The mechanisms regulating exocytosis of the salivary glands of the soft tick, *Ornithodoros savignyi*

by

Christine Maritz-Olivier

Submitted in partial fulfilment of the requirements for the degree

Philosophiae Doctor

in the

Faculty of Natural and Agricultural Science

Department of Biochemistry

University of Pretoria

Pretoria

July 2005

CONTENTS

Chapter 1:   Literature review

Chapter 2:   Signaling pathways regulating protein secretion from the salivary glands of unfed female *Ornithodoros savignyi*.

Chapter 3: Investigations into the conserved core machinery of regulated exocytosis in the salivary glands of *O. savignyi*

Chapter 4:   Investigation into protein-protein interactions between rat brain secretory proteins and an *O. savignyi* cDNA library by means of the GAL4 two-hybrid system

**Chapter 5:   Investigating   SNARE-interactions   by   functional
              complementation in *Saccharomyces cerevisiae* and pull-
              down assays with α-SNAP**

LIST OF ABBREVIATIONS

A	Adenosine / Alanine
AA	Arachidonic acid
AD	Activation domain
Ade	Adenine
AMP	Adenosine monophosphate
Amp	Ampicillin
αSNAP	α-Soluble NSF attachment protein
ATP	Adenosine triphosphate
BD	Binding domain
BLAST	Basic local alignment search tool
bp	Base pairs
°C	Degrees Celcius
C	Cytosine / Cysteine
cAMP	Cyclic adenosine monophosphate
CCV	Clathrin-coated vesicle
cDNA	Complementary DNA
cfu	Colony forming units
CgB	Chromogranin B
CHX	Cycloheximide
COX	Cyclooxygenase
C-terminal	Carboxy terminal
D	Aspartic acid
Da	Dalton
dA	Deoxy adenosine
DAG	Diacyl glycerol
dC	Deoxy cytosine
DDO	Double dropout
DEPC	Diethyl pyrocarbonate
dG	Deoxy guanosine

vi

DIG	Digoxygenin
DNA	Deoxyribonucleic acid
DNA-BD	DNA-binding domain
DNAse	Deoxyribonuclease
dNTP	Deoxynucleotide triphosphate
DO	Dropout
ds	Double stranded
dT	Deoxy thymidine
DTT	Dithiothreitol
E	Glutamic acid
E. coli	*Escherichia coli*
EDTA	Ethylene diamine tetra acetic acid
EE	Early endosome
EGTA	Ethylene-bis (oxyethylene nitrilo) tetra acetic acid
ELISA	Enzyme linked immunosorbent assay
F	Phenylalanine
G	Guanidine / Glycine
GAL4	Galactose 4 regulatory protein
G_i	Inhibitory G-protein
G_s	Stimulatory G-protein
H	Histidine
I	Inosine / Isoleucine
InsP	Inositol phosphate
IP_3	Inositol 1,4,5-triphosphate
IPTG	Isopropyl-β-D-thiogalactopyranoside
ISG	Immature granule
K	Lysine
kDa	Kilo Dalton

L	Leucine
lacZ	β-Galactosidase gene
LB	Luria-Berthani
LDCV	Large dense core vesicle
LD-PCR	Long distance PCR
M	Methionine
MCS	Multiple cloning site
μM	Micromolar
μmol	Micromole
mg	Milligram
min	Minutes
mM	Millimolar
mRNA	Messenger RNA
MSG	Mature secretory granule
N	Asparagine
NCBI	National Centre for Biotechnology Information
ng	Nanogram
NLS	Nuclear localization signal
nmol	Nanomole
NSF	N-Ethylmaleimide sensitive factor
N-terminal	Amino terminal
ORF	Open reading frame
ori	Origin of replication
P	Proline
PAGE	Polyacrylamide gel electrophoresis
PCR	Polymerase chain reaction
PEG	Poly-ethylene glycol
PG	Prostaglandin
PGE_2	Prostaglandin E_2

PIP$_2$	Phosphatidyl inositol 4,5-bisphosphate
PKA	Protein kinase A
PKC	Protein kinase C
PLC	Phospho lipase C
pmol	Picomole
pS	picoSiemens
Q	Glutamine
QDO	Quadruple dropout
R	Arginine
RACE	Random amplification of cDNA ends
RNAse	Ribonuclease
RNA	Ribonucleic acid
RRP	Rapidly releasable pool
RSP	Regulated secretory protein
RT-PCR	Reverse transcription PCR
S	Serine
SAP	Shrimp alkaline phosphatase
SD	Standard dropout
SDS	Sodium dodecyl sulfate
SEM	Scanning electron microscopy
SG	Secretory granule
SNAP	Soluble NSF attachment protein
SNARE	SNAP receptor
SRP	Slowly releasable pool
ss	Single stranded
SSV	Small synaptic vesicle
syt	Synaptotagmin
T	Thymidine / Threonine
TAE	Tris-acetate EDTA buffer
Taq	*Thermus aquaticus*

TBS	Tris buffered saline
TDO	Triple dropout
TEM	Transmission electron microscopy
TGN	*trans*-Golgi network
T_m	Melting temperature
Tris	Tris(hydroxymethyl) aminomethane
tRNA	Transfer RNA
U	Units
UAS	Upstream activating sequences
V	Valine
VAMP	Vesicle associated membrane protein
W	Tryptophan
WT	Wild type
X-gal	5-Bromo-4-chloro-3-indolyl-β-D-galactopyranoside
Y	Tyrosine

LIST OF FIGURES

LIST OF TABLES

APPENDIX

ACKNOWLEDGEMENTS

I am extremely grateful towards the following:

- Prof. A.W.H. Neitz, my supervisor at the Department of Biochemistry, University of Pretoria, whom inspired my love for biochemistry during the first lecture he presented on proteins during my 2nd year undergraduate studies; for opening numerous research opportunities, his continued support, interest and guidance during the duration of my post-graduate life.

- Prof. A.I.Louw, my co-supervisor at the Department of Biochemistry, University of Pretoria, for valuable advice, teaching me to write proper science, continued interest in this project and creating a passion for molecular biology.

- Prof. J.R. Sauer at the Department of Entomology, Oklahoma State University, USA for opening up his laboratory and home to me during my visit. Your Christian values and life will continue to be an inspiration throughout my life.

- Prof. H. Moolman-Smook at the Department of Medical Biochemistry, University of Stellenbosch, South Africa, for opening her laboratory to me, teaching me the art of the two-hybrid system and yeast, your support and valuable opinions.

- Dr. Fourie Joubert and Mr. Tjaart de Beer for their tireless advice on Bioinformatics, computational analyses of data and protein modeling.

- Dr. Ben Mans for the numerous discussions and philosophical talks on life. Your love for ticks inspired me to become a life-long tick person!

- Mrs. S. van Wyngaardt, for her support, advice, helping hands and guidance during this project.

- My fellow students and friends, for always inspiring me to do better!

- My parents, family and friends. Your love, motivation and prayer make life worth living.

- My husband, Nicholas Olivier, who supported me throughout my postgraduate studies. Your kindness, inspiration, guidance, prayer and love are the center of my being.

- The Andrew F. Mellon Foundation for the Mellon Foundation Postgraduate Mentoring Fellowship. This opportunity opened a tremendous amount of opportunities during this study. The scientific exposure I received shaped me into the scientist I am today.

- The National Research Foundation of South Africa for their financial assistance during this study.

- My heavenly Father, thanks for always being the same, unchangeable Rock of my life. Your presence kept me going throughout the good and bad times of this study. I admire your creation, in awe!

CHAPTER 1
LITERATURE REVIEW

1.1. TICKS: AN OVERVIEW

Ticks are believed to have originated 120 million years ago (MYA), and that they speciated by ~92 MYA into the main tick families as we know them today (Mans 2002a). Currently, they are classified as belonging to the subclass Acari, the dominant subclass of the Arachnida. The approximately 850 species are divided into two major and one small subfamily. The first family is the Ixodidae or 'hard ticks', so called because of their sclerotized dorsal scutal plate. The second family is the Argasidae or 'soft ticks', so called because of their flexible, leathery skin/cuticle. A third family, the Nutalliellidae, contains only one species, *Nuttaliella namaqua* (Sonenshine 1991).

Ixodidae

The family Ixodidae is by far the largest and economically most important family. It contains 13 genera and approximately 650 species (Sonenshine 1991). They are characterized by the presence of a tough, sclerotized plate (scutum) on the dorsal body surface, which functions as the site of attachment for various muscle groups (Figure 1.1).
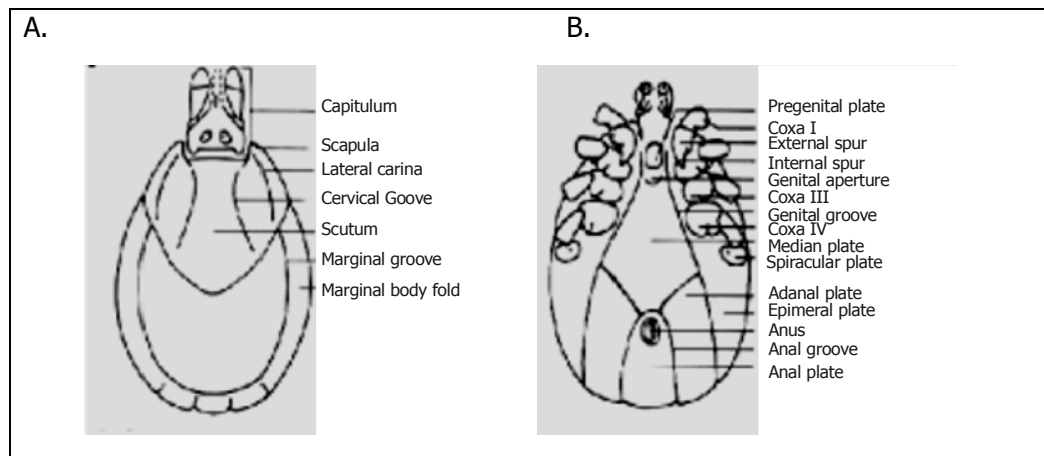
Figure 1.1. Diagram illustrating ixodid adult tick body structures (Sonenshine 1991). The *(A) Female ixodid tick, dorsal aspect, and (B) male, ventral aspects are shown.*

In males, the scutum covers the entire dorsal surface, limiting the expansion of the body during feeding. In females, nymphs and larvae, the scutum is limited to the anterior dorsal body region and allows for significant expansion of the body during feeding. In fully

engorged specimens, the scutum appears as a small plate on an extended body. Anterior to the scutum, the mouthparts protrude beyond the body and are visible when the specimens are viewed from the dorsal aspect (Sonenshine 1991).

During the life cycle of Ixodidae (Figure 1.2), eggs hatch into a single nymphal instar, which will molt to larvae. The nymphal and larval stages resemble adults, but lack the external genital pores, porose areas and foveal pore clusters. In larvae, only three pairs of walking legs occur, with the fourth pair represented by limb buds that develop into legs with the molt to the nymphal state (Sonenshine 1991).
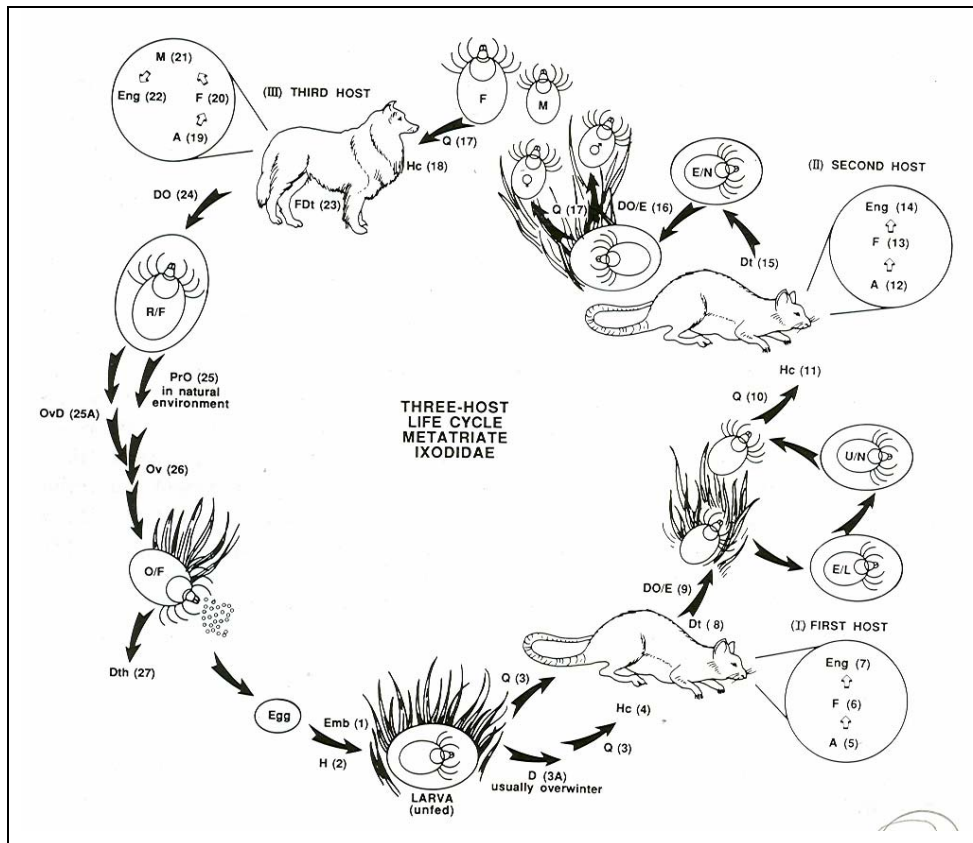
Figure 1.2. Diagram illustrating the typical 3-host cycle characteristic of most ixodid ticks (Sonenshine 1991). *The parasitic phases, i.e. when the different life stages are on the host, are shown in the exploded circles. The different events in the life cycle are indicated by a number in parentheses, (1) egg, (2) hatching, (3) larvae, (4) host contact, (5) attachment, (6) feeding, (7) engorgement, (8) detachment, (9) drop off, (10) nymph, (11-15) entire cycle of host contact, attachment, feeding, engorgement, and detachment, (16) nymphs drop off, (17) adults, (18) host contact, (19,20) attachment and feeding, (21) mating, (22) mated females, (23) fed females detach, (24) drop off, (25) pre-ovipositional development, (26) oviposition and (27) death of female.*

Argasidae

The family Argasidae comprises 5 genera and approximately 170 species (Sonenshine 1991). In contrast to the Ixodidae, the Argasidae lack the scutum and have a leathery cuticle (Figure 1.3).

A.

Hood

Discs

Mammillae

Dorso-ventral groove

B.

Hood
Mouthparts

Coxa
Eye

Coxal fold

Preanal groove

Median postanal groove
Transverse postanal groove
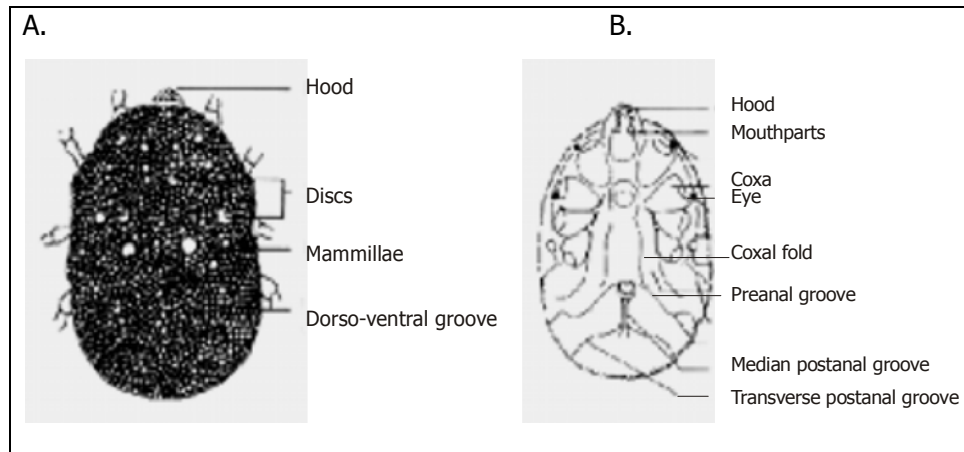
Figure 1.3. Diagram illustrating argasid adult tick body structures (Sonenshine 1991). *The generalized argasid tick ventral view (A) and dorsal view (B) is shown.*

Biologically, argasid ticks differ from ixodid ones in the number of nymphal stages (Figure 1.4). Argasid species may have from 2 to 8 nymphal instars, but usually have only 3 or 4. The number of nymphal instars is not fixed and depends on the size of the blood meal in preceding stages. During feeding, nymphs can increase their body weight 3-5 times, swelling as they feed. Usually males require fewer instars than females (Sonenshine 1991). Argasid ticks exhibit remarkable diversity in their patterns of development and feeding. They feed rapidly and the females oviposit frequently. Similar to mosquitoes and some blood-feeding insects, argasid ticks have multiple gonotrophic cycles (Figure 1.4).

A second characteristic of argasid ticks is the short time in which they feed. Adults and nymphs of most species feed rapidly (minutes to hours), in contrast to the lengthy (days), complex feeding process of ixodid ticks. During feeding, numerous bioactive compounds are secreted from the salivary glands into the host bloodstream (via saliva) to ensure continuous feeding (Table 1.1).
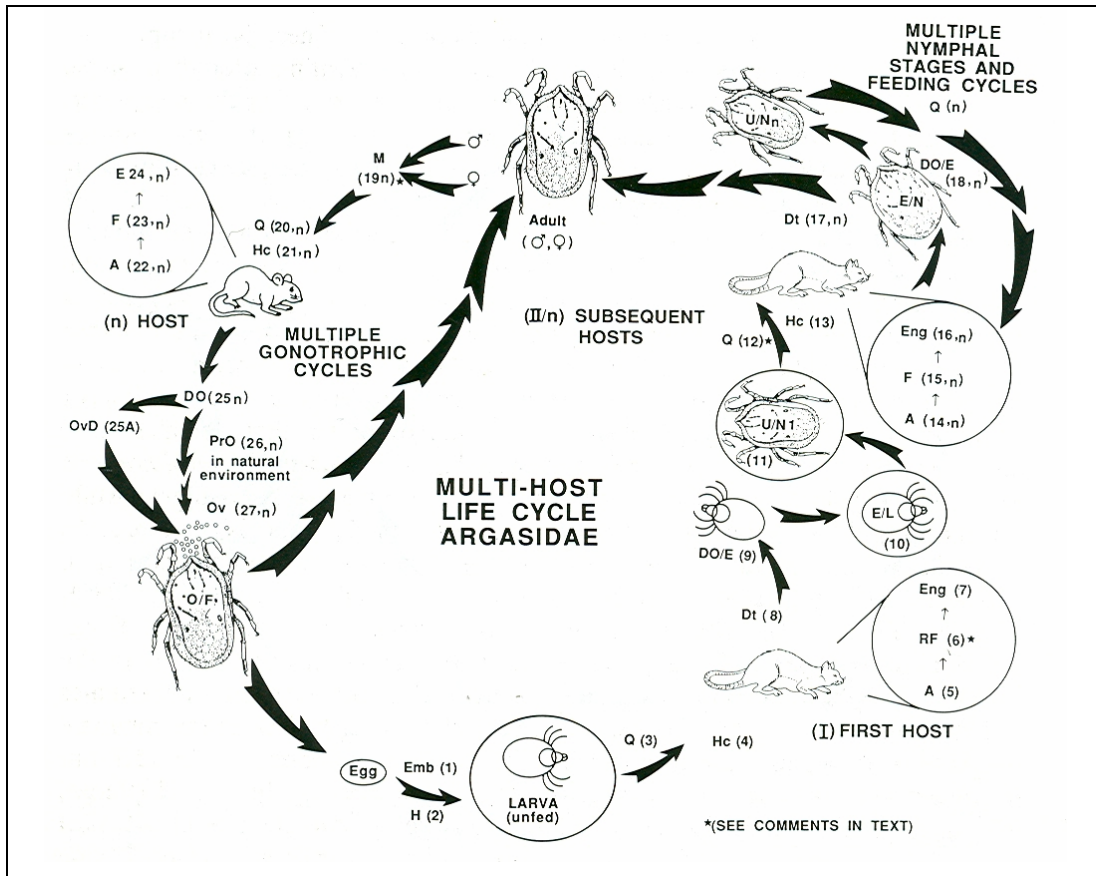
Figure 1.4. Diagram illustrating the typical argasid multi-host life cycle with multiple parasitic phases and repeated gonotrophic cycles (Sonenshine 1991). *The different events in the life cycle are indicated by a number in parentheses, (1) embryogenesis, (2) hatching of larvae, (3) host contact, (4) attachment, (5) feeding, (6) engorgement, (7) drop off, (8) ecdyse and molt into first nymphal stage, (9-12 & 13-21) entire cycle of host contact, attachment, feeding, engorgement, and detachment repeat twice, (22) adults mate, (23) host contact, (24) adults feed rapidly, (25) engorge, (26) drop off, (27) mated females oviposit, (28-36) adults seek hosts, feed and engorge several times and fed mated females oviposit after each bloodmeal. The number of gonotrophic cycles is indeterminate.*

During this study, the argasid tick *Ornithodoros savignyi* was studied (Figure 1.5). This species is found in sandy regions, giving rise to the local name 'sand tampan', throughout the North Western parts of South Africa and also Egypt, Arabia, Ethiopia, Kenya and Zimbabwe (Paton and Evans 1929). *O. savignyi* is diploid (2n=20), with the presence of sex-chromosomes, XY and XX for males and females, respectively (Howell 1966).

Currently these ticks are controlled by chemical treatment of the soil, since ticks avoid these treated areas (Paton and Evans 1929) . But since these ticks have a lifespan of 15-20 years and need to feed only occasionally (every 5-6 years), starvation is a not an option (Mans

2002a). Apart from the various bioactive compounds secreted by this species (Table 1.1), much emphasis is placed on it due to its local economic importance in that it kills many domestic animals, especially young calves and lambs. Originally death of the host was contributed to exsanguinations, but later it was shown that death is caused by a toxin which causes serious allergic reactions in humans (Howell *et al.* 1975). Later studies indicated the presence of two toxins (TSGP2 and TSGP4), which affects the cardiac system of the host (Mans *et al.* 2002c).

1 cm
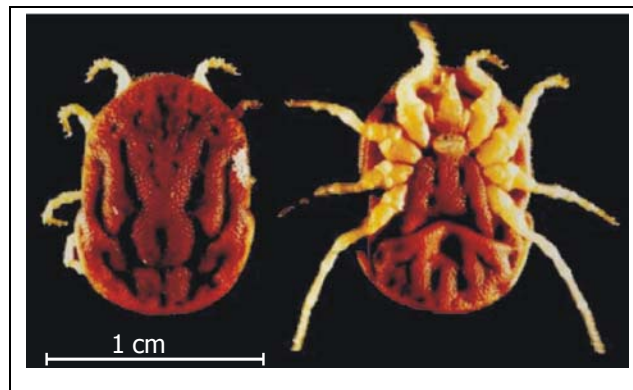
Figure 1.5. External anatomy of a female *O. savignyi. *The folded integument, position of the capitulum and genital opening is visible. Scale bar =1 cm. (Photograph: B.J. Mans, 1996).*

Table 1.1. Properties of the granule components secreted by argasid ticks.

Species	Compound	Target in host	Reference
Platelet aggregation factors			
O. moubata	Apyrase	ADP	(Ribeiro *et al.* 1991)
	Moubatin	Collagen	(Waxman and Connolly 1993)
	TAI	Collagen	(Karczewski *et al.* 1995)
	Disagregin	$\alpha_{IIb}\beta3$	(Karczewski *et al.* 1994)
O. savignyi	Apyrase	ADP	(Mans *et al.* 1998)
	Savignygrin	$\alpha_{IIb}\beta3$	(Mans *et al.* 2002b)
Anticoagulants			
O. moubata	Inhibitors	fxa	(Waxman *et al.* 1990)
		Trombin	(van de Locht *et al.* 1996)
O. savignyi	Inhibitors	fxa	(Gaspar *et al.* 1996; Joubert *et al.* 1998)
		Trombin	(Nienaber *et al.* 1999)
Toxins			
Argas (P.) walkerae	Paralysis toxin	Na$^+$ channel	(Viljoen *et al.* 1990; Maritz *et al.* 2000; Maritz *et al.* 2001)

Nuttaliellidae

This family is based on a single species, *Nuttalliella namaqua*, specimens of which were collected from localities in Namibia, South Africa and Tanzania from nests of rock hyraxes and swallows. Nuttaliellidae exhibits features of both the ixodid and argasid ticks. Female have a pseudo-scutum, which is a plate-like structure resembling the scutum in outline. It does not, however, share the smooth appearance of the sclerotized plate of the Ixodidae. Unique to this family is the fact that ball and socket joints articulate the leg segments, a feature not seen in any other species of tick. Other noteworthy features include the lack of eyes, spiracular plates, genital grooves and also dorso-ventral grooves (Sonenshine 1991).

1.2. BIOGENESIS OF SECRETORY GRANULES

As described above, it is clear that all stages and species of ticks require a bloodmeal in order to molt, oviposit and ultimately survive. During these feeding stages, the salivary glands fulfill a core function in ensuring a continuous blood flow from the host, preventing blood clotting in the tick, and counteracting the host's defense mechanisms. To date, bioactive compounds, which enable these processes, have been identified in all tick species. These are synthesized and stored in the salivary glands in diverse granules/vesicles, and are secreted upon stimulation, i.e. regulated exocytosis. The structure and function of argasid salivary glands and the various granules are discussed in great detail in Chapter 2. In this study, we investigated the proteins involved in regulated exocytosis of the salivary glands of O. *savignyi*. Therefore, the mechanisms underlying granule formation, maturation and regulated exocytosis are of significance to this study.

Secretory granules (SGs) can be viewed as alternative organelles capable of accommodating high concentrations of secretory compounds and sensitive to stimulus-induced exocytosis. In most cells SGs appear to represent an entirely new class of organelle, although in some cell types (e.g. hemopoietic cells) they share several properties with lysosomes, such as containing lysosomal markers, are accessible via the endocytic pathway and dense-core formation occurs in multi-vesicular bodies (Burgoyne and Morgan 2003). Furthermore, conventional lysosomes can undergo stimulus-induced fusion with the plasma membrane in a wide range of cells, and therefore it may be that classical secretory granules evolved from a lysosomal progenitor. In contrast to secretory lysosomes found in hemopoietic cells, granules found in endocrine, exocrine and neuronal cells are products of the biosynthetic pathway alone, i.e. they do not resemble lysosomes (Burgoyne and Morgan 2003).

6

Initial formation of immature granules (ISGs) occurs at the *trans*-Golgi network (TGN) and does not require a coat-driven budding process. Instead it is thought that membrane deformation may result from the aggregation of secretory proteins in the TGN (Burgoyne and Morgan 2003). Once formed, immature SGs must be processed and remodeled to form mature secretory granules (MSGs). In endocrine and neuroendocrine cells this involves both fusion with other immature secretory granules and removal of misrouted material via budding to increased size and density of mature granules (Burgoyne and Morgan 2003). Proteins retained in the MSG are called regulated secretory proteins (RSPs) and secretion of these will only occur from MSGs when the cell receives an external stimulus (Tooze *et al.* 2001). The widely accepted model for the biogenesis of secretory granules comprises four distinct steps (Figure 1.6). These steps are: (1) aggregation of the RSP and sorting of the RSP to the membrane in the TGN, (2) budding from the TGN, (3) homotypic fusion of ISGs, and (4) remodeling of the ISG membrane and content (Tooze *et al.* 2001).
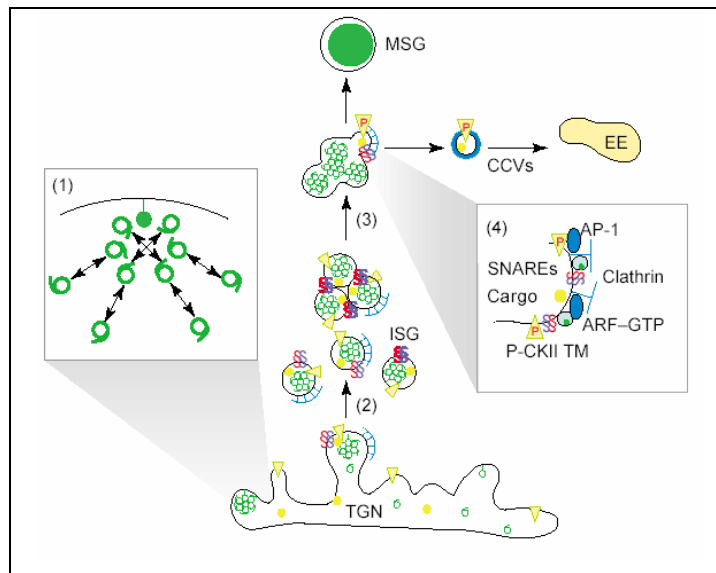
Figure 1.6. Biogenesis of secretory granules in neuroendocrine cells (Tooze *et al.* 2001). *Step (1) Regulated secretory proteins (RSPs; green spheres with curly tail) become associated with a specialized region of the trans-Golgi network (TGN) and assemble into oligomers with each other and with a membrane associated form of RSPs (filled green circle with stalk) in the lumen of the TGN. The assembly of the RSPs into oligomers, and later multimers, is the basis of the aggregation of the RSPs. (2) Additional components, including SNARE molecules (blue and red '§'), other soluble non-secretory granule proteins, or cargo (yellow spheres) and non-secretory granule membrane proteins (yellow triangles), are included into the nascent bud. Immature secretory granules (ISGs) form from the specialized region of the TGN containing the RSP, the cargo and the SNAREs. (3) After formation, ISGs undergo homotypic fusion mediated by SNAREs, followed by membrane remodeling (4). Remodeling is achieved by the interaction of GTP-bound ADP-ribosylation factor (ARF), AP-1 and clathrin to form clathrin-coated vesicles (CCVs), which remove SNAREs, cargo and non-secretory granule membrane proteins that are not destined for the mature secretory granule (MSG) in a process often dependent on phosphorylation (P) by casein kinase II (CKII). Abbreviation: EE, early endosome.*

Aggregation of RSPs

To date much effort has been spent on defining a specific domain of the RSPs responsible for sorting into ISGs. Conventional transfection screening was not successful due to the propensity of exogenous and endogenous RSPs to co-aggregate in the slightly acidic, high calcium milieu of the TGN. Proteins such as the family of granins, that includes chromogranin A, -B, secretogranin and 7B2, could be aggregation vehicles for a variety of proteins. Studies, where chromogranin B (CgB) was expressed in cells where endogenous protein synthesis was shut down, indicated that CgB has an N-terminal loop that acted as a signal for sorting into ISGs in the absence of any other RSPs. Deletion of the N-terminal allowed CgB to be sorted through aggregation only in the presence of other RSPs, indicating that the C-terminal may facilitate sorting indirectly (Tooze *et al.* 2001).

A variety of RSPs, containing a chromogranin-like N-terminal loop, is involved in some aspect of RSP sorting. It is believed that the loop either mediates interactions between monomers of RSPs, or by binding directly to a so-called loop receptor. Mutations and deletions in the loop region of various RSPs, as well as their effects, are summarized in Table 1.2.

Table 1.2. Effects of altered loop-regions in various proteins. (Tooze *et al.* 2001).

Cell Type / Protein	Chemical treatment/ Mutation of loop-domain	Effect
PC12 / CgB	DTT disruption	Constitutive secretion of CgB
GH$_4$C1 / CgB	DTT disruption	No effect
CgA	Neutral pH	Loop mediated homo-dimerization
GH$_4$C1 / CgA	Deleted C-terminal domain	Incorrect sorting
PC12 / CgA	Deleted C-terminal domain	No effect
α1-antitrypsin (AT)	Fused with N-terminal CgB loop domain	AT no longer constitutively secreted, directed into ISGs
α1-antitrypsin (AT)	Fused with N- and C-terminal CgB loop domains	Sorted more efficiently into ISGs, increased membrane binding of AT

During granule formation RSPs containing dibasic amino acid cleavage sites are processed by pro-hormone convertases, the so-called PC (Prohormone) enzymes. These enzymes are endopeptidases that process prohormones and require low pH and calcium (Tooze *et al.* 2001). Furin is related to the PC enzymes and is responsible for the processing of PCs in the Golgi. Inhibitors of these enzymes include chaperones, serpins and granin-like proteins. The most important inhibitor found in secretory granules is a serpin called endopin 1, which functions by inhibiting basic-residues cleaving proteases (Tooze *et al.* 2001). Since the initiation and efficiency of processing by PC enzymes varies depending on the cell-type and the RSPs, the question as to whether PCs are relevant in sorting is a much debated topic (Tooze *et al.* 2001).

Some RSPs adopt different strategies and rely on different signals to ensure inclusion into ISGs. Examples of the latter include prolactin and growth hormone, which forms a detergent-insoluble aggregate after it exits from the endoplasmic reticulum and, unlike other RSPs such as CgB, does not require an acidic pH to aggregate (Tooze *et al.* 2001). Another strategy that RSPs might use to promote inclusion into ISGs is the recruitment of

aggregation chaperones. The first chaperone to be found in the lumen of the secretory pathway was the granin 7B2 protein (Tooze *et al.* 2001). This protein binds to proPC2 and is essential for its transport from the ER to the ISG. Studies on the expression of his-tagged 7B2 *in vivo* indicated an increase in the aggregation of pro-enkephalin and CgA. The question must, however, be asked whether the overexpression of his-tagged proteins influence the concentration of divalent cations or pH in the TGN, and hence creating a more favorable environment for the RSP to aggregate.

Sorting of RSPs

Association of RSPs with the membrane is required for efficient sorting into nascent ISGs. Although none of the well-studied RSPs are membrane proteins, evidence suggests that many RSPs exist in two forms: a soluble form and a form that is tightly associated with the membrane. From this data several models have been proposed to explain the association of RSPs with the TGN to form ISGs, i.e (1) a subpopulation of RSPs that are tightly associated with the membrane, (2) a membrane protein or (3) a lipid. To date, a combination of models 1 and 3 are favored and is depicted in Figure 1.7.

It is believed that clustering of the soluble and membrane-bound forms of RSPs results in the formation of large aggregates in a specialized subdomain (lipid raft) of the TGN from which an ISG will form. This has been proven for epithelial cells as well as thyroglobulin (a RSP of the thyroid) where the RSP is targeted to a lipid microdomain. By manipulating the lipid levels in cells, the role of cholesterol and sphingolipids could be demonstrated (see Table 1.3).
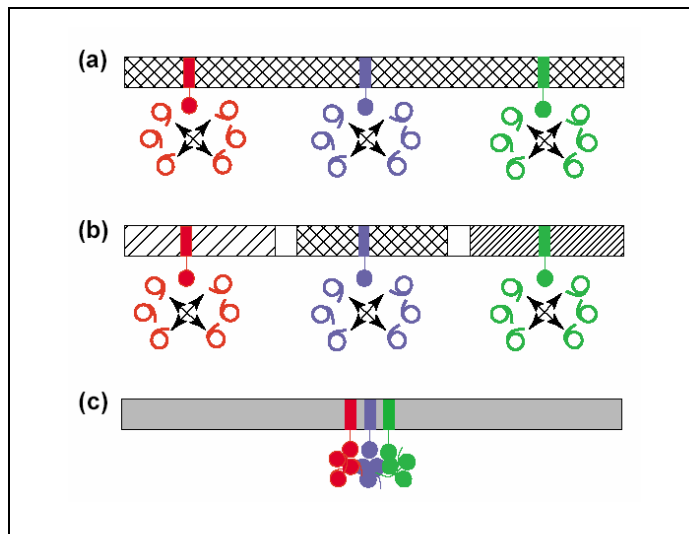
Figure 1.7. Sorting of regulated secretory proteins (RSPs) in the _trans_-Golgi network (TGN) by protein–lipid interactions (Tooze _et al._ 2001). _A subpopulation of RSPs is membrane-associated owing to their interaction with lipids. These protein/lipid complexes are contained within lipid rafts (hatched or striped boxes). The different membrane associated RSPs (filled circles shown in red, blue and green) bind to a lipid (rectangles shown in red, blue and green) either in (a) a single lipid raft or (b) separate lipid rafts. Aggregation of the different RSPs with each other, mediated by the N-terminal loops and aggregation domains, and perhaps the associated lipids, promotes the assembly of a specialized domain in the TGN (gray shading) from where immature secretory granules (ISGs) will form (c)._

Table 1.3. Examples of RSPs associated with lipid microdomains (Tooze _et al._ 2001).

Cell Type	Chemical treatment	Effect	Reference
AtT20	Lovostatin (Depletes cholesterol)	- Inhibition of secretory granule formation - Reversible upon addition of cholesterol	(Wang _et al._ 2000)
Various	Addition of cholesterol	Increased ISG production	(Wang _et al._ 2000)
Chromaffin	None	PC2 and GPIII are associated with lipid rafts	(Palmer and Christie 1992; Blazquez _et al._ 2000)
AtT20	Fumonisin (Inhibitor of sphingolipid biosynthesis)	Sphingolipids are required for PC2 sorting	(Blazquez _et al._ 2000)
Bovine pituitary	Methyl-β-cyclodextrin (Deplete cholesterol)	- CPE no longer sorted and occur in soluble fraction - Reduction in the N-terminal loop of POMC binding to granule membranes	(Dhanvantari and Loh 2000)

11

Maturation of ISGs

Surprisingly, in some cell types immature granules can undergo regulated exocytosis, indicating that the process of granule maturation does not confer plasma membrane fusion competence, but rather inhibits homotypic granule-granule fusion. In contrast, maturation actually increases stimulus-secretion coupling in other cells, as newly formed granules are poorly responsive to secretagogues relative to mature granules (Burgoyne and Morgan 2003).

(a) Remodeling of ISGs

In all endocrine and neuroendocrine cells studied to date, a feature of maturation is the removal of soluble proteins, peptides and membrane proteins from the ISG (Step 3, Figure 1.6). Soluble peptides and hormones removed from the ISG often appear to be secreted from the cell in a non-regulated manner, leading to the description of 'constitutive-like' secretion. Removal of membrane proteins occurs in clathrin-coated vesicles (CCVs), which are targeted to either endosomes or the TGN (Tooze *et al.* 2001). The CCVs may also function to remove soluble proteins destined for constitutive-like secretion.

In AtT20 cells newly formed granules were found to be poorly responsive to secretagogues relative to mature granules. This is believed to be due to the presence of synaptotagmin IV on immature granules that inhibits the putative exocytotic calcium receptor synaptotagmin I. Once it is removed during maturation, normal calcium-dependent release occurs (Burgoyne and Morgan 2003).

(b) Homotypic fusion

Maturation of ISGs involves a change in size; either increased via homotypic fusion or decreased via budding of vesicles from the ISG (Step 3, Figure 1.6). Reconstitution of homotypic fusion in cell-free extracts reveals that the cytosolic components NSF and α-SNAP (involved in all membrane fusion events) are required for ISG-ISG fusion by priming the SNAREs (SNAP receptors). Since the SNAREs present on ISGs differ from those of MSGs, it is hypothesized that they are essential for maturation. To date the mechanism underlying maturation of ISGs by SNAREs has been proven for VAMP 4 (Eaton *et al.* 2000) and syntaxin 6 (Klumperman *et al.* 1998; Dittie *et al.* 1999), which is believed to act by recruiting the proteins ARF and AP-1 (Figure 1.6).

1.3. THE EXOCYTOTIC PATHWAYS

Regulated exocytosis has been dissected into a number of functionally defined, sequential stages (Burgoyne and Morgan 2003). These include physical movement of vesicles to the subplasmalemmal region of the cell, tethering and then docking at release sites on the plasma membrane, ATP-dependent priming steps to convert the vesicles into a fully releasable state, triggered membrane fusion, release of granule content, and finally retrieval of the granule membrane (Figure 1.8)
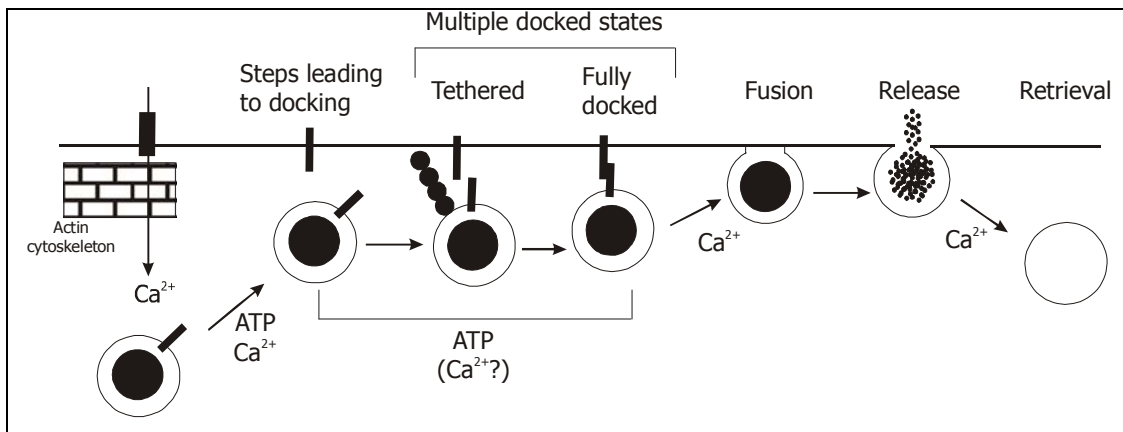
Figure 1.8. Schematic representation of the steps leading to secretory granule exocytosis (Burgoyne and Morgan 2003). *This representation is based on neuroendocrine cells undergoing calcium-triggered exocytosis. In this case, calcium entry leads to the disassembly of the cortical actin cytoskeleton, allowing granule recruitment to the plasma membrane where tethering and docking of the granule can occur, followed by fusion and release of granule contents.*

Tethering and Docking

The first physical linkage between two membranes destined to fuse appears to be mediated by tethering factors, which may also trigger the engagement of *trans*-SNARE complexes (Ungar and Hughson 2003). Although tethering factors are structurally diverse, they can be divided into two main classes (Table 1.4). Firstly, a group of long coiled-coil proteins that form homodimeric coiled coils with lengths up to several times the diameter of a vesicle. The current model suggests that they are anchored at one end to a membrane, which allows them to search the surrounding space for a passing vesicle, which is then bound by the other end (Whyte and Munro 2002). Secondly, a group of large, hetero-oligomeric complexes have been proposed to play a role in vesicle tethering at distinct trafficking steps. To date, seven conserved complexes have been identified and described (Table 1.4). These tethering complexes are also known to interact with various SNAREs and Rab GTPases located

throughout the secretory pathway (Ungar and Hughson 2003). The various interacting partners are listed in Table 1.4.

Table 1.4. Properties and binding partners of tethering proteins (Lipschutz and Mostov 2002; Whyte and Munro 2002; Ungar and Hughson 2003). *Abbreviations of subcellular compartments: (TGN) trans-Golgi network, (PM) plasma membrane, (ER) endoplasmic reticulum.*

Tethering Protein	Location *in vivo*	Receptor	Interacting SNARE / Rab
Coiled-coil proteins			
p115/Uso1p	Golgi	On vesicle: Giantin On Golgi: GM130	Bet1, Bos1, Sec22, Ykt6, Gos28, Membrin, syntaxin 5
EEA1	Early endosome	Unknown	Syntaxin 6 & 13
Hetero-oligomeric complexes			
COG (Conserved oligomeric Golgi complex)	Golgi	Unknown	Bet1, Sec22, Ykt6, Gos1p, Sed5p,
GARP / VFT (Golgi-associated retrograde protein)	Golgi	Unknown	Tlg1p
TRAPP I and II (Transport protein particle)	TGN, Cytosol	Unknown	Bet1
Exocyst (Sec6/8 complex)	PM, TGN	Unknown	Sec4, Rho3, RalA, Rho1
HOPS/ C-Vps complex	Vacuole	Unknown	Vam3
Dsl1p complex	Golgi / ER	Unknown	Sec22, Ufe1

After tethering of the granule/vesicle, *trans*-SNARE complexes are formed. SNAREs are membrane proteins that are localized to various intracellular organelles and are identified by a characteristic heptad repeat sequence known as the SNARE motif. Three proteins namely syntaxin, VAMP/synaptobrevin (vesicle associated membrane protein) and SNAP-25 form a SNARE complex, first described in synapses by Sollner *et al.* (Sollner *et al.* 1993). Since VAMP is localized on the vesicle membrane and syntaxin and SNAP-25 localize to the plasma membrane, SNAREs were originally classified as vesicle (v-) or target (t-) SNAREs, and the SNARE-hypothesis was formed. The latter states that each class of transport vesicle contains a specific protein (v-SNARE) that is capable of associating with a receptor protein (t-SNARE), specific to the appropriate acceptor membrane (Sollner *et al.* 1993; Bajjalieh and Scheller 1995). Later studies, however, indicated that the specificity is not due to SNARE-interactions alone, but is the product of numerous interactions involving non-SNARE proteins. Since the

SNARE proteins are the ones investigated during this study, they are discussed in more detail in the following chapters.

Priming

In neuronal and non-neuronal systems there is substantial evidence that docked vesicles are not intrinsically fusion-competent (Klenchin and Martin 2000). Priming is an essential pre-fusion step, determining the release probabilities of a vesicle by rendering them competent for Ca^{2+}-triggered fusion (Figure 1.9). This has been well described for small synaptic vesicles (SSVs), but currently it is believed that priming of SSVs differ from that of large dense core vesicles (LDCVs) in being more efficient. Rapidly releasable pool (RRP) sizes for LDCVs are estimated as ~100 vesicles out of a membrane-docked pool of ~1000 LDCVs in chromaffin cells, in contrast to neurons where the releasable pool corresponds closely to the full docked complement of SSVs (Martin 2003). In studies of secretory granule exocytosis, priming is a term used to describe any functionally detected ATP-dependent process that occurs before fusion (Burgoyne and Morgan 2003).
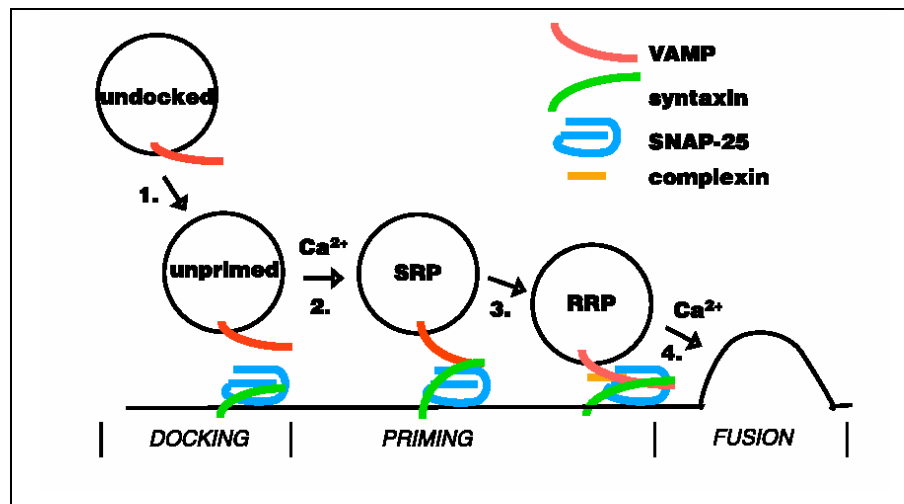
Figure 1.9. LDCV exocytosis viewed as sequential stages of docking, priming and fusion (Martin 2003). *Cytoplasmic or undocked vesicles undergo docking (1). Priming of docked vesicles may occur in two stages to generate SRP (slowly releasable pool) and RRP (rapidly releasable pool) of vesicles (2 and 3). The first priming step requires moderate increases in cytoplasmic Ca^{2+}. Activating levels of Ca^{2+} trigger fusion of vesicles from either the SRP (not shown) or from the RRP (4). Each step is thought to be reversible although they are depicted as single arrows in the figure. Priming reactions are thought to involve assembly of trans SNARE complexes, which may be initiated by anchoring of N-terminal domains of SNARE motifs and their subsequent "zippering" to C-terminal, membrane proximal regions. In SV exocytosis, complexins may stabilize trans SNARE complexes at a late stage of assembly rendering them fusion-ready upon Ca^{2+} influx.*

To date, p145/CAPS has been identified as essential for the priming of LDCVs by rendering the LDCVs calcium-sensitive (Martin 2003). Furthermore, CAPS is also regarded as a tethering protein since it interacts with both the LDCV and the plasma membrane via PIP_2 (Phosphatidyl inositol 4,5-bisphosphate; which is essential for LDCV exocytosis). In PC12 cells, the priming reaction for which CAPS is essential is strongly ATP-dependent. It is believed that ATP is required for maintaining the slow releasable vs. the rapid releasable pool of vesicles, thereby enabling its replenishment (Martin 2003).

Synaptotagmins (Syt) are a second class of protein involved in priming of LDCVs. In PC12 cells cross-linking studies showed that Syt proximity to SNARE complexes increases when exocytosis-triggering levels of calcium are provided. This suggests that the majority of docked LDCVs in PC12 cells are in an unprimed state in which *trans*-SNARE complex formation has yet to be initiated. The calcium dependence of the priming step may be mediated by Syt proteins, which catalyze *trans*-SNARE complex formation (Martin 2003).

The ATPase NSF (<u>N</u>-ethylmaleimide <u>s</u>ensitive <u>f</u>actor) has also been linked to priming of vesicles in non-neuronal cells, although not conclusively to dense core vesicles. In PC12 cells, neutralizing NSF antibodies were found to inhibit the ATP-dependent priming of docked vesicles, indicating that NSF may function to promote the ATP-dependent disassembly of *cis*-SNARE complexes that are largely resident on the plasma membrane of PC12 cells (Klenchin and Martin 2000). In chromaffin cells, N-ethylmaleimide treatment resulted in a reduced refilling of the rapidly releasable pool (RRP) of vesicles, similar to the results obtained in a temperature-sensitive allele of *Drosophila* NSF. Further studies indicated that docked vesicles accumulated at the membrane, but that they were fusion-incompetent, indicating that NSF functions in vesicle priming (Klenchin and Martin 2000). Finally, the protein Munc13-1 is also believed to act as a priming factor, since overexpression promotes priming of LDCVs in chromaffin cells (Martin 2003).

Interesting to note is the fact that priming is regulated by various protein kinases. In chromaffin cells, phorbol ester stimulation of protein kinase C (PKC) increased the size of the RRP and enhanced the rate of refilling the RRP without affecting vesicle fusion probabilities, an indication that PKC regulates vesicle priming. The role of protein kinase A (PKA) during priming has been shown in β-insulin secreting cells (Klenchin and Martin 2000).

Membrane fusion

In 1980 Chandler and Heuser reported the first image of an expanding fusion pore in degranulating mast cells by using rapid freezing techniques. They were able to show that membrane-lined pores of 20-100 nm in diameter provided a water path for secretory products to exit the vesicle interior into the extracellular space. Due to the smoothness of the membrane lining the pores, it was believed that pores are made exclusively of lipids (Lindau and deToledo 2003). By using more advanced techniques, such as admittance analysis (which monitor changes in cell surface areas), the groups of Almers and Zimmerberg independently provided the first estimations of fusion pore conductance and kinetics in degranulating mouse mast cells (Lindau and deToledo 2003). It was concluded that the initial fusion pore conductance was 200-300 pS (pico Siemens) in a lipid bilayer with a diameter of ~2 nm. This value, similar to the conductance of the potassium channel or a gap junction channel, is consistent with a fusion pore made of proteins. Later experiments by Monck and Fernandez indicated fusion pore conductances as low as 50 pS in eosinophils and neutrophils, which proposed that fusion pores are lipidic. These two extreme hypotheses led to a debate still unresolved (Lindau and deToledo 2003).

Another debate regarding membrane fusion entails full fusion versus transient fusion. Full fusion means that following the formation of a fusion pore, the pore expands to a large size and the vesicle membrane becomes fully incorporated into the plasma membrane. Transient fusion (kiss-and-run fusion) means that the pore opens, and maybe expands, but then closes again in order for the vesicle to retain its integrity when it discharges its contents (Figure 1.10)

Although to date no clear model exists for the fusion pore, it is widely believed that pore formation is a consequence of structural changes in the SNARE complex. Present models envision the C-terminal ends of VAMP and syntaxin to be located close to each other in the center of the pore, while the C-terminal of SNAP25 is located near the transmembrane domains of VAMP and syntaxin (Lindau and deToledo 2003). The SNARE hypothesis of fusion suggests that the initial fusion pore may be a proteolipid structure. In neurons and chromaffin cells, the SNARE proteins VAMP, syntaxin and SNAP25 are thought to form and expand the fusion pore. The dependence of membrane fusion on the concentration of soluble VAMP2 coil domains has suggested that three SNARE complexes mediate fusion of a vesicle (Lindau and deToledo 2003).
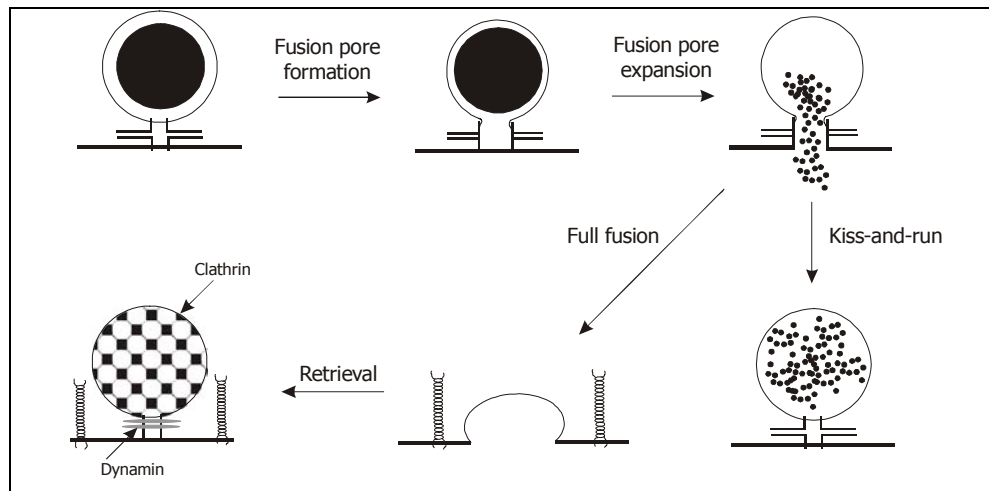
Figure 1.10. Comparison of kiss-and-run exocytosis and full fusion (Burgoyne and Morgan 2003). *Membrane fusion initially occurs by the formation of a fusion pore. Fusion pore expansion allows release of granule content. This can be limited by rapid re-closure of the fusion pore (kiss-and-run). Alternatively, full emptying of the granule can be followed by a retrieval mechanism involving dynamin and clathrin.*

The SNARE fusion hypothesis is, however, not accepted by all scientists, since SNAREs could only be responsible for membrane merging with fusion being executed by other proteins (Jahn and Grubmuller 2002). Support for the latter came from (a) the identification of several proteins, which operate downstream of SNAREs, such as protein phosphatase I, calmodulin, the V_0 subunit of the vacuolar ATPase and Vac8 as well as (b) observations showing that SNAREs appear to be expendable for fusion (Jahn and Grubmuller 2002).

Fusion pores also seem to be influenced by calcium levels. In PC12 cells, overexpression of syt I prolonged the lifetime of the fusion pore, whereas syt IV shortened this time. Later studies performed in eosinophils indicated that initial fusion pore formation does not depend on the intracellular calcium concentration, but that the rate of fusion pore expansion is regulated by the intracellular calcium concentration. A role for activation of PKC was also shown to influence pore expansion (Lindau and deToledo 2003).

In biological systems, the tight coupling between exocytosis and endocytosis must always be considered. Rapid endocytosis is often considered equivalent to kiss-and-run, although direct evidence is usually not available. This was shown in PC12 cells where membrane sheets revealed that ~30% of exocytosed vesicles were recaptured. The recapturing was not simple fusion pore flickering, but involved dynamin, indicating a tight coupling between exo- and endocytosis (Lindau and deToledo 2003).

1.4. PROTEIN-PROTEIN INTERACTIONS: A TARGET FOR THERAPY?

Protein trafficking and secretion, similar to various other cell processes, occur via protein-protein interactions. Proteins interact in complicated ways because of the complexity of their 3-dimensional structures. Amino acid side chains that are exposed on the surface of the molecule create pits or bumps of different shapes and sizes, which are then exploited by proteins producing binding pockets and recognition sites with varying degrees of specificity and subtlety of interaction. It is this versatility of protein-protein interactions that makes them such a tempting prospect to exploit in the search for new drugs (Buckingham 2004).

Apart from being promising, targeting protein-protein interactions present serious obstacles such as the range of concentrations over which proteins might interact. Affinities between proteins can vary depending on the cellular function and the immediate chemical environment, especially the pH and calcium concentration. Peptides and small molecules used for disrupting protein interactions must also be able to reach the inside of the cell as well as the site of interaction.

To date, two methods have proven successful in identifying new targets for disrupting protein- protein interactions. Dale Boger at the Scripps Research Institute, San Diego, was the first to be successful in using peptidomimetics, i.e. short, synthesized peptide fragments that mimic the most common motifs such as α-helix or β-sheet (Buckingham 2004). He used a technique called solution-phase combinatorial chemistry to generate a library of some 40,000 variants of these peptidomimetics and was successful in identifying a compound that blocks the interactions between integrin ($\alpha_v\beta_3$) and MMP2, two proteins that initiate angiogenesis in tumors. This compound was found to interfere with the site that controls the localization of MMP2 within the cell (Buckingham 2004).

An alternative approach to combinatorial chemistry is to screen a number of small organic compounds, called fragments, in order to identify the ones that bind to the protein of interest (Buckingham 2004). These small molecules can either bind directly to the site of interaction, or can allosterically induce conformational changes that hides the desired domain (Dev 2004). The fragments can be screened using nuclear magnetic resonance, or by an ingenious technique called 'tethering' which was pioneered by Jim Wells from Sunesis Pharmaceuticals (Buckingham 2004). Tethering commences by engineering the target protein with a cysteine mutation near a known interaction site. The protein is then probed

with test fragments containing disulphide bonds. When a fragment hits the target area, it becomes chemically bonded to the cysteine and can subsequently be identified using mass spectroscopy. The main advantage of this approach is that it starts with an enriched source of lead compounds, themselves good starting points because they are less hydrophobic and are therefore likely to be good building blocks for drugs. To date the group of Wells was successful in identifying two sub-sites on the interleukin receptor, IL-2, a rigid one and a more flexible one, of which the latter proved more effective in binding the fragment (Buckingham 2004).

SNARE proteins, which are involved in exocytosis, have been extensively investigated for the identification of new therapeutics because of the implication of neuro-secretion in the pathogenesis of several human neurological disorders (Blanes-Mira *et al.* 2003). Thus far, clostridial neurotoxins and peptides patterned after the protein domains of SNAREs have been the only molecules able to modulate the assembly and stability of the core complex (Apland *et al.* 2003; Blanes-Mira *et al.* 2003). One such an example is that of small peptides patterned after the N-terminal domain of SNAP25 (Figures 1.11 and 1.12). Two peptides, which are identical to the N-terminal of native SNAP25, SNAP25_N1 (residues 1-21) and SNAP25_N2 (residues 22-44), inhibited 25% and 50% of complex formation, respectively. Mechanistically, the peptides act by disrupting the interaction of the parental protein (SNAP25) with syntaxin (Figure 1.11). By using another peptide SNAP_N4, which resemble the core of peptide SNAP25_N2 (residues 26-28) it was shown that the SNAP25_N4 peptide can establish up to seven interactions with syntaxin and the SNAP25 C-terminal. As shown in Figure 1.11, residue 30Arg on the peptide forms a salt bridge with 145 Glu on the C-terminal of SNAP25, while 31Arg and 28Ser interact with 206Glu on syntaxin. Furthermore, 36Glu on SNAP25_N4 pairs with 213His on syntaxin. In addition of these interacting pairs, several hydrophobic interactions notably contribute to peptide binding (Inset, Figure 1.11). *In vivo*, these were found to inhibit SNARE complex assembly, regulate inhibited calcium-dependent exocytosis from excitable cells and are able to translocate through the plasma membrane of intact cells (Blanes-Mira *et al.* 2004).
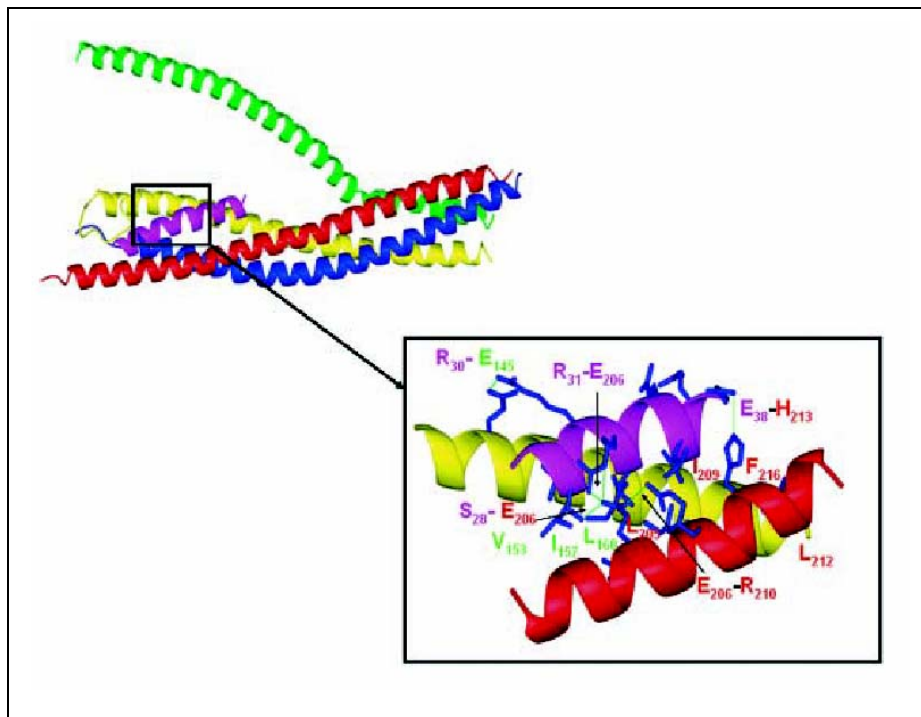
Figure 1.11. Structural model illustrating the putative binding site of peptides SNAP25_N2 on the SNARE complex (Blanes-Mira *et al.* 2004). *(Top) Putative interaction of SNAP25_N2 peptide (residues 22-44) on the SNARE complex preventing the interaction of the N-terminus domain of SNAP25. (Bottom) Enlargement showing the interactions of peptide SNAP25_N4 (residues 26-38) with syntaxin (red), the C-terminus of SNAP25 (yellow) and VAMP (blue). Peptide is shown in magenta. Interactions are highlighted.*

The group of Ferrer-Montiel has recently provided the first description of peptides with sequences unrelated to the SNARE proteins that are capable of inhibiting the assembly of the core complex. They were able to identify SNARE modulators that inhibit exocytosis from an α-helix constrained, mixture-based, 17-mer combinatorial peptide library composed of 137 180 sequences (Blanes-Mira *et al.* 2003). By screening the peptides for their ability to prevent the formation of the SDS-resistant SNARE core complex, eight peptides were identified. The most potent 17-mer peptide (acetyl-SAAEAFAKLYAEAFAKG-NH$_2$, Figure 1.12.A) abolished both calcium-evoked catecholamine secretion from chromaffin cells and L-glutamate release from hippocampal primary cultures (syntaxin, SNAP25, VAMP). The structures are shown in Figure 1.12.
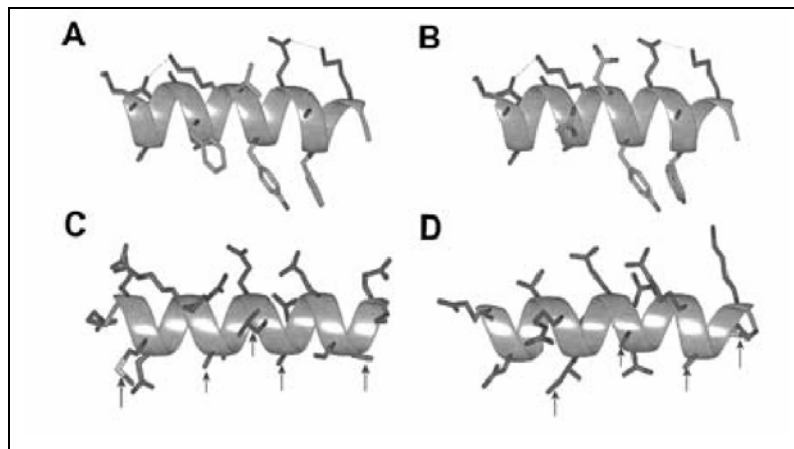
Figure 1.12. α-Helical models of peptides identified from an α-helical constrained combinatorial peptide library (Blanes-Mira *et al.* 2003). *Models are shown for the most (SAAEAFAKLYAEAFAKG; A) and least SAAEAEAKQYAEAWAKG; (B) active peptides for inhibition of SNARE complex formation, and for peptides patterned after the N-terminus (EEMQRRADQLADESLES; C) and C-terminus (DSNKTRIDEANQRATKM; D) of SNAP25. The helical structure for SNAP25 peptides was obtained from the three-dimensional structure of SNAP25 in the SNARE complex. Arrows indicate hydrophobic residues involved in core coiled-coil interactions in the SNARE complex.*

Another novel set of fusion peptides, which inhibits activity of the NSF ATPase and blocks exocytosis, has been described by Matsushita *et al*. (Matsushita *et al.* 2005). These NSF inhibitors are fusion polypeptides composed of an 11 amino acid HIV TAT domain fused to a 22 amino acid NSF domain. These TAT-NSF fusion polypeptides cross endothelial cell membranes, inhibit NSF hydrolysis of ATP, decrease NSF disassembly of the SNARE complex, and block exocytosis (Matsushita *et al.* 2005).

Excitingly, known drugs are being re-investigated to determine their mode of action. In some cases, they are only now being linked to SNARE proteins. One such an example is the anti-epileptic drugs carbamazepine (CBX) and zonisamide (ZNS). Recent findings indicate that in neuronal cells they reduce P-type voltage-gated calcium channel/synaptobrevin-related exocytosis mechanisms during the depolarization stages, and simultaneously enhance N-type voltage-gated calcium channel/syntaxin-related exocytosis mechanisms at the resting stage (Okada *et al.* 2002).

Taking into account the advances in this field during the past few years, targeting protein-protein interactions in order to inhibit exocytosis, seems feasible. If one can identify and study the proteins and their interacting partners regulating exocytosis in the salivary glands of ticks, it would be possible to design or screen for an anti-tick feeding compound.

1.5. AIMS OF THIS THESIS

By understanding the mechanism of exocytosis in tick salivary glands, the various pathways and compounds regulating the process can be used for the rational design of an anti-tick feeding drug or vaccine. In the long run, successful disruption of exocytosis can inhibit tick feeding (hence the lifecycle of ticks) and possibly also affect pathogen transmission.

During this study we investigated the signaling pathways, as well as the proteins involved in regulated exocytosis of protein from large dense core granules from the salivary glands of *O. savignyi*. Since significant information is available regarding the signaling pathways of ixodid ticks, we compared the mechanism to that found in the argasid tick, *O. savignyi*.

Furthermore, since SNAREs and their binding partners have been implicated in controlling regulated exocytosis, we used molecular biological tools as well as methods exploiting protein-protein interactions, in order to identify homologous partners in *O. savignyi*. Antibodies (Chapter 3), degenerative primers (Chapter 3), the yeast two-hybrid system (Chapter 4), functional complementation in yeast (Chapter 5) and affinity chromatography with recombinant SNAREs (Chapter 5) were used.

1.6. REFERENCES

Apland, J.P., Adler, M., Oyler, G.A. (2003). Inhibition of neurotransmitter release by peptides that mimic the N-terminal domain of SNAP-25. *Journal of Protein Chemistry* **22**(2): 147-53.

Bajjalieh, S.M., Scheller, R.H. (1995). The biochemistry of neurotransmitter secretion. *The Journal of Biological Chemistry* **270**: 1971-1974.

Blanes-Mira, C., Merino, J.M., Valera, E., Fernandez-Ballester, G., Gutierrez, L.M., Viniegra, S., Perez-Paya, E., Ferrer-Montiel, A. (2004). Small peptides patterned after the N-terminus of SNAP25 inhibit SNARE complex assembly and regulate exocytosis. *Journal of Neurochemistry* **88**: 124-135.

Blanes-Mira, C., Pastor, M.T., Valera, E., Fernandez-Ballester, G., Merino, J.M., Gutierrez, L.M., Perez-Paya, E., Ferrer-Montiel, A. (2003). Identification of SNARE modulators that inhibit exocytosis from an alpha-helix constrained combinatorial library. *Biochemical Journal* **375**: 159-166.

Blazquez, M., Thiele, C., Huttner, W.B., Docherty, K., Shennan, K.I. (2000). Involvement of the membrane lipid bilayer in sorting prohormone convertase 2 into the regulated secretory pathway. *Biochemical Journal* **349**: 843-852.

Buckingham, S. (2004). Picking the pockets of protein-protein interactions. *Nature, Horizon Symposia: Charting chemical space.*(April): 1-4.

Burgoyne, R.D., Morgan, A. (2003). Secretory granule exocytosis. *Physiology Reviews* **83**: 581-632.

Dev, K.K. (2004). Making protein interactions druggable: Targeting PDZ domains. *Nature Reviews Drug Discovery* **3**: 1047-1056.

Dhanvantari, S., Loh, Y.P. (2000). Lipid raft association of carboxypeptidase E is necessary for its function as a regulated secretory pathway sorting receptor. *The Journal of Biological Chemistry* **275**: 29887-29893.

Dittie, A.S., Klumperman, J., Tooze, S.A. (1999). Differential distribution of mannose-6-phosphate receptors and furin in immature secretory granules. *Journal of Cell Science* **112**(Pt22): 3955-3966.

Eaton, B., A., Haugwitz, M., Lau, D., Moore, H.P. (2000). Biogenesis of regulated exocytotic carriers in neuroendocrine cells. *Journal of Neuroscience* **20**(19): 7334-7344.

Gaspar, A.R.M.D., Joubert, A.M., Crause, J.C., Neitz, A.W.H. (1996). Isolation and characterization of an anticoagulant from the salivary glands of the tick, *Ornithodoros savignyi* (Acari: Argasidae). *Experimental and Applied Acaralogy* **20**: 583-598.

Howell, C.J. (1966). Studies on karyotypes of South African Argasidae. 1. *Ornithodoros savignyi* Audouin (1827). *Onderstepoort Journal of Veterinary Research* **33**: 93-98.

Howell, C.J., Neitz, A.W.H., Potgieter, D.J.J. (1975). Some toxic and chemical properties of the oral secretion of the sand tampan, *Ornithodoros savignyi* Audouin (1825). *Onderstepoort Journal of Veterinary Research* **43**: 99-102.

Jahn, R., Grubmuller, H. (2002). Membrane fusion. *Current Opinion in Cell Biology* **14**: 488-495.

Joubert, A.M., Louw, A.I., Joubert, F., Neitz, A.W.H. (1998). Cloning, nucleotide sequence and expression of the gene encoding factor Xa inhibitor from the salivary glands of the tick, *Ornithodoros savignyi*. *Experimental and Applied Acarology* **22**: 603-619.

Karczewski, J., Endris, R., Connolly, T.M. (1994). Disagregin is a fibrinogen receptor antagonist lacking the Arg-Gly-Asp sequence from the tick, *Ornithodoros moubata*. *The Journal of Biological Chemistry* **269**(6702-6708).

Karczewski, J., Waxman, L., Endris, R., Connolly, T.M. (1995). An inhibitor from the argasid tick *Ornithodoros moubata* of cell adhesion to collagen. *Biochemical and Biophysical Research Communications* **208**(532-541).

Klenchin, V.A., Martin, T.F.J. (2000). Priming in exocytosis: Attaining fusion-competence after vesicle docking. *Biochimie* **82**: 399-407.

Klumperman, J., Kuliawat, R., Griffith, J.M., Geuze, H.J., Arvan, P. (1998). Mannose-6-phsophate receptors are sorted from immature secretory granules via adaptor protein AP-1, clathrin, and syntaxin 6 positive vesicles. *Journal of Cell Biology* **141**(2): 359-371.

Lindau, M., deToledo, G.A. (2003). The fusion pore. *Biochimica et Biophysica Acta* **1641**: 167-173.

Lipschutz, J.H., Mostov, K.E. (2002). Exocytosis: The many masters of the Exocyst. *Current Biology* **12**: R212-214.

Mans, B.J. (2002a). Functional perspectives on the evolution of argasid tick salivary gland protein superfamilies. *Biochemistry*. Pretoria, University of Pretoria.

Mans, B.J., Louw, A.I., Gaspar, A.R.M.D., Neitz, A.W.H. (1998). Apyrase activity and platelet aggregation inhibitors in the tick *Ornithodoros savignyi*. *Experimental and Applied Acaralogy* **22**: 353-366.

Mans, B.J., Louw, A.I., Neitz, A.W.H. (2002b). Savignygrin, a platelet aggregation inhibitor from the soft tick, *Ornithodoros savignyi*, presents the RGD integrin recognition motif on the Kunitz-BPTI fold. *The Journal of Biological Chemistry* **277**(24): 21371-21378.

Mans, B.J., Steinmann, C.M., Venter, J.D., Louw, A.I., Neitz, A.W.H. (2002c). Pathogenic mechanisms of sand tampan toxicoses induced by the tick, *Ornithodoros savignyi*. *Toxicon* **40**: 1007-1016.

Maritz, C., Louw, A.I., Gothe, R., Neitz, A.W.H. (2000). Detection and micro-scale isolation of a low molecular mass paralysis toxin from the tick, *Argas (Persicargas) walkerae*. *Experimental and Applied Acaralogy* **24**: 615-630.

Maritz, C., Louw, A.I., Gothe, R., Neitz, A.W.H. (2001). Neuropathogenic properties of *Argas (Persigarcas) walkerae* larval homogenates. *Comparative Biochemistry and Physiology A* **128**: 233-239.

Martin, T.F.J. (2003). Tuning exocytosis for speed: fast and slow modes. *Biochimica et Biophysica Acta* **1641**: 157-165.

Matsushita, K., Morrell, C.N., Lowenstein, C.J. (2005). A novel class of fusion polypeptides inhibits exocytosis. *Molecular Pharmacology* **67**(4): 1137-44.

Nienaber, J., Gaspar, A.R.M.D., Neitz, A.W.H. (1999). Savignin, a potent thrombin inhibitor isolated from the salivary glands of the tick, *Ornithodoros savignyi* (Acari: Argasidae). *Experimental Parasitology* **93**(82-91).

Okada, M., Zhu, G., Yoshida, S., Kanai, K., Hirose, S., Kaneko, S. (2002). Exocytosis mechanism as a new targeting site for mechanisms of action of antiepileptic drugs. *Life Sciences* **72**: 465-473.

Palmer, D.J., Christie, D.L. (1992). Identification of molecular aggregates containing glycoporteins III, J, K (carboxypeptidase H) and H (Kex2-related proteases) in the soluble and membrane fractions of adrenal medullary chormaffin cells. *The Journal of Biological Chemistry* **267**: 19806-19812.

Paton, W.S., Evans, G.O. (1929). *Insects, ticks, mites and venomous animals of medical and veterinary importance. Part I.* Croydon. Great Britian.

Ribeiro, J.M.C., Endris, T.M., Endris, R. (1991). Saliva of the soft tick *Ornithodoros moubata* contains anti-platelet and apyrase activity. *Comparative Biochemistry and Physiology* **100A**: 109-112.

Sollner, T., Whiteheart, S.W., Brunner, M., Erdjument-Bromage, H., Geromanos, S., Tempst, P., Rothman, J.E. (1993). SNAP receptors implicated in vesicle targeting and fusion. *Nature* **362**: 318-324.

Sonenshine, D.E. (1991). *Biology of ticks*. New York, Oxford, Oxford University Press.

Tooze, S.A., Martens, G.J.M., Huttner, W.B. (2001). Secretory granule biogenesis: Rafting to the SNARE. *Trends in Cell Biology* **11**(3): 116-122.

Ungar, D., Hughson, F.M. (2003). SNARE protein structure and function. *Annual Reviews in Cell Developmental Biology* **19**: 493-517.

van de Locht, A., Stubbs, M.T., Bode, W., Friedrich, T., Bollschweiler, C., Hoffken, W., Huber, R. (1996). The ornithodorin-thrombin crystal structure, a key to the TAP enigma? *EMBO Journal* **15**: 6011-6017.

Viljoen, G.J., van Wyngaardt, S., Gothe, R., Visser, L., Bezuidenhout, J.D., Neitz, A.W.H. (1990). The detection and isolation of a paralysis toxin present in *Argas (Persicargas) walkerae*. *Onderstepoort Journal of Veterinary Science* **57**: 163-168.

Wang, Y., Thiele, C., Huttner, W.B. (2000). Cholesterol is required for the formation of regulated and constitutive secretory vesicles from the trans-Golgi network. *Traffic* **1**(12): 952-962.

Waxman, L., Connolly, T.M. (1993). Isolation of an inhibitor selective for collagen-stimulated platelet aggregation from the soft tick *Ornithodoros moubata*. *The Journal of Biological Chemistry* **268**(5445-5449).

Waxman, L., Smith, D.E., Arcuri, K.E., Vlasuk, G.P. (1990). Tick anticoagulant peptide (TAP) is a novel inhibitor of blood coagulation factor Xa. *Science* **248**: 593-596.

Whyte, J.R.C., Munro, S. (2002). Vesicle tethering complexes in membrane traffic. *Journal of Cell Science* **115**: 2627-2637.

CHAPTER 2

SIGNALING PATHWAYS REGULATING PROTEIN SECRETION FROM THE SALIVARY GLANDS OF UNFED FEMALE *Ornithodoros savignyi*

2.1. INTRODUCTION

2.1.1. General anatomy of tick salivary glands

The salivary glands are the largest glands in the tick's body. They are complex, heterogeneous organs. In both argasid and ixodid ticks, the salivary glands consist of a pair of grape-like clusters of acini (alveoli) comprising 2 major types, the agranular and granular acini (Sonenshine 1991). A myo-epithelial sheath surrounds the salivary glands of argasid ticks, while it is absent in ixodid ticks (Figure 2.1). The salivary glands surround the paired salivary ducts, which extend through the basis capituli and open into the salivarium (Sonenshine 1991). It is via these ducts that tick saliva gets secreted into the host's bloodstream and allow for successful feeding.
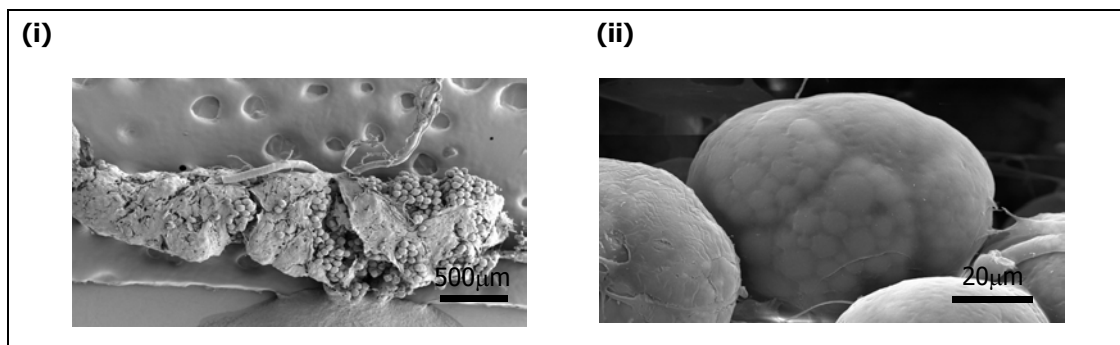
Figure 2.1. SEM analysis of salivary glands from *O. savignyi (Mans 2002a)*. *(i) An intact salivary gland with the myo-epithelial sheath visible, as well as single acini (40-70 μM diameter). Scale bar = 500 μm. (ii) An acini at high electron voltage (30 keV) show the packing of the salivary gland granules through the cell membrane. Scale bar = 20 μm.*

The organization of the salivary glands of ixodid ticks has been best described for the adult female *Rhipicephalus appendiculatus*. In these glands, there are about 1400 acini of three types (I, II, III) in contrast with the 1350 acini of four types (I, II, III, IV) found in males (Sauer and Hair 1986). In both the ixodid and argasid ticks, the agranular acini (type I) occur near the anterior end of the gland and are located adjacent to the main salivary duct. These acini open directly into the main duct. In contrast, the granular types II, III and IV

acini occur more posteriorly and comprise grape-like clusters surrounding secondary ducts that ramify among lobes. Most of the granular acini open into secondary ducts (Sonenshine 1991). The most important features of these acini are summarized in Table 2.1.

Table 2.1. General features of female ixodid tick salivary gland acini ((Sonenshine 1991).

Acini Type	Function	Location in acinus
I (Agranular)	Osmoregulation	Along the main duct
II (Granular)	Secretion (Granule containing)	Arranged radially around a small lumen
III (Granular)	Secretion (Granule containing)	Terminal branches of the duct at the periphery of the gland

Type I acini consist of a single central cell and a number of peripheral cells, also called the pyramidal cells. Both of these cell types contain an abundance of mitochondria, an inconspicuous Golgi complex, and little or no endoplasmic reticulum. The cytoplasm is poor in ribosomes but contains widely dispersed α and β particles of glycogen. No granules are present but small dense lysosome-like bodies and lipid droplets of various sizes are common. This acinus has been reported to show little change in structure during tick feeding. Support for their function in osmoregulation came from studies by Needham and Coons who indicated significant differences in acini I between dehydrated and rehydrated ticks (Sauer and Hair 1986).

Type II acini contain a bewildering diversity of glandular cell types. Binnington has designated these in 1978 as a, b, c_1, c_2, c_3 and c_4 in the tick *Boophilus microplus* (Sauer and Hair 1986). Their identification at light microscope level was largely based upon size, staining properties and histochemical reactions of their secretory granules. In 1983, Binnington reported that the gland of *R. appendiculatus* was similar to that of *Boophilus* with 6 granular cell types in acinus II (Sauer and Hair 1986). The most important features of these 6 cell types are summarized in Table 2.2.

Type III acini are the best studied, since they are the site of sporogony of *Theileria parva*, the protozoan parasite that causes African East Coast fever. The acinus contains three glandular cell types (d, e and f), and their characteristics are summarized in Table 2.3.

Table 2.2. General features of the cell types found in the type II acinus of the ixodid tick, *R. appendiculatus* (Sauer and Hair 1986).

Cell type	Granule characteristics	Location
a	- Large compound granules visible with light microscope - Large membrane-bound secretory granules (3 μm) with round subunits (0.5 μm) - Subunits are pale and matrix darker - Stain negative with PAS for carbohydrates - Secrete a component of the cement	Hilus of acinus
b	- Stain intensely with PAS - Large secretory granules (up to 2 μm) - Granules exhibit inhomogeneity	Adjacent to a-cell
C_1	- Small, PAS positive granules (up to 0.75 μm) - Affinity for basic dyes - Exhibit most esterase activity in acinus - Lowest density of c-series during electron microscopy - Hypertrophy in course of feeding - May have a very large nucleus with multiple nucleoli	Fundus of acinus
C_2	- Large secretory granules (up to 2 μm) - Pale pink PAS staining reaction - Granules are homogenous and moderately dense	Polar or equatorial region of acinus, adjacent to an a-cell.
C_3	- Granules are smaller than C_2 (up to 1.7 μm) - Stain more intense with PAS - Smooth-contoured and more dense than c2-granules	
C_4	- Small granules (0.75 - 1 μm) - Stain intensely with PAS - Electron dense	Interspersed among C_1-cells at the fundus of the acinus

Table 2.3. General features of the cell types found in the type III acinus of ixodid ticks (Sauer and Hair 1986).

Cell type	Granule characteristics	Location
d	- Secretory granules (up to 3 μm) with large subunits - Density of subunits are inconsistent - Secretory product accumulates during questing. In unfed ticks large numbers of granules are found throughout the cell. - Cytoplasma is rich in mitochondria and narrow cisternal profiles of endoplasmic reticulum. - Golgi is rarely observed - Secrete cement at onset of feeding - Little evidence of continuing synthetic activity during feeding	Around hilus of acinus
e	- Largest granules (4 μm) in the gland - Endoplasmic reticulum cisternae occupy most of cytoplasma - Granules are of low density and composed of closely packed subunits (60 - 100 nm) - Also contain denser granules (100-150 nm diameter) scattered around in cytoplasma - Secrete during feeding and the cells remain active and provide an opportunity to study the role of the organelles in the formation of secretory granules.	Dominant cell type in type III acinus
f	In unfed ticks: - These cells are slender and undifferentiated - Cytoplasm is rich in ribosomes - Few membranous organelles present - No secretory granules are present In feeding ticks: - Cells rapidly enlarge - Differentiate into typical glyco-protein secretory cells - Extensive endoplasmic reticulum becomes visible - Prominent Golgi complex forming dense secretory granules are evident - Only active secretion for 2 days before protein synthesis machinery is dismantled by autophagy. After autophagy: - Body of each f-cell is surrounded by an intricate filigree of slender cell processes forming the ablumenal portion of a very elaborate basal labyrinth. - The ablumenal interstitial cells hypertrophy and undergo proliferation of their mitochondria. They increase in size and elongate, extending towards the periphery of the acinus. - Both the f-cells and the ablumenal interstitial cells terminate in contact with the membrane. - The glandular epithelium of acinus III has thus been converted to an epithelium of unparalleled complexity specialized for fluid transport.	Clustered at the fundus of acinus III

Classical studies performed in 1972 by Roshdy on the glands of *Argas persicus* indicated that at least three granular cell types (a, b and c) are present in the salivary glands of argasid ticks (Roshdy 1972). Roshdy and Coons confirmed this data in 1975 during ultra-structural studies of the salivary glands of *Argas arboreus* (Roshdy and Coons 1975). El Shoura

described similar granular types in 1985 during ultra-structural studies of the salivary glands of *Ornithodoros moubata* (El Shoura 1985).

During recent studies on the argasid tick *Ornithodoros savignyi* four cell types was described (Mans 2002a). Cell type 'a' contains dense core granules (diameter 3 - 5 μm), which stains positive for the proteins apyrase and savignygrin (Figure 2.2.i). The granular content of these cells are released during feeding. Type 'b' cells contain homogenous granules (diameter 4 – 10 μm), which could be immature precursors of the dense core granules. These granules also stained positive for apyrase and savignygrin (Figure 2.2.ii). Type 'c' cells contain smaller granules (diameter 1 – 2 μm) with electron lucent cores. They stained positive for carbohydrates during the Thiery test. Finally, a fourth cell type (d) was described. These cells have a similar morphology and histochemical basis as type b-cells but stained negative for savignygrin.
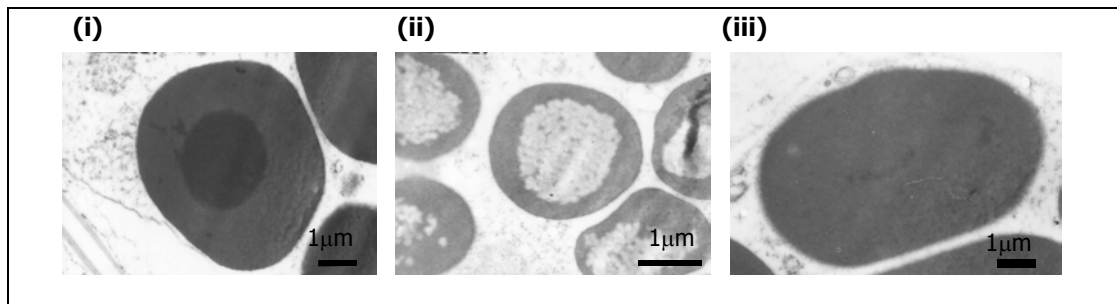
Figure 2.2. TEM micrographs of the granules of type II granular alveoli (Mans 2002a). *(i) Type a cell granules consist of a peripheral carbohydrate region and a dense protein core. (ii) Type b cells are composed of a dense, finely textured material that stains positively for polysaccharides, while the granules show a negative reaction for protein. (iii) Type C cell granules possess electron-dense and electron-lucent zones.*

During feeding of *O. savignyi*, it could be shown that all cells that displayed granule release retained several granules. Also organelles such as mitochondria not previously observed in these cells became prominent. After feeding, the glands resumed the general morphology observed for unfed ticks within one day, except for a dilated lumen that was still visible (Mans 2002a).

2.1.2. Extracellular stimuli

The group of Schmidt, Essenberg and Sauer described the first evidence for neuronal control of fluid secretion from tick salivary glands in 1981, when a D_1-type dopamine receptor was identified in *Amblyomma americanum* (Schmidt *et al.* 1981). To date, 5 types of dopamine

receptors are known (Table 2.4) (Watling 2001). The D_1-dopamine receptor is known as a stimulating G-protein (G_s) that is associated with the activation of adenylyl cyclase (AC) and causes elevated levels of intracellular cAMP upon binding of its ligand, dopamine.

Table 2.4: Structural classification of dopamine receptors (Watling 2001).

Type	D_1	D_2	D_3	D_4	D_5
Structural Information	446 aa (human)	Short: 414 aa (human) Long: 443 aa (human)	400 aa (human)	386 aa (rat)	477 aa (human)
Family	D1	D2	D2-like family	D2-like family	D1-like family
Mechanism	**Gs** Increase cAMP	**Gi** cAMP modulation **Gq/11** Increase IP_3 / DAG	**Gi** cAMP modulation	**Gi** - cAMP modulation - ↑ Arachidonic acid release - Stimulate phospholipid methylation	**Gs** Increase cAMP

Dopamine is a neurotransmitter synthesized from the amino acid tyrosine (Figure 2.3). It is also the substrate for dopamine β-hydroxylase for the synthesis of norepinephrine, which is converted to epinephrine by the enzyme phenylethanolamine N-methyltransferase. AC from the salivary glands of *Amblyomma americanum* is stimulated by several derivatives of phenylethylamine, dopamine, noradrenaline, adrenaline and isoproterenol (a β-adrenergic agonist). Octopamine and L-DOPA have no effect on basal adenylate cyclase activity. Dopamine has the highest potency and the lowest k_a (0.4 μM), followed by adrenaline and noradrenaline (23 μM) and isoproterenol (0.15 mM). The most potent inhibitors of gland AC activity are the dopamine receptor antagonists. The phenothiazine drugs (thioridazine, chlorpromazine and fluphenazine) are more effective than the butyrophenone drug (haloperidol). The k_i for the phenothiazine drugs are 60 nM for thioridazine, 1.9 μM for chlorpromazine and 2.3 μM for fluphenazine. The inhibition of AC activity is specific for the (+) enantiomer of butaclamol (a stereospecific dopamine receptor antagonist), suggesting that the Lone Star tick AC has a D_1 type dopamine receptor (Schmidt *et al.* 1981).
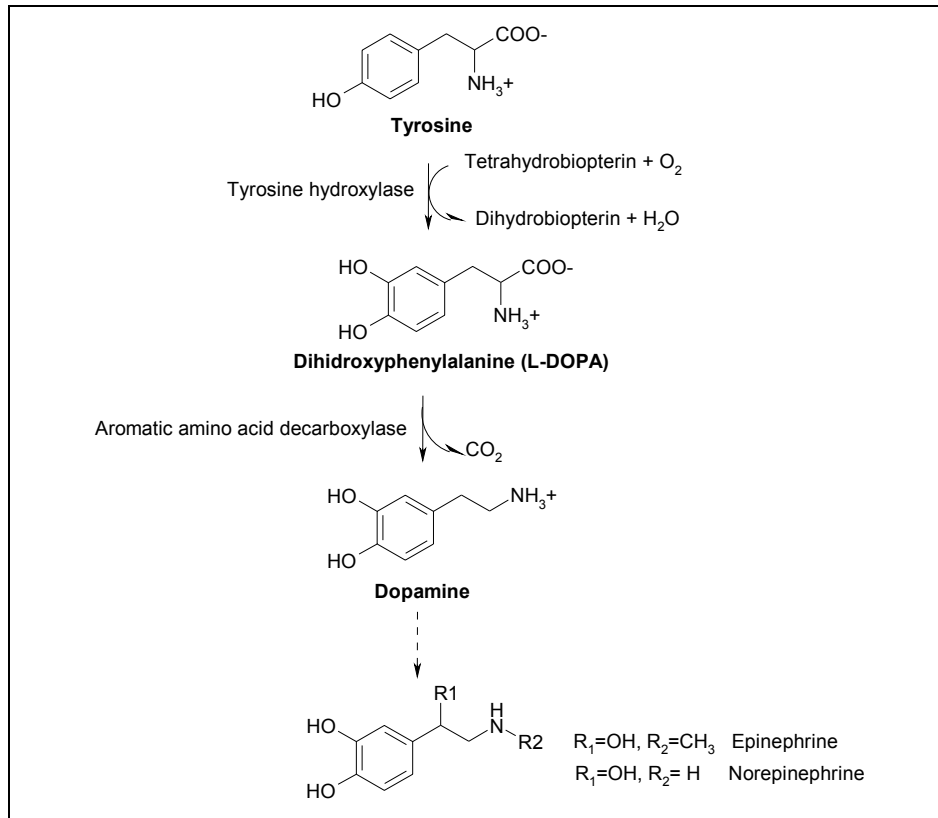
Figure 2.3: Biosynthesis of the physiologically active amines dopamine, epinephrine and norepinephrine (Voet and Voet 1995).

Apart from dopamine, other effectors of signal transduction pathways could also elicit oral secretion from the salivary glands of *A. americanum*. Overall, the volume of oral secretion produced by partially fed ticks in response to the effectors and pharmacological agents varied widely. The volume and rate of oral secretion stimulated by pharmacological agents were: pilocarpine > (dopamine and theophylline) = (dopamine, theophylline and GABA) > (dopamine, theophylline and phorbol 12 myristate 13-acetate; an activator of phospholipase C) (McSwain *et al.* 1992a).

Pilocarpine is often used to induce tick oral secretion, and it is believed to stimulate cholinergic receptors in the tick synganglion, which relay information to nerves innervating the salivary glands. Cholinergic agents fail to stimulate secretion in isolated salivary glands (McSwain *et al.* 1992a). Theophylline, GABA as well as the phorbol esters had no effect when injected individually. Co-injection of the phorbol ester PMA with dopamine and theophylline was inhibitory, indicating an essential role for PKC in eliciting oral secretion.

SDS-PAGE analysis of the secreted proteins showed variable results in response to different agonists. The highest number of proteins was detected from ticks in the earliest stages of feeding. In some ticks, proteins were identified at one collection time but not at another time in secretions from the same tick stimulated by the same agent. One such an example is pilocarpine, which stimulated secretion of different proteins in the same tick after multiple injections. In the case of dopamine, theophylline and GABA, protein secretion was consistent (McSwain *et al.* 1992a).

Other evidence indicates that Ca^{2+} is essential for secretion. Removal of Ca^{2+} from the support medium greatly inhibits dopamine and cAMP-stimulated secretion from isolated salivary glands (McSwain *et al.* 1992a). This is similar to results obtained in salivary duct cells of the cockroach, *Periplaneta americana*. In this study, dopamine evoked a slow and reversible dose-dependent elevation in $[Ca^{2+}]_i$ in salivary duct cells. The dopamine-induced elevation in $[Ca^{2+}]_i$ is absent in Ca^{2+}-free saline and is blocked by La^{3+}, indicating that dopamine induces an influx of Ca^{2+} across the basolateral membrane of the duct cells. Stimulation with dopamine depolarizes the basolateral membrane and is also blocked by 100 μM La^{3+} and abolished when the Na^+ concentration in the solution is reduced from physiological concentrations to 10 mM (Lang and Walz 1999).

GABA, as mentioned before, does not stimulate secretion by itself (McSwain *et al.* 1992a). The enhancing effect of GABA on dopamine-stimulated fluid secretion of isolated salivary glands occurred only at high concentrations (Lindsay and Kaufman 1986). Activation of another receptor by GABA may potentiate secretion by another, but poorly understood, mechanism. A model was proposed and experimentally investigated by Linday and Kaufman in 1996 (Figure 2.4). Their data indicated that GABA and spiperone binds to the same receptor, and that this reaction can be inhibited by sulpiride without diminishing the effect of dopamine. Another receptor, the so-called ergot alkaloid sensitive receptor, which can also be blocked by sulpiride without altering the response to dopamine, was also detected but its function remains unknown. In conclusion, the authors suggested that GABA might play an important neuromodulatory role in salivary fluid secretion (Lindsay and Kaufman 1986). Interestingly, spiperone is also a subtype selective antagonist for the 5-HT$_{1A}$ serotonin receptor, and it has been reported that serotonin, a known agonist of salivary secretion in the insect, *Calliphora erythrocephala*, inhibits basal cyclase activity (Schmidt *et al.* 1981;

Watling 2001). Therefore, the possible inhibitory effect of serotonin on the GABA activated signaling pathway should be investigated.
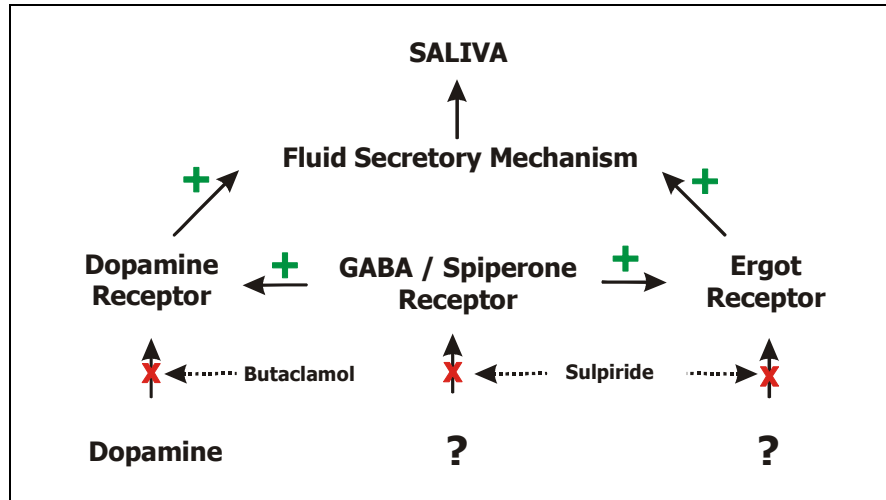
Figure 2.4. A model to demonstrate the receptors involved in salivary fluid secretion in ixodid ticks (Lindsay and Kaufman 1986). *A spiperone receptor in some way modulates the dopamine and ergot alkaloid receptors, resulting in an increased maximum response. Because spiperone has no intrinsic activity, its receptor has no direct link to the fluid secretory mechanism.*

2.1.3. Adenylyl cyclase and cAMP

As mentioned before, it has been demonstrated in ixodid ticks that the dopamine D_1-receptor activates adenylyl cyclase (AC) activity (Schmidt *et al.* 1981). This activation is most likely through the dopamine surface receptor linked via heterotrimeric ($\alpha\beta\gamma$) stimulatory (G_s) guanine nucleotide-dependent regulatory proteins (G proteins). To date, ten distinct adenylyl cyclase isozymes have been identified, and all but one isozyme is activated by $G\alpha_s$. Activation by $G\alpha_s$ occurs through its interaction with the C_2 domain of AC, yielding the active enzyme GTP•α_s•C. Inhibition by G proteins may occur by a direct effect of $G\alpha_I$ with the C_1 domain of AC or by the recombination of $\beta\gamma$ with $G\alpha_s$ (Watling 2001).

A substrate binding cleft is formed between the C_1•C_2 domains upon activation of AC (Watling 2001). The active site catalyzes a cation-dependent attack of the 3'-OH on the α-phosphate of a nucleoside triphosphate (ATP), with pyrophosphate as the leaving group. cAMP subsequently binds to a cAMP-dependent protein kinase (R_2C_2) whose catalytic subunit (C), when activated by the dissociation of the regulatory dimer as R_2•cAMP$_4$, activates various cellular proteins by catalyzing their phosphorylation (Figure 2.5).
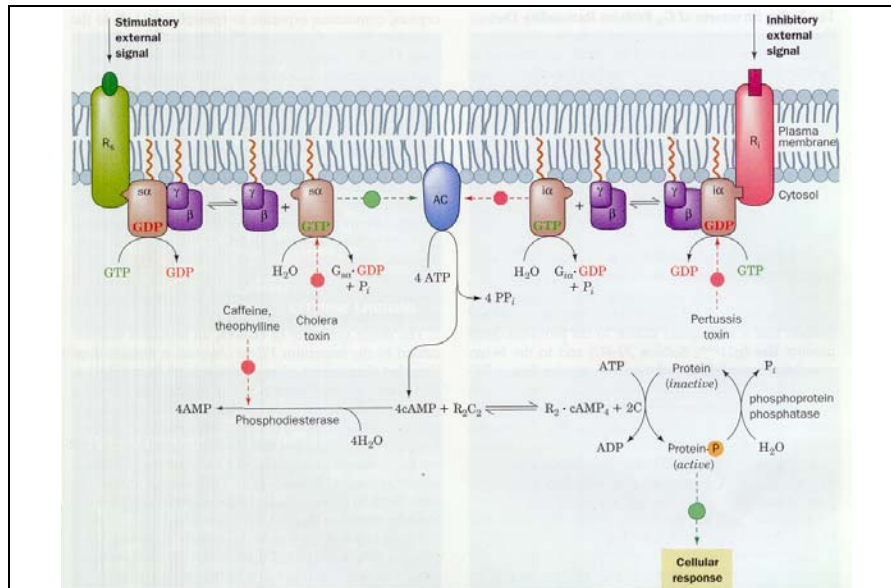
Figure 2.5. The mechanism of receptor-mediated activation / inhibition of adenylyl cyclase (Voet and Voet 1995). *The binding of hormone to a stimulatory receptor (Rs) induces it to bind Gs protein, which in turn stimulates the Gsα subunit of this hetero-trimer to exchange its bound GDP for GTP. The Gsα•GTP complex then dissociates and stimulates adenylyl cyclase to convert ATP to cAMP. Binding of hormone to an inhibitory receptor (Ri) triggers an almost identical chain of events except that the Giα.GTP complex inhibits AC from producing cAMP. R_2C_2 represents a cAMP-dependent protein kinase whose catalytic subunit (C), when activated by dissociation of the R_2•cAMP complex, activates various cellular proteins by means of phosphorylation.*

Studies regarding the cAMP mediated phosphorylation of endogenous proteins in the ixodid tick *A. americanum* indicated 12 proteins. Ten of these were dephosphorylated after dopamine stimulation was attenuated with the dopaminergic antagonists thioridazine and d-butaclamol. The most prominent proteins were those with molecular weights of 62, 47 and 45 kDa. By comparing the proteins phosphorylated upon stimulation with respectively, dopamine and cAMP, 7 proteins (148, 102, 62, 55, 47, 45 and 37 kDa) were identical. Therefore, it could be concluded that a dopamine-sensitive AC is present (McSwain *et al.* 1985). Later studies by Mane *et al* in 1985 and 1987 resulted in the identification of the cAMP-dependent protein kinase, as well as the kinetics of the phosphotransferase reaction of the catalytic subunit of the kinase from the salivary glands of *A. americanum* (Mane *et al.* 1985; Mane 1987).

In most eukaryotes, cAMP-dependent kinases (PKA or cAPK) occur as two enzymes (type I and II). These exist as tetramers (R_2C_2), consisting of two regulatory- and two catalytic subunits (Table 2.5). In the absence of it's activating ligand cAMP, PKA exists as an inactive holoenzyme, which can be anchored to specific compartments via interaction of their

36

regulatory subunits with specific PKA anchoring proteins. Upon binding of four cAMP molecules to the regulatory subunits, the catalytic subunits are released. These then catalyze the transfer of the γ-phosphate of ATP to serine and threonine residues of many cellular proteins containing the –R-R/K-X-S/T consensus sequence. It must be noted that exceptions to this consensus sequence have been observed (Watling 2001).

Table 2.5: Structural classification of Protein kinases A / cAMP-dependent kinases (Watling 2001).

Name	PKA I (RI$_2$C$_2$) and PKA II (RII$_2$C$_2$)		
Structural Information	Tetramer of 2 regulatory (R) and two catalytic (C) subunits		
	RI	**RII**	**C**
	RIα: 381 aa	RIIα: 404 aa	Cα: 351 aa
	RIβ: 381 aa	RIIβ: 418 aa	Cβ: 351 aa
			Cγ: 351 aa
Subcellular localization	Cytoplasm	Cytoskeletal structures, Organelles, membranes	_
Activators	cAMP	cAMP	_

Three isoforms of cAMP-dependent kinase catalytic subunits have been identified in the tick, *A. americanum,* to date (Palmer *et al.* 1999). These are believed to be the product of alternative RNA processing of a single cAPK-C gene. The cDNAs contain unique N-termini of variable lengths, which are linked to a common region containing the αA helix, catalytic core, and a C-terminal tail (Figure 2.6). The common region is highly similar to both insects and vertebrate cAPK-Cs. Although three isoforms have been identified, only a single cAPK isoform (i.e. cAPK-C) is expressed in the salivary glands of both unfed and feeding female ticks (Palmer *et al.* 1999).
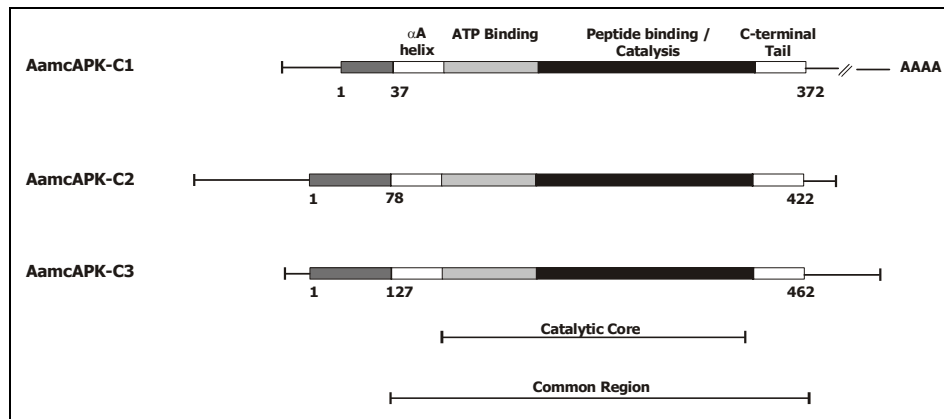
Figure 2.6. Schematic representation of *A. americanum* cAPK-cDNAs and proteins (Palmer *et al.* 1999). *Structure of the three AamcAPK-C cDNAs containing unique 5' termini linked to a common region that includes 1108 bp of open reading frame and the 3' UT sequences. The translated sequences contain unique amino termini of 37, 78 and 127 amino acids that precede a common region containing the catalytic core. Shown above are the αA helix that precedes the catalytic core, the regions involved in ATP binding and peptide binding and catalysis, and the C-terminal tail.*

2.1.4. Prostanoids

Prostanoids were first discovered in the 1930s, when it was shown by Von Euler that semen compounds are able to lower blood pressure in animals (Versteeg *et al.* 1999). Today it is known that prostanoids comprise prostaglandins (PGs), thromboxanes (Txs) and the most recent addition, isoprostanes. The synthesis of prostanoids is shown in Figure 2.7, from which it is evident that synthesis is regulated by the release of the precursor lipid arachidonic acid (AA) from plasma membrane phospholipids. Either cytosolic phospholipase A_2 ($cPLA_2$) or the combined action of phospholipase C, a diglyceride- and a monoglyceride lipase, produces AA (Versteeg *et al.* 1999). Since a cytosolic phospholipase A_2 ($cPLA_2$) is essential for exocytosis from the ixodid tick *A. americanum*, some characteristics of the class is given in Table 2.6.

Upon its release, AA is converted by cyclooxygenase (COX) to PGG_2, and subsequently to PGH_2, which is converted to other prostanoids via a specific prostaglandin synthetase. The isoprostanes are synthesized through non enzymatic conversions of arachidonic acid. Five primary prostanoids are distinguished: PGD_2, PGE_2, PGI_2, $PGF_{2\alpha}$ and TXA_2 with the exact metabolites synthesized dependent on the tissue type and stimulus. For instance, TXs, PGD_2, PGI_2, $PGF_{2\alpha}$ are major metabolites in platelets, mast cells, endothelial cells, and kidney glomerulus cells, respectively. In contrast, a broad range of cell types synthesize PGE_2 (Versteeg *et al.* 1999).

Table 2.6: Structural classification of the phospholipases A$_2$ (Watling 2001).

Group	Secreted / Cytosolic	Molecular Weight (kDa)	Cofactor
IA	Secreted	13-15	mM Ca^{2+}
IB	Secreted	13-15	mM Ca^{2+}
IIA	Secreted	13-15	mM Ca^{2+}
IIB	Secreted	13-15	mM Ca^{2+}
IIC	Secreted	15	mM Ca^{2+}
III	Secreted	16-18	mM Ca^{2+}
IV	Cytosolic	85	μM Ca^{2+}
V	Secreted	14	mM Ca^{2+}
VI	Cytosolic	80-85	None
VII	Secreted	45	None
VIII	Cytosolic	29	None
IX	Secreted	14	< mM Ca^{2+}
X	Secreted	14	mM Ca^{2+}
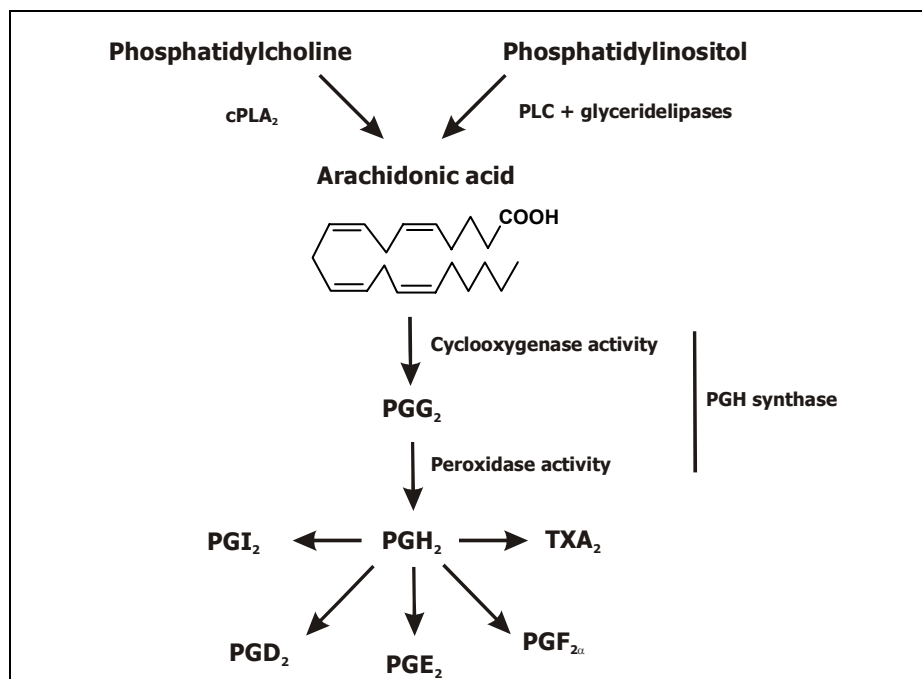
Figure 2.7. Schematic representation of the prostanoid synthesis pathway (Narumiya *et al.* 1999; Versteeg *et al.* 1999). *Either a cytosolic PLA$_2$ (cPLA$_2$) or the combined effect of phospholipase C (PLC) and glyceridelipases releases arachidonic acid from the plasma membrane. The conversion of arachidonic acid to PGG$_2$ and then to PGH$_2$ are catalyzed by PGH synthase and subsequent conversion of PGH$_2$ to each prostaglandin or thromboxane is catalyzed by the specific prostanoid / thromboxane synthase.*

Prostanoids mediate their effect on cells via prostanoid receptors (see Table 2.7). In general these receptors belong to either the superfamily of the G-protein coupled rhodopsin type receptors, or to the superfamily of nuclear steroid/thyroid hormone receptors (Versteeg *et al.* 1999). All prostanoid-induced effects are transduced either through modulation of the activity of adenylyl cyclase or inositol phospholipid hydrolysis and calcium mobilization (Watling 2001).

Table 2.7: Structural classification of prostanoid receptors (Watling 2001).

	EP1	EP2	EP3	EP4
Structural Information	402 aa (human)	358 aa (human)	4 splice variants 390, 388, 365, 374aa (human)	488 aa (human)
Receptor selective prostanoid	PGE_2	PGE_2	PGE_2	PGE_2
Receptor selective antagonists	None	None	None	None
Signal Transduction Mechanisms	$G_{q/11}$ Increase IP_3/DAG	G_s Increase cAMP	$G_{q/11}$ Increase IP_3/DAG G_i cAMP modulation	G_s Increase cAMP
	DP	**FP**	**IP**	**TP**
Structural Information	359 aa (human)	358 aa (human)	386 aa (human)	343 aa (human)
Receptor selective prostanoid	PGD_2	PGF_{2a}	PGI_2	TxA_2
Receptor selective antagonists	Various	None	None	Various
Signal Transduction Mechanisms	G_s Increase cAMP	$G_{q/11}$ Increase IP_3/DAG	G_s Increase cAMP $G_{q/11}$ Increase IP_3/DAG	$G_{q/11}$ Increase IP_3/DAG

Studies regarding changes in the lipid content of the salivary gland of *A. americanum* during feeding indicated that most of the fatty acids were associated with the phospholipids, with the most abundant phospholipids molecules at all feeding stages being phosphatidylcholine (PC) and phosphatidylethanolamine (PE).

During feeding it was found that arachidonic acid (AA, 20:4) levels increased dramatically, up to 40 times. Interestingly, virgin female ticks (which do not increase to more than 40 mg during feeding) had a percentage AA content similar to fed/mated females (250 mg) despite the fact that mating is required for females to acquire a large bloodmeal (Shipley *et al.* 1993). Similar to other organisms, the majority of 20:4 fatty acids (>83%) were found to be stored in cell membranes esterified at glycerol C2 of phospholipids (the diacyl phospholipids subclass). Shipley et al showed in 1994 that [^{3}H]-20:4 were primarily incorporated into the *sn-2* position of diacyl PC > PE, with some incorporation into triglycerides (Shipley 1994). Later, Bowman *et al.* investigated the origin of AA since most arthropods studied to date are able to synthesize AA from dietary linoleic acid (18:2). It was found that ticks have the ability to synthesize mono-unsaturated fatty acids, but not poly-unsaturated fatty acids such as AA, which are sequestered from the host bloodmeal (Bowman 1995a; Sauer *et al.* 2000). This inability to convert linoleate to arachidonate is highly unusual, and has only been described for the domestic cat, rainbow trout and mosquito, *Culex pipiens* (Bowman *et al.* 1995b). Furthermore, when ticks were fed [^{3}H] arachidonic acid, the radioactivity was incorporated solely into the PC and PE phospholipids fraction of the salivary glands (Bowman 1995a).

The next question involved the biosynthesis of salivary prostaglandins from the obtained bloodmeal arachidonic acid. This is important, since prostaglandins are postulated to aid the tick in overcoming hemostasis, inflammatory responses and host immunity. For example, PGE_2 and prostacyclin (PGI_2) can prevent platelet aggregation and cause vasodilation, which maintains a generous supply of blood flowing to the tick during feeding. Furthermore, PGE_2 and PGI_2 also inhibit mast cell degranulation (which minimizes release of inflammatory mediators) and suppress secretion of interleukin-1 and –2, causing inhibition of T-cell clonal expansion (Shipley *et al.* 1993). In 1993, it was described that *A. americanum* possesses a calcium-sensitive PLA_2 which is capable of increasing free AA levels in the SG following calcium ionophore stimulation (Bowman *et al.* 1993). Prostaglandin synthetase (PGS) activity was also detected in dopamine-stimulated glands. PGE_2 was always the major product together with appreciable quantities of $PGF_{2\alpha}$ and PGD_2 (Bowman 1995d). A later study by Pedibhotla *et al.* describes the subcellular localization of prostaglandin H synthase and prostaglandin synthesis in *A. americanum* (Pedibhotla *et al.* 1995).

Since PGS activity could only be detected after dopamine stimulation, the mechanism for regulating the concentration of free AA by dopamine was investigated by Bowman *et al*. It

was found that dopamine was as effective as the calcium ionophore A23187 in stimulating PLA_2 activity. This effect was abolished in the presence of the calcium channel blocking agent, verapamil, and the PLA_2 substrate analogue, oleyloxyethyl phosphorylcholine, in a dose dependent manner. It was concluded that free AA levels are increased through activation of a type IV-like PLA_2 (due to its insensitivity to merthiolate), following an increase of intracellular calcium caused by the opening of a voltage-gated calcium channel upon dopamine stimulation (Bowman 1995c).

In 1997 a specific PGE_2 receptor was identified in the plasma membrane fraction of the salivary glands of *A. americanum*. The receptor exhibited a single, high affinity PGE_2 binding site with a $K_d \sim 29$ nM, which is saturable, reversible, PGE_2 specific and coupled to a cholera toxin sensitive guanine nucleotide regulatory protein (Qian *et al.* 1997). Since PGE_2 was found not to affect adenylyl cyclase activity similar to EP1 and EP3 (see Table 2.7), it was suggested that the PGE_2 receptor stimulates an alternate pathway. Data obtained from using GTPγS strongly suggested that the tick PGE_2 receptor is linked to a G_s-like, rather than a G_i-protein, but later studies indicated that PGE_2 have no effect on plasma membrane adenylyl cyclase activity (Qian *et al.* 1997).

Since PGE_2 receptors in mammals are known to affect either adenylyl cyclase or the mobilization of calcium, the effects of PGE_2 and inositol 1,4,5-triphosphate (IP_3) were investigated. The results of Qian *et al.* indicated that exogenous PGE_2 does not stimulate an influx of calcium, but resulted in significant secretion of anticoagulant protein at concentrations ranging from 1 nM to 1 μM PGE_2. Lower or higher concentrations of PGE_2 had no effect on protein secretion (Qian *et al.* 1998). Protein secretion was also possible using the PGE_2 EP1 receptor antagonist, AH-6809, indicating an EP1-like salivary gland PGE_2 receptor. Upon PGE_2 stimulation, a rise in IP_3 and intracellular calcium (released from microsomes) were observed. Therefore, the authors hypothesized that PGE_2 is both secreted into the saliva and functions as a local hormone by interacting with a PGE_2 receptor to increase IP_3. IP_3 mobilizes intracellular calcium, which is important for regulating exocytosis of salivary gland proteins (McSwain 1992b; Qian *et al.* 1998). This hypothesis was supported by data obtained in 2000 by Yuan *et al*. They were able to show that the effect of PGE_2 can be inhibited by TMB-8, an antagonist of IP_3 receptors (Yuan *et al.* 2000). Also, it was shown that the PGE_2 receptor increases IP_3 levels via activation of a cholera-sensitive G-protein coupled phospholipase C (PLC).

2.1.5. Phospholipase C and intracellular calcium

The hydrolysis of a minor membrane phospholipid, phosphatidyl inositol 4,5-bisphosphate (PIP_2), by a specific PLC is one of the earliest key events in the regulation of various cell functions by more than 100 extracellular signaling molecules. This reaction produces two intracellular messengers, diacylglycerol (DAG) and inositol 1,4,5-triphosphate (IP_3), which mediate the activation of protein kinase C (PKC) and intracellular calcium release, respectively (Figure 2.8).
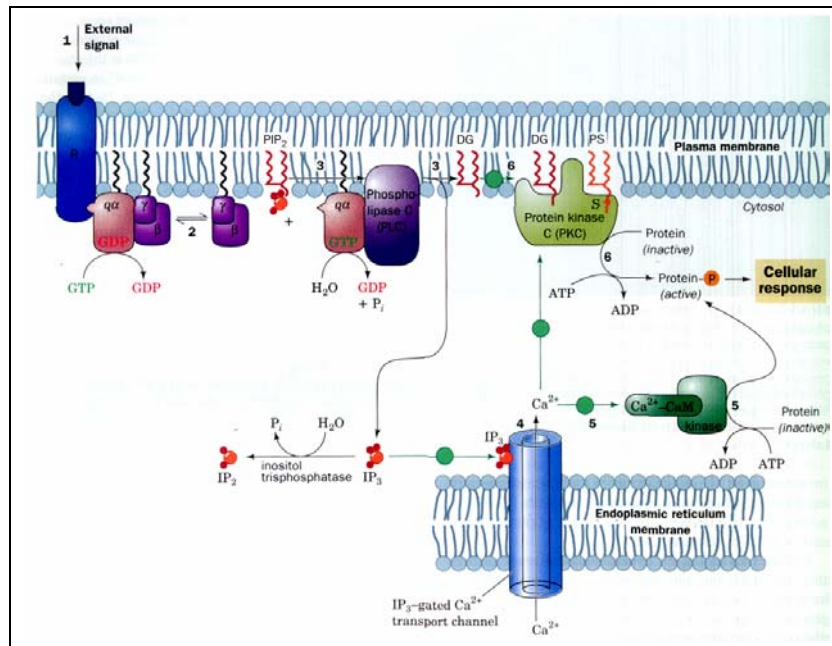
Figure 2.8. A schematic representation of the activation of PLC and the role of PIP_2 in intracellular signaling (Voet and Voet 1995). *Binding of an angonist to a surface receptor activates PLC through a G-protein. In some cases it is via a receptor tyrosine kinase or a non-receptor tyrosine kinase. PLC catalyzes the hydrolysis of PIP_2 to diacylglycerol (DG) and inositol 1,4,5-triphosphate (IP_3). IP_3 stimulates the release of calcium from the endoplasmic reticulum, which in turn activates numerous cellular processes through CaM and its homologues. DG remains membrane associated where it activates PKC (only in the presence of phosphatidylserine and calcium), which in turn phosphorylates numerous cellular proteins.*

A decrease in PIP_2 itself is an important signal because PIP_2 is an activator of phospholipase D and phospholipase A_2, modulates actin polymerization by interacting with various actin-binding proteins, and serves as a membrane attachment site for many signaling proteins that contain pleckstrin (PH) domains. Consequently, the activity of PLC is strictly regulated through several distinct mechanisms that link PLC isoforms to various receptors (Watling 2001).

In *A. americanum*, a trypsin-sensitive factor from tick synganglion was found to stimulate phosphoinositide hydrolysis in tick salivary glands (McSwain *et al.* 1989). Diacylglycerol, the other product of PLC, activates salivary gland protein kinase C (PKC) in the presence of calcium and phosphatidylserine. Activators of PKC, phorbol 12-myristate 13-acetate (PMA) and 1-oleoyl-2-acetyl-sn-glycerol (OAG) did not stimulate fluid secretion and scarcely affected the ability of dopamine to stimulate fluid secretion and intracellular levels of cAMP (McSwain 1992b; Sauer *et al.* 2000).

2.1.6. Current model for the control and mechanism of secretion in ixodid ticks

A current model for the control and mechanism of secretion from the salivary glands of ixodid ticks is depicted in Figure 2.9. Dopamine is released at the neuroeffector junction and interacts with D1-subtype receptor, which is coupled to a stimulatory guanine nucleotide protein (Gs) that activates adenylyl cyclase to synthesize cAMP. In response to cAMP, a cAMP-dependent protein kinase is activated and numerous gland proteins are phosphorylated, e.g. Aquaporin (AQP-5). The latter then translocates to the plasma membrane and is responsible for fluid transport. Dopamine also opens a voltage-gated calcium channel, allowing the influx of extracellular calcium. This influx of calcium stimulates a cytosolic phospholipase A_2 ($cPLA_2$) to liberate free arachidonic acid (AA). AA is then converted into a variety of prostaglandins, including PGE_2, via the cyclooxygenase pathway (COX). High levels of PGE_2 are secreted into the host via saliva. Additionally, PGE_2 also interacts with a EP1-subtype receptor on the same or neighboring cells. Upon activation of the EP1 receptor, PLC is activated by a G-protein and generates diacylglycerol (DAG) and IP_3. The IP_3 interacts with and opens the IP_3-receptor channel in the endoplasmic reticulum releasing calcium into the cytosol. The increased calcium appears to regulate the exocytosis of anticoagulant protein from secretory vesicles into the saliva.
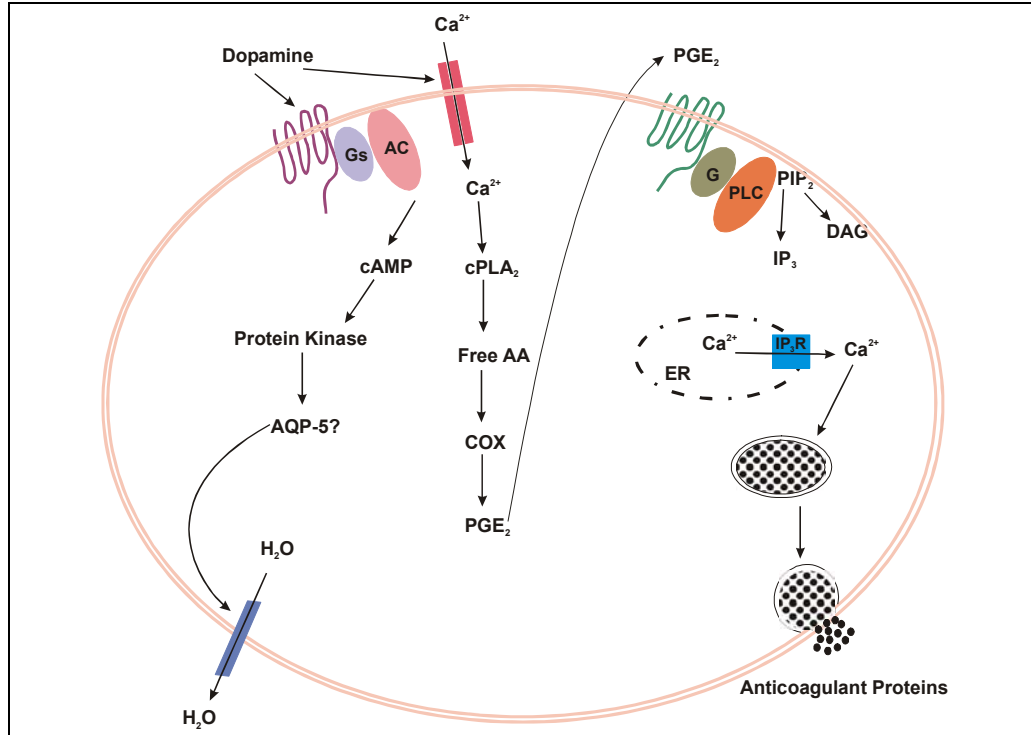
Figure 2.9. Known and hypothesised factors and events controlling secretion in ixodid female salivary glands (Sauer *et al.* 2000). Dopamine released at the neuro-effector junction interacts with a dopamine (D1-subtype) receptor coupled to a stimulatory guanine nucleotide protein (Gs) that activates adenylate cyclase leading to increased levels of cAMP. Numerous gland proteins are phosphorylated by a cAMP-dependent protein kinase. It is speculated that a water channel protein (AQP-5) is phosphorylated, moves to the cell membrane and is responsible for fluid transport observed in dopamine- and cAMP-stimulated glands. Dopamine also opens a voltage-gated Ca^{2+} channel allowing an influx of extracellular Ca^{2+}, thus, increasing intracellular Ca^{2+} levels and stimulating a cytosolic phospholipase A_2 ($cPLA_2$). The free arachidonic acid (AA) liberated by the $cPLA_2$ is converted by the cyclooxygenase pathway (COX) into a variety of prostaglandins, including PGE_2. Additionally, on the same or neighbouring cells, PGE_2 interacts with an EP1-subtype receptor coupled to a guanine nucleotide protein (G) that activates PLC and generates diacylglycerol (DAG) and IP_3. The IP_3 interacts with and opens the IP_3-receptor channel in the endoplasmic reticulum releasing Ca^{2+} into the cytosol. The increased Ca^{2+} appears to regulate the exocytosis of anticoagulant protein from secretory vesicles into the saliva.

2.2. HYPOTHESIS

- The signaling mechanisms involved in controlling protein secretion from ixodid ticks are similar to those involved in the argasid tick, *Ornithodoros savignyi*.

2.3. AIMS

- To compare key molecules involved in the regulated exocytosis of proteins from large dense core granules between ixodid and argasid ticks using various agonists and/or antagonists.

2.4. MATERIALS

Ticks were collected from the North West Province of South Africa by sifting of sand and were kept in sand at room temperature. Dopamine, isoproterenol, carbachol, oleyloxyethyl phosphorylcholine (OPC), digitonin, verapamil, Ouabain, N-ethylmaleimide, anti-phosphoserine, anti-phosphothreonine, phosphatase inhibitor cocktail, Wortmannin, U73122, cytochalasin D, colchicine and HEPES were purchased from Sigma-Aldrich Co. Theophylline was a kind gift from Prof. J. R. Sauer, Oklahoma State University, USA. PGE_2, cAMP, $GTP\gamma S$, ATP, IP_3 and glucose were from ICN (Separations). NaCl, ethylene diamine tetra-acetic acid (EDTA), glycine, ammonium persulphate Tris(hydroxymethyl)aminomethane, N,N,N′,N′-tetramethyl-ethylenediamine (TEMED) and methanol were obtained from Merck, Germany. Acrylamide, bisacrylamide, sodium dodecyl sulphate (SDS), $CaCl_2$, MgCl were from BDH Laboratory Supplies LTD., England. Hybond-P membranes were from Amersham Pharmacia Biotech. Super Signal® chemiluminescent substrate and the Protein Assay kit were from Pierce, USA (Separations). X-ray film, photographic developer and fixer were from Konica. Low molecular weight marker proteins were purchased from Pharmacia, USA. All materials were of analytical grade and double distilled, deionized water was used in all experiments.

2.5. METHODS

2.5.1. TICK SALIVARY GLAND DISSECTION

Female ticks were embedded in molten wax with their dorsal sides visible. The integument was removed by lateral dissection of the cuticle with a scalpel under a 0.9% NaCl solution using a binocular stereomicroscope (10 x magnification). Salivary glands were removed with fine forceps and placed on ice in calcium free Hanks balanced salt solution (HBSS, 5.4 mM KCl, 0.3 mM Na_2HPO_4, 0.4 mM KH_2PO_4, 4.2 mM $NaHCO_3$, 0.5 mM $MgCl_2$, 0.6 mM $MgSO_4$, 137 mM NaCl, 5.6 mM Glucose, 10 mM HEPES, pH 7.2).

2.5.2. APYRASE ACTIVITY ASSAY

In female *O. savignyi* ticks the enzyme apyrase has been localized to the 'a' cell types where it is stored in large dense core vesicles / granules (LDCV, 3-5 μm) and released during feeding (Mans 2002a). Therefore, by investigating the release of apyrase, one can gain insight into the mechanisms involved in regulated exocytosis of LDCVs. In order to create a higher throughput system and also compensate for the numerous variables between individual salivary glands (such as size, age, amount of active apyrase etc.), we created a 96-well assay that is shown and described below (Table 2.8).

Table 2.8. Schematic presentation of the micro-titer plate setup in the secretion assay.

		Assay #1			Assay #2			Assay #3			Assay #4		
		1	2	3	4	5	6	7	8	9	10	11	12
A	Glands	SG	SG	SG	SG	SG	SG	SG	SG	SG	SG	SG	SG
B	Secreted	10μl											
C		10μl											
D		10μl											
E		10μl											
F	Dilutions of crude	Crude											
G		1/10											
H		1/10											

In the 96-well test, we were able to perform 4 individual assays, each in 12-fold (i.e. n=12), on a single plate. Briefly, glands were dissected and cut in half. Four randomly selected halves were placed in the wells of row A in 100 μl of HBSS containing the appropriate compound of interest (see 2.5.3). After stimulation, 10 μl of the medium was removed and placed in rows B-E containing 90 μl of apyrase reaction medium (20 mM Tris-HCl, 150 mM NaCl, 5 mM $MgCl_2$, 2 mM ATP, pH 7.6) per well. The remaining salivary glands were sonified with a Branson Model B-30 sonifier (Branson Sonic Power Co.) at 10 pulses at 10% duty cycles at an output control of 2. Fractions (10 μl) were taken and diluted into 90 μl apyrase reaction medium in row F, and subsequently diluted twice in rows G and H. The plate was covered and incubated at 37°C for 30 min. The reactions were terminated by the addition of 33 μl molybdic acid mixture to each sample or standard orthophosphate sample (100 μl) in a microtiter well (25 ml of 2.5% molybdate and 13.3% concentrated sulphuric acid were added to 8 ml of a 1% ascorbic acid solution and mixed thoroughly). The reactions were shaken for 10 minutes and the absorbance determined at 620 nm using a SLT 340 ATC scanner (SLT Labinstruments). The amount of phosphate released was calculated from an orthophophate standard curve and one enzyme unit (U) was defined as 1 μmole of inorganic phosphate released per minute. The apyrase activity secreted, as well as the apyrase activity remaining in the salivary glands (crude) after stimulation were determined. Data is expressed as the % apyrase secreted (i.e. apyrase secreted / apyrase remaining in the glands x 100) in order to normalize data obtained from various sizes and metabolic states of the salivary glands. Data was statistically evaluated by means of the student's t-Test.

2.5.3. AGONIST AND ANTAGONIST TREATMENT

Salivary glands were made accessible for treatment with various compounds by dividing the glands into half using a sterile blade, hence rupturing the surrounding myo-epithelial sheath. Two halves of non-paired glands were placed in a microtiter plate well containing 100 μl calcium-free HBSS. By using a calcium specific electrode (Model 93-20, Orion Research, USA), the free calcium concentration in HBSS was determined to be less than 0.1 μM (Micro-processor ionalyzer Model 910, Orion Research, USA). The latter concentration is the lower detection limit of the electrode. Glands were washed three times with 100 μl HBSS and excess fluid was removed using a sterile 25G x 1" needle linked to a vacuum pump. Permeabilized cells were prepared by incubating the salivary gland sections in HBSS containing digitonin (40 μg / ml HBSS) at 4°C for 5 minutes. Digitonin-containing HBSS was removed by washing the cells three times with HBSS prior to incubation with the molecule of interest. Various conditions were investigated and these are described in the result section.

2.5.4. PHOSPHORYLATION ASSAY

Ten salivary glands were dissected, cut in half and placed on ice in 100 μl HBSS containing 0.1 mg/ml penicillin, 0.25 mg/ml fungizone, 0.1 mg/ml streptomycin sulphate, 1 μg/ml leupeptin, 20 μg/ml aprotonin, 0.5 mM PMSF (phenylmethylsulfonyl fluoride) and 5 μl phosphatase inhibitor cocktail (Sigma). Intact salivary glands were stimulated for 10 minutes at 37ºC with 10 μM dopamine, while broken cells (hand homogenated using a teflon pestle, on ice for 2 minutes) were stimulated with 10 μM cAMP and 10 mM theophylline. A 5 μl aliquot of sample was removed and used to determine the protein concentration of the various fractions. The phosphorylation reaction was terminated by adding 30μl stop buffer (6 μl of 1M Tris, pH 6.8, 10 μl of 20% SDS, 8 μl of 80% glycerol, 5 μl mercapto-ethanol, 1 μl of 1% bromophenol blue) and boiling the samples for 10 minutes. Equal amounts of protein from each sample was subjected to SDS-PAGE and Western Blotting (as described in chapter 3) using monoclonal mouse-anti-phosphothreonine IgG$_{2b}$ or mouse-anti-phosphoserine IgG$_1$ as the primary antibody and a goat-anti-mouse IgG (heavy and light chain) coupled to horseradish peroxidase as secondary antibody.

2.6. RESULTS AND DISCUSSION

2.6.1.   DOPAMINE / ISOPROTERENOL / CARBACHOL

It is well established that tick salivary glands (ixodid and argasid) are stimulated by dopamine, a neurotransmitter secreted at the neuroeffector junction (Sauer *et al.* 2000). In order to determine the optimal concentration of dopamine required for stimulation of salivary glands of *O. savignyi*, intact glands were stimulated in the presence and absence of added extracellular calcium in HBSS (see sections 2.5.2 and 2.5.3). In the presence of an excess added calcium (1.3 mM), maximal stimulation was obtained with 0.5 μM dopamine, in contrast to the 10 μM dopamine required in the absence of extracellular calcium (Figure 2.10). This 20-fold difference clearly indicates that the intracellular effect of dopamine is tightly regulated by extracellular calcium, which has been indicated for ixodid ticks as the opening of a voltage-gated calcium channel by dopamine. The k_a for dopamine in ixodid ticks has been established as 0.4 μM, which is in a range similar to that observed in this study, i.e. 0.5 μM. Free calcium levels in the HBSS buffer were not affected by the addition of salivary glands (see section 2.5.3).
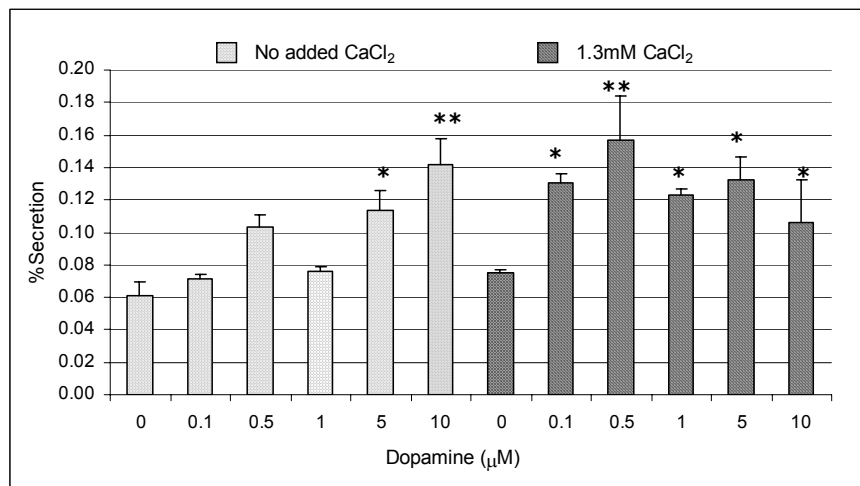
Figure 2.10. The effect of dopamine and extracellular calcium on apyrase secretion from the salivary glands of *O. savignyi*. *Salivary glands were incubated in HBSS without added calcium (dotted bars) or HBSS containing 1.3 mM CaCl$_2$ (striped bars) and stimulated with various concentrations of dopamine. The % apyrase secreted from the salivary glands is indicated. Error bars represent SD with n=12. (*) p<0.005, (**) p<0.001.*

Upon testing the effect of isoproterenol (a β-adrenoceptor agonist) in concentrations similar to that of dopamine (in the presence of extracellular calcium), no significant stimulation above baseline was detected (p>0.05 of a t-test assuming unequal variance; Figure 2.11).

The absence of apyrase secretion in the presence of isoproterenol can be explained by the high k_a described for isoproterenol in ixodid ticks, i.e. 0.15 mM, which greatly exceed the concentrations tested in this study.
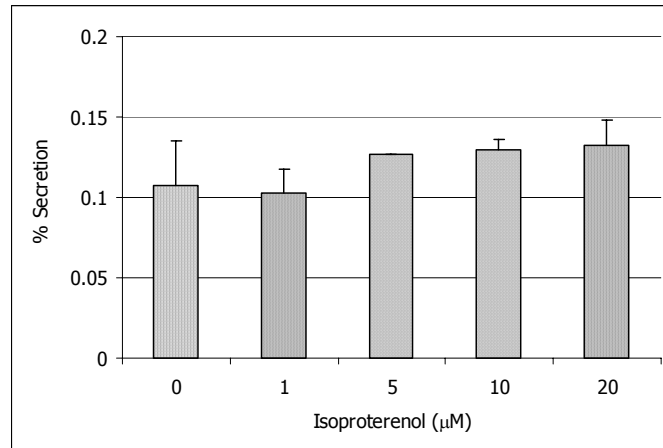
Figure 2.11. The effect of isoproterenol on apyrase secretion from the salivary glands of *O. savignyi*. *Salivary glands were incubated in HBSS containing 1.3 mM CaCl$_2$ and stimulated with various concentrations of isoproterenol. The % apyrase secreted from the salivary glands is indicated. Error bars represent SD with n=12. In all cases p>0.005.*

Injecting ticks with pilocarpine (a nonselective muscarinic acetylcholine receptor agonist) has been described for inducing salivation. In ixodid ticks it is believed that pilocarpine does not stimulate the salivary glands directly, but rather acts upon the synganglion, which then in response stimulates secretion from the salivary glands (personal communication with Prof. J.R. Sauer). By using the non-selective cholinergic agonist, carbachol (carbamyl chloride), the activation of cholinergic receptors on the salivary glands were investigated. The results indicated no stimulation, but rather inhibition of secretion (Figure 2.12). One explanation could be the observation that carbachol causes apoptosis in some cells (Sigma-Aldrich 2002). Upon apoptosis, cell caspases are processed into proteolytically active forms that initiate the 'caspase' cascade of cell destruction, including the collapse of the cytoskeleton and degradation of proteins involved in DNA replication and repair (Watling 2001).
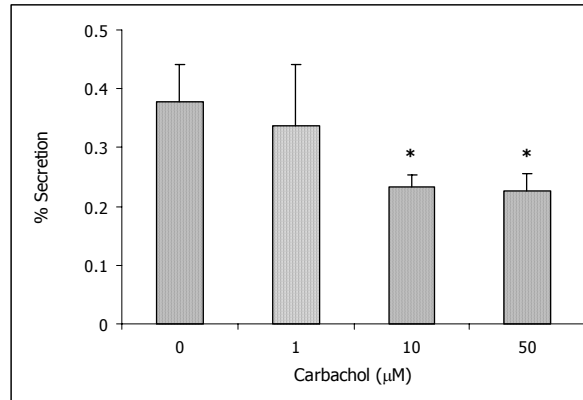
Figure 2.12. The effect of carbachol on apyrase secretion from the salivary glands of *O. savignyi*. *Salivary glands were incubated in HBSS containing 1.3 mM CaCl$_2$ and stimulated with various concentrations of carbachol. Error bars represent SD with n=12. (*) p<0.005.*

2.6.2.   INTRACELLULAR CALCIUM

In most, if not all secretory cells, the final step of regulated exocytosis is triggered by a burst of intracellular calcium. The effect of intracellular calcium in salivary glands was investigated by permeabilizing glands and placing them in a calcium-free buffer containing an excess of EGTA (5 mM), which will sequester any free calcium released intracellularly upon dopamine stimulation. In the presence of EGTA, a 1.5 fold increase in signal was observed when compared with the baseline (i.e. unstimulated permeabilized cells). In contrast, a 2.6 fold increase was observed in the absence of EGTA (Figure 2.13). Firstly, this indicates that an increase in intracellular calcium is essential for secretion from argasid salivary glands. Secondly, it also indicates that intracellular calcium is released in response to dopamine.
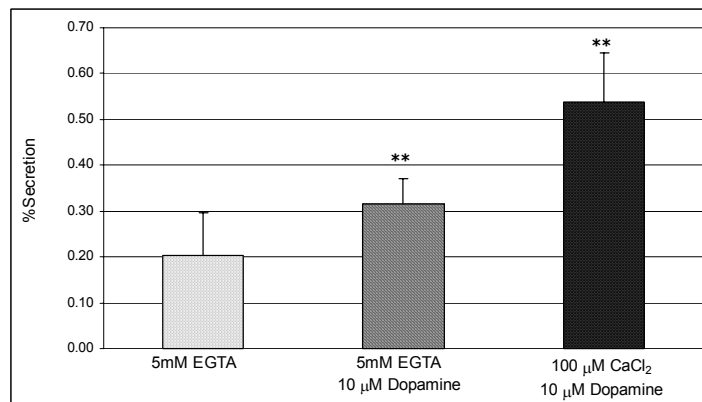
Figure 2.13. The effect of intracellular calcium on dopamine-stimulated apyrase secretion from permeabilized salivary glands of *O. savignyi*. *Salivary glands were permeabilized with digitonin and incubated in HBSS with 5 mM EGTA (bars 1 and 2) or HBSS with 100 μM CaCl$_2$ (bar 3). Cells were stimulated with 10 μM dopamine. The % apyrase secreted from the salivary glands is indicated. Error bars represent SD with n=12. (**) p<0.001.*

2.6.3.   PROSTAGLANDINS

In the case of *A. americanum* it has been proven that PGE_2 plays an important role in stimulating protein secretion from the salivary glands (Sauer *et al.* 2000). It has been shown that activation of a PGE_2 receptor on the plasma membrane results in activation of PLC, production of IP_3 and a rise in intracellular calcium (Qian *et al.* 1998). PGE_2 in the ixodid salivary glands are synthesized from arachidonic acid via two key enzymes, a cytosolic phospholipase A2 (cPLA2) and PGH synthase that is essential to the COX-pathway. In order to investigate whether the synthesis of prostaglandins are essential for exocytosis from *O. savignyi* salivary glands, glands were permeabilized and treated with the PLA_2 inhibitory substrate analogue oleyloxyethyl phosphorylcholine (OPC), similar to the studies performed by Qian *et al.* (Qian *et al.* 1997). In the case of cells treated with OPC, apyrase release was greatly abolished (3,5 fold) in the presence of as little as 5 μM OPC (Figure 2.14, bars 4 and 5). This indicates that dopamine cannot bring about exocytosis without an active PLA_2, and hence it seems that liberation of free arachidonic acid from the plasma membrane and possibly prostaglandin synthesis is necessary for exocytosis from argasid salivary glands.
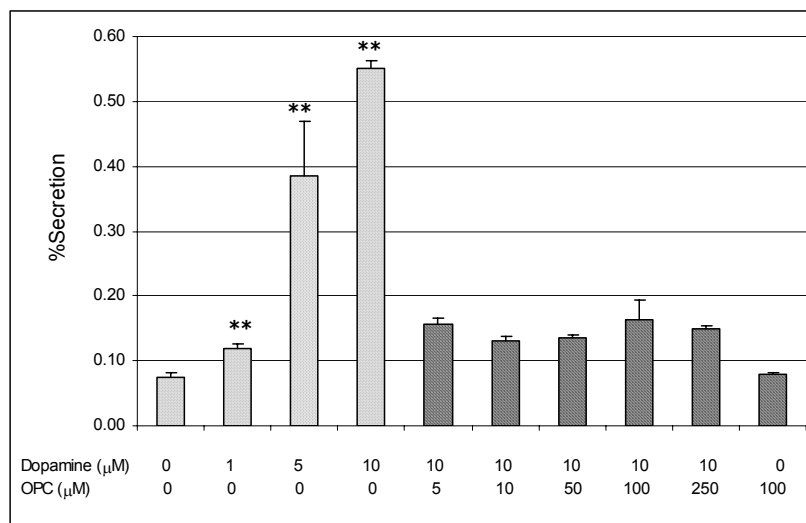
Figure 2.14. The effect of OPC on dopamine-stimulated apyrase secretion from permeabilized salivary glands of *O. savignyi*. *Salivary glands were permeabilized with digitonin and incubated in HBSS containing 1.3 mM $CaCl_2$ and various concentrations of OPC. After washing the cells, they were stimulated with 10 μM dopamine. The % apyrase secreted from the salivary glands is indicated. Error bars represent SD with n=12. (**) p<0.001.*

The following question is whether PGE_2 by itself can bring about apyrase secretion in argasid salivary glands. Since the PGE_2-receptor of *A. americanum* is localized on the plasma

membrane and directly accessible to PGE_2 in intact glands, intact *O. savignyi* salivary glands were incubated with HBSS containing calcium and stimulated with various concentrations of PGE_2. The results obtained (Figure 2.15) indicate that exogenous PGE_2 is unable to induce apyrase secretion.
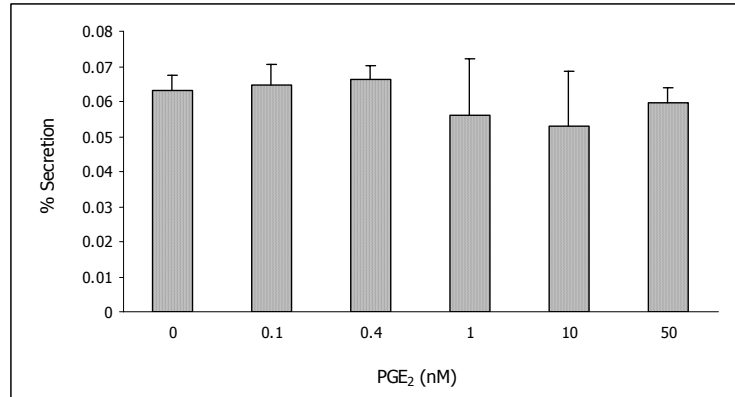
Figure 2.15. PGE_2 stimulated apyrase secretion from intact salivary glands in the presence of HBSS with calcium. *Salivary glands were incubated in HBSS containing 1.3 mM $CaCl_2$ and stimulated with various concentrations of PGE_2. The % apyrase secreted from the salivary glands is indicated. Error bars represent SD with n=12.*

In order to remove excess endogenous PGE_2 (as suggested by Prof. J.R. Sauer) and to also investigate the possibility of an intracellular PGE_2 receptor, glands were permeabilized with digitonin for 15 minutes and washed extensively. Glands were subsequently incubated with various concentrations of PGE_2. The results indicated that PGE_2 was unable to stimulate apyrase secretion (Figure 2.16). In contrast, PGE_2 had an inhibitory effect on secretion at concentrations as low as 10nM. We were also unable to rescue cells treated with OPC by incubating cells with PGE_2 (Figure 2.17). Therefore the possibility of side effects of OPC must be further investigated as well as rescue studies using arachidonic acid. If an active PLA_2 is however required, one can deduce that generating free AA (arachidonic acid) and its metabolites are essential for secretion. A suitable positive control (such as *A. americanum* salivary glands) should also be investigated to confirm that PGE_2 is bioactive.
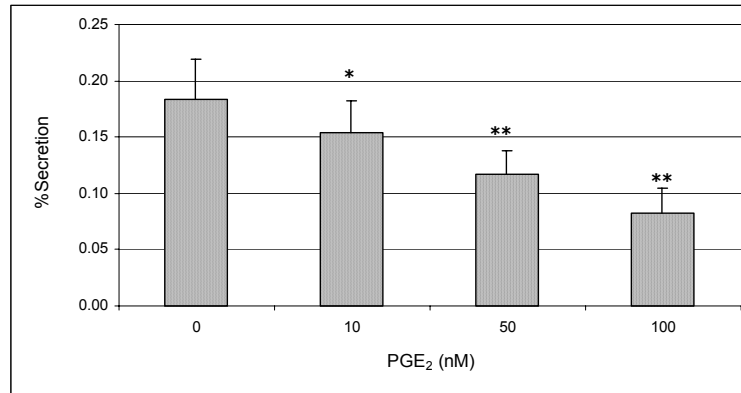
Figure 2.16. PGE$_2$ stimulated apyrase secretion from permeabilized salivary glands in the presence of HBSS with calcium. *Salivary glands were incubated in HBSS containing 1.3 mM CaCl$_2$ and digitonin. After washing the cells, they were stimulated with various concentrations of PGE$_2$. The % apyrase secreted from the salivary glands is indicated. Error bars represent SD with n=12. (*) p<0.05, (**) p<0.001.*
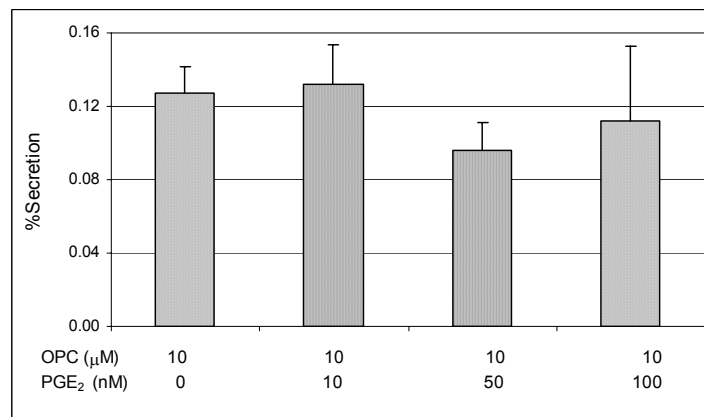
Figure 2.17. Rescue of OPC treated cells with PGE$_2$. *Salivary glands were permeabilized with digitonin and incubated in HBSS containing 1.3 mM CaCl$_2$ and 5 μM OPC. After washing the cells, they were stimulated with various concentrations of PGE$_2$. The % apyrase secreted from the salivary glands is indicated. Error bars represent SD with n=12.*

2.6.4.   cAMP

cAMP is a widely used secondary messenger synthesized by adenylyl cyclase (AC). In ixodid tick salivary glands it has been shown that although cAMP levels are elevated during dopamine stimulation (via activation of AC), it is important for fluid secretion and not for protein secretion (Schmidt *et al.* 1981). Similar to the studies performed by McSwain *et al.*, intact argasid salivary glands were stimulated with milli-molar concentrations of exogenous cAMP (in HBSS with calcium) (McSwain *et al.* 1985). Limited stimulation of the glands was detected, i.e. apyrase secretion, was observed at 1 and 5 mM (Figure 2.18).
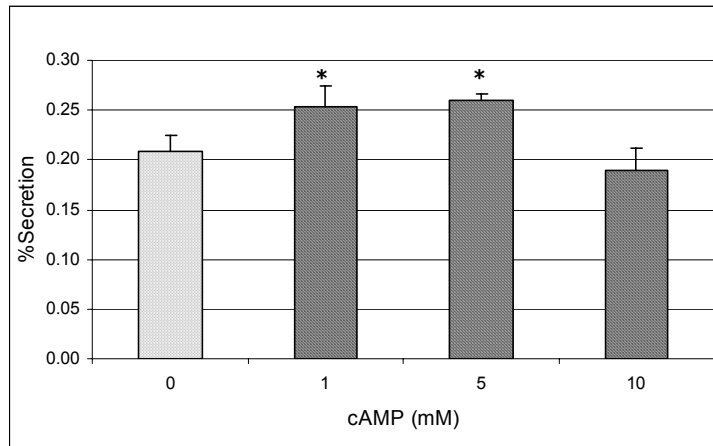
Figure 2.18. The effect of elevated extracellular cAMP levels on apyrase secretion from intact salivary glands of *O. savignyi*. *Salivary glands were incubated in HBSS containing 1.3 mM CaCl$_2$ and stimulated with various concentrations of exogenous cAMP. The % apyrase secreted from the salivary glands is indicated. Error bars represent SD with n=12. (*) p<0.002.*

In the case of stimulating digitonin-permeabilized salivary glands with lower (micro-molar) concentrations of cAMP (in HBSS containing calcium), an inhibition of apyrase secretion was detected (Figure 2.19). The effect of intracellular cAMP on dopamine-stimulation of permeabilized cells was also investigated. In the presence of Ca^{2+}, cAMP inhibited dopamine-stimulated secretion of apyrase (Figure 2.20).
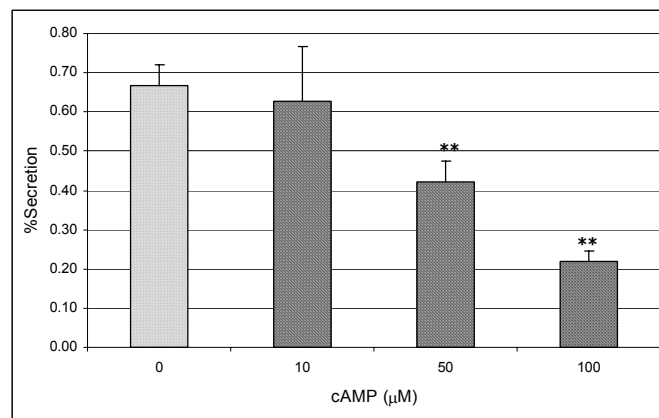
Figure 2.19. The effect of elevated intracellular cAMP levels on apyrase secretion from permeabilized salivary glands of *O. savignyi*. *Salivary glands were permeabilized with digitonin and incubated with HBSS containing various concentrations of cAMP. The % apyrase secreted from the salivary glands is indicated. Error bars represent SD with n=12. (**) p<0.001.*
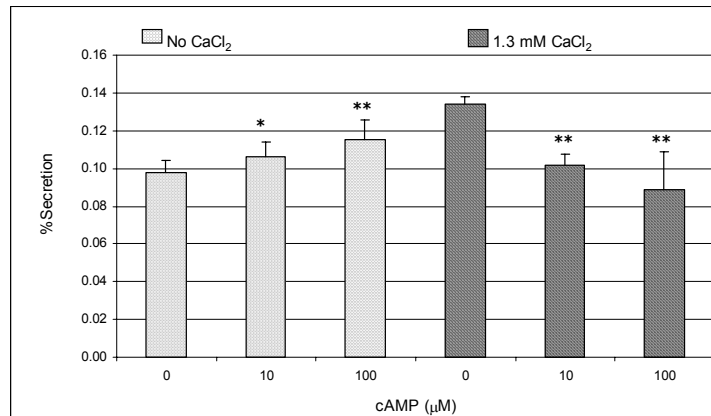
Figure 2.20. The effect of elevated intracellular cAMP levels on dopamine-stimulated apyrase secretion from permeabilized salivary glands of *O. savignyi*. *Salivary glands were permeabilized with digitonin, washed, incubated with HBSS containing various concentrations of cAMP and stimulated with 10 μM dopamine. The % apyrase secreted from the salivary glands is indicated. Error bars represent SD with n=12. (*) p<0.05, (**) p<0.001.*

This inhibition of secretion by intracellular cAMP can be explained firstly by the change in amplitude and duration of the signal, i.e. change in normal physiological signal. Secondly, the increase in cAMP will increase PKA activity resulting in the phosphorylation and change in activity of numerous proteins. Thirdly, cAMP-regulated guanine (GTP/GDP) exchange factors of small G-proteins, as well as cAMP-regulated ion channels, will be activated. All of the above could contribute to the inhibition of apyrase secretion.

These results do, however, indicate that elevated levels of cAMP are not sufficient to bring about apyrase secretion. Whether adenylyl cyclase and the production of cAMP are essential for exocytosis should be addressed by inactivating adenylyl cyclase. It has, however, been shown that cAMP-dependent kinase phosphorylation of proteins are essential for protein secretion, since they regulate phosphorylation of secretory proteins such as SNAP25 (Risinger and Bennett 1999), α-SNAP (Hirling and Scheller 1996) and rabphillin (Lonart and Sudhof 2001) in neurons, syntaxin 4 in non-neuronal cells (Foster *et al.* 1998), secretory granule membrane proteins of rat parotid glands (Marino *et al.* 1990) and t-SNAREs in yeast (Marash and Gerst 2001).

2.6.5.   VERAPAMIL

The phenylalkylamines (e.g. verapamil) have long been used to distinguish between the various calcium channels (Jeziorski *et al.* 2000; Watling 2001). Only the L-type is verapamil

sensitive, while the T, N, P, Q and R-types are all insensitive (Watling 2001). Both the L and T type of calcium channels are found on endocrine cells. Upon stimulating intact salivary glands with dopamine in the presence of verapamil (in HBSS, with calcium), apyrase secretion was inhibited. At a concentration of 1, 50 and 100 μM verapamil, secretion was inhibited by 14%, 22% and 53%, respectively (Figure 2.21). This indicates an important role for a L-type calcium channels in argasid tick secretion, and also explains the need for extracellular calcium for optimal dopamine-stimulated secretion. Since these studies were performed on intact salivary glands, the L-type channels is deduced to be localized on the plasma membrane.
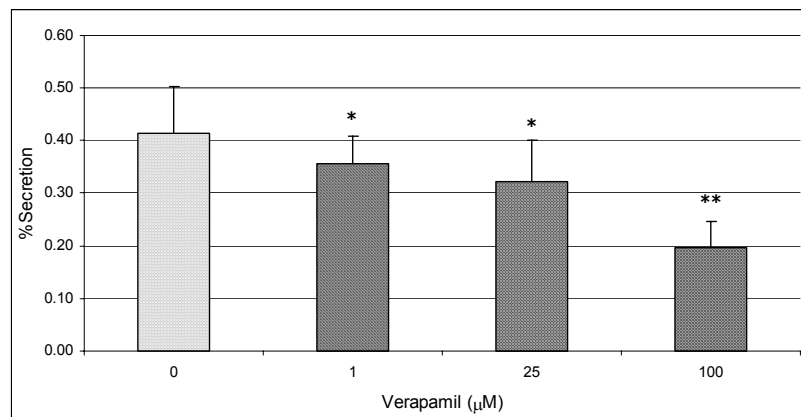
Figure 2.21. The effect of verapamil on dopamine-stimulated apyrase secretion from intact salivary glands. *Salivary glands were incubated in HBSS containing 1.3 mM $CaCl_2$ and various concentrations of verapamil. After washing the cells, they were stimulated with 10 μM dopamine. The % apyrase secreted from the salivary glands is indicated. Error bars represent SD with n=12*. *(*) p<0.05, (**) p<0.001.*

The possible activation of CaM via this influx of extracellular calcium should also be investigated, since this is involved in the phosphorylation (and thus the metabolic control) of numerous proteins, the regulation of adenylyl cyclase, inactivation of voltage-gated calcium channels and cyclic nucleotide phosphodiesterases (Watling 2001).

2.6.6.   OUABAIN

Na^+-K^+-ATPases of plasma membranes were first isolated in 1957 by Jens Skou (Voet and Voet 1995). The enzyme is often referred to as the Na^+-K^+-Pump because it pumps Na^+ out of and K^+ into the cell with the simultaneous hydrolysis of intracellular ATP. This extrusion of Na^+ enables animal cells to control their water content osmotically. Without functioning Na^+-K^+-ATPases, cells lacking cell walls (like animal cells) would swell and burst. In neuronal

cells, the electrochemical potential gradient generated by Na^+-K^+-ATPases is responsible for the electrical excitability of nerve cells, while in other cells (such as intestinal epithelium and erythrocytes) it provides the free energy for active transport of glucose and amino acids.

Ouabain is a glycoside that blocks the effective efflux of Na^+ and reuptake of K^+ by blocking the movement of the H5 and H6 transmembrane domains of Na^+-K^+-ATPases (Sigma-Aldrich 2002). In ixodid ticks it has been described that the correlation to fluid secretion and activities is highest in the salivary glands of mated, rapidly feeding females (Sauer *et al.* 2000). Furthermore, it has been shown that the Na^+-K^+-ATPases are sensitive to Ouabain and that the volume of saliva secreted is dependent on an active Na^+-K^+-ATPase. This indicates that Na^+-K^+-ATPases in ixodid ticks are involved in regulating cell volume. In argasid ticks we were able to show that Ouabain also inhibits apyrase secretion. In the presence of 10, 20 and 50 μM Ouabain secretion was inhibited by 12%, 41% and 47%, respectively (Figure 2.22).
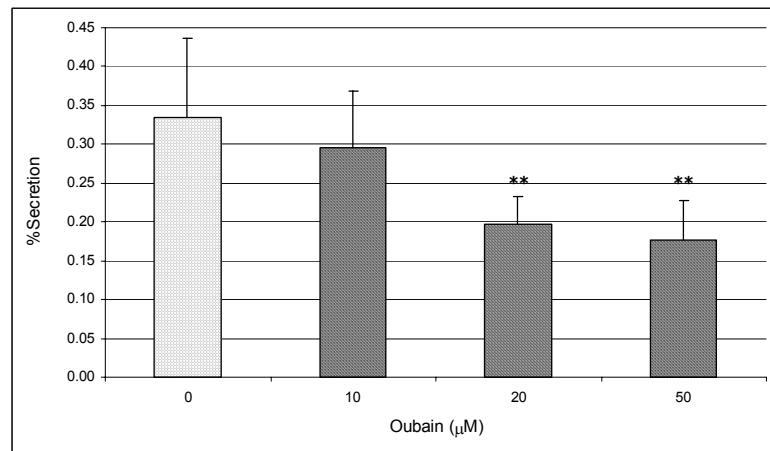
Figure 2.22. The effect of Ouabain on dopamine-stimulated apyrase secretion in HBSS with calcium. *Salivary glands were incubated in HBSS containing 1.3 mM $CaCl_2$ and various concentrations of Ouabain. After washing the cells, they were stimulated with 10 μM dopamine. The % apyrase secreted from the salivary glands is indicated. Error bars represent SD with n=12. (**) p<0.001.*

In various cells it has been found that by inactivating Na^+-K^+-ATPases, exocytosis is also affected (Finkelstein *et al.* 1986; Troyer and Wightman 2002). In ixodid ticks, the inactivation of the Na^+-K^+-ATPase did not affect protein secretion, but the volume of saliva secreted was affected. Therefore it was hypothesized that Na^+-K^+-ATPases are involved in maintaining cellular osmolarity. By inhibiting Na^+-K^+-ATPases with Ouabain in the salivary

glands of *O. savignyi* we observed 41-47% inhibition of apyrase secretion when using concentrations between 20-50 μM. This indicates that an active Na^+-K^+-ATPase is required for protein secretion from argasid salivary glands. The current hypothesis for the role of Na^+-K^+-ATPases in exocytosis are based on vesicle / granule swelling which occurs due to the displacement of associated cations in the granule with hydrated cations such as Na^+ from the external solution (Troyer and Wightman 2002). Whether osmotic swelling is a driving force in argasid tick salivary gland exocytosis must be further examined by determining the effect of high and low osmolarity solutions on apyrase secretion, similar to the studies done on mast- and chromaffin cells (Troyer and Wightman 2002).

2.6.7. EXTRACELLULAR AND INTRACELLULAR CONDITIONS (Membrane potential)

It has long been known that elevating the extracellular K^+ concentration (thereby depolarizing the membrane) can bring about neurotransmitter release from neuronal cells (Adam-Vizi 1992). In order to investigate the effect of depolarizing the salivary gland plasma membrane potential, the effect of dopamine-stimulated secretion was investigated under conditions reflecting an extracellular environment (high Na^+, low K^+, high $Ca2^+$, low ATP; HBSS) and conditions reflecting an intracellular environment (low Na^+, high K^+, low $Ca2^+$, high ATP; AISS) similar to the studies performed by Chaturvedi *et al*. (Chaturvedi *et al.* 1999). From the results it is evident that membrane depolarization of salivary glands is not sufficient to bring about optimal apyrase secretion (Figures 2.23 and 2.24). Therefore, the mechanism underlying apyrase secretion is not identical to that of neurotransmitter release. Also, in the case of HBSS with calcium, again it could be seen that 0.5 μM of dopamine stimulated optimal secretion of apyrase (Figure 2.23). In the case of AISS, five times less (0.1 μM) dopamine was sufficient to stimulate optimal apyrase secretion (Figure 2.24).
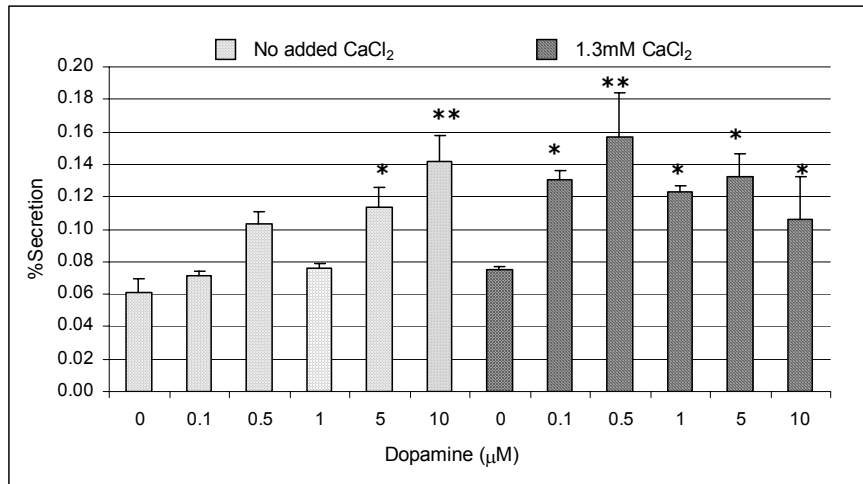
Figure 2.23. The effect of dopamine and extracellular calcium on apyrase secretion from the salivary glands of *O. savignyi* in HBSS. *Salivary glands were incubated in HBSS without calcium (dotted bars) or HBSS containing 1.3 mM $CaCl_2$ (striped bars) and stimulated with various concentrations of dopamine. The % apyrase secreted from the salivary glands is indicated. Error bars represent SD with n=12. (*) p<0.005, (**) p<0.001.*
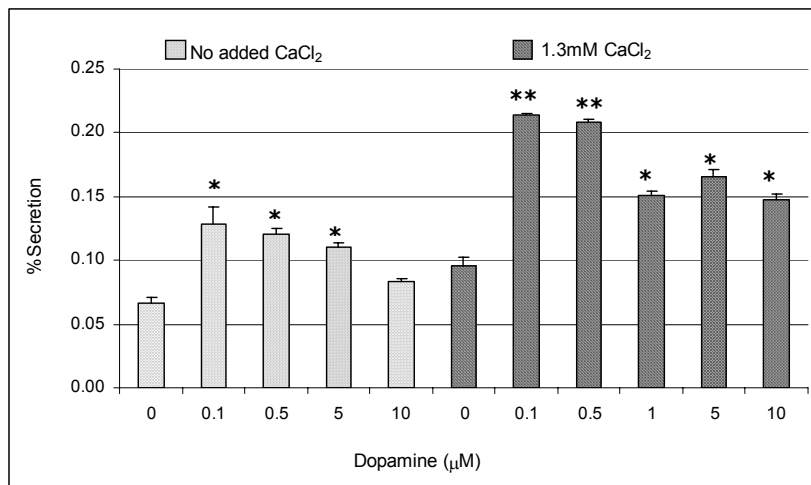
Figure 2.24. The effect of dopamine and extracellular calcium on apyrase secretion from the salivary glands of *O. savignyi* in AISS. *Salivary glands were incubated in AISS without calcium (dotted bars) or HBSS containing 1.3 mM $CaCl_2$ (striped bars) and stimulated with various concentrations of dopamine. The % apyrase secreted from the salivary glands is indicated. Error bars represent SD with n=12. (*) p<0.005, (**) p<0.001.*

2.6.8.   N-ethylmaleimide (NEM)

N-ethylmaleimide is a well-known alkylating agent. During studies on the exocytotic machinery of various cells, a NEM-sensitive fusion protein called NSF (N-ethylmaleimide sensitive factor) was identified and isolated. NSF was shown to be a homo-oligomeric

ATPase. It's ATP-dependent activity is involved in rearranging soluble NSF attachment protein (SNAP) receptor (SNARE) protein complexes during ATP-dependent priming (Banerjee 1996a).

By incubating permeabilized salivary glands with NEM, we were able to observe a 41% decrease in apyrase secretion at 100 μM NEM (Figure 2.25). At concentrations of 500 μM and 1000 μM NEM, apyrase secretion was inhibited by 53% and 74%, respectively. Only concentrations lower than 1 mM was tested since higher concentrations have been described to have cellular side effects (Chaturvedi *et al.* 1999).
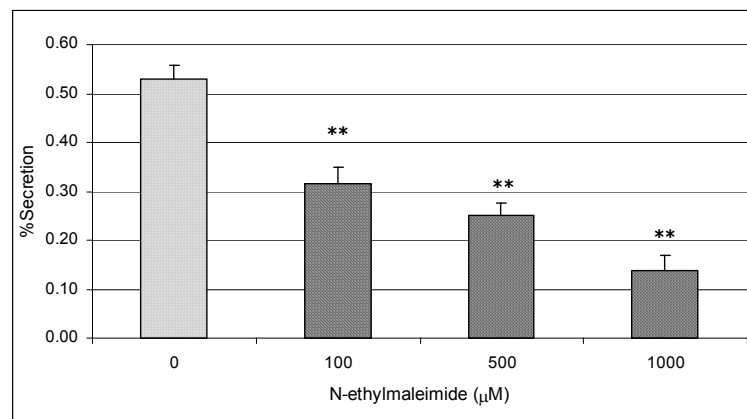
Figure 2.25. Effect of N-ethylmaleimide on dopamine-stimulated apyrase secretion. *Salivary glands were permeabilized with digitonin, washed, incubated with HBSS containing various concentrations of NEM and stimulated with 10 μM dopamine. The % apyrase secreted from the salivary glands is indicated. Error bars represent SD with n=12. (**) p<0.001.*

2.6.9. GTPγS

GTPγS is a non-hydrolyzable GTP analog, known for its role as a G-protein and GTPase activator. In order to test the effect of GTP-binding proteins in apyrase secretion, cells were incubated and stimulated with HBSS containing GTPγS. The results obtained (Figure 2.26) indicate that activation of GTP-binding proteins is sufficient for inducing apyrase secretion without further extracellular stimulation. At concentrations of 50, 100 and 250 μM GTPγS, we observed a 19%, 61%, 91% increase in secretion from the baseline values.
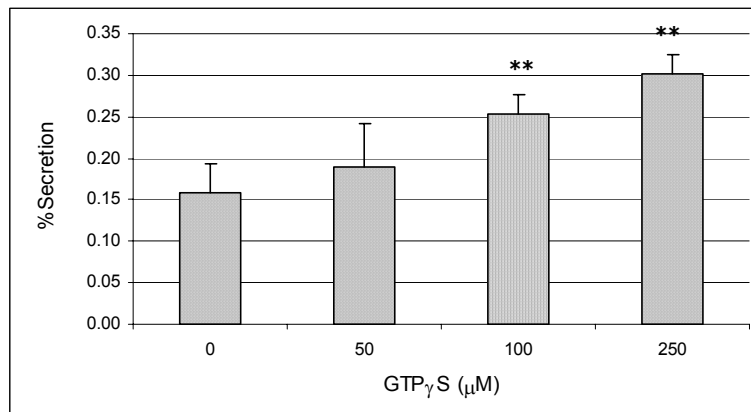
Figure 2.26. Effect of GTPγS on apyrase secretion. *Salivary glands were permeabilized with digitonin, washed, incubated with HBSS (with calcium) containing various concentrations of GTPγS. The % apyrase secreted from the salivary glands is indicated. Error bars represent SD with n=12. (**) p<0.001.*

2.6.10.   cAMP-DEPENDENT PHOSPHORYLATION

In ixodid ticks dopamine activates a D1-type receptor linked to a Gs-protein that activates adenylyl cyclase to produce cAMP (Schmidt *et al.* 1981). This increase in cAMP activates a cAMP-dependent kinase that mediates the phosphorylation of various proteins. In studies performed by McSwain *et al.*, it was shown that the increase in cAMP activates a cAMP-dependent kinase that mediates the phosphorylation of 12 endogenous proteins in *A. americanum*. Upon attenuating dopamine stimulation with dopaminergic antagonists, ten of these proteins were dephosphorylated, indicating the presence of a dopamine-sensitive AC (McSwain *et al.* 1985).

We investigated the effect of dopamine and cAMP (in the presence of the phosphodiesterase inhibitor theophylline) stimulation on the phosphorylation of endogenous proteins in the salivary glands of *O. savignyi* by means of Western blotting with both anti-phosphothreonine and anti-phosphoserine antibodies, similar to the studies of McSwain *et al.* (McSwain *et al.* 1985). In all cases, equal amounts of protein were subjected to SDS-PAGE in order to allow for comparison. No phospho-proteins could be detected using the anti-phosphoserine antibodies. We were able to identify 6 proteins that are phosphorylated via threonine residues in response to both dopamine and cAMP (Figure 2.27 lane 2 and 3). The molecular masses of these are 76, 68, 52, 37, 27 and 22 kDa, respectively. By comparing the molecular masses of the proteins phosphorylated in *A. americanum* (masses indicated in brackets) and *O. savignyi*, the masses are similar for the 76 (74), 68 (62), 52 (55), 37 (37) and 27 (29) kDa proteins, respectively (Table 2.9). These results indicate that a dopamine activated

cAMP-dependent kinase is present, and that dopamine therefore activates adenylyl cyclase similar to the model proposed for ixodid ticks. The possibility of phosphorylated tyrosine residues as well as dephosphorylation studies on the identified phoshothreonine proteins must still be investigated.
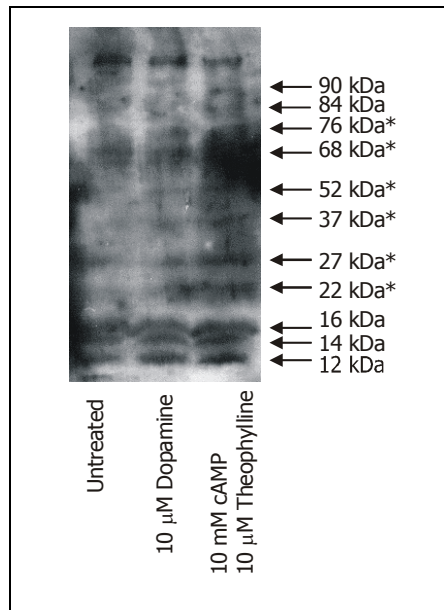
Figure 2.27. Western blotting of dopamine and cAMP treated salivary glands using a monoclonal anti-phosphothreonine IgG. *Lane 1 indicates intact untreated salivary glands, lane 2 indicate intact salivary glands treated with 10 μM dopamine and lane 3 homogenated salivary glands treated with 10 μM cAMP, 10 μM theophylline. Bands that increased in density in response to stimulation is indicated with *.*

Table 2.9. Molecular masses of proteins phosphorylated by a dopamine-sensitive cAMP-kinase in the salivary glands of the ixodid tick *A. americanum* (McSwain *et al.* 1985) and the argasid tick *O. savignyi*.

A. americanum	*O. savignyi*
93.5	
74	76
62	68
55	52
49	
47	
45	
37	37
34	
29	27
	22

2.6.11.   PI-3-KINASE INHIBITOR (WORTMANNIN)

In the tick *A. americanum*, a trypsin-sensitive brain factor was identified that induced the formation of inositol phosphates in tick salivary glands (McSwain *et al.* 1989). In secretory cells an increased turnover of inositol phospholipids correlate with exocytosis (Huijbregts *et al.* 2000). To date, 3- and 4-phosphorylated inositol lipids have been indicated in membrane trafficking. 4-Phosphorylated inositol lipids are believed to function in membrane trafficking e.g. priming of dense core granules in neuroendocrine cells by activation of a calcium-dependent activator protein for secretion (CAPS). 3-Phosphorylated inositol lipids are not only involved in both regulated exocytosis and protein sorting, but by interacting with FYVE-domain containing proteins (such as EEA1, early endosome associated antigen), the PtdIns-3-P signals are integrated with the activation of Rab GTPases (Huijbregts *et al.* 2000). The fact that phosphoinositides regulate membrane trafficking suggests that enzymes dedicated to phosphoinositide turnover will also exert modulatory effects. One such an enzyme is synaptojanin, which contains a catalytic domain with both inositol 3- and 4-phosphatase activity, and is required for endocytosis (Huijbregts *et al.* 2000).

During this study we investigated the possible role of PI-3-kinases type I, which is involved primarily in the synthesis of PtdIns(3,4,5)P$_3$. Our interest in PI-3-kinases type I came from the recent studies indicating a role for this enzyme in exocytosis and also the fact that PI-3-kinases are activated by the βγ-subunits of G-proteins. The reason for the latter is the observation that PLCβ (1,2, and 3 subfamilies) could also be regulated by βγ dimers (Bonacci *et al.* 2005). If one can indicate the presence of active PI-3-kinases, it can be hypothesized that βγ dimers are activators in argasid ticks and thus the possibility of PLC activation by βγ dimers must be investigated.

Wortmannin (from *Penicillium funiculosum*) is a potent and specific phophatidylinositol 3-kinase (PI3-K) inhibitor (Sigma-Aldrich 2002). In cells there are two types of PI3-kinases (type 1A and 1B) that are affected by Wortmannin (see Table 2.10). Since the type 1B is only localized in hemopoietic cells, one can assume that by investigating the effect of Wortmannin on salivary glands, one would determine the effects of a Type 1A phophatidylinositol 3-kinases (Watling 2001; Sigma-Aldrich 2002).   A summary of the functions of the various kinases as well as the reaction inhibited by Wortmannin is shown in Figure 2.28.

Table 2.10. Characteristics of Type 1A and 1B phophatidylinositol 3- kinases sensitive to Wortmannin (Watling 2001).

Kinase	Type 1A PI3K	Type 1B PI3K
Reaction *in vivo*	PtdIns(4,5)P$_2$ > PtdIns(3,4,5)P$_3$	PtdIns(4,5)P$_2$ > PtdIns(3,4,5)P$_3$
Structure	p85 (α,β) or p55γ regulatory subunit; p110 (α,β or γ) catalytic subunit	p101 regulatory subunit p101γ catalytic subunit
Control/Comments	- P85 SH2 domain interacts with P-Tyr residues - P110 activated by p85 and by activated Ras -Activated by insulin receptor/ growth factor receptors and $\beta\gamma$-complexes liberated from activated Gs proteins	- P101 complexes activated by $\beta\gamma$-complexes liberated from activated Gi and/or Go proteins. - Receptors that influence motility and the bacterial oxidative burst of neutrophils
Localization	Various cells	Hemopoietic cells
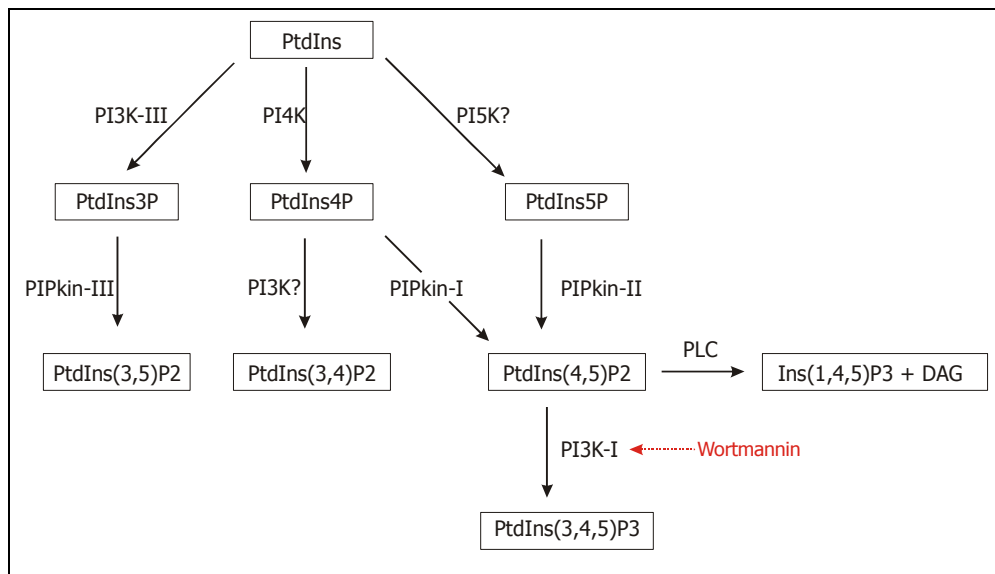
Figure 2.28. A schematic presentation of the functions of the various reactions catalyzed by cellular phosphoinositide kinase isozymes (Watling 2001). *The reaction affected by Wortmannin is indicated in red.*

PtdIns(3,4,5)P$_3$, which is the product formed by PI3K-I, is a remarkable membrane-associated second messenger molecule. It appears to have many direct target proteins, each interacting with highly PtdIns(3,4,5)P$_3$-selective pleckstrin (PH) domains. Some of these are protein kinases, while others include regulators of small GTPases, e.g. GTP/GDP exchange factors and GTPase-activated factors (Watling 2001). Recent work indicated that PI3-kinases may be one of the important regulatory exocytotic components involved in the signaling cascade controlling actin rearrangements (blocking of actin disassembly) required for

catecholamine secretion from chromaffin cells by affecting myosin-actin ATPase activity (Chasserrot-Golaz *et al.* 1998; Neco *et al.* 2003). Inhibitors of PI3-kinase also significantly decrease heterophil degranulation (Kogut *et al.* 2002). PI3-kinases are also required for the efficient routing of proteins through FYVE-domain proteins such as EEA1. Inhibition of PI3-kinase activity by agents such as Wortmannin effects release of EEA1 from endosomal membranes, and correspondingly inhibits endosome fusion (Huijbregts *et al.* 2000).

Upon stimulating permeabilized salivary glands in the presence of 1, 10 and 100 nM of Wortmannin we observed a 15, 29 and 36% inhibition of apyrase secretion, respectively (Figure 2.29). Since inhibitor concentrations used were in the nano-molar range we can conclude that other enzymes such as myosin light-chain kinase, PLA_2 and some PI4-kinases were not affected. The latter have been reported in literature to be affected by Wortmannin when used in the micro molar range (Chasserrot-Golaz *et al.* 1998). This indicates that a dopamine activated (direct / indirect) G_s-$\beta\gamma$ subunit is most likely involved in activating PI3-kinases and that PtdIns(3,4,5)P_3 is an important signaling lipid during regulated exocytosis of apyrase. Furthermore, we hypothesize that these PI3-kinases are regulated by $\beta\gamma$-dimers, similar to all other secretory cells. The role of these $\beta\gamma$-dimers must be investigated by future studies to determine their role in activation of PLC.
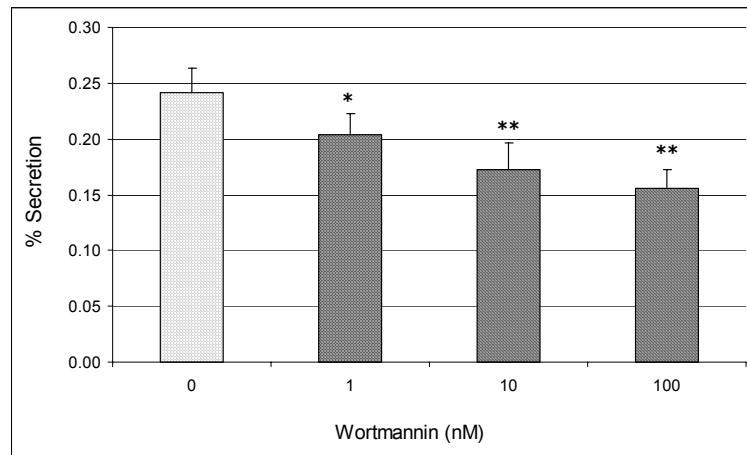
Figure 2.29. Effect of Wortmannin on dopamine-stimulated apyrase secretion. *Salivary glands were permeabilized with digitonin, washed, incubated with HBSS containing various concentrations of Wortmannin and stimulated with 10 μM dopamine in the presence of calcium. The % apyrase secreted from the salivary glands is indicated. Error bars represent SD with n=12. (*) p<0.01, (**) p<0.001.*

## 2.6.12.   Inositol (1, 4, 5) tri-phosphate (IP$_3$)

In the ixodid tick *A. americanum* it has been clearly indicated that IP$_3$ levels are raised in response to PGE$_2$. In response to IP$_3$, intracellular calcium was released from microsomes and exocytosis of salivary gland proteins occurred. In order to investigate the effect of elevated levels of IP$_3$ on the exocytosis of apyrase from argasid salivary glands, permeabilized cells were stimulated with HBSS containing IP$_3$. The results (Figure 2.30) indicate that elevated IP$_3$ levels are insufficient for inducing secretion. This finding indicates that elevated IP$_3$ (and hence elevated intracellular calcium levels) are not sufficient for inducing exocytosis by itself and that other signaling pathways are also required for inducing exocytosis in *O. savignyi*.
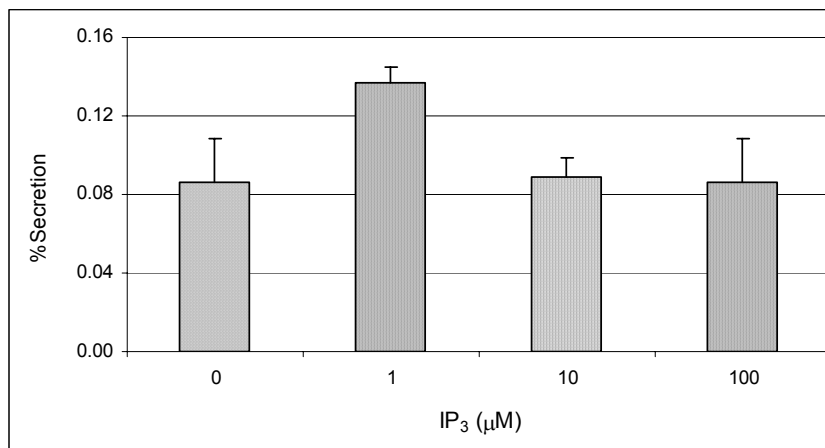
Figure 2.30. Effect of IP$_3$ on apyrase secretion from permeabilized salivary glands of *O. savignyi*. *Salivary glands were permeabilized with digitonin, washed, incubated with HBSS containing various concentrations of IP$_3$. The % apyrase secreted from the salivary glands is indicated. Error bars represent SD with n=12.*

2.6.13.   PLC INHIBITOR (U73,122)

As described previously, IP$_3$ and increased intracellular calcium are key processes in regulated exocytosis in secretory cells. IP$_3$ is synthesized by phospholipase C (PLC) that is in turn activated by either the α-subunits of the G$_{q/11}$ subfamily or by the G$_{\beta\gamma}$ dimers. Since ixodid ticks contain an EP1-type of PGE$_2$ receptor, it most likely is linked to G$_{q/11}$ and PLC-β. In order to determine whether a PLC-activated pathway is involved in exocytosis in *O. savignyi*, we investigated the effect of the PLC inhibitor U73,122 (1-(6-[([17b]-3-methoxyestra-1,3,5[10]-trien-17-yl)-amino]hexyl)-1H-pyrrole-2,5-dione) which is a non-specific inhibitor of the PLC-β, PLC-γ and PLC-δ isoforms. The results (Figure 2.31) indicate

68

that an active PLC is required for exocytosis of apyrase. At concentrations of 10, 50 and 100 μM U73,122 we observed complete inhibition of apyrase secretion when cells were stimulated by dopamine. This indicates that the normal products produced by PLC (i.e. IP$_3$ and DAG) are required for exocytosis.
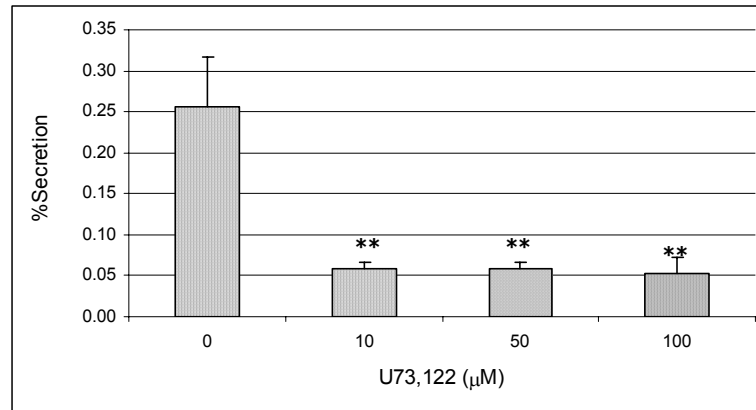
Figure 2.31. Effect of U73,122 on dopamine-stimulated apyrase secretion from permeabilized salivary glands of *O. savignyi*. *Salivary glands were permeabilized with digitonin, incubated with HBSS containing various concentrations of U73122, washed and stimulated with HBSS containing 1.3 mM calcium and 10 μM dopamine. The % apyrase secreted from the salivary glands is indicated. Error bars represent SD with n=12. (**) p<0.001.*

2.6.14.   Actin inhibitor (Cytochalasin D)

Early ultrastructural studies of actively secreting cells, such as pancreatic or neuronal cells, revealed an extensive actin network and a dense sub-plasmalemmal actin cortex. It is predicted that this zone creates an obstacle that obstructs exocytosis and endocytosis at the plasma membrane, the so-called actin-physical barrier model (Eitzen 2003). Data from various experiments support this model and imply that depolymerization of F-actin is needed in order for vesicles to gain access to their appropriate docking and fusion sites. However, not all data support this model. Other hypotheses to explain the role of actin in exocytosis include (a) actin remodeling that includes a rearrangement to form structures that spatially restrict fusogenic proteins to active fusion sites and/or (b) the ability to apply a constrictive force on membranes during membrane fusion to overcome the large electrostatic force between two lipid bilayers that opposes their juxtapositioning (Eitzen 2003).

To date the entire mechanism of actin to facilitate membrane fusion and exocytosis is not clearly defined. In numerous cells (adrenal chromaffin-, alveolar type II-, egg-, GH$_3$-, HIT-

T15 -, anterior pituitary-, mast-, pancreatic β -, parotid acinar-, posterior pituitary terminal-, sperm-, WRK-1 cells and synapses) it has been shown that the actin cytoskeleton function as a barrier and disassembles upon exocytosis stimulus induction (Burgoyne and Morgan 2003). Also, actin is required for the active transport of secretory granules to the plasma membrane (Burgoyne and Morgan 2003).

Cytochalasin D (from *Zygosporium mansonii*) is a cell permeable fungal toxin that disrupts actin microfilaments and inhibits actin polymerization. In a study by Orci *et al.*, the mild application (10 μg/ml) of cytochalasin D significantly increased the secretion of insulin, indicating the presence of an actin-barrier (Orci *et al.* 1972; Eitzen 2003). However, higher concentrations (50 μg/ml) resulted in inhibition of secretion, indicating a dual role for actin (such as a need for actin during the final stages of exocytosis).

During confocal imaging using an anti-actin antibody, we observed an increased sub-plasmalemmal localization of actin (Chapter 3). In order to investigate the possibility of an actin-barrier in the salivary glands of *O. savignyi*, cells were treated with low concentrations (nM) of cytochalasin D and stimulated with dopamine. From the results (Figure 2.32), it is evident that cytochalasin D increased apyrase secretion. At concentrations of 10 and 100 nM, secretion increased with 17% and 49%, respectively. This data indicate that actin plays an important role in apyrase secretion in a manner supporting the actin-physical barrier model. Similar to the work of Orci *et al.*, disassembly of actin was not sufficient for inducing exocytosis. Based on the sub-plasmalemmal localization of actin visible during confocal imaging using an anti-actin antibody (Chapter 3), we propose a barrier function for actin in the salivary glands of *O. savignyi*. In numerous cell types it was shown that actin disassembly is activated by elevation of cytosolic calcium and by activation of PKC (Burgoyne and Morgan 2003). The latter, as well as a function for actin in transport must be investigated in future studies.
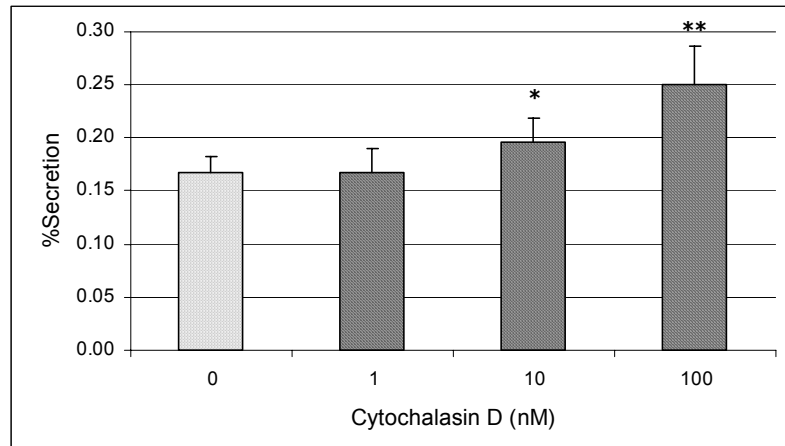
Figure 2.32. The effect of cytochalasin D on dopamine-stimulated apyrase secretion. *Salivary glands were incubated with HBSS containing various concentrations of cytochalasin D for 15 minutes, washed and stimulated with 10µM dopamine. The % apyrase secreted from the salivary glands is indicated. Error bars represent SD with n=12. (*) p<0.05, (**) p<0.001.*

2.6.15.   Tubulin Inhibitor (Colchicine)

Colchicine is an antimitotic agent that disrupts microtubules by binding to tubulin and prevents its polymerization, stimulating the intrinsic GTPase activity of tubulin. Similar to actin, tubules contain various motors such as myosins, kinesins and dyneins required for the transport and delivery of proteins throughout the entire secretory pathway (Apodaca 2001; Neco *et al.* 2003). The effect of disrupting the tubules in salivary glands was investigated by incubating permeabilized glands with colchicine and investigating the effect on dopamine stimulated exocytosis. From the results obtained (Figure 2.34) it is evident that disruption of tubules results in an inhibition of apyrase secretion. At 10 µM colchicine, a 23% decrease in secretion was observed while at higher concentrations such as 50 and 100 µM colchicine a 42% and 44% decrease, respectively, were observed. This indicates that tubules are involved in regulated exocytosis and most likely via the transport of granules to the plasmamembrane where fusion occurs.
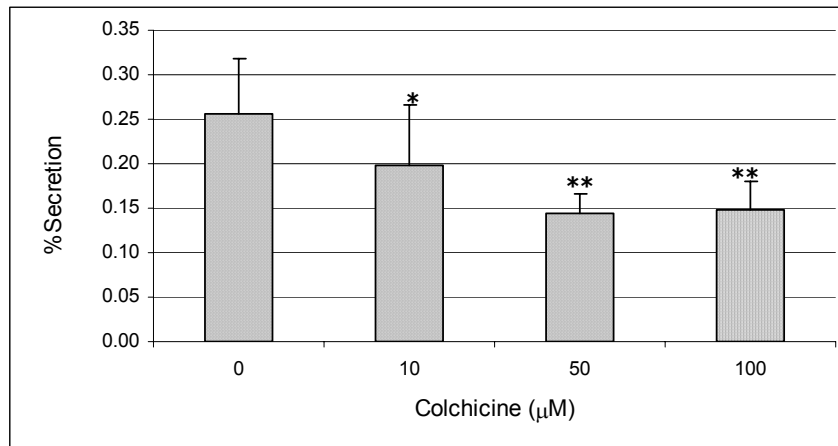
Figure 2.34. The effect of colchicine on dopamine-stimulated apyrase secretion. *Salivary glands were permeabilized with digitonin, incubated with HBSS containing various concentrations of colchicine for 15 minutes, washed and stimulated with 10 μM dopamine. The % apyrase secreted from the salivary glands is indicated. Error bars represent SD with n=12. (*) p<0.05, (**) p<0.001.*

2.7.   CONCLUSION

All of the signaling pathways (steps) investigated during this study are summarized and compared with known pathways of the ixodid tick, *A. americanum* in Table 2.11.

Table 2.11. Comparison between the signaling pathways regulating exocytosis from the salivary glands of *A. americanum* (Ixodidae) and *O. savignyi* (Argasidae).

Signaling step	*A. americanum* (Ixodidae)	*O. savignyi* (Argasidae)
Dopamine/ Adrenergic agonists	- Stimulate exocytosis - Dopamine (D1) receptor $K_a = 0.4\ \mu M$ - Isoproterenol $K_a = 0.15$ mM	- Stimulate exocytosis - Isoproterenol is less sufficient in stimulating exocytosis
Cholinergic agonist	- No effect	- No effect (Carbachol)
Adenylyl cyclase & cAMP	-Activation via dopamine receptor linked to Gs protein -cAMP dependent protein kinase identified - PKA phosphorylate 12 proteins - 3 PKA isoforms identified from cDNA	-Dopamine sensitive adenylyl cyclase -cAMP dependent protein kinase identified -Thr phosphorylation of 6 proteins -No serine phosphorylation
Extracellular Ca^{2+}	- Voltage gated Ca^{2+} channel required. -L-type (Verapamil sensitive)	- Voltage gated Ca^{2+} channel required. -L-type (Verapamil sensitive)
Intracellular Ca^{2+}	- Increase is stimulated by IP_3 in response to PGE_2	- Essential for secretion - Mechanism of release unknown
Prostaglandins	- Cytosolic PLA_2 required (OPC sensitive) -AA increase during feeding -PGE_2 receptor (EP1) K_d ~29 nM, linked to cholera sensitive G protein, activates PLC	- Cytosolic PLA_2 required (OPC sensitive)
Na^+-K^+-ATPase	-Volume saliva (fluid) secreted is decreased in the presence of Ouabain -Function in regulating cell volume	-Ouabain inhibits apyrase secretion, i.e. exocytosis.
Membrane potential	Unknown	-Depolarization is unsufficient for inducing exocytosis
N-ethylmaleimide	Unknown - NSF ATPase has been identified	- Exocytosis is NEM sensitive - Role for NSF ATPase in exocytosis
GTPγS	Unknown	- Exocytosis is G-protein regulated and increase in the presence of GTPγS

PI-3 Kinases	Unknown	-PI-3 kinases are involved in exocytosis (Wortmannin sensitive)
Phospholipase C & IP$_3$	- PLC activated by EP1 receptor - IP$_3$ increase [Ca^{2+}]$_i$	-PLC is required for exocytosis (U73,122 sensitive)
Actin	Unknown	- Actin disassembly is required for exocytosis (Cytochalasin D sensitive)
Microtubules	Unknown	-Intact microtubules are required for exocytosis (Colchicine sensitive).

In order to summarize, we constructed a schematic representation of the known and hypothesized factors regulating apyrase secretion from LDCV (Figure 2.35). Dopamine binds to an extracellular D1 type receptor which activates a L-type voltage gated calcium channel, as well as AC via the Gα subunit to produce cAMP. Elevated cAMP levels activate PKA which phosphorylates threonine residues of various target proteins. We propose that the G$_{\beta\gamma}$ subunits activate PI3-kinases to produce PIns (3,4,5)P3. The possibility of activation of PLC by the G$_{\beta\gamma}$ subunits must be investigated. We propose that the activation of PI3-kinases, and hence the production of PIns(3,4,5)P3 is essential for exocytosis since it acts as a secondary messenger which regulates various kinases, GTPases and protein routing throughout the secretory pathway. Activation of PLC, which results in the production of IP3 and DAG, is essential for exocytosis. We hypothesize that IP$_3$ causes elevated intracellular calcium levels and DAG is involved in the activation of PKC. Since GTPγS stimulation results in exocytosis, one can conclude that GTP binding proteins (GTPases) are involved in exocytosis. Disruption of the actin cytoskeleton resulted in enhanced exocyotosis, indicating the possibilty of an actin web forming a barrier between the granules and plasmamebrane and inhibiting non-specific exocytosis. In contrast, disruption of microtubules inhibited exocytosis. This could be due to tubules regulating granule transport.

Inhibition of exocytosis by N-ethylmaleimide indicates that the ATPase NSF, which forms part of the exocytosis machinery, is involved in driving fusion. A striking difference between ixodid and argasid ticks is the inabilty to stimulate apyrase secretion by exogenous PGE$_2$. Since the PLA$_2$ inhibitor OPC completely inhibited exocytosis, one can conclude that the production of free arachidonic acid is essential. The question still remains what the end product of AA is after metabolism, and it's function is in exocytosis. Also, we cannot comment on the activation of the PLA$_2$ since it was not investigated. We propose in Figure 2.35 that it is activated by an influx of extracellular calcium, similar to ixodid ticks.
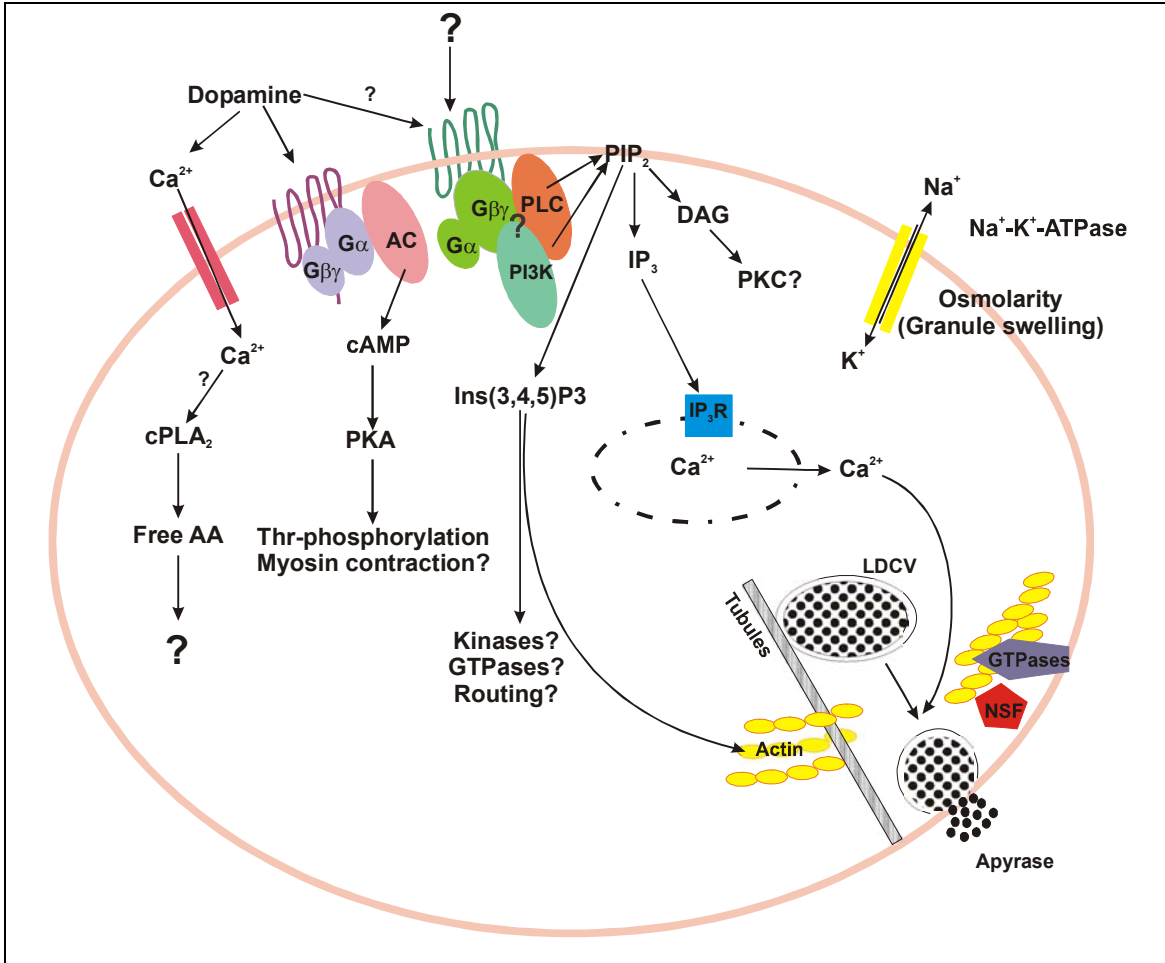
Figure 2.35. Schematic representation of the proposed mechanisms underlying regulated exocytosis of apyrase from LDCVs from the salivary glands of *O. savignyi*.

2.8. REFERENCES

Adam-Vizi, V. (1992). External calcium-independent release of neurotransmitters. *Journal of Neurochemistry* **58**: 395-405.

Apodaca, G. (2001). Endocytic traffic in polarized epithelial cells: Role of the actin and microtuble cytoskeleton. *Traffic* **2**: 149-159.

Banerjee, A., Barry, V.A., DasGupta, B.R., Martin, T.F.J. (1996a). N-ethylmaleimide sensitive factor acts at a prefusion ATP-dependent step in calcium-activated exocytosis. *The Journal of Biological Chemistry* **271**(34): 20223-20226.

Bonacci, T.M., Ghosch, M., Malik, S., Smrcka, A.V. (2005). Regulatory interactions between the amino terminus of G-protein βγ subunits and the catalytic domain of phospholipase Cβ2. *The Journal of Biological Chemistry* **250**(11): 10174-10181.

Bowman, A.S., Dillwith, J.W., Madden, R.D., Sauer, J.R. (1995a). Uptake, incorporation and redistribution of arachidonic acid in isolated salivary glands of the lone star tick. *Insect Biochemistry and Molecular Biology* **25**(4): 441-447.

Bowman, A.S., Dillwith, J.W., Madden, Sauer, J.R. (1995c). Regulation of free arachidonic acid levels in isolated salivary glands from the lone star tick: A role for dopamine. *Archives of Insect Biochemistry and Physiology* **29**: 309-327.

Bowman, A.S., Sauer, J.R., Neese, P.A., Dillwith, J.W. (1995b). Origin of arachidonic acid in the salivary glands of the lone star tick, *Amblyomma americanum*. *Insect Biochemistry and Molecular Biology* **25**(2): 225-233.

Bowman, A.S., Sauer, J.R., Shipley, M.M., Gengler, C.L., Surdick, M.R., Dillwith, J.W. (1993). *Tick salivary prostaglandins: their precursors and biosynthesis.* Vero Beach, Florida, University of Florida-IFAS.

Bowman, A.S., Sauer, J.R., Zhu, K., Dillwith, J.W. (1995d). Biosynthesis of salivary prostaglandins in the lone star tick, *Amblyomma americanum*. *Insect Biochemistry and Molecular Biology* **25**(6): 735-741.

Burgoyne, R.D., Morgan, A. (2003). Secretory granule exocytosis. *Physiology Reviews* **83**: 581-632.

Chasserrot-Golaz, S., Hubert, P., Thierse, D., Dirrig, S., Clahos, C.J., Aunis, D., Bader, M.-F. (1998). Possible involvement of Phosphatidylinositol-3-Kinase in regulated exocytosis: Studies in chromaffin cells with inhibitor LY294002. *Journal of Neurochemistry* **70**(6): 2347-2356.

Chaturvedi, S., Qi, H., Coleman, D., Rodriquez, A., Hanson, P.I., Striepen, B., Roos, D.S., Joiner, K.A. (1999). Constitutive calcium-independent release of *Toxoplasma gondii* dense core granules occurs through the NSF/SNAP/SNARE/Rab machinery. *The Journal of Biological Chemistry* **274**(4): 2424-2431.

Eitzen, G. (2003). Actin remodeling to facilitate membrane fusion. *Biochimica et Biophysica Acta* **1641**: 175-181.

El Shoura, S.M. (1985). Ultrastructure of salivary glands of *Ornithodoros moubata* (Ixodoidea: Argasidae). *Journal of Morphology* **186**: 45-52.

Finkelstein, A., Zimmerberg, J., Cohen, F.S. (1986). Osmotic swelling of vesicles: Its role in the fusion of vesicles with planar phospholipid bilayer membranes and its possible role in exocytosis. *Annual Reviews in Physiology* **48**: 163-174.

Foster, L.J., Yeung, B., Mohtashami, M., Ross, K., Trimble, W.S., Klip, A. (1998). Binary interactions of the SNARE proteins syntaxin-4, SNAP23 and VAMP-2 and their regulation by phosphorylation. *Biochemistry* **37**: 11089-11096.

Hirling, H., Scheller, R.H. (1996). Phosphorylation of synaptic vesicle proteins: Modulation of the alpha-SNAP interaction with the core complex. *Proceedings of the National Academy of Science of the United States of America* **93**: 11945-11949.

Huijbregts, R.P.H., Topalof, L., Bankaitis, V.A. (2000). Lipid metabolism and regulation of membrane trafficking. *Traffic* **1**: 195-202.

Jeziorski, M.C., Greenberg, R.M., Anderson, P.A.V. (2000). The molecular biology of invertebrate voltage-gated calcium channels. *The Journal of Experimental Biology* **203**: 841-856.

Kogut, M., Lowry, V.K., Farnell, M. (2002). Selective pharmacological inhibitors reveal the role of Syk tyrosine kinase, phospholipase C, phosphatidylinositol-3-kinase, and p38 mitogen-activated protein kinase in Fc receptor-mediated signaling of chicken heterophil degranulation. *Int Immunopharmacology* **2**(7): 963-973.

Lang, I., Walz, B. (1999). Dopamine stimulates salivary duct cells in the cockroach *Periplaneta americana*. *The Journal of Experimental Biology* **202**: 729-738.

Lindsay, P.J., Kaufman, R. (1986). Potentiation of salivary fluid secretion in ixodid ticks: A new receptor system for gamma-aminobutyric acid. *Canadian Journal of Physiology and Pharmacology* **64**: 1119-1126.

Lonart, G., Sudhof, T.C. (2001). Characterization of rabphillin phosphorylation using phospho-specific antibodies. *Neuropharmacology* **41**: 643-649.

Mane, S.D., Darville, R.G., Sauer, J.R., Essenberg, R.C. (1985). Cyclic AMP-dependent protein kinase from the salivary glands of the tick, *Amblyomma americanum*. *Insect Biochemistry* **15**(6): 777-787.

Mane, S.D., Essenberg, R.C., Sauer, J.R. (1987). Kinetics of the phosphotransferase reaction of the catalytic subunit of the tick salivary gland cAMP-dependent protein kinase. *Insect Biochemistry* **17**(5): 665-672.

Mans, B.J. (2002a). Functional perspectives on the evolution of argasid tick salivary gland protein superfamilies. *Biochemistry*. Pretoria, University of Pretoria.

Marash, M., Gerst, J.E. (2001). t-SNARE dephosphorylation promotes SNARE assembly and exocytosis in yeast. *The EMBO Journal* **20**(3): 411-421.

Marino, C.R., Castle, D., Gorelick, F.S. (1990). Regulated phosphorylation of secretory granule membrane proteins of the rat parotid gland. *American Journal of Physiological* **259**(1Pt1): G70-G77.

McSwain, J.L., Essenberg, R.C., Sauer, J.R. (1985). Cyclic AMP mediated phosphorylation of endogenous proteins in the salivary glands of the lone star tick, *Amblyomma americanum* (L.). *Insect Biochemistry* **15**(6): 789-802.

McSwain, J.L., Essenberg, R.C., Sauer, J.R. (1992a). Oral secretion elicited by effectors of signal transduction pathways in the salivary glands of *Amblyomma americanum* (Acari: Ixodiddae). *Journal of Medical Entomology* **29**(1): 41-48.

McSwain, J.L., Masaracchia, R.A., Essenberg, R.C., Tucker, J.S., Sauer, J.R. (1992b). *Amblyomma americanum* (L.): Protein kinase C independent fluid secretion by isolated salivary glands. *Experimental Parasitology* **74**: 324-331.

McSwain, J.L., Tucker, J.S., Essenberg, R.C., Sauer, J.R. (1989). Brain factor induced formation of inositol phosphates in tick salivary glands. *Insect Biochemistry* **19**: 343-349.

Narumiya, S., Sugimoto, Y., Ushikubi, F. (1999). Prostanoid receptors: Structures, properties and functions. *Physiological Reviews* **79**(4): 1193-1226.

Neco, P., Giner, D., Frances, M., Viniegra, S., Gutierrez, L.M. (2003). Differential participation of actin- and tubulin-based vesicle transport systems during secretion in bovine chromaffin cells. *European Journal of Neuroscience* **18**: 733-742.

Orci, L., Gabbay, K.H., Malaisse, W.J. (1972). Pancreatic beta-cell web: its possible role in insulin secretion. *Science* **175**: 1128-1130.

Palmer, M.J., McSwain, J.L., Spatz, M.D., Tucker, J.S., Essenberg, R.C., Sauer, J.R. (1999). Molecular cloning of cAMP-dependent protein kinase catalytic subunits isoforms from the lone star tick, *Amblyomma americanum* (L.). *Insect Biochemistry and Molecular Biology* **29**: 43-51.

Pedibhotla, V.K., Sarath, G., Sauer, J.R., Stanley-Samuelson, D.W. (1995). Prostaglandin biosynthesis and subcellular localization of prostaglandin H synthase activity in the lone star tick, *Amblyomma americanum*. *Insect Biochemistry and Molecular Biology* **25**(9): 1027-1039.

Qian, Y., Essenberg, R.C., Dillwith, J.W., Bowman, A.S., Sauer, J.R. (1997). A specific prostaglandin E2 receptor and its role in modulating salivary secretion in the female tick, *Amblyomma americanum* (L.). *Insect Biochemistry and Molecular Biology* **27**(5): 387-395.

Qian, Y., Yuan, J., Essenberg, R.C., Bowman, A.S., Shook, A.L., Dillwith, J.W., Sauer, J.R. (1998). Prostaglandin E2 in the salivary glands of the female tick, *Amblyomma americanum* (L.): calcium mobilization and exocytosis. *Insect Biochemistry and Molecular Biology* **28**: 221-228.

Risinger, C., Bennett, M.K. (1999). Differential phosphorylation of syntaxin and synaptosome associated protein of 25 kDa (SNAP-25) isoforms. *Journal of Neurochemistry* **72**(2): 614-624.

Roshdy, M.A. (1972). The subgenus *Persicargas* (Ixodoidae, Argasidae, *Argas*). 15. Histology and histochemistry of the salivary glands of *A. (P.) persicus (Oken)*. *Journal of Medical Entomology* **9**: 143-148.

Roshdy, M.A., Coons, L.B. (1975). The subgenus Persicargas (Ixodidea: Argasidae: Argas). 23. Fine structure of the salivary glands of unfed *A. (P.) arboreus* (Kaiser, Hoogstraal and Kohls). *Journal of Parasitology* **61**: 743-752.

Sauer, J.R., Essenberg, R.C., Bowman, A.S. (2000). Salivary glands in ixodid ticks: control and mechanism of secretion. *Journal of Insect Physiology* **46**: 1069-1078.

Sauer, J.R., Hair, J.A. (1986). *Morphology, physiology and behavioral biology of ticks.* New York, Chichester, Brisbane, Toronto, Halsted Press: A division of John Wiley & Sons.

Schmidt, S.P., Essenberg, R.C., Sauer, J.R. (1981). Evidence for a D1 dopamine receptor in the salivary glands of *Amblyomma americanum* (L.). *Journal of Cyclic Nucleotide Research* **7**(6): 375-384.

Shipley, M.M., Dillwith, J.W., Bowman, A.S., Essenberg, R.C., Sauer, J.R. (1993). Changes in lipids of the salivary glands of the lone star tick, *Amblyomma americanum*, during feeding. *Journal of Parasitology* **79**(6): 834-842.

Shipley, M.M., Dillwith, J.W., Bowman, A.S., Essenberg, R.C., Sauer, J.R. (1994). Distrubution of arachidonic acid among phospholipid subclasses of the lone star tick salivary glands. *Insect Biochemistry and Molecular Biology* **24**(7): 663-670.

Sigma-Aldrich (2002). *Cell signaling and Neuroscience*. Missouri, USA, Sigma-Aldrich Corporation.

Sonenshine, D.E. (1991). *Biology of ticks*. New York, Oxford, Oxford University Press.

Troyer, K.P., Wightman, R.M. (2002). Temporal separation of vesicle release from vesicle fusion during exocytosis. *The Journal of Biological Chemistry* **277**(32): 29101-29107.

Versteeg, H.H., van Bergen, P.M.P., van Deventer, S.J.H., Peppelenbosch, M.P. (1999). Cyclooxygenase-dependent signalling:molecular events and consequences. *FEBS Letters* **445**: 1-5.

Voet, D., Voet, J.G. (1995). *Biochemistry*. New York, Chichester, Brisbane, Toronto, Singapore, John Wiley & Sons, Inc.

Watling, K.J. (2001). *The Sigma-RBI handbook of receptor classification and signal tranduction*. Natick, MA, Sigma-Aldrich Research Biochemicals Incorporated.

Yuan, J., Bowman, A.S., Aljamali, M., Payne, M.R., Tucker, J.S., Dillwith, J.W., Essenberg, R.C., Sauer, J.R. (2000). Prostaglandin E2-stimulated secretion of protein in the salivary glands of the lone star tick via a phosphoinositide signallling pathway. *Insect Biochemistry and Molecular Biology* **30**: 1099-1106.

CHAPTER 3

INVESTIGATIONS INTO THE CONSERVED CORE MACHINERY OF REGULATED EXOCYTOSIS IN THE SALIVARY GLANDS OF *O. savignyi*

3.1. INTRODUCTION

In essentially all cells a process known as constitutive exocytosis occurs, where secretory vesicles fuse to the plasma membrane in order to insert new cell membrane and membrane components. In many cells a second pathway, termed regulated exocytosis, also exists where fusion occurs only in response to a physiological signal (Burgoyne and Morgan 2003). To date, the process of regulated exocytosis has been most extensively studied in cells with a crucial physiological or pathophysiological interest. The wide variety of secretory granule-containing cells in mammalian species are shown in Table 3.1.

Table 3.1. Cells with secretory granules (Burgoyne and Morgan 2003)

Class of cell	Cell Type	Granule
Neuron	Various	Dense-core vesicles
Endocrine neurons	Hypothalamic	Large dense core-vesicles
	Posterior pituitary	Large dense core-vesicles
	Median eminence	Large dense core-vesicles
Neuroendocrine/endocrine cells	Adrenal chromaffin	Chromaffin granules
	Anterior pituitary	Secretory granules
	Atrial myocytes	Secretory granules
	Carotid body glomus cells	Secretory granules
	Gut enteroendocrine cells	Secretory granules
	Gastric enterochromaffin-like cells	Secretory granules
	Gastric G cells	Secretory granules
	Intestinal I cells (cholecystokinin)	Secretory granules
	Kidney juxtaglomerulat cells (rennin)	Secretory granules
	Pancreatic A cells (glucagon)	Secretory granules
	Pancreatic B cells (Insulin)	Secretory granules
	Pancreatic D cells (Somatostatin)	Secretory granules
	Pancreatic F cells (Pancreatic polypeptide)	Secretory granules
	Parathyroid cells (Parathyroid hormone)	Secretory granules
	Pineal glands	Secretory granules
	Posterior pituitary	Secretory granules
	Thyroid C cells (calcitonin)	Secretory granules

Exocrine	Airway goblet cells	Mucin granules
	Alveolar type II epithelial cells	Lamellar body
	Gastric chief cells	Secretory granules
	Intestinal goblet cells	Mucin granules
	Lacrimal	Zymogen granules
	Mammary epithelial cells	Casein vesicles
	Pancreatic acinar cells	Zymogen granules
	Parotid	Zymogen granules
	Submaxillary	Zymogen granules
Hemopoietic	Basophils	Lysosome-related granule
	Eosinophils	Lysosome-related granule
	Macrophages	Multiple granules
	Mast cells	Lysosome-related granule
	Neutrophils	Multiple granules
	Platelets	Lysosome, dense and α-granules
	T-cells	Lysosome-related granule
Other	Endothelial cells	Weibel-Palade body
	Melanocytes	Melanosomes
	Sperm	Acrosome
	Egg	Cortical granules
	All cell types	Lysosomes

3.1.1. Conserved core machinery for regulated exocytosis

The idea of stimulation-secretion coupling during regulated exocytosis, with calcium as the key trigger, was generally accepted by the 1970's (Burgoyne and Morgan 2003). The downstream mechanisms leading to membrane fusion was, however, unknown. The first enhancement to our understanding of membrane fusion came from the work of Novick and Schekman who isolated the first secretory (sec) mutant sec1 from mutagenized yeast cells, after screening for temperature-sensitive secretion mutants (Novick and Schekman 1979). The second breakthrough came from the work of Rothman who identified NSF, which was purified from isolated Golgi complexes and cytosol based on its ability to reconstitute intra-Golgi transport after blockage by N-ethylmaleimide (Rothman 1994). Analysis of the NSF gene indicated that the coding sequence of NSF is 48% identical to that of the yeast *SEC18* gene. Later, it was shown that sec18 could substitute for NSF in mammalian *in vitro* assays of endosome fusion, intra-Golgi transport and granule exocytosis. This suggests that NSF and sec18 contribute similar functions to an evolutionary ancient molecular mechanism of membrane fusion in all cells (Burgoyne and Morgan 2003).

This hypothesis was supported when protein-protein interaction studies revealed that NSF and its co-factor, α-soluble NSF attachment protein (α-SNAP; Sec17 in yeast), interact with membranes via a SNAP receptor (SNARE) complex comprising VAMP/synaptobrevin (Snc1/2 in yeast), syntaxin (Sso1/2 in yeast) and SNAP-25 (Sec9 in yeast). Realization that two additional protein families, namely the Rabs and the Sec1 homologs, were also involved in multiple vesicular transport processes led to the concept of a universal mechanism of membrane fusion (Burgoyne and Morgan 2003). The key proteins involved in regulated exocytosis are listed in Table 3.2.

Table 3.2. Key proteins that function in exocytosis in neurons and in secretory granule exocytosis (Burgoyne and Morgan 2003)

Protein class	Neuronal Protein	Endocrine	Homologues in non-neuronal cells
SNAREs	Syntaxin SNAP-25 VAMP (Synaptobrevin)	Yes Yes Yes	Syntaxin isoforms SNAP-23 Yes
SNARE regulators	α-SNAP NSF Munc18 / nSec1 Munc 13	Yes Yes Yes Yes	Yes Yes Isoforms ?
Rabs and effectors	Rab3 Rabphillin Rim Noc2	Yes Yes Yes Yes	Other Rabs Yes ? Endocrine cells
Calcium binding proteins	Synaptotagmin Calmodulin CAPS	Yes Yes Yes	Yes Yes ?
Others	Csp Synapsins	Yes No	Yes Neuron specific

a. The SNAREs

SNAREs are membrane proteins that are localized to various intracellular organelles and are identified by a characteristic heptad repeat sequence known as the SNARE motif. Three proteins namely syntaxin, VAMP/synaptobrevin (vesicle associated membrane protein) and SNAP-25 form a SNARE complex, first described in synapses by Sollner et al. (Sollner et al. 1993). Since VAMP is localized on the vesicle membrane and syntaxin and SNAP-25 localize to the plasma membrane, SNAREs were originally classified as vesicle (v-) or target (t-)

SNAREs. More recently a rival classification system has been proposed based on whether a conserved glutamine (Q) or arginine (R) is present in the SNARE motif in the so-called zero layer (Figure 3.1.). In the SNARE complex, syntaxin contributes one Q-containing helix; SNAP-25 contributes two Q-containing helices and VAMP one R-containing helix. Characterized SNARE complexes always contain three Q-helices and one R helix. This code of 3Q:1R helices has been shown to be an essential combination which, in a lock-and-key fashion, allows specific SNARE pairing and consequent membrane fusion (Katz and Brennwald 2000). The Q and R residues are not essential for membrane fusion, but mutation impairs disassembly of the SNARE complex by NSF and α-SNAP (Graham *et al.* 2001).
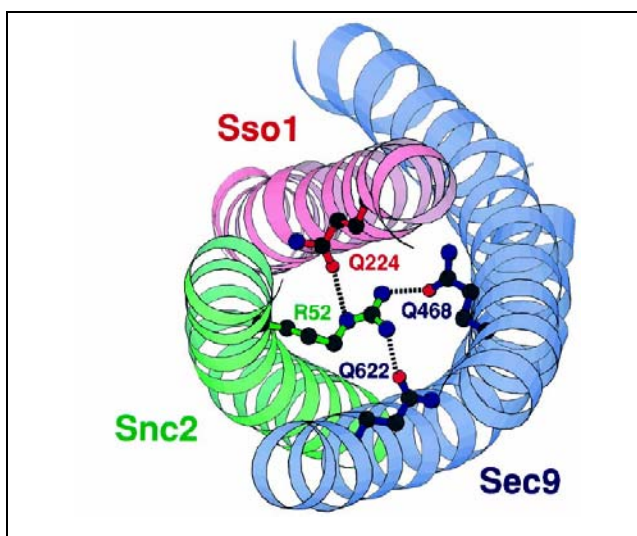
Figure 3.1. Model of the ionic layer of the yeast post-Golgi SNARE complex (Katz and Brennwald 2000). *The yeast post-Golgi SNARE complex is a parallel four-helix bundle with most of the layers composed entirely of hydrophobic residues. Roughly halfway along the axis of the helical bundle is a unique ionic layer (also known as zero layer) consisting of an arginine and three glutamines. Within this layer, the arginine is contributed by the v-SNARE Snc2 (synaptobrevin) and the glutamines are contributed by the t-SNAREs Sec9 (SNAP-25) and Sso1 (Syntaxin). The glutamine and arginine residues form an extensive network of hydrogen bonds with each other. The flanking hydrophobic layers stabilize the ionic layer by protecting the polar interactions from exposure to the surrounding environment.*

By using either mutational studies, clostridial neurotoxins, SNARE-directed antisera or peptides it could be shown that SNAREs are essential for regulated granule exocytosis in various cell types such as adrenal chromaffin cells, PC12 cells, pancreatic B-cells, pancreatic acinar cells, AtT-20 cells, eosinophils, platelets, peptiderigic hypothalamic neurons, gastric enterochromaffin-like cells and sperm (Burgoyne and Morgan 2003). Based on various observations, it is believed that SNAREs are involved in regulated exocytosis by driving

membrane fusion. The accepted model comprises of four steps. First, syntaxin is unavailable for SNARE complex formation due to its association with munc18. Secondly, dissociation of munc18 renders syntaxin in the open conformation. Thirdly, the SNAREs interact and assemble into the four-helical bundle. Finally, as the complex is fully assembled, the lipid bilayers of the plasma membrane and vesicle are brought close enough for bilayer fusion to occur.

Syntaxin

All eukaryotes examined to date contain syntaxin-like sequences. In mammals, the syntaxin family consists of 15 genes and in yeast of 7 genes (Teng *et al.* 2001). Alternative splicing generates additional diversity within the family. All mammalian syntaxins (excluding syntaxin 11) are transmembrane proteins (~35 kDa) anchored by their C-terminal tail; therefore the amino-terminus and polypeptide face the cytoplasm. The SNARE-domain of approximately 60-residues is conserved in all syntaxins and mediates interactions with SNARE domains of other target membrane SNARE proteins (Teng *et al.* 2001). These include other syntaxins, SNAP-25 and VAMP. The amino terminus of some syntaxins serves as an auto-inhibitory domain by folding back onto the membrane proximal SNARE domain. In this case, the formation of a fusion complex is inhibited and the molecule is said to be in a 'closed' configuration (Figure 3.2). The chaperone protein n-Sec1 / munc18 binds to this closed conformation of syntaxin and dissociates upon a structural change induced by Rab GTPases to yield an 'open' configuration (Teng *et al.* 2001; Burgoyne and Morgan 2003).
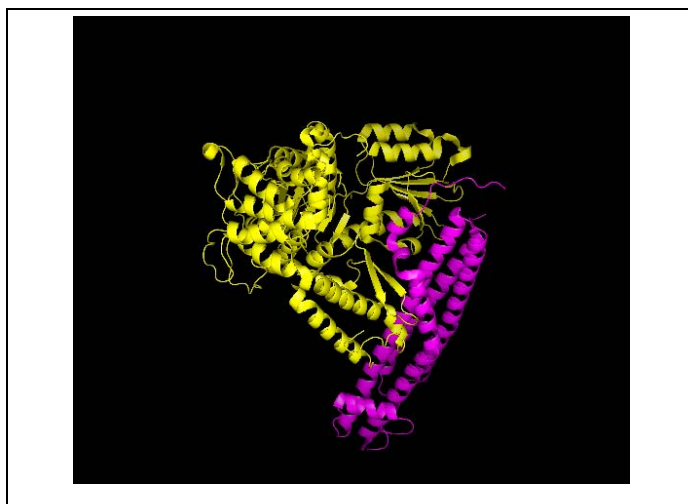
Figure 3.2. Crystal structure of the neuronal Sec1/syntaxin 1a complex (Misura *et al.* 2000). *The four helical bundles of syntaxin (purple) and nSec1 (yellow) bound to the N-terminal of syntaxin are shown.*

Syntaxins are localized to various subcellular locations where they function in anterograde, endocytotic/retrograde flow of traffic and known membrane transport steps (Table 3.3). They have also been shown to interact with a range of proteins other than their SNARE partners. These include vesicle coat proteins (Teng *et al.* 2001), Rab GTPases and effectors (Takai *et al.* 2001; Torii *et al.* 2002), tethering factors (Takai *et al.* 2001), channels such as the sodium channel, CFTR chloride channel (Kleizen *et al.* 2000) and voltage-sensitive calcium channels (Atlas 2001), as well as munc proteins (Betz *et al.* 1997; Kauppi *et al.* 2002).

Table 3.3. Cellular and functional information about mammalian syntaxins (Teng *et al.* 2001).

Isoform	Cellular Localization	Tissue Distribution	Known Function
Syntaxin 1 (A, B and C)	Presynaptic plasma membrane	Neuronal cells Secretory cells	Neuronal exocytosis Regulated exocytosis
Syntaxin 2 (A, B, C and D)	Plasma membrane	Ubiquitous	Exocytosis Morpho-regulator during development
Syntaxin 3 (A, B, C and D)	Plasma membrane	Ubiquitous	Exocytosis
Syntaxin 4	Plasma membrane	Ubiquitous	Glut4 translocation
Syntaxin 5 (Long and short form)	ER-Golgi boundary	Ubiquitous	ER-Golgi transport
Syntaxin 6	TGN	Ubiquitous	TGN-endosome transport Endosome-TGN transport Fusion of immature secretory granules
Syntaxin 7	Endosome	Ubiquitous	Late endosome fusion Late endosome-lysosome fusion
Syntaxin 8	Endosome	Ubiquitous	Late endosome fusion
Syntaxin 10	TGN	Ubiquitous	Unknown
Syntaxin 11	TGN / Late endosome	Ubiquitous	Unknown
Syntaxin 12 / 13	Endosome	Ubiquitous	Recycling of surface protein Early endosome fusion
Syntaxin 16 (A, B and C)	Golgi / TGN	Ubiquitous	Early endosome-TGN transport
Syntaxin 17	Smooth ER	Steroidogenic tissues	Trafficking to smooth ER
Syntaxin 18	ER	Unknown	ER-Golgi transport ER homotypic fusion

A recent study by Karim *et al.*, identified syntaxin isoforms 1 and 2 in the salivary gland of the lone star tick, *A. americanum* by means of Western blotting. Both syntaxin isoforms 1

and 2 proteins have a molecular mass of 35 kDa (similar to that in brain extracts) and are enriched in the membrane fraction obtained by centrifugation at 100,000 x g (Karim *et al.* 2002). Preliminary studies using partially purified plasma membrane indicated that tick syntaxins are localized on the plasma membrane since they co-localize with the Na^+/K^+-ATPase following sucrose density centrifugation (Karim *et al.* 2002).

Synaptobrevin / VAMP (<u>V</u>esicle <u>a</u>ssociated <u>m</u>embrane <u>p</u>rotein)

The synaptobrevin / VAMP family members are small type II membrane proteins of about 120 amino acids (~18 kDa). They consist of a variable region of 25-35 amino acids located at the amino terminus, followed by either one extended or two short (helix 1 and 2) amphiphatic α-helical segments, which form coiled-coil structures and have a transmembrane domain located at their carboxyl terminus (Gerst 1999). Helix 1 is unusually hydrophobic and may interact with lipids during the process of membrane fusion while helix 2 is involved in SNARE-SNARE interactions (Grote *et al.* 1995). Various isoforms and spliced variants have been identified to date (Table 3.4).

Table 3.4. Cellular and functional information of synaptobrevins (Gerst 1999; Jahn 1999).

Protein	Synonym	Localization	Trafficking event
Synaptobrevin 1	VAMP1	Synaptic vesicles Clathrin-coated vesicles	Regulated exocytosis
Snc1 and Snc2	Yeast equivalent of VAMP1 / 2	Plasma membrane	Golgi to Plasma membrane
Synaptobrevin 2	VAMP2	Synaptic vesicles / Secretory granules Clathrin-coated vesicles	Regulated and Constitutive exocytosis
Cellubrevin	VAMP3	Ubiquitous Microvesicles Clathrin-coated vesicles	Regulated and Constitutive exocytosis
VAMP 4	Synaptobrevin 4	Unknown	Unknown
VAMP 5/6	Synaptobrevin 5/6	Myogenesis skeletal muscle and heart Plasma membrane Intravesicular structures	Constitutive exocytosis
Ti-VAMP	VAMP 7 / Synaptobrevin-like protein	Apical membrane Secretory granules Endosomes	Regulated and Constitutive exocytosis
Endobrevin	VAMP 8	Early Endosomes	Endocytosis?

The study of Karim *et al*. also identified VAMP2 in the salivary glands of *A. americanum* (Karim *et al.* 2002). The protein identified by Western blotting with an anti-VAMP2 antibody, co-migrated with the 18 kDa VAMP protein in rat brain. By purifying secretory granules and vesicles by means of a two-step sucrose gradient centrifugation, it could be shown that VAMP-2 localize to the granule fraction (chromogranin B positive) and not the plasma membrane fraction.

SNAP 25

SNAP-25 belongs to a family of evolutionary conserved proteins whose members are essential for membrane fusion. SNAP-25 is a hydrophilic protein of 206 amino acids. It associates with membranes through palmityl residues, which are thioester-linked to four closely spaced cysteine residues at the centre of the protein (Hodel 1998). The N- and C terminals are highly conserved and are predicted to form intermolecular coiled coils. Proteolysis by botulinum toxins A, E and C1 truncates SNAP-25 by cleaving a single peptide bond near the C-terminus. Syndet and SNAP-23 are ubiquitously expressed homologues of SNAP-25 with a sequence homology of ~60%. These homologues are thought to mediate constitutive exocytosis by interacting with other isoforms of the SNAREs syntaxin and VAMP at the plasma membrane (Figure 3.3) (Hodel 1998).
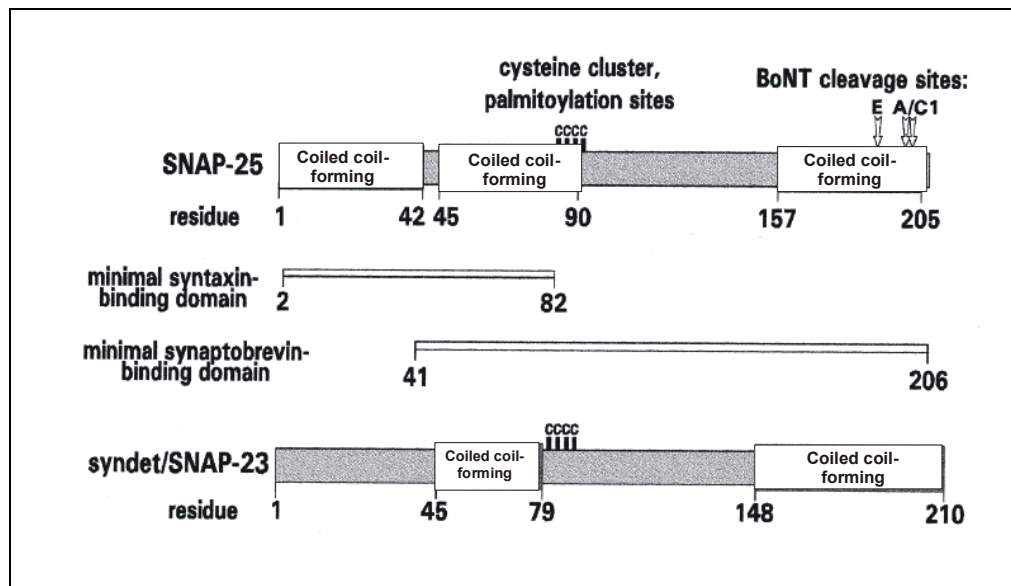
Figure 3.3. Protein structure of neuronal SNAP-25 and ubiquitously expressed homologues (Hodel 1998).

Although SNAP-25 is predominantly expressed in neuronal cells, it has been shown to be essential for the exocytosis of large dense core vesicles from neuroendocrine cells (Hodel 1998), PC12 cells (Banerjee *et al.* 1996b) and chromaffin cells (Tagaya *et al.* 1996). Apart from forming the SNARE complex, SNAP-25 has also been shown to bind and negatively modulate calcium channels (Hodel 1998). It also binds the calcium sensor synaptotagmin (Gerona *et al.* 2000). When part of the SNARE complex, SNAP-25 mediates subsequent binding of α-SNAP (Marz *et al.* 2003).

In a study by Castle *et al.* SNAP-23 has been implicated as a link between signaling and exocytosis in mast cells. Their findings indicated stimulus-induced relocation of SNAP-23 from foci in the plasma membrane to putative sites of membrane fusion both at the cell surface and intracellularly between granules (Castle *et al.* 2001).

Niemeyer and Schwarz have identified a new member of the family, SNAP-24 in Drosophila. Unlike SNAP-25, SNAP-24 is not concentrated in synaptic regions but can form complexes with both synaptic- and non-synaptic v-SNAREs. High levels of SNAP-24 were found in larval salivary glands, where they localized mainly to granule membranes. During a massive exocytotic event of these glands, SNAP-24 containing granules fused with one another and the apical membrane. This suggests that SNAP-24 is a mediator of secretion and granule-granule fusion in salivary glands (Niemeyer and Schwarz 2000).

b. NSF and SNAPs

NSF is a homo-oligomeric ATPase consisting of three 76 kDa subunits, which function together with SNAPs to disassemble SNARE complexes (Burgoyne and Morgan 2003). Owing to the extreme stability of the SNARE complex, disassembly requires ATP hydrolysis which is provided by NSF. Each identical subunit of NSF has a N-terminal domain required for binding to α-SNAP, followed by two ATPase domains (D1 and D2) with distinct, essential functions. The ability to hydrolyze ATP is unique to the D1 domain, whereas the function of the inactive D2 domain is to establish the oligomeric complex. Conformational changes in NSF upon ATP hydrolysis are transduced to α-SNAP to unwind the four helices of the SNARE complex. Apart from disassembling SNARE complexes, NSF has also been shown to function independently of SNAREs by binding different receptors (or their interacting proteins) and to regulate their insertion or removal from the plasma membrane. Such receptors include the AMPA receptor,

the β_2-adrenergic receptor, β-arrestin and the GABA$_A$ receptor-associated protein (Burgoyne and Morgan 2003).

Soluble NSF-attachment proteins (SNAPs) were identified in 1990 because of their ability to restore intracellular vesicular protein transport after salt extraction of Golgi-membranes (Stenbeck 1998). SNAPs are required to mediate membrane attachment of the cytosolic protein NSF. In mammals there are three isoforms, α-, β- and γ-SNAP. All are soluble and have molecular masses between 33-36 kDa. α and γ-SNAP are expressed ubiquitously while β-SNAP is restricted to the brain (Stenbeck 1998). In chromaffin cells, both α and β-SNAPs enhance exocytosis induced by micromolar calcium, but only α-SNAP does so at sub-micromolar calcium levels. Binding of α- and β-SNAPs to the SNARE complex induces a conformational change that renders it competent for binding and activating the ATPase activity of the D1 domain of NSF. The function of γ-SNAP remains unclear (Burgoyne and Morgan 2003).

To date, functional evidence supports a role for α-SNAP and/or NSF in granule exocytosis in chromaffin cells, PC12 cells, pancreatic β-cells, spermatozoa and platelets. Certain observations also suggest a chaperone function for NSF and α-SNAP, continually disassembling *cis* complexes (granule-granule) to release SNARE proteins to engage in *trans* (granule-plasma membrane) and hence further membrane fusion events (Burgoyne and Morgan 2003).

c. The Sec1 / Munc proteins

Genetic studies have established the importance of Sec-1 related genes in vesicle fusion in a wide variety of organisms such as yeast, plants, nematodes, flies and mice. Since the isolation of the first sec proteins from yeast (Sec1), three Sec1 orthologs have been isolated in mammals. These include the neuronal/endocrine munc18-1/nSec1 proteins, the ubiquitous munc18-2 and the munc18-3 isoforms. Sec1 family members from numerous organisms have been shown to interact with syntaxin homologs. In yeast, the syntaxins Sso1 and Sso2 act as suppressors of sec1-1 mutants while in neuronal tissue it has been shown that Sec1/munc18 bind syntaxin with nanomolar affinity *in vitro* to form a complex that precludes syntaxin-binding to other SNAREs. These observations suggest that Sec1 proteins act as syntaxin chaperones, preventing SNARE complex assembly until signaled to release syntaxin (Burgoyne and Morgan 2003).

Sec1 proteins have been implicated in granule exocytosis in pancreatic cells, platelets, pancreatic acinar cells, PC12 cells and chromaffin cells (Burgoyne and Morgan 2003). In the tick, *A. americanum*, it was shown that an anti-human nSec1 polyclonal antibody reacts with a 68 kDa protein in various salivary gland fractions. Several low molecular bands also cross-reacted both in the salivary gland fractions and the rat brain tissue, used as positive control (Karim *et al.* 2002).

d. Rabs and Rab-effectors

Rab GTPases (Ras-related in brain) belongs to the Ras family of small GTPases and form the largest branch of the small G protein superfamily (Stenmark and Olkkonen 2001). They exist in all eukaryotic cells, and to date more than 60 Rab proteins and isoforms have been identified in mammalian cells (Pfeffer 2001; Takai *et al.* 2001). At first it was thought that Rab proteins regulate intracellular vesicle trafficking, but it is now emerging that Rab proteins are key to the recruitment of membrane-tethering and docking factors that facilitate membrane traffic. In some cases, Rabs are important for the formation of transport vesicles and the recruitment of motor proteins onto vesicles to allow vesicle motility. But how do Rabs facilitate all these different functions? The answer lies in the various scaffolds built by the various Rabs (Pfeffer 2001).

Within cells, Rabs are reversibly localized between the cytosolic face of distinct intracellular membranes and the cytosol. This reversible location depends on the post-translational modification of a cysteine motif (CXXX, CC, CXC, CCXX or CCXXX where X is any amino acid) at the C-terminal, with one or more highly hydrophobic geranylgeranyl groups. This modification entails the recognition of the newly synthesized Rab by a Rab escort protein (REP), which presents it to the geranylgeranyl transferase. REP also functions as a chaperone that keeps the hydrophobic geranylated Rab soluble and delivers it to the appropriate membrane. The REP-Rab GTPase is in the GDP-form, but upon membrane delivery GDP/GTP exchange is catalyzed by a GDP/GTP exchange factor (GEF) that causes the release of the REP.

Rab proteins then cycle between the GDP-bound inactive and GTP-bound active forms and between the cytosol and membrane (Figure 3.4). At steady state, 10-50% of a given Rab protein is detected in the cytosol (Takai *et al.* 2001). Prenylated Rabs are bound to the GDP-GTP dissociation inhibitor (GDI) in the cytosol. This complex has the capacity to deliver the

Rabs to the correct compartment in their GDP-bound forms. A proteinaceous factor named GDI-displacement factor (GDF) releases a Rab from the GDI, permitting the Rab to insert into the adjacent membrane. Activation by a GDP-GTP exchange factor (GEF) follows and conversion to the GTP-bound form enables effector binding (Pfeffer 2001).
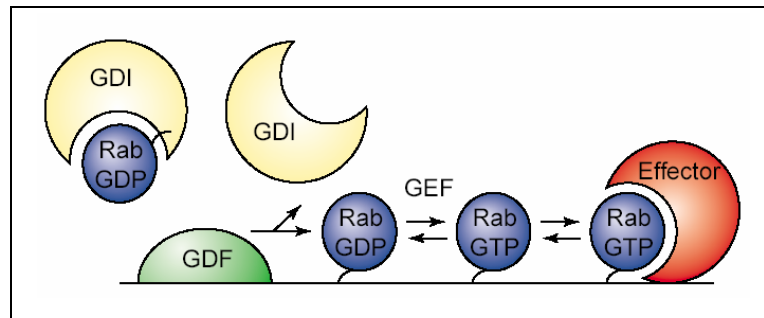
Figure 3.4. A model for Rab recruitment (Pfeffer 2001). *Prenylated Rabs are bound to GDP-GTP dissociation factor (GDI) in the cytosol. This complex has the ability to deliver Rabs to the correct compartment in their GDP-bound forms. A GDI-displacement factor (GDF) releases a Rab from the GDI, permitting Rab to insert into the adjacent membrane. Activation by a GDP-GTP exchange factor (GEF) follows; conversion to the GTP-bound form enables effector binding.*

Organelles have always been classified by the marker molecules present, for example in the Golgi stack where each cisterna houses a separate set of enzymes. The early Golgi contains mannosidase I, medial Golgi contains N-acetylglucosmaine transferase I, and the late Golgi galactosyl transferase, and so on. For endocytic compartments, the classification was less clear until the realization that different compartments in the exocytic and endocytic pathways contain distinct Rab GTPases on their surfaces (Pfeffer 2001). Furthermore, Rabs are now known to collect integral and peripheral membrane proteins into a specific domain (or scaffold) on an organelle. One such an example is Rab1, which enables the Golgi to recognize incoming cargo by the GM130-GRASP65 scaffold. Rab1 has been shown to interact with a complex of GM130-GRASP65, thereby facilitating the delivery of transport vesicles to the Golgi (Pfeffer 2001). Rab1 also provides a link between vesicles leaving the ER and their destination (the Golgi) by binding to p115, a protein that interacts with the Golgi scaffold. The localization and function of some other Rabs are summarized in Table 3.5.

Numerous genetic and biochemical studies indicated that the key to the function of Rab proteins is the recruitment of effector molecules, which bind exclusively to Rabs in their GTP-form. Crystallographic data indicated that Rab proteins adopt two different conformations when in the GDP- and GTP-bound states and that binding between Rabs and their effectors

is via the switch domains. These domains are described as the two major nucleotide-induced conformation-changing domains and are located in loops 2 and 5 on the surface of the Rab protein. Rab effectors are a very heterogeneous group of proteins: some are coiled-coil proteins involved in membrane tethering or docking, while others are enzymes or cytoskeleton-associated proteins (Stenmark and Olkkonen 2001). The effectors recognized by some selected Rabs are listed in Table 3.5.

Rab proteins also interact with SNAREs. During *in vivo* studies it was shown by Grote and Novick that these interactions are non-selective in the absence of effector proteins (Grote and Novick 1999). Recent studies also indicated the important role of tethering/docking factors in this recognition process. Tethering factors involved in vesicle targeting/docking include Uso1, TRAPP, p115, exocyst and EEA1, and these all bind membranes before the formation of SNARE complexes (Takai *et al.* 2001). EEA1, which is involved in the homotypic endosome fusion process, has recently been found to be an effector of Rab5. It is likely that the events that precede stable SNARE-dependent docking of membranes are the result of a network of interactions between many proteins including tethering and Rab proteins. Direct interactions between Rabs and Sec4 as well as Rabs and the exocyst have also been described. Therefore Rabs are likely candidates for orchestrating vesicle targeting through tethering proteins (Takai *et al.* 2001).

To date, no tethering proteins have been identified in tick tissues. Karim *et al.* did however identify a 25 kDa putative Rab3 in the salivary glands of *A. americanum* using a polyclonal antibody to human Rab3a. The molecular mass of the identified tick protein was similar to that observed in rat brain. Various fractions, such as the pellet and supernatant obtained after a 2000 x g centrifugation fractionation and the pellet obtained after 150,000 x g centrifugation, tested positive. The supernatant obtained after 150,000 x g, the plasma membrane fraction obtained from sucrose gradient membrane fractionation and saliva, tested negative (Karim *et al.* 2002).

Table 3.5. Localization, function and effectors of selected Rab GTPases (Watson 1999; Pfeffer 2001; Stenmark and Olkkonen 2001; Takai *et al.* 2001). *Subcellular compartment abbreviations: ER (endoplasmic reticulum), SV (synaptic vesicles), EE (early endosome), CCV (clathrin coated vesicles), PM (plasma membrane), LE (late endosome). TGN (trans Golgi network) and RE (recycling endosome). Effector abbreviations: RIM (rab interacting protein), EEA (early endosome associated protein).*

Name	Yeast Homologue	Localization	Expression	Function	Effector
Rab1a	Ypt1p	ER / *cis*-Golgi	Ubiquitous	ER-Golgi transport	
Rab2a		ER / *cis*-Golgi	Ubiquitous	Golgi-ER retrograde transport	
Rab3a Rab3		SV Granules	Neurons Ubiquitous	Regulated exocytosis	Rabphillin-3A RIM
Rab4a		EE	Ubiquitous	Endocytic recycling	
Rab5a	Ypt51p	EE, CCV, PM	Ubiquitous	Budding, motility and fusion in exocytosis	Rabaptin-5 Rabenosyn-5 EEA1
Rab6a	Ypt6p	Golgi	Ubiquitous	Retrograde Golgi traffic	Rabkinesin-6
Rab7	Ypt7p	LE	Ubiquitous	Late endocytic traffic	
Rab8a	Sec4p	TGN, PM	Ubiquitous	TGN-PM traffic	Pab8ip (Ser/ Thr kinase)
Rab9a		LE	Ubiquitous	LE-TGN traffic	p40
Rab11a	Ypt31p	RE, TGN	Ubiquitous	Endocytic recycling via RE and TGN	Rab11BP/Rabphillin-11
Rab27a		Melanosomes Granules	Melanocytes Platelets Lymphocytes	Movement of lytic granules and melanosomes towards PM	

e. Calcium binding proteins

The near universal role of calcium as the trigger for granule exocytosis predicts the existence of conserved protein(s) capable of activating the fusion machinery upon binding calcium (Burgoyne and Morgan 2003). Several different candidate proteins have been suggested to play such as role. Since synaptotagmins have attracted most of the attention, they will be discussed in more detail.

Synaptotagmins belong to the large family of C2 domain proteins since it contains two identical repeats that share homology with the protein kinase C (PKC) C2 domain. To date they have been detected in numerous eukaryotes but have not been found in yeast, suggesting that they are not part of the basic membrane trafficking machinery (Marqueze *et al.* 2000).

Synaptotagmin I (sytI) is abundantly expressed in neuronal and endocrine cells where they localize to the synaptic vesicles and secretory granules, respectively. Synaptotagmin I interacts with various binding partners (Figure 3.5) including the key components of the exocytosis-endocytosis machinery: syntaxin (Chapman *et al.* 1995), SNAP25, β-SNAP as well as various channels, lipids, neurexins (Perin 1996), the clathrin adaptor protein AP-2 (Haucke and De Camilli 1999) and calmodulin (Perin 1996). These interactions are regulated via phosphorylation by casein kinase II, calmodulin kinase II and PKC. Although sytI is most abundant in neuronal tissue, it has been detected in other tissues such as chromaffin cells where it localizes to the large dense core vesicles (LDCVs). By means of sytI deficient cells, it could be shown that sytI is required for rapid, highly calcium sensitive LDCV exocytosis, and that it regulates the equilibrium between a slowly releasable and a readily releasable state of the fusion machinery (Voets *et al.* 2001).
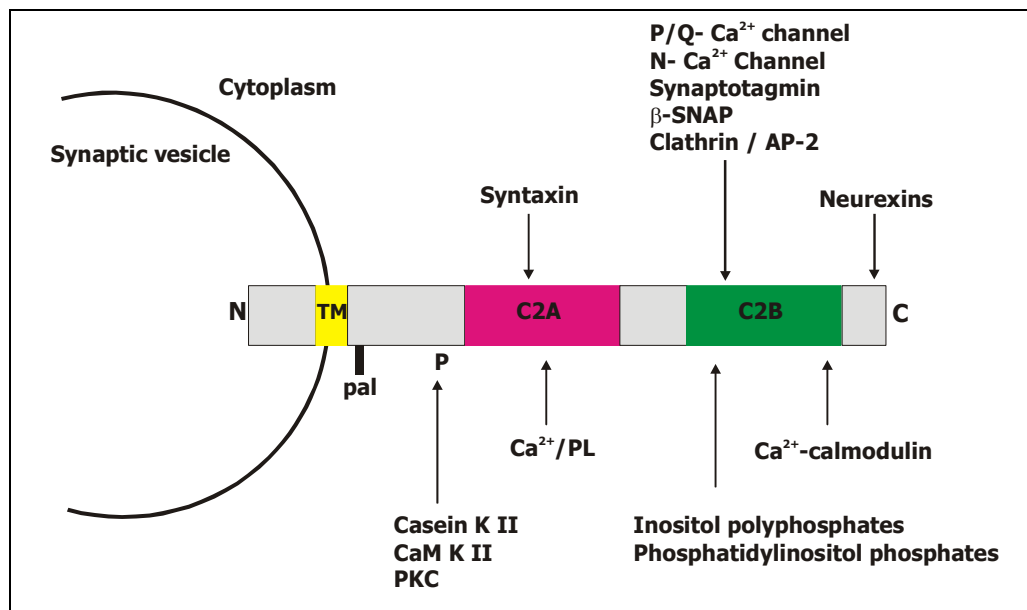
Figure 3.5. Diagram of the domain structure of synaptotagmin I (Marqueze *et al.* 2000). *The interaction sites with the major binding partners are indicated. Abbreviations corresponds to: (C) carboxy-terminus; (CaM Kinase II) Ca2+/calmodulin kinase II; (Casein K II) casein kinase II; (N) amino-terminus; (P) phosphorylation sites; (pal) palmitoylation site; (PL) phospholipids; (PKC) protein kinase C   and (TM) transmembrane domain.*

Synaptotagmin II (sytII) shares the highest homology with sytI and is assumed to also function similarly. Hetero-oligomers have been described and proposed to modulate the properties of the synaptotagmins in neuro-secretion. Properties of the other synaptotagmin isoforms are listed in Table 3.6.

Table 3.6. Properties of various synaptotagmin isoforms (Marqueze *et al.* 2000; Sudhof 2002).

Subcellular compartment abbreviations: SLMVs: synaptic like microvesicles, LDCVs: Large dense core vesicles.

Isoform	cDNA identification	Protein expression, properties and function
I	Peptides of the protein were used to design oligonucleotides and screening of a cDNA library	-Synaptic vesicles from rat brain - SLMVs from adrenal medulla - LDCVs from PC12 cells, posterior pituitary - Secretory granules of insulin secreting cells - Parotid secretory granules - Ca^{2+} sensor for fast exocytosis - N-glycosylated N terminus
II	Screening of a genomic library using sytI probes	- Growth cones - Synaptic vesicles - Secretory granules of insulin secreting cells - Ca^{2+} sensor for fast exocytosis - N-glycosylated N terminus
III	RT-PCR with sytI primers	- Mouse neuromuscular junction - Secretory vesicles of pancreatic B-cells - Ca^{2+} sensor for exocytosis - Disulfide bonds at N-terminus - Determine secretory granule size (Grimberg *et al.* 2003)
IV	- Differential screening of an induced PC12 cDNA library - PCR with C2 domain degenerative primers	- Rat brain membranes (62 kDa) - Drosophila heads membranes (55 kDa) - SLMVs and LDCVs of PC12 cells (46 kDa) - Unknown function - Asp → Ser substitution in C2A-domain
V	Screening of a cDNA library with sytI probe (Hudson and Birnbaum 1995)	- Kidney, Adipose tissue, lung, Heart - Ca^{2+} sensor for exocytosis - Disulfide bonds at N-terminus
VI	Screening of a libraries using syt probes	- ~50 KDa protein - Not in synaptic vesicles - Intestine, Kidney, Pancreas, Testis - Ca^{2+} sensor for exocytosis - Disulfide bonds at N-terminus - No consensus Ca^{2+} binding sites
VII	Screening of a libraries using syt probes	- Brain (several proteins), Heart, Lung, Spleen - Ca^{2+} sensor for exocytosis ->12 splice isoforms

VIII	Screening of a libraries using syt probes	- Renal cortex and medulla (52 kDa), Heart, Cerebral cortex - No consensus Ca^{2+} binding sites
IX (sytV)	-Screening of rat adipose tissue cDNA library with sytI probe -E17 rat forebrain cDNA library	- Brain, PC12 cells (50 kDa), Adipose tissue, Heart, Kidney - Unknown function
X	Differential display PCR	- Dentate granule cells of cortex after kainic acid-induced seizures - Ca^{2+} sensor for exocytosis - Disulfide bonds at N-terminus
XI	PCR with primers designed in a human syt EST sequence	- Brain - Unknown function - Asp→ Ser substitution in C2A-domain
srg1	Screening of cDNA library for thyroid hormone up-regulated genes	- Brain

The various isoforms differ mostly regarding their calcium-dependent phospholipid binding capability, binding to other synaptotagmins, calmodulin and AP-2 binding as well as the EC_{50} of the C2A domain for calcium. The ability to interact with both membranes and the fusion machinery in response to the spectrum of calcium levels that drive exocytosis, suggests that synaptotagmins may be ubiquitous exocytotic calcium-sensors (Marqueze *et al.* 2000; Burgoyne and Morgan 2003).

It is possible that various classes of calcium-sensors determine the distinct calcium dependency of granule exocytosis. PKC, rabphillin 3A, Doc2, RIM and munc13, all proteins involved in exocytosis, share the C2 domains of synaptotagmin. Although rabphillin has originally been isolated as a Rab3 binding protein, recent studies indicate a function independently of Rab3 in various systems during exocytosis. Doc2 (double C2) overexpression in PC12 cells indicated its involvement in granule exocytosis by interacting with both munc18/nSec1 and another C2 domain containing protein, munc13. Overexpression of munc-13 in chromaffin cells increases the magnitude of both the exocytotic burst and the subsequent slower phase of release, suggesting a role in priming. The final C2 domain-containing protein implicated in exocytosis is RIM (Rab Interacting Molecule). Studies in PC12 cells, β-cells, β-cell lines and chromaffin cells indicated a function for RIM in exocytosis that is unrelated to Rab3 (Burgoyne and Morgan 2003).

Two proteins, calmodulin and p145/CAPS, that lack C2 domains have also been implicated in granule exocytosis. Calmodulin binds calcium via its four EF-hand domains and was one of the first proteins suggested to be involved in the late calcium-activated triggering of exocytosis. Its mechanism of action is unclear as it binds to several proteins implicated in exocytosis, including synaptotagmin I, Rab3, VAMP and the SNARE complex. Recently, p145/CAPS has emerged as a granule exocytosis–specific calcium sensor. Originally identified as a cytosolic factor that reconstituted secretion from GH3 and PC12 cells, CAPS has since been shown to regulate dense-core vesicle exocytosis in nerve terminals, chromaffin cells and pituitary melanotrophs. CAPS is known to act in the late calcium-activated triggering stage, but its mechanism of action is unknown. In particular, its calcium affinity (K_d=270 μM) appears too low to explain its effect on granule exocytosis (Burgoyne and Morgan 2003).

To date, the only calcium-sensor detected in ticks is synaptotagmin using western blotting and an rabbit-anti-rat synaptotagmin polyclonal antibody (Karim *et al.* 2002). The molecular mass of 65 kDa is similar to synaptotagmins I and II found in brain tissue.

3.2. HYPOTHESIS

- Salivary glands of the soft tick *Ornithodoros savignyi* contain homologues of the conserved core machinery involved in regulated exocytosis, i.e. syntaxin, SNAP-25 and VAMP.

3.3. AIMS

- Identification of the conserved core machinery (syntaxin, SNAP-25 and VAMP) and the Rab3 GTPase by means of Western Blotting using polyclonal antibodies against the rat brain isoforms.
- Localization of the SNARE proteins using subcellular fractionation by ultra-centrifugation and confocal microscopy.
- Isolation of the cDNA transcripts encoding the SNARE protein syntaxin and the calcium-binding protein synaptotagmin from argasid ticks by means of degenerative primers and 3'-RACE.

3.4. MATERIALS

New Zealand white rabbits were obtained from the NICD (National Institute for Communicable Diseases), Johannesburg, South Africa. The rabbits resided at the animal unit of the Medical Research Council (MRC), Pretoria, South Africa. All animal studies were also conducted at the MRC with the help of Mr. K. Venter. Recombinant synaptotagmin was a kind gift from Prof. R.H. Scheller, Stanford University Medical Center, USA. Diethyl pyrocarbonate (DEPC) and dithiothreitol (DTT) were obtained from Sigma Chemical Co. Tris(hydroxymethyl)aminomethane, NaCl, ethylene diamine tetra-acetic acid (EDTA), methanol, acetic acid, glycine, ammonium persulphate, N,N,N',N'-tetramethyl-ethylenediamine (TEMED) were obtained from Merck, Darmstadt, Germany. Acrylamide, bisacrylamide, sodium dodecyl sulphate (SDS) were from BDH Laboratory Supplies LTD., England. Chemiluminescent molecular weight marker proteins, Super Signal® chemiluminescent substrate and Protein Assay kit were from Pierce, USA (Separations). TaKaRa Ex Taq (5 U/μl) and Taq (5 U/μl) were from Takara Bio Inc., Japan (Separations). X-ray film, photographic developer and fixer were from Konica. The RNeasy total RNA isolation kit and the Super Smart cDNA synthesis kit were obtained from Qiagen (Southern Cross Biotechnology). SNARE antibodies were a gift from Prof. J. R. Sauer, Oklahoma State University, USA. All primers were synthesized by Inqaba Biotech, Pretoria, South Africa. Isopropyl β-D-thiogalactopyranoside (IPTG), 5-bromo-4-chloro-3-indolyl β-D-galacto-pyranoside (X-gal), RNAse, High Pure plasmid isolation kit, RNase-inhibitor, PCR nucleotide mix (10 mM deoxynucleotides solution), DIG (Digoxigenin) labeled dUTP, blocking solution, anti-Digoxigenin alkaline phosphatase and CDP-Star™ were from Roche Diagnostics. Yeast extract and tryptone were purchased from Oxoid Ltd. (Basingstoke, Hampshire, England). SuperScript II Rnase H⁻ reverse transcriptase was from Invitrogen Life Technologies.

3.5. METHODS

3.5.1. SALIVARY GLAND FRACTIONATION

Salivary glands (10 pairs) were homogenized in 1 ml extraction buffer (20 mM Tris-HCl, 150 mM NaCl, 1 mM DTT, 2.5 mM EDTA, 1 μg/ml leupeptin, 20 μg/ml aprotinin, 0.5 mM phenylmethylsulfonylfluoride) and fractionated by ultra centrifugation (Sorvall®, Ultra Pro™ 80, Du Pont) for 60 minutes at 4º C. Fractions were collected after the 2000 x g and 100 000 x g centrifugation steps and protein concentrations determined. Protein fractions (100 μg) were separated by SDS-PAGE and subjected to Western blotting.

3.5.2. PROTEIN GEL ELECTROPHORESIS

SDS-PAGE was performed using a 5% stacking gel (0.625 M Tris-HCl, 0.5% SDS, pH 6.8) and 12% separating gel (1.88 M Tris-HCl, 0.5% SDS, pH 8.8). The acrylamide gels and the electrophoresis buffer were prepared from an acrylamide stock (30% acrylamide, 0.8% N',N'-methylene bisacrylamide) and electrophoresis buffer stock (0.02M Tris-HCl, 0.06% SDS, 0.1 M glycine, pH 8.3). The gel solutions were polymerized with the addition of 30 μl of 10% ammonium persulphate and 5 μl TEMED. Samples were diluted 1:1 in reducing sample buffer (0.06 M Tris-HCl, 2% SDS, 0.1% glycerol, 0.05% β-mercaptoethanol, 0.025% bromophenol blue) and boiled at 95ºC for 5 minutes. Pre-stained molecular mass markers (Pierce, USA) were dissolved in 10 μl water. Electrophoresis was carried out in a Biometra electrophoresis system (Biometra GmbH, Germany) with an initial voltage of 60 V for 45 minutes and thereafter 100 V. When chemiluminescent Blue Ranger® Prestained Peroxidase-labeled protein molecular weight markers (Pierce, USA) were used, SDS was omitted from the gels and the marker sample was not boiled.

3.5.3. WESTERN BLOTTING

Proteins were blotted onto PVDF (polyvinylidine-difluoride, Merck) membranes using a Trans-Blot semi-dry transfer cell (Bio-Rad) and 10 mM CAPS (3-(cyclohexylamino)-1-propane sulphonic acid) at 20 V for 45 minutes. Membranes were blocked with 1% skim milk powder in TBS (20 mM Tris-HCl, 150 mM NaCl, pH 7.4-7.6) overnight at 4ºC. Blots were then incubated with the primary antibodies at a dilution of 1:1000 in blocking buffer. The antigen-antibody complexes were visualized with alkaline peroxidase conjugated anti-rabbit or anti-mouse IgG (whole molecule) at a dilution of 1: 10 000 and detected with Super Signal® chemiluminescent substrate (Pierce, USA).

3.5.4. IMMUNO-FLUORESCENT LOCALIZATION USING CONFOCAL MICROSCOPY

Glands of unfed female ticks were dissected in PBS and immediately fixed in 1% formaldehyde and 0.1% gluteraldehyde for 3 hours. These fixed glands were permeabilized in a graded series of methanol solutions (1-100%) before rehydration in PBS. Glands were subsequently incubated overnight in 100 mM NaBH$_4$ at 4ºC with the Eppendorf caps open to minimize auto-fluorescence. Glands were washed 3 time with TBSN buffer (10 mM Tris-HCl, pH 7.4, 155 mM NaCl, 0.1% Triton X100) for 90 minutes with constant rotation before blocking with 2% BSA in TBSN overnight at 4ºC. Glands were incubated with 50x dilution of primary antibody in PBS and 2% BSA for 8 hours. Glands were washed with TBSN for a

further 48 hours with buffer washes every 8-12 hours before incubation with the appropriate FITC-coupled secondary antibody in TBSN, 2% BSA for 8 hours at 4ºC in the dark. Glands were washed in TBSN for 48 hours before dehydration in a graded series of methanol solutions (0-100%) over 90 minutes. Glands were mounted on microscope slides in clearing solution and viewed with a Zeiss LSM-410 confocal laser scanning microscope and Zeiss Own™ imaging software.

3.5.5. DEGENERATIVE PRIMER DESIGN

The NCBI (National Centre for Biotechnology Information) SwissProt database was searched for known SNARE proteins and serine protease amino acid sequences. The Clustal W Program was used to create multiple alignments of the homologous amino acid sequences in order to identify conserved areas (Thompson *et al.* 1994). The homologous regions were used as templates to design a primer sequence using the Oligo Version 4.0 program (National Biosciences, USA)(Rychlik and Rhoades 1989). Inosine was included at positions of high redundancy. The Tm was calculated by the equation: 69.3 + 0.041 x (% G/C) – (650 / length) (Rychlik *et al.* 1990).

3.5.6. TOTAL RNA ISOLATION

Total RNA was isolated from either unfed (200 glands) or fully engorged (30 glands) female *O. savignyi* salivary glands. Ticks were fed to completion (30-45 minutes) on New Zealand white rabbits and dissected within 2 hours. Glands were transferred to 750 μl TRI-REAGENT$^{®}$ (Molecular Research Center, INC). Total RNA was isolated according to the manufacturer's instructions up to the step where the total RNA fraction was in the aqueous fraction. The RNA was not precipitated immediately as suggested, but loaded onto a RNA isolation column (RNeasy$^{®}$, Qiagen) for further purification. The column was washed according to the instructions and the RNA eluted in 50 μl DEPC-treated water. The purity and quantity of RNA was determined spectrophotometrically by measuring the 260/280 nm ration and the 260 nm value, respectively. RNA quality was assessed by denaturing agarose gel electrophoresis on a 1% agarose gel prepared in 40 mM MOPS, 10 mM sodium acetate, 1 mM EDTA and 18% formamide in DEPC treated double distilled deionized water. Electrophoresis was conducted at 70 V for 30 minutes.

3.5.7. CONVENTIONAL cDNA SYNTHESIS

Single strand cDNA was prepared using Superscript™ II (Life Techonologies) and the anchor-dT primer (Joubert *et al.* 1998). Total RNA (1 μg) in 7.5 μl DEPC treated water was denatured at 70ºC for 3 minutes and snap cooled on ice. Five pmoles of anchor-dT primer (1 μl), 3 μl DTT (0.1 M), 200 units Superscript™ II (1 μl), 4 μl 5x first strand buffer (250 mM Tris-HCl, 375 mM KCl, 15 mM MgCl2, pH 8.3) was added and incubated at 42 ºC for 60 minutes before inactivation at 70 ºC for 2 minutes. The cDNA was stored at – 70ºC.

3.5.8. SUPER SMART™ cDNA SYNTHESIS

The Super SMART™ PCR cDNA synthesis kit (Qiagen) provides a novel, PCR-based method for producing high-quality cDNA from nanogram quantities of total RNA. A modified oligo(dT) primer, the 3' CDS Primer IIA primes the first-strand synthesis reaction (Figure 3.6). When the MMLV (Moloney murine leukemia virus) reverse transcriptase (RT) reaches the 5' end of the mRNA, the enzyme's terminal transferase activity adds a few (up to 5) additional nucleotides, primarily deoxycytidine, to the 3' end of the cDNA. The SMART™ oligonucleotide, which has an oligo(G) sequence at its 3' end, base-pairs with the deoxycytidine stretch, creating an extended template. RT then switches templates and continues replication to the end of the oligonucleotide. The resulting full-length, single-stranded cDNA contains the complete 5' end of the mRNA as well as sequences that are complementary to the SMART™ oligonucleotide. The SMART™ anchor sequence and the poly(A) sequence serve as universal priming sites for end-to-end cDNA amplification. In contrast, cDNA without these sequences, such as prematurely terminated cDNAs, contaminating genomic DNA or cDNA transcribed from poly(A)⁻ RNA will not be exponentially amplified (Clontech Laboratories 2001a). Since the terminal transferase activity of the RT adds a random number of deoxycitidine to the first strand, directional cloning and expression of these fragments are possible since various reading frames were generated randomly.
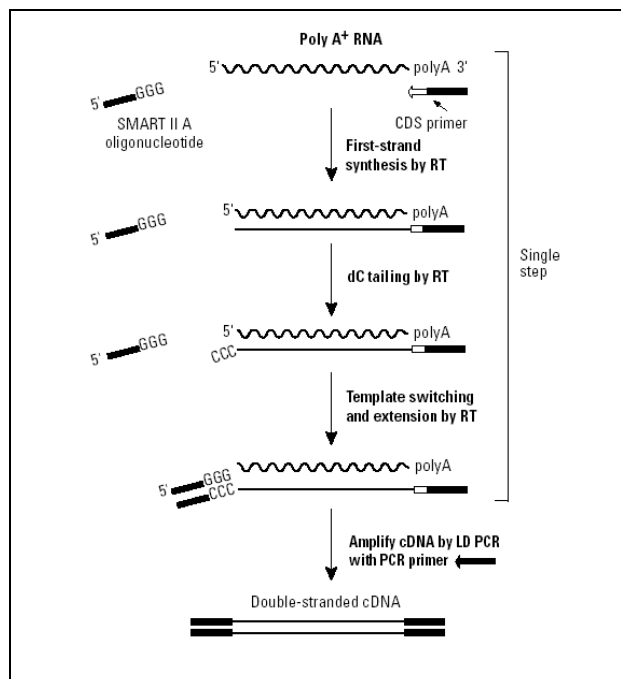
Figure 3.6. Flow chart of Super SMART™ cDNA synthesis (Clontech Laboratories 2001a).

First strand cDNA synthesis was performed by combining 500 ng total RNA, 7 μl of the 3'
SMART CDS III primer (12 μM), 7 μl SMART IV primer (12 μM) and water up to a final
volume of 64 μl. See Table 3.10 for primer properties. The contents were mixed with a
pipette and collected by brief centrifugation. The RNA was denatured at 65ºC for 2 minutes
and then kept at 42ºC. 20 μl of 5x First-strand buffer, 2 μl DTT (100 mM), 10 μl 50x dNTP
(10 mM), 2.5 μl RNAse inhibitor (40 U/μl), 2.5 μl SuperScript II RNase H- reverse
transcriptase (200 U/μl) and 5 μl water were added. The mixture was mixed by gently
pipetting and then centrifuged briefly. Since full-length cDNAs were required for downstream
applications, the mixture was incubated for 90 minutes at 42ºC. Finally the reaction was
terminated with the addition of 2 μl of 0.5 M EDTA.

To purify the SMART cDNA from unincorporated nucleotides and small (<0.1 kb) cDNA
fragments, the cDNA was subjected to column chromatography using the NucleoSpin®
Extraction kit (Machery Nagel, Germany). Three volumes of buffer NT2 (details of buffer
composition withheld by supplier) were added to each cDNA synthesis reaction, mixed by
pipetting and loaded onto the column. The column was centrifuged at 13 000 x g for 1
minute and the flow through discarded. The column was washed three times with 500 μl
buffer NT3 (details of buffer composition withheld by supplier) and centrifuged (13 000 x g,
1 minute). In order to remove any remaining ethanol, the column was placed in a clean tube

and again centrifuged. Water (50 μl) was added to the column filter and soaked for 2 minutes before eluting the cDNA into a clean tube with centrifugation. The elution process was repeated with 35 μl water using the same collection tube. The total recovered elution volume was 80-85 μl per sample. The cDNA was stored at –70ºC until used.

3.5.9. cDNA amplification by LD-PCR

Based on the guidelines provided by Clontech, 5 μl of ss cDNA was used for cDNA amplification by long distance PCR (LD-PCR). The ss cDNA was diluted in 79 μl water to which 10 μl of ExTaq buffer, 2 μl 50x dNTP mix (10 mM) and 2 μl 5' PCR Primer II (12 μM) was added (see Table 3.10 for primer properties). The mixture was mixed well by pipetting and centrifuged briefly. The tube was placed in a preheated thermal cycler and incubated for 1 minute at 94ºC before lowering the temperature to 80ºC and adding 2 μl ExTaq polymerase (5 U/μl). PCR cycling was performed at 95ºC for 15 seconds, 65ºC for 30 seconds and elongation at 68ºC for 6 minutes. After 15 cycles, 30 μl was removed for optimization of the number of PCR cycles. The remaining 70 μl was stored at 4ºC and 25 μl of the optimization fraction returned to the thermal cycler. After every 3 cycles, 5 μl was removed up to a final of 30 cycles. The 5 μl fractions were analyzed on a 1.2% agarose / ethidium bromide gel alongside DNA molecular size markers. The optimal number of cycles required for each sample was determined as one cycle fewer than is needed to reach the plateau, ensuring that the ds cDNA remains in the exponential phase of amplification. The remaining 70 μl was returned to the thermal cycler and subjected to the number of additional cycles. Usually, 24 cycles were optimal for 500 ng of salivary gland cDNA. Finally the ds cDNA was purified using the NucleoSpin extract kit (as described earlier) and the yield determined at 260 nm on the Gene Quant Pro system (Biochrom Ltd., Cambridge, Supplied by Amersham Biosciences). On average 1,8 -2,2 μg of SMART cDNA was obtained after purification.

3.5.10. RANDOM AMPLIFICATION OF 3' cDNA ENDS (3'-RACE)

Both single stranded cDNA obtained after normal cDNA synthesis or ds cDNA obtained from SMART cDNA synthesis were used during 3'-RACE. In all cases, the optimal concentrations of cDNA, primers, MgCl$_2$, annealing temperature and number of cycles were optimized for every reaction using a Taguchi optimization matrix (Cobb and Clarkson 1994). Single-stranded cDNA (0.1- 0.5 μl) or SMART ds cDNA (50 ng) were combined with 10 pmol of the appropriated anchor primer, 5 - 50 pmol of the degenerative primer, 2 μl TaKaRa Taq™ PCR

buffer, 1 - 1.5 mM $MgCl_2$, 200 μM dNTP's and water to a final volume of 20 μl. The cDNA was denatured at 94ºC for 3 minutes and then cooled to 80ºC after which 5 μl of enzyme mix (2.5 U TaKaRa Taq diluted in 1x PCR buffer) was added. Amplification consisted of 21-30 cycles of DNA denaturation (94ºC, 30 seconds), annealing (at various temperatures depending on the Tm of the degenerative primer used, 30 seconds) and extension (72ºC, 2 minutes) followed by a final extension step (72ºC, 5 minutes). All amplification procedures were conducted in a Gene Amp PCR system 9700 (Perkin Elmer Applied Biosystems). The principle of 3'-RACE using degenerative primers is depicted in Figure 3.7.
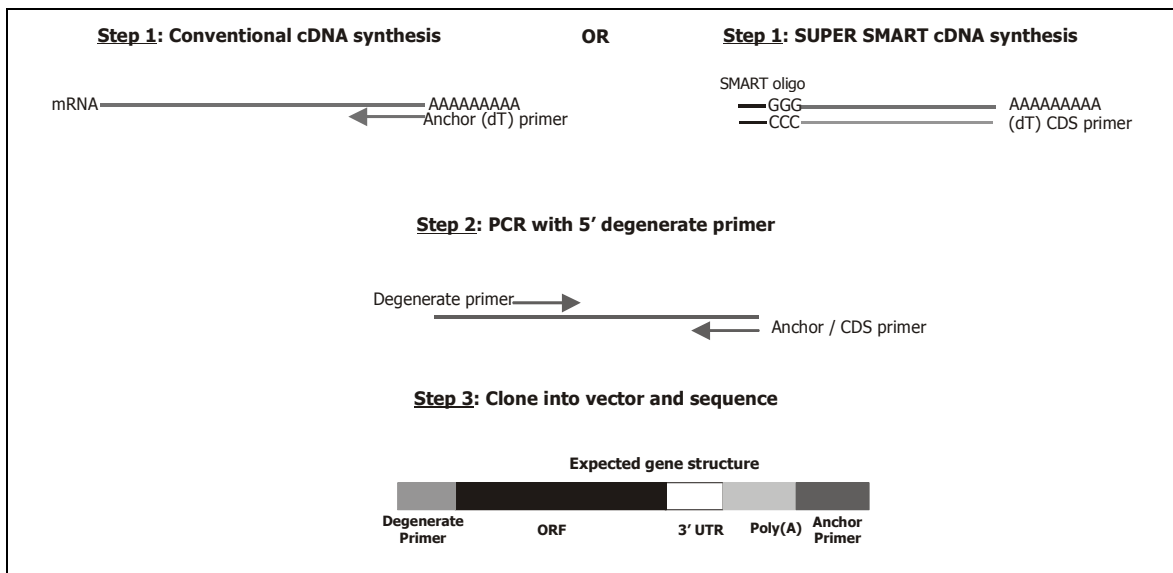
Figure 3.7. Cloning strategy during 3'-RACE (adopted from Mans, 2002). *(1) Single stranded cDNA was synthesized with an anchor (dT) primer and ds cDNA with the (dT) CDS and SMART primers. (2) A degenerate primer and an anchor primer was used to amplify the product of interest. (3) The product was cloned into the pGEM T-easy vector (Promega) and sequenced.*

3.5.11. DIG-LABELLING OF PROBES USING PCR

The synaptotagmin I probe was synthesized from the recombinant sytI plasmid obtained from Prof. Scheller. In order to use the T3 and T7 primers, the coding region of sytI was cloned into Bluescript. The PCR mixture consisted of 2 μl Takara Taq DNA polymerase (5 U/μl), 2 μl dNTPs, 0.25 nmol DIG-dUTP, 1.5 mM $MgCl_2$, 5 pmol of each primer, and 0.5 μl of template (1:10 000 dilution of 50 ng/μl stock) in a total volume of 20 μl. Twenty-three cycles were done with an annealing temperature of 50ºC for 30 seconds, denaturation at 94ºC for 30 seconds and extension at 72ºC for 2 minutes.

3.5.12. DNA DOT BLOTTING

DNA was denatured for 10 minutes at 95ºC and chilled immediately on ice to prevent re-annealing. DNA samples (1 μl, typically 10-100 ng) were spotted onto a Nylon membrane (Roche Molecular Biochemicals), allowed to dry and exposed to UV-light (Spectroline transilluminator, Spectronics Corporation, New York, USA, λ=312 nm) for 3 minutes to cross-link the DNA to the membrane. The membrane was placed in a hybridization bag containing standard hybridization solution (5x Sodium citrate saline solution (SSC), 0.1% N-lauroylsarcosine, 0.02% SDS, 1% blocking reagent) and incubated at 65ºC for 2 hours. The probe was diluted to a concentration of 25 ng/ml in standard hybridization solution and after removing the pre-hybridization buffer the membrane was incubated overnight at 65ºC with the probe. Excess probe was removed by washing the membrane twice for 15 minutes in 2x washing solution (2x SSC, 0.1% SDS) and twice for 15 minutes in 0.5x washing solution (0.5x SSC, 0.1% SDS) at 65ºC. The membrane was equilibrated in detection wash buffer (100 mM maleic acid, 150 mM NaCl, 0.3% Tween 20, pH 7.5) for 1 minute and then blocked in the detection buffer containing 1% blocking reagent for 60 minutes at 25ºC. Following the blocking step, the membrane was incubated with anti-digoxigenin alkaline phosphatase Fab fragments (1:20,000 dilution in blocking buffer) for 30 minutes at 37ºC and again washed twice for 15 minutes with detection wash buffer at 37ºC to remove unbound Fab fragments. The membrane was equilibrated for 2 minutes in detection buffer (100 mM Tris-HCl, pH 9.5, 100 mM NaCl) and incubated for 5 minutes in the CDP-Star™ substrate (diluted 1:100 in detection buffer). Exposing the membrane to X-ray film was used for the detection of the chemiluminescent signal.

3.5.13. AGAROSE GEL ELECTROPHORESIS

PCR products were analyzed by electrophoresis at 68 V using a 1, 1.5 or 2% analytical grade agarose gel (D-1 Low EEO Agarose, Conda, Spain). TAE (40 mM Tris, 1mM EDTA) was used as electrophoresis buffer in a mini gel apparatus (Biometra, GmbH). Molecular masses were calculated from the Rf-values of the molecular mass markers (Promega, Wisconsin, USA).

3.5.14. PCR PRODUCT PURIFICATION

PCR products were purified from either agarose gels or a PCR reaction mixture. In both cases, the NucleoSpin® Extract kit (Machery Nagel, Germany) was used. During purification from agarose gels, gel pieces were dissolved in 300 μl buffer NT1 and incubated at 50ºC until the gel slices were dissolved (5-10 min). The sample was loaded onto a NucleoSpin®

extract column, centrifuged (8000 x g, 1 min) and the flow through discarded. The column was washed with 600 μl buffer NT3 and centrifugation (11 000 x g, 1min) and then with 200 μl NT3 (11 000 x g, 2min). DNA was eluted in 40 μl elution buffer (5 mM Tris-HCl, pH 8.5) after centrifugation (11 000 x g, 1min). The procedure for isolation from PCR reactions is identical, except that the gel-dissolving step is omitted and the sample is diluted in 4 volumes of buffer NT2.

3.5.15.   QUANTIFICATION OF NUCLEIC ACIDS

All DNA and RNA samples were quantitated spectrophotometrically using the Gene Quant Pro™ system (Biochrom Ltd., Supplied by Amersham Biosciences) using a mini cuvette (10 μl).

3.5.16.   A/T CLONING OF PCR PRODUCTS INTO pGEM® T-EASY VECTOR

DNA products were ligated into 50 ng of the pGEM® T-Easy vector (Promega) at a 3:1 insert to vector ratio. Ligation was performed at 4ºC overnight with 1 μl T4 ligase and 5 μl 2x ligation buffer of the pGEM® T-Easy vector system (Promega, USA). Prior to transformation, the T4 ligase was inactivated at 70 ºC for 10 minutes.

3.5.17.   PREPARATION OF ELECTROCOMPETENT CELLS

A single colony of SURE or BL21 *E. coli* was inoculated into 15 ml Luria-Berthani Broth (LB Broth, 1% NaCl, 1% Tryptone, 0.5% yeast extract in deionized water, pH 7.4) and grown overnight at 30ºC with moderate shaking. Two 5 ml fractions of the overnight culture were diluted into 2 x 500 ml of pre-warmed LB broth in a sterile 2-liter flask, and grown at 37˚C with vigorous shaking until OD_{600} reached 0.5 to 0.6. The cultures were transferred into four pre-chilled 250 ml centrifuge bottles, placed on ice for 20 minutes and then centrifuged (10 000 x g, 20 min, 4ºC). The cell pellet was suspended in 10 ml ice cold H_2O with swirling, another 240 ml of ice cold water was added and the cells were collected by centrifugation (10 000 x g, 20 min, 4ºC). After another three washes with 250 ml water, the cell pellets were dissolved in 10 ml glycerol (10% v/v), pooled into two sterile 50 ml centrifuge tubes, incubated on ice for 60 minutes and again centrifuged to collect the cells. Finally, cell pellets were suspended in a total volume of 1 ml glycerol (10% v/v) and divided into 90 μl aliquots that were stored at –70ºC.

3.5.18. TRANSFORMATION BY ELECTROPORATION

To each ligation reaction, one-tenth volumes of tRNA (10 mg / ml) and sodium acetate (3 M, pH 5) as well as three volumes of 100% ethanol were added. The mixture was centrifuged (13 000 x g, 30 minutes, 4ºC) to collect the plasmid-tRNA complex. The precipitate was washed with 1 ml 70% ethanol, centrifuged (13 000 x g, 10 min, 4ºC) and dried *in vacuo*. The pellet was dissolved in 10 µl water and added to 90 µl electro-competent cells, which were thawed on ice. The complete 100 µl mixture was placed into a pre-chilled 0.1 cm gap electroporation cuvette and electroporated at 2.5 - 3 kV for 5 milli-seconds. Immediately after electroporation, the cells were removed from the cuvette, diluted in 1 ml LB-broth and incubated at 30ºC with moderate shaking for 60 minutes before plating 10-50 µl of transformed cells onto 1.5% agar that contained 50 µg/ml ampicillin, 40 µg/plate X-gal (20 mg/ml DMSO) and 4 µl/plate IPTG (400 mM). Positive colonies were selected using blue-white selection with conventional plasmid isolation and restriction enzyme digestion of plasmid to identify inserts with the correct size.

3.5.19. MINIPREP PLASMID ISOLATION

Positive colonies were grown overnight in a shaking incubator at 30 ºC in LB broth containing ampicillin (10 µg/ml). The cells of 2 ml culture were collected by centrifugation (12 000 x g, 10 minutes) and resuspended in 100 µl solution I (25 mM Tris-HCl, 50 mM glucose, 10 mM EDTA, pH 8). Cells were subsequently lyzed with the addition of 150 µl of solution II (200 mM NaOH, 1% SDS), mixed by gentle inversion and incubation at room temperature for 10 minutes. Chromosomal DNA and SDS were removed with the addition of 250 µl of solution III (3 M potassium acetate, pH 4.2) and incubation on ice for 10 minutes. The insoluble precipitate was removed by centrifugation (13 000 x g, 15 minutes, 4ºC). Plasmid DNA was precipitated from the supernatant with the addition of 1 ml cold, absolute ethanol and centrifugation (13 000 x g, 30 minutes, 4ºC). The pelleted plasmid was washed with 1 ml cold, 70% ethanol and again centrifuged. The pellet was dried using the Bachoffer vacuum concentrator and dissolved in 30-50 µl water.

3.5.20. HIGH PURE PLASMID ISOLATION

High purity plasmids were isolated by means of the High Pure™ plasmid purification kit (Roche Diagnostics). Cells from 2 ml of culture were isolated by centrifugation (13,000 x g, 2 minutes, 4ºC) and suspended in 250 µl suspension buffer (50 mM Tris-HCl, 10 mM EDTA, 0.1 ml/ml RNAse, pH 8). Cells were lyzed at room temperature for 5 minutes with the

addition of 250 μl lysis buffer (200 mM NaOH, 1% SDS). Afterwards, 350 μl binding buffer (4 M guanidine hipochloride, 0.5 M potassium acetate) were added to precipitate chromosomal DNA and increase the ionic strength for sufficient binding to the silica matrix. Chromosomal DNA was removed by centrifugation (12 000 x g, 15 minutes, 4ºC) and the supernatant loaded onto the High Pure filter tube, which contain the silica filter for binding of DNA in the presence of chaotropic salts. The solution was centrifuged (12 000 x g, 1 min) and the flow through discarded. The column was washed twice. First with 700 μl wash buffer I (5M guanidine hydrochloride, 20 mM Tris-HCl, pH 6.6, 40% ethanol) and then 700 μl wash buffer II (2 mM Tris-HCl, 20 mM NaCl, 80% ethanol, pH 7.5). In order to remove any residual ethanol, the filter was dried by centrifugation (12,000 x g, 2 minutes). The High Pure filter tube was transferred to a clean tube and plasmid eluted with 100 μl elution buffer (1 mM Tris-HCl, pH 8.5) and centrifugation (12 000 x g, 2 minutes).

3.5.21. AUTOMATED DNA SEQUENCING AND DATA ANALYSIS

Sequencing was performed with the Big Dye Sequencing kit (Perkin Elmer, Foster City) on an ABI Prism 377 DNA sequencer (Perkin Elmer Applied Biosystems, USA). Each reaction contained 2 μl Ready reaction mixture™, 3 μl 5x buffer (400 mM Tris-HCl, 10 mM MgCl$_2$, pH 9), 1 μl primer (3.2 pmol), 300 ng plasmid and water to a final volume of 20 μl. PCR sequencing was performed using 25 cycles of denaturation (96ºC, 10 seconds), annealing (50ºC, 5 seconds) and extension (60ºC, 4 minutes). The mixture was transferred to a siliconized tube before precipitation of the PCR product with the addition of 64 μl absolute ethanol and centrifugation (13,000 x g, 20 minutes, 4ºC). The pellet was washed with 100 μl 70% ethanol, centrifuged, dried and dissolved in 3 μl loading dye (5:1 ratio of deionized formamide and 25 mM EDTA, pH8 and blue dextran, 30 mg/ml). Samples were denatured at 95ºC (2 minutes), cooled on ice and analyzed.

Sequences obtained were analyzed using the BioEdit Program. DNA and deduced protein sequences were analyzed using BLAST-P, PSI-BLAST (www.ncbi.nlm.nih.gov/BLAST) and the threading program 3D-PSSM Web Server V 2.6.0 (www.igb.uci.edu/tools/scratch/). All alignments were performed with Clustal W (www.ebi.ac.uk/clustalw/).

3.6.   RESULTS AND DISCUSSION

3.6.1. Western blotting of salivary glands with anti-SNARE and anti-Rab3a antibodies

By means of polyclonal antibodies against the three core proteins of the fusion machinery, we were able to detect a syntaxin, SNAP25 and VAMP homologue in the salivary glands of *O. savignyi* (Figure 3.8). The molecular masses of the identified proteins correspond to those in literature for both the ixodid and brain proteins (Karim *et al.* 2002). In all cases the proteins were enriched in the membrane fractions (lanes 2 and 4) obtained after centrifugation. Syntaxin was also detected in the supernatant fractions.
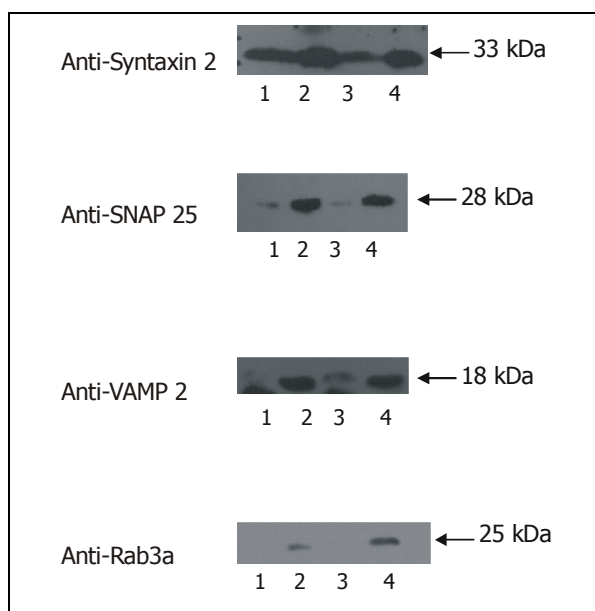
Figure 3.8. Identification of SNAREs and Rab3a using Western Blotting. *Salivary glands were homogenized and fractionated by centrifugation. The supernatant (lane 1) and pellet (lane 2) obtained after 2000 x g as well as the supernatant (lane 3) and pellet (lane 4) obtained after 100,000 x g was analyzed.*

Prior to fusion, SNARE tethering complexes are formed between syntaxin, SNAP25 and VAMP. These complexes are SDS-resistant and can be identified by comparing boiled and non-boiled samples during Western blotting. The presence of a high molecular mass complex in *O. savignyi* was investigated by using membrane fractions obtained after 100,000 x g centrifugation and anti-VAMP2 polyclonal antibodies. As a positive control, homogenized rat brain was subjected to centrifugation (100,000 x g) and the pellet fraction was analysed. From the results (Figure 3.9) we identified the rat brain 20S complex corresponding to 78 kDa (lane 1) and a high molecular mass complex (81 kDa) in the pellet of *O. savignyi* (lane

3). In both the boiled and non-boiled fractions obtained from *O. savignyi*, the monomeric VAMP (18 kDa) is visible, although it is enriched in the boiled fraction (lanes 2 and 3). This indicates that unlike brain tissue (lane 1), not all of the VAMP-proteins are present in complexes at one time. In both lanes 1 and 3 a second high molecular mass VAMP-containing complex is visible which could be the VAMP-synaptophysin complex described in literature (Edelman *et al.* 1995) since a synaptophysin homologue was also identified in *A. americanum* (Karim *et al.* 2002).
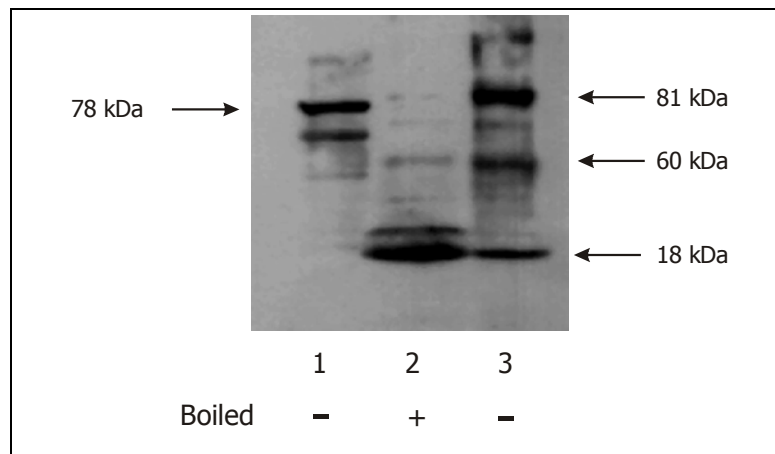
Figure 3.9. Identification of a high molecular mass core complex in the salivary glands of *O. savignyi*. *Western Blot analysis using anti-VAMP2 of non-boiled rat brain pellet (lane 1), boiled (lane 2) and non-boiled (lane 3) O. savignyi salivary gland pellet fractions obtained after centrifugation at 100,000 x g.*

The data obtained during Western blotting confirmed the presence of the core fusion proteins syntaxin, VAMP and SNAP25, as well the core fusion complex formed by these three proteins. Apart from the SNARE proteins, we also identified a Rab3a GTPase homologue in the salivary glands of *O. savignyi*.

3.6.2. Localization of SNAREs and cytoskeleton proteins using confocal microscopy

Syntaxin

Syntaxin isoforms 1A, 1B, 2, 3 and 4 are all located on the plasma membrane of cells (Teng *et al.* 2001). By using anti-syntaxin 2 polyclonal antibodies and a FITC-coupled secondary antibody, we were able to localize a syntaxin-2 homologue to the cell plasma membrane of *O. savignyi* (Figure 3.10). No intra-cellular syntaxin was detected.
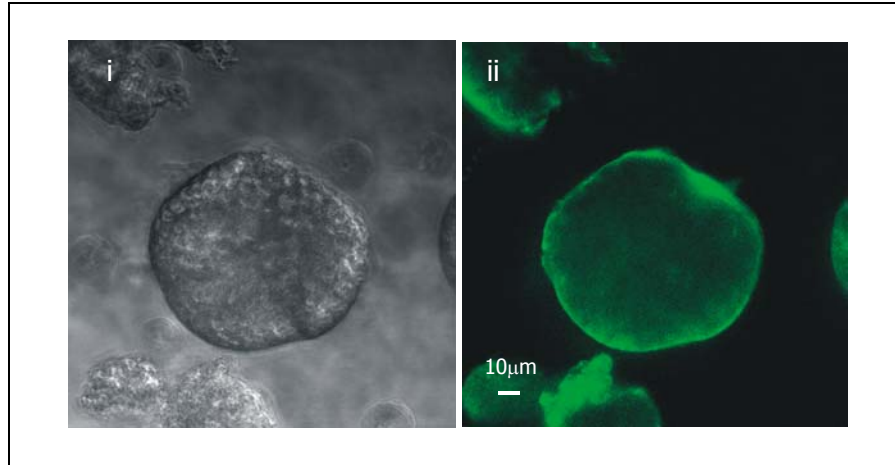
Figure 3.10. Immuno-localization of syntaxin in the salivary glands of *O. savignyi* using anti-rat brain syntaxin2 polyclonal antibodies. *Light microscopy (i) and fluorescence confocal image (ii) of a granular salivary gland cell.*

VAMP

Immuno-localization of VAMP using anti-rat brain VAMP2 polyclonal antibodies indicated VAMP to be localized to the granule membrane, since individual granules are visible (Figure 3.11.ii and iii). From Figure 3.11.iii it is evident that VAMP does not localize to the plasma membrane itself. In some acini, cells containing small granules enriched in VAMP were identified (Figure 3.11.iii). The identity of these small granules is unknown, but based on the size we hypothesize that these correspond to small granules (1-2 μm) of the 'c' cells as described previously (Chapter 2) and B.J. Mans (Mans 2002a).
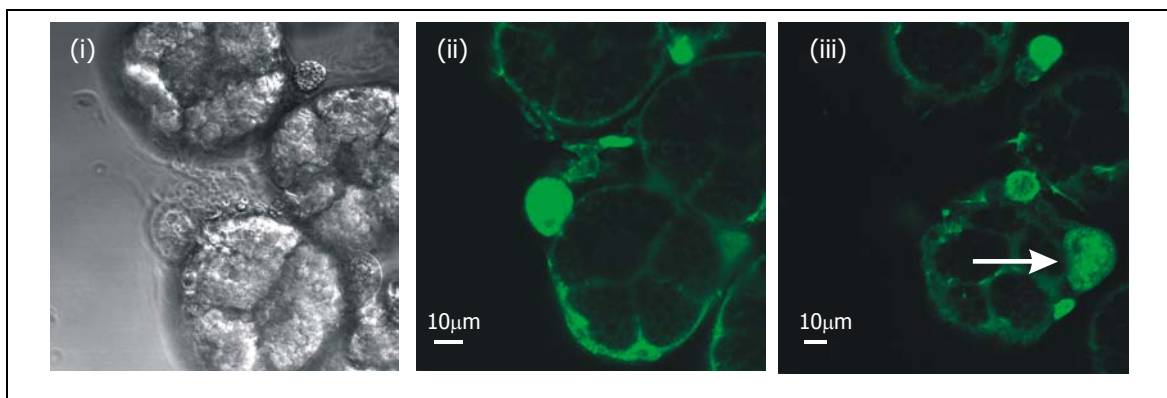
Figure 3.11. Immuno-localization of VAMP in the acini of *O. savignyi* using anti-rat brain VAMP2 polyclonal antibodies. *Light microscopy (i) and fluorescence confocal image (ii and iii) of granular salivary gland acini. The arrow in figure iii indicates the VAMP2 enriched small granules.*

Immuno-localization of VAMP in granular cells indicated VAMP to again localize to the granule membranes (Figure 3.12). In order to determine if VAMP is present on the plasma membrane, we performed 3D-scanning confocal microscopy. The results indicated that VAMP is not present on the plasma membrane of granular cells (Figure 3.12.ii).
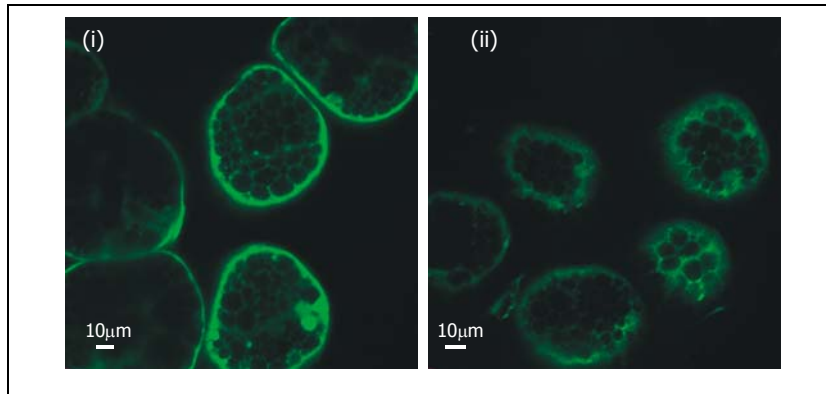
Figure 3.12. Immuno-localization of VAMP in granular cells of *O. savignyi* salivary glands. *VAMP localize to granule membranes (i), but not the cell plasma membrane (ii).*

SNAP 25

Immuno-localization of SNAP25 indicated small granules/vesicles enriched in SNAP25 (Figure 3.13.i). In acini, localization of SNAP25 to granule membranes was confirmed since individual granules are visible (Figure 3.13.ii).
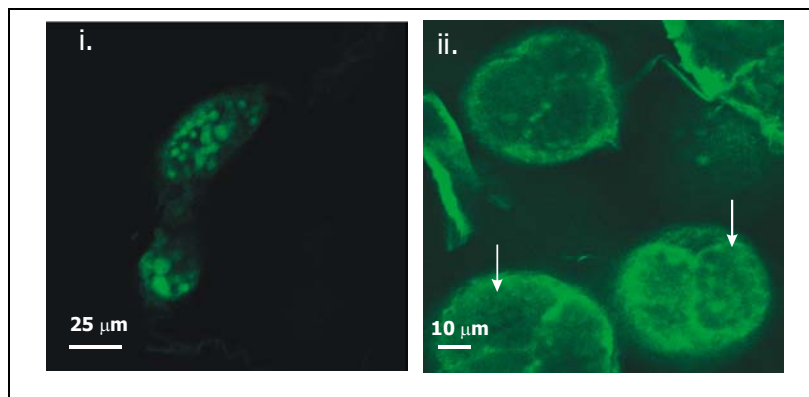
Figure 3.13. Immuno-localization of SNAP25 in acini of *O. savignyi*. *SNAP25 was localized to small granules (i) and granule membranes (ii). Arrows indicate individual granules.*

Cytoskeleton proteins: Actin and Tubulin

Both of the cytoskeleton proteins actin and tubulin play important roles during exocytosis. The actin cytoskeleton is believed to regulate exocytosis by forming a cortical actin network

beneath the plasma membrane and to also mediate the transport of secretory granules to exocytotic sites on the plasma membrane (Burgoyne and Morgan 2003). Immuno-localization of actin in granular cells of *O. savignyi* indicated actin to localize predominantly to the sub-plasma membrane region, supporting the presence of an actin barrier in tick salivary glands (Figure 3.14). Actin is also visible between the granules since individual granules are visible.
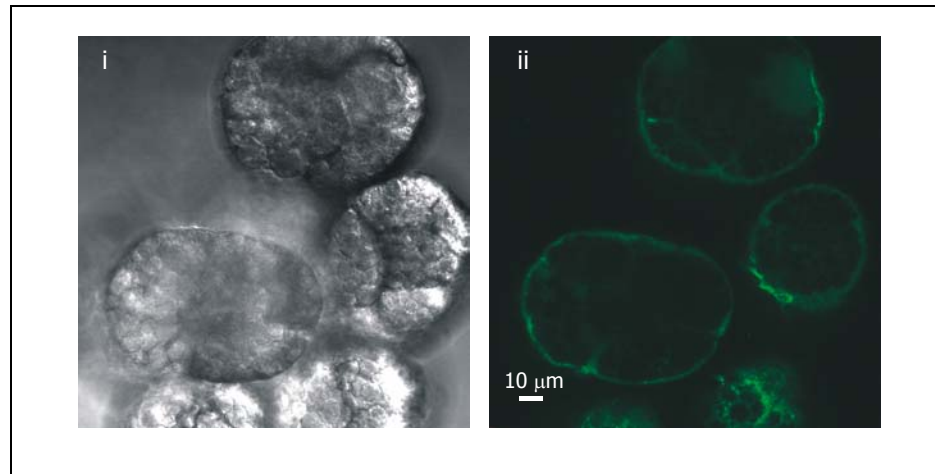
Figure 3.14. Immuno-localization of actin in acini of *O. savignyi*. *Actin localized to the plasma membrane region in granular acini. Both the light microscope image (i) and the fluorescence confocal image (ii) are shown.*

Similar to actin, tubules are required for the transport and delivery of proteins throughout the entire secretory pathway (Apodaca 2001; Neco *et al.* 2003). Localization of tubulin in acini was indicated to the sub-plasma membrane of the cells, as well as the intracellular tissue between the granules (Figure 3.15). Therefore, one can conclude that tick salivary glands do contain an extensive cytoskeletal structure and that it is involved in exocytosis (see Chapter 2).
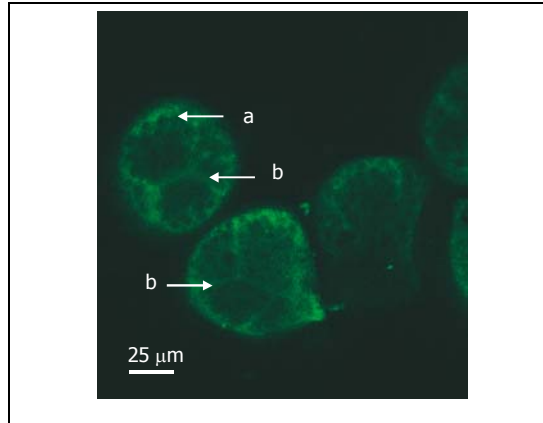
Figure 3.15. Immuno-localization of tubulin in the acini of *O. savignyi.* *Tubulin localized to either the (a) intra granular spaces or (b) the sub-plasma membrane region of granular cells.*

3.6.3. RNA isolation

Analysis of the total RNA isolated from the salivary glands of *O. savignyi* indicated only a 18S rRNA band, which is different from total RNA isolated from tissues containing 28S, 18S and 5S rRNA units. This observation has been described previously (Joubert *et al.* 1998; Mans 2002a). In contrast, RNA isolated from whole *O. savignyi* ticks (all tissues excluding salivary glands) and fed *Argas (P.) walkerae* larvae contained the 28S, 18S and 5S rRNA bands (Figure 3.16.ii and iii).
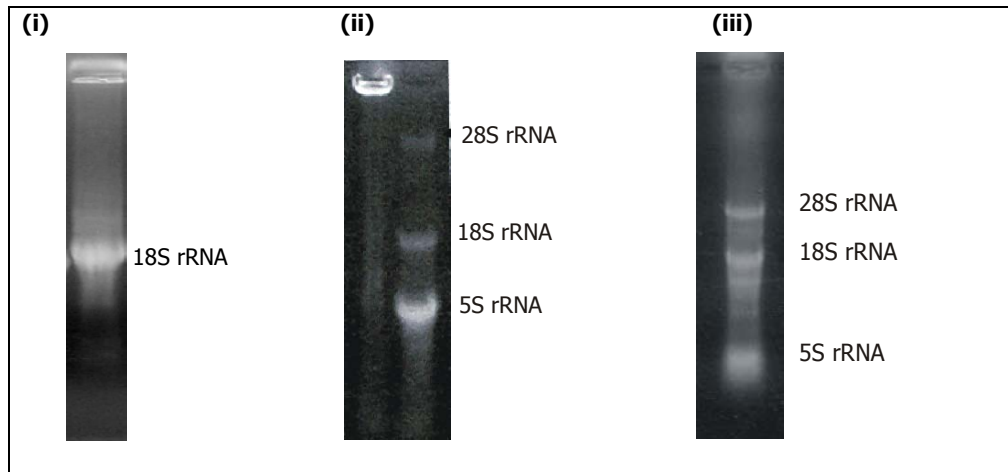
Figure 3.16. Electrophoretic analysis of total RNA. *Figures corresponds to total RNA isolated from (i) salivary glands of O. savignyi, (ii) the remaining tissues of O. savignyi, and (ii) whole Argas (P.) walkerae larvae.*

3.6.4 3'-RACE USING ss cDNA

cDNA was synthesized as described previously using the method of Joubert *et al.*, which employs an anchor-dT primer and reverse transcriptase (Joubert *et al.* 1998). 3'-RACE was subsequently performed with a degenerative primer and anchor primer (Figure 3.7).

Synaptotagmin

Based on the techniques used to date to identify synaptotagmin isoforms from various tissues (Table 3.6), we decided on exploiting a synaptotagmin I (sytI) probe as well as degenerative primers. The entire coding sequence of sytI was amplified from the recombinant sytI construct obtained from Prof. R.H. Scheller, using PCR and sequence specific primers. A single band corresponding to 975 bp was obtained (Figure 3.17). Identical conditions were used to amplify the sytI band in the presence of DIG-dUTP to create a DIG-labelled probe. The probe was purified using the NucleoSpin® Extract kit.
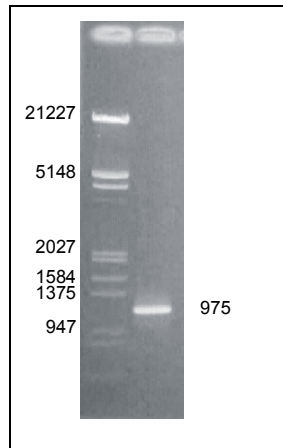
Figure 3.17. Agarose electrophoresis of the open reading frame amplified from recombinant synaptotagmin I.

Degenerative primers were designed on two conserved regions identified in synaptotagmin isoforms I, II, III, IV and V (Figure 3.18). The first sequence (FDRFS) is present in the PKC-C2A domain while the second sequence (SDPYVK) is present in both PKC-C2 (A and B) domains. The properties of the degenerative primers are listed in Table 3.7.

```
                                                                  •• ••
        SytV  vldkhqLGRL qYSLDYdFqt gQLlVgIlQA egLaALDlgG .sSDPYVsVY LLPDKRRRhe TKVHRqTLNP hFgETFaF.k VPYvELggRv LvmaVYDFDR
        SytI  pkeeekLGKL qYSLEYdFqn nQLlVgIiQA aeLPALDmgG .tSDPYVKVF LLPEKKKKfe TKVHRKTLNP vFnEqFtF.k VPYsELggKt LvmaVYDFDR
       SytII  ekepenLGKL qFSLEYdFqa nQLtVgVlQA aeLPALDmgG .tSDPYVKVF LLPDKKKKye TKVHRKTLNP aFnETFtF.k VPYqELggKt LvmaIYDFDR
      SytIII  geagapcGRI sFaLrYlYgs dQLvVrIlQA ldLPAkDsnG .fSDPYVKIY LLPDRKKKfq TKVHRKTLNP iFnETFqF.s VPlaELaqRk LhfsVYDFDR
       SytIV  ekq.eklGtL fLSLEYnFek kaFvVnIkeA qgLPAMDeqs mtSDPYIKmt iLPEKKHRvk TRVlRKTLdP vFgETFtFyg IPYphiqels LhftVlsFDR
   Consensus  .......G.. .o.L.Y.o.. ....V....A ..LPA.D... .SDPY.... .LP-++++.. T+V.R.TL.P .F.E.F.F.. .P........ L......FDR

        SytV  FSRnDaIGEV rVPMssVnLg rpvqa...WR ElqvapkEeq EkLGDicfSL rYvPTAGkLT ViVLeAKNLK KMDVgGLSDP YVKVhLlqgG KRvRKKKTTI
        SytI  FSKhDiIGEf kVPMntVDFg hvtee...WR DlqsaekEeq EkLGDicfSL rYvPTAGkLT VvILeAKNLK KMDVgGLSDP YVKIhLmqnG KRlKKKKTTI
       SytII  FSKhDiIGEk kVPMntVDLg qpiee...WR DlqggekEep EkLGDictSL rYvPTAGkLT VcILeAKNLK KMDVgGLSDP YVKIhLmqnG KRlKKKKTTV
      SytIII  FSRhDlIGqV .VldnllELa eqppdrplWR DileggsEka D.LGElnfSL cYlPTAGilLT VtIikAsNLK aMDltGFSDP YVKasLiseG rRlKKRKTSI
       SytIV  FSRdDvIGEV lIPLsgIELs d..gkmlmtR Eiikrnakks sgrGEllvSL cYqsTtntLT VvVLkARhLp KsDVsGLSDP YVKVnLyhak KRisKKKThV
   Consensus  FS+.D.IG.. .......... .......R -......... ...G-...SL .Y..T...LT V....A..L. ..D..G.SDP YVK..L.... +R..K+KT..

                      ****
        SytV  KKnTLNPyYN EaFsFEVPcD qVqkVqVelt VLDYDKlGKN EaIGRvaVGt avgGaglR.H WaDMLANPRR PIAQWHsLrp pdrarpipap. ..........
        SytI  KKnTLNPyYN EsFsFEVPfE qIqkVqVvvt VLDYDKiGKN DaIdKvfVGy nstGaelR.H WsDMLANPRR PIAQWHtLqv eeevdamlavk k.........
       SytII  KKkTLNPyFN EsFsFEIPfE qIqkVqVvvt VLDYDKlGKN EaIGKifVGs natGtelR.H WsDMLANPRR PIAQWHsLkp eeevdallgkn k.........
      SytIII  KKnTLNPtYN EaLvFDVapE sVenVglsia VvDYDciGHN EvIGvcrVGp eaadphgReH WaEMLANPRK PVeHWHqLve ektlssftkgg kglsekense
       SytIV  KKcTpNavFN ElFvFDIPcE sleeIsVefl VLDsERgsRN EvIGRlvlGa taeGsgg.gH WkEicdfPRR qIAKWHmLcd g.......... ..........
   Consensus  KK.T.N..oN E...F-.... .......... V.D.-...+N -.I.....G. .........H W.-....PR+ ....WH.L.. .......... ..........
```

Figure 3.18. Amino acid similarity among five synaptotagmin isoforms (Hudson and Birnbaum 1995). *Amino acid sequences of the five synaptotagmin isoforms are aligned. Conserved and identical amino acids are capitalized. A consensus sequence appears on the bottom, depicting only amino acids that are identical among all isoforms. In the consensus sequence, completely conserved acidic or basic residues are indicated with a (–) or (+), respectively, and conserved aromatic residues are indicated by (o). The PKC-C2 domains are overlined with a solid line while the NPXY sequence is denoted by asterisks (X indicates any amino acid).*

Table 3.7. Properties of the synaptotagmin degenerative primers. *Degenerate nucleotide nomenclature corresponds to: (W) is A or T, (N) is any nucleotide, (R) is A or G, (S) is G or C, (M) is A or C and (Y) is C or T.*

Name	Sequence	Degeneracy	Tm (ºC)
Syt_1 (SDPYVK)	WST GAY CCT TAY GTN AAR	128	48.77
Syt_2 (FDRFS)	TTY GAY TTY GAY MGT TT	32	45.4

Using the Syt_1 primer we were able to identify various bands during PCR using cDNA from both salivary glands and whole *O. savignyi* ticks (Figure 3.19). As a control, cDNA from rat brain was used. The expected size was 735 bp for the open reading frame of rat brain sytI (excluding the 3' UTR and polyA tail). In lanes 11-13 an intense band was observed at ~800 bp for the brain samples, while two bands (~950 and 1100 bp) were observed for the *O. savignyi* samples.
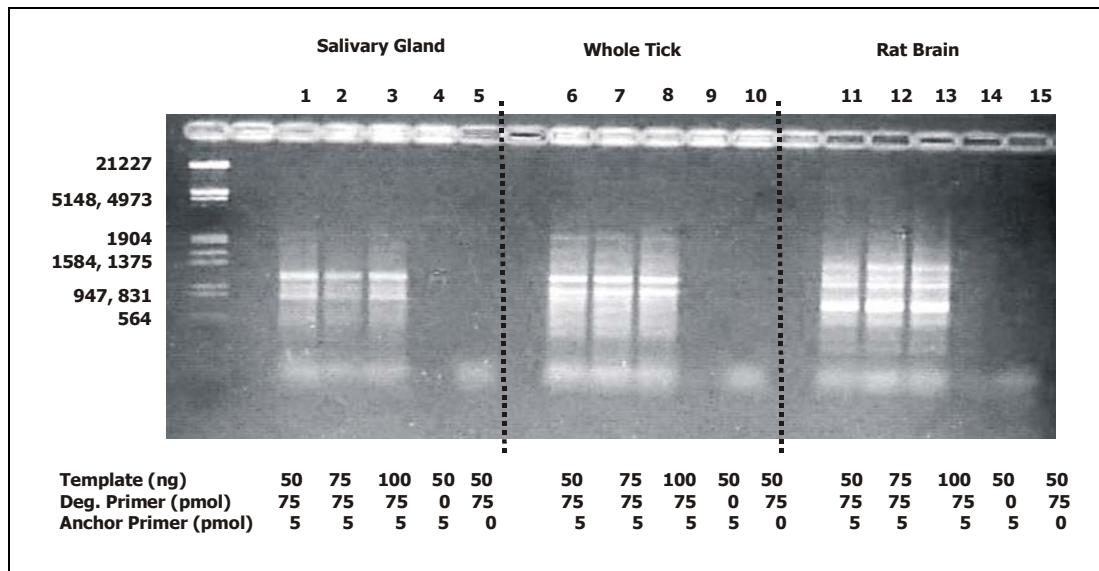
Figure 3.19. 3'-RACE with synaptotagmin primer 1 (SDPYVK) and cDNA created from salivary glands of *O. savignyi*, whole *O. savignyi* ticks and rat brain (positive control). *The conditions used during 3'-RACE are listed for each sample.*

Since the PCR could not be optimized to obtain only single specific bands, the bands were excised, purified and cloned into the pGEM-T easy vector. Using restriction enzyme mapping unique clones were identified. These were grown, subjected to high pure plasmid isolation and hybridization with the sytI probe. All positive clones were subjected to DNA sequencing. The results obtained from all of the *O. savignyi* samples indicated no similarity to synaptotagmin (results not shown). Synaptotagmin was, however, successfully cloned and identified from the rat brain samples.

3'-RACE performed with the syt_2 primer yielded a single band of ~500 bp (Figure 3.20). Once again the rat brain cDNA, which was used as positive control, yielded a similar mass band (~600 bp). The various bands were purified, cloned and screened via restriction enzyme digestion and hybridization with the sytI probe (Figure 3.21). All unique positive clones were subjected to DNA sequencing. Once again, no similarity to synaptotagmin was obtained for the tick clones (results not shown).
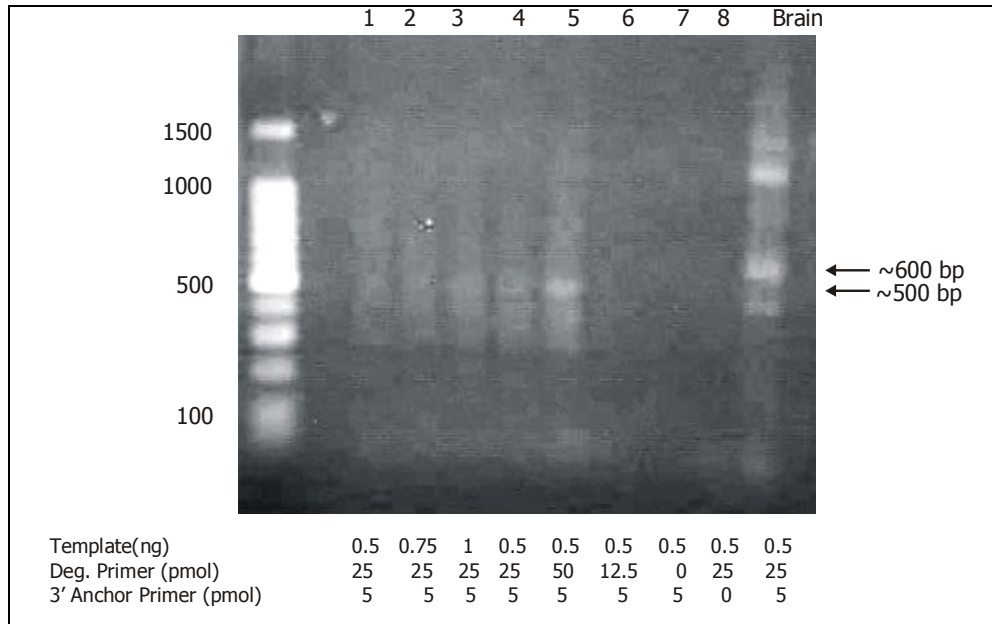
Figure 3.20. 3'-RACE with salivary gland RNA and the syt_2 primer. *The conditions used during 3'-RACE are listed for each sample.*
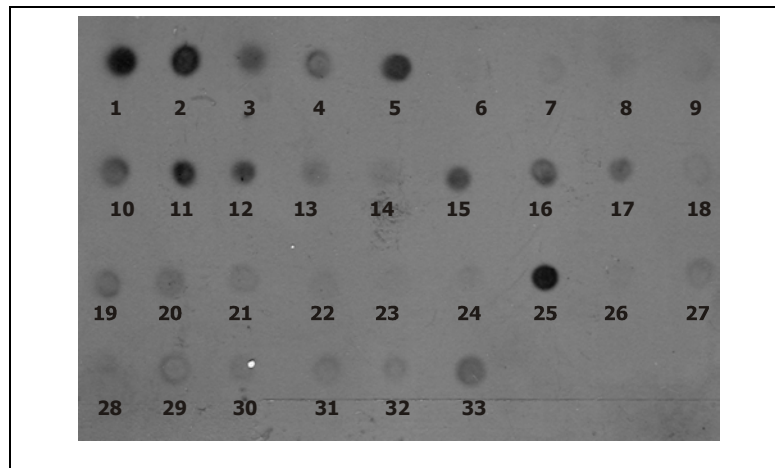
Figure 3.21. Hybridisation of the putative synaptotagmin clones obtained with the DIG-labelled sytI probe.

Syntaxin

Amino acid sequence alignment of various syntaxin isoforms from various diverged organisms indicated five conserved regions (Figure 3.22). The RKFVEVM and VESQGEM regions were used for designing degenerative primers for 3'-RACE due to the lower degeneracy of the codons encoded for in these amino acid sequences. The properties of the two primers are listed in Table 3.8.

119

```
D78271_Loligo              DKISDNVDAVKKKHSDILSAPQTDDQMKEELEELMTDIKRTANKVRGKLK 97
Y14575_Loligo              DKISDNVDAVKKKHSDILSAPQTDDQMKEELEELMTDIKRTANKVRGKLK 97
U03123_Aplysia             DKIASNVDEVKKKHSAILSAPQTDDKMKEELEELMSEIKKNANKVRAKLK 96
U85807_Hirudo              DKIAVDVDEVKKKHSAILSAPQTDDKTKEELEDLMAEIKKTANKVRGKLK 100
L37732_Drosophila          DKVQDNVEVKKKHSAILSAPQTDEKTKQELEDLMADIKKNANRVRGKLK 97
AB008844_Caenorhabditis    DIIANNVEEVKKKHSAILSNPVNDQKTKEELDELMAVIKRAANKVRGKLK 96
AB008843_Caenorhabditis    DIIANNVEEVKKKHSAILSNPVNDQKTKEELDELMAVIKRAANKVRGKLK 96
AB008842_Caenorhabditis    DIIANNVEEVKKKHSAILSNPVNDQKTKEELDELMAVIKRAANKVRGKLK 96
AF015486_Strongylocentrotus DKISKNVDEVKKKHSDILSAPQADEKVKDELEELMSDIKKTANKVRAKLK 76
U12918_Human               DKIAENVEEVKRKHSAILASPNPDEKTKVELEELMSDIKKTANKVRSKLK 65
X90581_Human               DKISEHVEEAKKLYSIILSAPIPEPKTKDDLEQLSTEIKKRANNVRNKLK 86
AJ002077_Human             --ISEHVEEAKKLYSIILSAPIPEPKTKDDLEQLTTEIKKRANNVRNKLK 48
                             :  .*: .*: :* **: *  : : * :*::* : **: **.** ***


                                              Primer1
D78271_Loligo              TIELNIEQEEHSNKSSADLRIRKTQYSTISRKFVEVMSDYNTTQIDYRDR 147
Y14575_Loligo              TIELNIEQEEHSNKSSADLRIRKTQYSTISRKFVEVMSDYNTTQIDYRDR 147
U03123_Aplysia             VIEQNIEQEEHTNKSSADLRIRKTQHATLSRKFVEVMNDYNACQIDYRER 146
U85807_Hirudo              VLEQKIEQEEETNKSSADLRIRKTQHSTILRKFIEVMNQYNAAQVDYRDG 150
L37732_Drosophila          GIEQNIEQEEQQNKSSADLRIRKTQHSTLSRKFVEVMTEYNRTQTDYRER 147
AB008844_Caenorhabditis    LIENAIDHDEQG-AGNADLRIRKTQHSTLSRRFVEVMTDYNKTQTDYRER 145
AB008843_Caenorhabditis    LIENAIDHDEQG-AGNADLRIRKTQHSTLSRRFVEVMTDYNKTQTDYRER 145
AB008842_Caenorhabditis    LIENAIDHDEQG-AGNADLRIRKTQHSTLSRRFVEVMTDYNKTQTDYRER 145
AF015486_Strongylocentrotus MMDQSIERRRVPRRTQTDVRIRKTQHSTLSRKFVEVMTDYNSTQTDYRER 126
U12918_Human               SIEQSIEQEEGLNRSSADLRIRKTQHSTLSRKFVEVMSEYNATQSVYRER 115
X90581_Human               SMEKHIEEDEVR--SSADLRIRKSQHSVLSRKFVEVMTKYNEAQVDFRER 134
AJ002077_Human             SMEKHIEEDEVR--SSADLRIRKSQHSVLSRKFVEVMTKYNEAQVDFRER 96
                             ::   *:. .     .:*:****:*::.: *:*:***..**  *  :*:


D78271_Loligo              CKARIKRQMEITGRTTTNEELEDMLESGNPAIFTQGIIMETQQAKQTLAD 197
Y14575_Loligo              CKARIKRQMEITGRTTTNEELEDMLESGNPAIFTQGIIMETQQAKQTLAD 197
U03123_Aplysia             CKGRIKRQLAITGKTTTNEELEDMIESGNPAIFTQGIIMETQQANETLAD 196
U85807_Hirudo              CKKRLQRQMEITGRATTNEELEDMLESGNPAIFTQGIITDTQQAKQSLMD 200
L37732_Drosophila          CKGRIQRQLEITGRPTNDDELEKMLEEGNSSVFTQGIIMETQQAKQTLAD 197
AB008844_Caenorhabditis    CKGRIQRQLDIAGKQVGDEDLEEMIESGNPGVFTQGIITDTQQAKQTLAD 195
AB008843_Caenorhabditis    CKGRIQRQLDIAGKQVGDEDLEEMIESGNPGVFTQGIITDTQQAKQTLAD 195
AB008842_Caenorhabditis    CKGRIQRQLDIAGKQVGDEDLEEMIESGNPGVFTQGIITDTQQAKQTLAD 195
AF015486_Strongylocentrotus CKGRIQRQLEITGKSTTDAELEDMLESGNPAIFTSGIIMDTQQAKQTLRD 176
U12918_Human               CKGRIQRQLEITGRTTTSEELEDMLESGNPAIFASGIIMDSSISKQALSE 165
X90581_Human               SKGRIQRQLEITGKKTTDEELEEMLESGNPAIFTS-GIIDSQISKQALSE 183
AJ002077_Human             SKGRIQRQLEITGKKTTDEELEEMLESGNPAIFTS-GIIDSQISKQALSE 145
                            .* *::**: *:*: . . :**.*:*.**..:*:.  * ::. ::::* :


                                              Primer2
D78271_Loligo              IEARHADIMKLETSIRELHDMFMDMAMLVESQGEMIDRIEYNVEAAVDYI 247
Y14575_Loligo              IEARHADIMKLETSIRELHDMFMDMAMLVESQGEMIDRIEYNVEAAVDYI 247
U03123_Aplysia             IEARHNDIMKLETSIRDLHDMFMDMAMLVESQGEMIDRIEYNVEQAVDYI 246
U85807_Hirudo              IEARHNDIMKLEQSIRELHDMFMDMAMLVESQGEMIDRIEHNVEKAVDYV 250
L37732_Drosophila          IEARHQDIMKLETSIKELHDMFMDMAMLVESQGEMIDRIEYHVEHAMDYV 247
AB008844_Caenorhabditis    IEARHNDIMKLESSIRELHDMFMDMAMLVESQGEMVDRIEYNVEHAKEFV 245
AB008843_Caenorhabditis    IEARHNDIMKLESSIRELHDMFMDMAMLVESQGEMVDRIEYNVEHAKEFV 245
AB008842_Caenorhabditis    IEARHNDIMKLESSIRELHDMFMDMAMLVESQGEMVDRIEYNVEHAKEFV 245
AF015486_Strongylocentrotus IEARHNDIIKLESSIRELHDMFMD------------------------- 200
U12918_Human               IETRHSEIIKLENSIRELHDMFMDMAMLVESQGEMIDRIEYNVEHAVDYV 215
X90581_Human               IEGRHKDIVRLESSIKELHDMFMDIAMLVENQGEMLDNIELNVMHTVDHV 233
AJ002077_Human             IEGRHKDIVRLESSIKELHDMFMDIAMLVENQ----------------- 177
                            ** ** :*::** **::******
```

Figure 3.22. Amino acid sequence alignment of various syntaxins. *Sequences were obtained from the NCBI databank. Identical (*), similar charge (:), and similar polarity (.) of residues are indicated. Conserved regions indicated in red were considered for degenerative primer design.*

Table 3.8. Properties of the syntaxin degenerative primers. *Degenerate nucleotide nomenclature corresponds to: (W) is A or T, (N) is any nucleotide, (R) is A or G, (S) is G or C, (Y) is C or T and (M) is A or C.*

Name	Sequence	Degeneracy	Tm (ºC)
Syn_1 (VESQGEM)	GTI GAR WSI CAR GGN GAR ATG	128	58.0
Syn_2 (RKFVEVM)	MGI AAR TTY GTI GAR GTN ATG	64	53.0

PCR amplification using the syn_1 degenerative primer and cDNA from the salivary glands of *O. savignyi* identified a single band of ~700 bp, which is in the expected size region. This band was however not cloned since the PCR was driven only by the degenerative primer and not both the degenerative and anchor primers (Figure 3.23). PCR amplification using cDNA obtained from fed *Argas walkerae* larvae (another argasid tick used as control) yielded a single band, which was amplified by both primers (Figure 3.24). This band was purified, cloned and subjected to DNA sequencing. The obtained nucleotide and protein sequence is given in Figure 3.25.

	1	2	3
Syn_1	+	+	-
Anchor	+	-	+
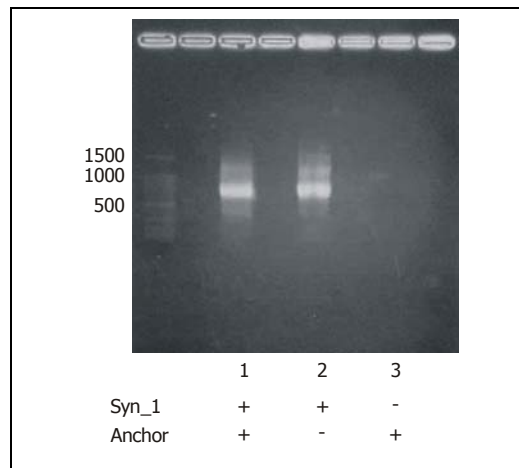
Figure 3.23. PCR amplification of syntaxin using the syn_1 degenerative primer from *O. savignyi* salivary gland cDNA.

	1	2	3
Syn_1	+	-	+
Anchor	-	+	+
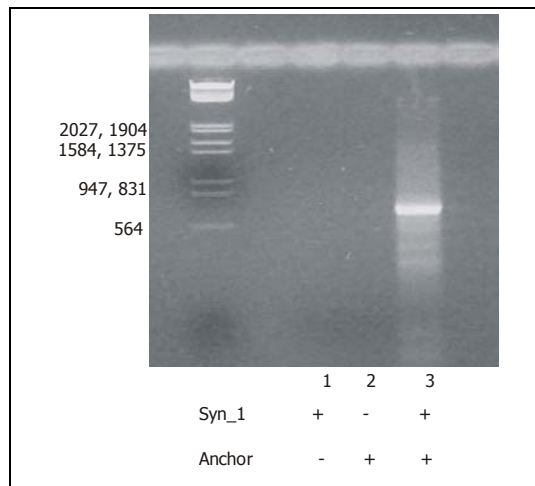
Figure 3.24. PCR amplification of syntaxin using the syn_1 degenerative primer from *Argas (P.) walkerae* cDNA.

```
gtggagtggcagggcgagatgtttgagaggccaggaaagctgtctgactactttccatct
 V   E   W   Q   G   E   M   F   E   R   P   G   K   L   S   D   Y   F   P   S
ccataccccaatgaagaggcagcaagagcagcgaataatggtgctcttccacctgacctc
 P   Y   P   N   E   E   A   A   R   A   A   N   N   G   A   L   P   P   D   L
agcttcatcacgaatgctaaacatggcggagaggactacattttcgcactgttgacggga
 S   F   I   T   N   A   K   H   G   G   E   D   Y   I   F   A   L   L   T   G
tactgcgatccacccgcaggagtgacgatccaagaaggtcagtactacaaccccctacttc
 Y   C   D   P   P   A   G   V   T   I   Q   E   G   Q   Y   Y   N   P   Y   F
ccaggggggagctatcggcatggcccaagctctctacaatgaggccatggaatactctgat
 P   G   G   A   I   G   M   A   Q   A   L   Y   N   E   A   M   E   Y   S   D
ggcacaccggccactactagtcagatggcaaaggatgtactactttcctcaggttctgca
 G   T   P   A   T   T   S   Q   M   A   K   D   V   L   L   S   S   G   S   A
cggagccanagtttgatgaccgcaaacgcatgtttatcaagggcatgatgatctgtcact
 R   S   X   S   L   M   T   A   N   A   C   L   S   R   A   -   -
gctgcttgntacgacctggtacttgnaaccggcagaatggatgac
```

Figure 3.25. DNA nucleotide and amino acid sequence of *A. walkerae* clone obtained with syn_1. *The primer region is indicated in red and the stop codon (-) is visible.*

Both BLAST_P and PSI-BLAST analysis of the deduced protein sequence indicated a significant similarity to the cytochrome C1 heme protein as well as the cytochrome C1 precursor, with E-values of $2x10^{-41}$ and $3x10^{-39}$, respectively. Threading analysis indicated 53% identity to the sequence and structure of the cytochrome C1 transmembrane subunits.

PCR amplification using the syn_2 primer, based on the amino acid sequence RKFVEVM, was optimized using a Taguchi optimization matrix (Cobb and Clarkson 1994). The three conditions that were varied were the $MgCl_2$ concentration, syn_2 primer concentration and amount of template (cDNA/RNA equivalents). A single ~550 bp band was obtained under numerous conditions (Figure 3.26). This band was purified (Figure 3.27), cloned and subjected to DNA sequencing. The nucleotide and deduced amino acid sequence is given in Figure 3.28. Both BLAST-P and PSI-BLAST analysis were unable to detect any possible identity of the encoded protein. Threading indicated similarity to DNA binding proteins (25%), various collagen isoforms (25-26%) and insect defensins (28%). Therefore, degenerative primers and 3'-RACE was not successful in amplifying a syntaxin homologue from *O. savignyi*.
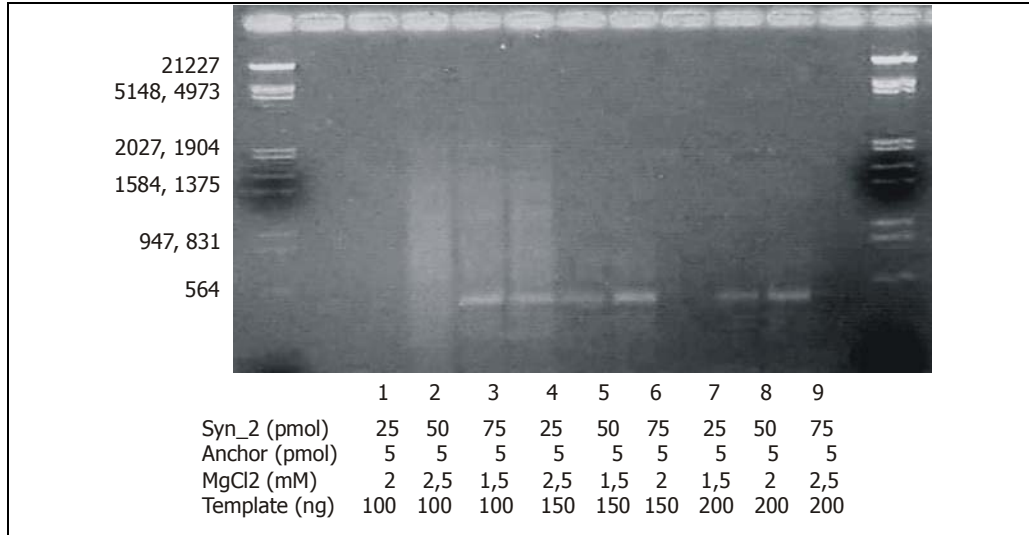
Figure 3.26. Taguchi-PCR with syn_2 using salivary gland cDNA from *O. savignyi*. *The conditions used during 3'-RACE are listed for each sample.*
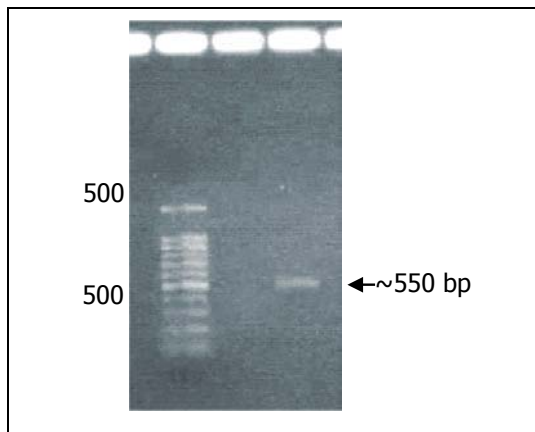
Figure 3.27. High Pure isolation of the 500 bp band obtained with syn_2.

```
aggaaattcgtggaggttatgtatgttacgcacggtctcagtgtaagcttaagagcaccc
 R  K  F  V  E  V  M Y  V  T  H  G  L  S  V  S  L  R  A  P
catctaccgctacctgggacttcgaggtgtgtggcatgcacgagatgcattggagaaat
 H  L  P  G  T  S  R  C  V  A  C  T  R  C  I  G  E  N
caaaatgagatgacgttgattagtgaggttacatcagttgactgcgattgatttagctta
 Q  N  E  M  T  L  I  S  E  V  T  S  V  D  C  D  -  F  S  L
cacagattttgtttctttgtttagttgcaccaatgacaacgtatggcctactacatcgc
 H  R  F  L  F  L  C  L  V  A  P  M  T  T  Y  G  L  L  H  R
gtatcccgctacgcactgtactgtatggtgccgaaattctgcaatgacatgtacgtcgat
 V  S  R  Y  A  L  Y  C  M  V  P  K  F  C  N  D  M  Y  V  D
agggtacagctgcgtgcacttcgcgttgttcagaaattgggtattaacagggtatctaaa
 R  V  Q  L  R  A  L  R  V  V  Q  K  L  G  I  N  R  V  S  K
gcagcatgtacgactccacagtgaagaaaatactccgcgtatgtcgagattggtaaatga
 A  A  C  T  T  P  Q  -
ggaacatgacttaattgtacggaaaaaaaaaaaaaaaa
```

Figure 3.28. Nucleotide and amino acid sequence of the 500 bp band obtained with syn_2 primer from salivary gland cDNA. *The primer sequence is indicated in purple. The stop codon (-) and poly(A) tail is visible.*

123

Serine protease (Positive control)

As a positive control, we designed a primer against possible high abundance salivary gland proteins such as serine proteases. The serine proteases are divided into two families: the trypsins and subtilisins. The trypsin family is the largest and is found in vertebrates, as well as fungi and prokaryotic cells (http://www.diapharma.com). A degenerative primer was designed against the most conserved region (GDSGGPL), which was identified from aligned serine protease amino acid sequences. The properties of the primer are given in Table 3.9.

Table 3.9. Properties of the serine protease degenerative primer. *Degenerate nucleotide nomenclature corresponds to: (W) is A or T, (N) is any nucleotide, (S) is G or C and (Y) is C or T.*

Name	Sequence	Degeneracy	Tm (ºC)
Ser1 (GDSGGPLV)	GTG AYW STG GTG GTC CIY TIG TN	64	61.5

Initial PCR studies using total RNA from unfed *O. savignyi* salivary glands revealed only a smear and no distinct bands could be observed. After optimization, two bands (~200 and 300bp, respectively) were obtained. DNA sequencing and analysis of the bands indicated that none of the bands displayed significant similarity to any known protein. These results indicated that (i) the transcript is not present in the cDNA pool, or (ii) the transcript is present in very low abundance, or (iii) the primer is not suitable for the identification of a serine protease. These conclusions also applied to the previously described PCRs for the identification of synaptotagmin and syntaxin. Therefore, we decided to firstly use RNA from fed ticks in which transcription is enhanced and secondly, to equalize the cDNA using suppression PCR.

3.6.5 3'-RACE USING SUPER SMART™ ds cDNA

RNA was isolated from fully engorged ticks. There was an approximate 3.5 fold increase in tick weights. During ds DNA synthesis using the Super SMART™ principle, only a single primer is used during LD-PCR, since the 5' sequence (obtained form the SMART IV primer) and the 3' sequence (obtained from the CDS III primer) are complementary (Table 3.10). Therefore, during PCR amplification of the ds DNA, intra-molecular annealing events can result in the formation of panhandle-structures (Figure 3.29), which will not be amplified. This is more likely to occur in high abundance transcripts, allowing the exponential amplification of low abundance transcripts and hence establishing a representative cDNA library.

Table 3.10. Super SMART™ primers used for cDNA synthesis and LD-PCR.

Name	Sequence
SMART IV	AAG CAG TGG TAT CAA CGC AGA GTG GCC ATG GAG GCC GGG
CDS III	ATT CTA GAG GCC TCC ATG GCC GAC ATG T_{30}VN
3' PCR	ATT CTA GAG GCC TCC ATG GCC GAC ATG
5' PCR	AAG CAG TGG TAT CAA CGC AGA GT
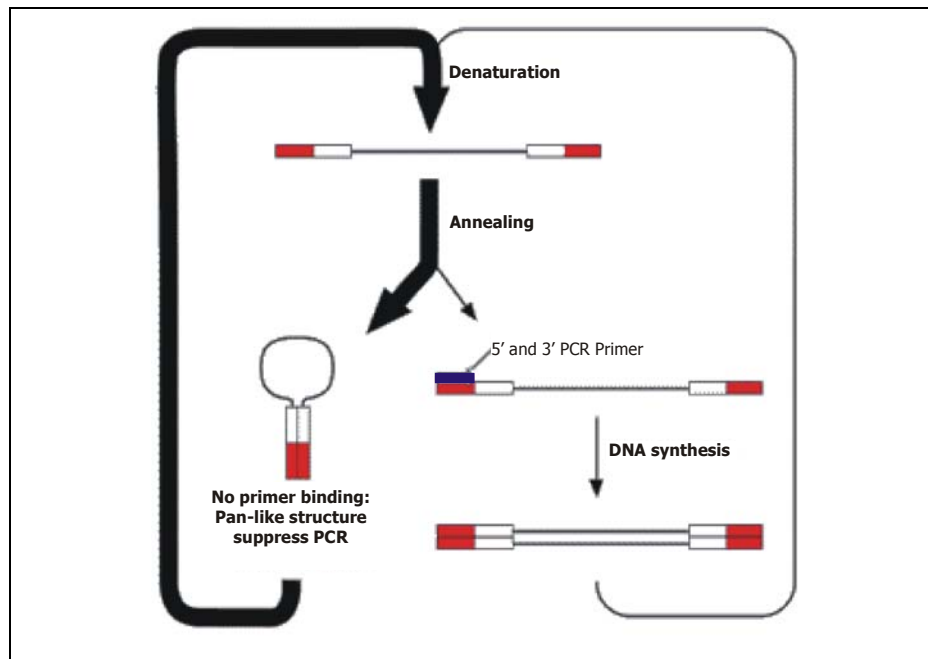
Figure 3.29. Schematic presentation of the suppression PCR effect. Adapted from (Lukyanov *et al.* 1997).

Figure 3.30 shows a typical gel profile of ds cDNA synthesized using the Super SMART™ cDNA synthesis and amplification system. The optimal amount of cycles (1 cycle less than needed to reach the plateau) was determined as 25 for both the salivary gland and whole tick (include all tissues and organs except salivary glands) RNA samples. A smear between 200-2000 bp was obtained from salivary gland RNA, while a 200-5000 bp smear was obtained from the RNA isolated of the remaining tissues of *O. savignyi* (Figure 3.30). Following amplification, the ds DNA was purified using the NucleoSpin® kit and used for 3'-RACE.
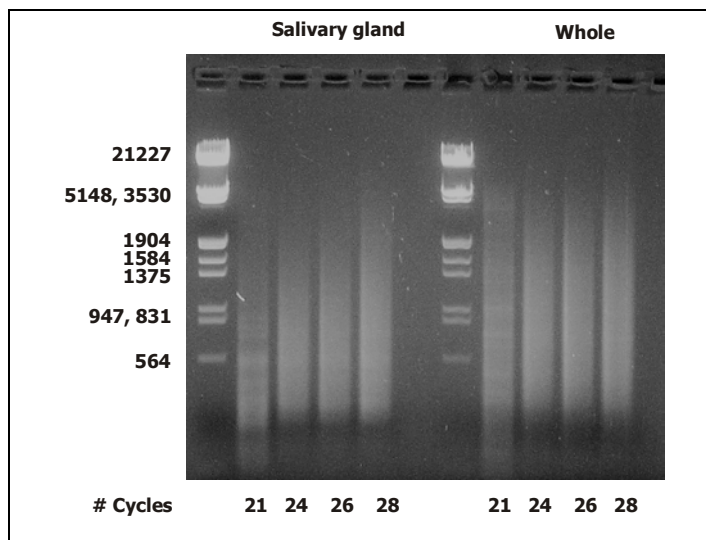
Figure 3.30. Analysis of ds cDNA amplification by LD-PCR using Super SMART™ technology. *The number of cycles used to determine the plateau is indicated for each sample.*

3′ - RACE using SuperSMART™ ds DNA

During 3′-RACE using SuperSMART ds DNA as template, the identical degenerative primers as described previously were used, but the anchor primer was replaced by the 3′ PCR primer (Table 3.10).

Serine protease (Positive control)

3′-RACE using the serine protease degenerative primer yielded two bands. These were purified, cloned and sequenced. BLAST analysis of the inserts indicated similarity to serine proteinase-1 from *Rhipicephalus appendiculatus* with a significant E-value of 1×10^{-6}, as well as serine proteases from bovine, rat and human origin. This indicates that the degenerative primer was correctly designed and that the previous inability to identify the correct transcript was most probably due to low abundance or absence of the mRNA transcript.

Syntaxin

Taguchi optimisation of the 3′-RACE conditions using the syn_1 primer indicated a prominent band at ~ 450 bp and a smear (Figure 3.31). Optimization of the conditions resulted in the amplification and purification of the 450 bp band (Figure 3.32). This band was cloned and sequenced.
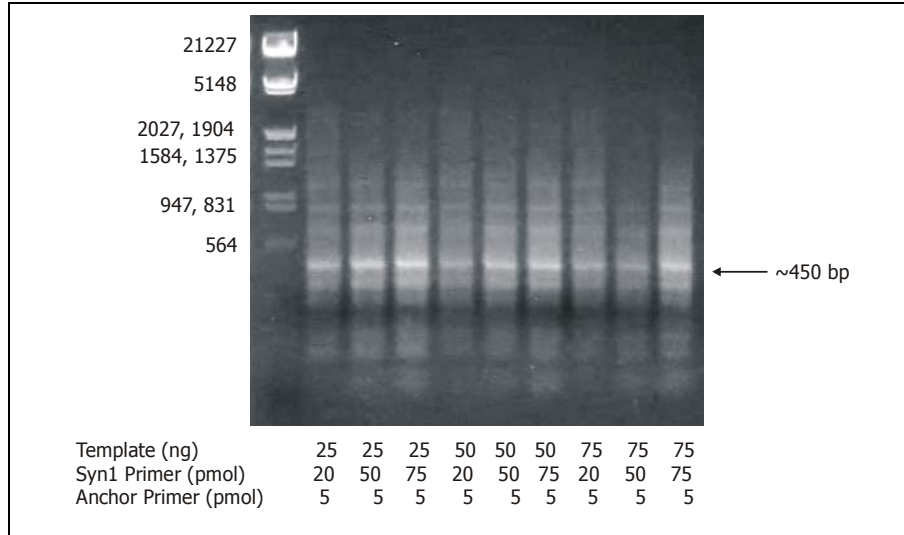
Figure 3.31. Taguchi_PCR with the syn_1 primer using ds SMART DNA from salivary glands of *O. savignyi.* *The various conditions used during 3'-RACE are listed for each sample.*
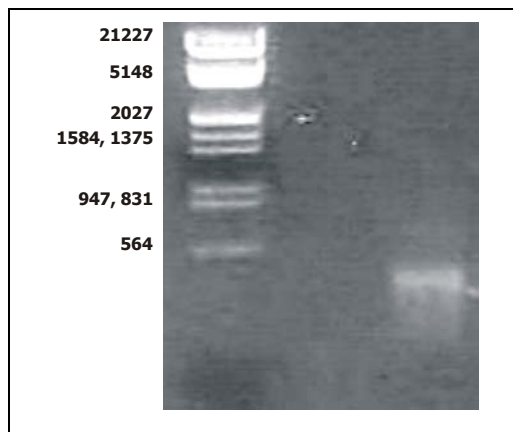
Figure 3.32. Agarose electrophoresis of the purified 450 bp product obtained with syn_1 and SMART DNA.

```
gtggagtggcaggggggagatgaaagacaaggcggaaatcctcttccnctacgaggaacag
 V   E   W   Q   G   E   M   K   D   K   A   E   I   L   F   X   Y   E   E   Q
tctcaagtcaaagatgaacttactcaagaggttggagagctgcacgccgcattagagcaa
 S   Q   V   K   D   E   L   T   Q   E   V   G   E   L   H   A   A   L   E   Q
gaacgttccaaggtccattccttgcaaacggagctcaagaagccaggcaaaagggacaac
 E   R   S   K   V   H   S   L   Q   T   E   L   K   K   P   G   K   R   D   N
cggtgatggtggcagccccttatttttttcaagtcattttggccagtcttccaaaggatc
 R   -
tggagacagtattaacgggaacaggatccagaagctttccttcattttgtatatagcagc

tgtgggataaaattcatttccggcagaaaaaaaaaaaaaaaaaaaaaaaaaaaaaaa
```

Figure 3.33. Nucleotide and amino acid sequence of 450bp band obtained with syn_1 primer from SMART salivary gland cDNA. *The primer region is indicated in red. The stop codon (-) and poly(A) tail is visible.*

127

BLAST-P and PSI-BLAST analysis of the encoded protein identified highest similarity to the GKAP-42 protein (E-value: 8 x 10^{-11}) and protein kinase anchoring proteins (E-value: 1 x 10^{-9}). Threading identified various proteins, all belonging to the all-alpha protein class, such as the Eps15 homology domain and the RAP domain of alpha-2-macroglobulin receptor associated protein. Again, no similarity to syntaxin was detected.

Syntaxin isoforms 2 and 3

In order to investigate whether tick syntaxins share sequence similarity to isoforms other than syntaxin 1, we aligned mouse, rat, human and rabbit syntaxin 2 and 3 isoforms (Figure 3.34). Various conserved regions suitable for degenerative primer design were identified. The less degenerative primer could be designed against the MLESG-region and the properties of the primer are listed in Table 3.11. During 3'-RACE, two distinct bands were obtained at 450 and 350 bp, respectively. These bands were purified, cloned and subjected to DNA sequencing.

```
MusEpim     SIILSAPNPEGKIKEELEDLDKEIKKTANRIRGKLKSIEQSCDQDENGNRTSVDLRIRRT 118
Rat_2A      SIILSAPNPEGKIKEELEDLNKEIKKTANRIRGKLKAIEQSCDQDENGNRTSVDLRIRRT 119
Rat_2C      SIILSAPNPEGKIKEELEDLNKEIKKTANRIRGKLKAIEQSCDQDENGNRTSVDLRIRRT 119
Rat_2B      SIILSAPNPEGKIKEELEDLNKEIKKTANRIRGKLKAIEQSCDQDENGNRTSVDLRIRRT 119
EPIM_Homo   SIILSAPNPEGKIKEELEDLNKEIKKTANKIAAKLKAIEQSFDQDESGNRTSVDLRIRRT 117
Rat_3A      SIILSAPIPEPKTKDDLEQLTTEIKKRANNVRNKLKSMEKHIEEDE--VRSSADLRIRKS 118
Human_3     SIILSAPIPEPKTKDDLEQLTTEIKKRANNVRNKLKSMEKHIEEDE--VRSSADLRIRKS 118
Orycto_3    --------------DDLEQLTTEIKKRANNVRNKLKSMERHIEEDE--VRSSADLRIRKS 44
                      ::**:*  :*** **.:  ***::*:  :::*   *:*.*****::


                                                            Primer
MusEpim     QHSVLSRKFVDVMTEYNEAQILFRERSKGRIQRQLEITGRTTTDDELEEMLESGKPSIFI 178
Rat_2A      QHSVLSRKFVDVMTEYNEAQILFRERSKGRIQRQLEITGRTTTDEELEEMLESGKPSIFI 179
Rat_2C      QHSVLSRKFVDVMTEYNEAQILFRERSKGRIQRQLEITGRTTTDEELEEMLESGKPSIFI 179
Rat_2B      QHSVLSRKFVDVMTEYNEAQILFRERSKGRIQRQLEITGRTTTDEELEEMLESGKPSIFI 179
EPIM_Homo   QHSVLSRKFVEAMAEYNEAQTLFRERSKGRIQRQLEITGRTTTDDELEEMLESGKPSIFT 177
Rat_3A      QHSVLSRKFVEVMTKYNEAQVDFRERSKGRIQRQLEITGKKTTDEELEEMLESGNPAIFT 178
Human_3     QHSVLSRKFVEVMTKYNEAQVDFRERSKGRIQRHVEITGKKTTDEELEEMLESGNPAIFT 178
Orycto_3    QHSVLSRKFVEVMTKYNEAQVDFRERSKGRIQRQLEITGKKTTDEELEEMLESGNPAIFT 104
            ***.******:.*::** :*   :*:*.*.****::****:.**::***:*****: :**


MusEpim     SDIISDSQITRQALNEIESRHKDIMKLETSIRELHEMFMDMAMFVETQGEMVNNIERNVV 238
Rat_2A      SDIISDSQITRQALNEIESRHKDIMKLETSIRELHEMFMDMAMFVETQGEMVNNIERNVV 239
Rat_2C      SDIISDSQITRQALNEIESRHKDIMKLETSIRELHEMFMDMAMFVETQGEMVNNIERNVV 239
Rat_2B      SDIISDSQITRQALNEIESRHKDIMKLETSIRELHEMFMDMAMFVETQGEMVNNIERNVV 239
EPIM_Homo   SDIISDSQITRQALNEIESRHKDIMKLETSIRELHEMFMDMAMFVETQGEMINNIERNVM 237
Rat_3A      SGII-DSQISKQALSEIEGRHKDIVRLESSIKELHDMFMDIAMLVENQGEMLDNIELNVM 237
Human_3     SGII-DSQISKQALSEIEGRHKDIVRLESSIKELHDMFMDIAMLVENQGEMLDNIELNVM 237
Orycto_3    SGII-DSQISKQALSEIEGR---------------------------------------- 123
            ..*   ***::***.*** *
```

Figure 3.34. Amino acid sequence alignment of various syntaxin isoforms 2 and 3. *Sequences were obtained from the NCBI databank Identical (*), similar charge (:), and similar polarity (.) of residues are indicated. Conserved regions indicated in yellow were considered for degenerative primer design.*

Table 3.11. Properties of the syn_2/3 degenerative primer. *Degenerate nucleotide nomenclature corresponds to: (W) is A or T, (N) is any nucleotide, (R) is A or G, (S) is G or C and (Y) is C or T.*

| Name	Sequence	Degeneracy	Tm (ºC)
Syn_2/3 (MLESGK)	GAR GAT ATG YTT GAR WSN GG	96	58
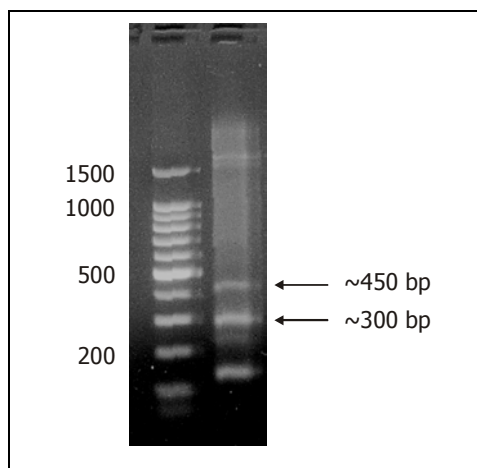
Figure 3.35. 3'-RACE with the syn_2/3 primer using ds SMART DNA from salivary glands of *O. savignyi*.

The nucleotide sequence was analysed in all three reading frames in order to determine the encoded protein sequence (Table 3.12). BLAST-N of the nucleotide sequences indicated no homology to any known protein. PSI-BLAST and P-BLAST analysis of the amino acids sequences also indicated no homology to any known proteins. Threading indicated the highest similarity to neurotoxins such as the omega-conotoxin mviia2 as well as microbial and mitochondrial isozyme 2.

Table 3.12. Amino acid sequence of the proteins encoded for in the 450 bp and 300 bp bands amplified with the syn_2/3 primer.

Name	Amino acid sequence
450 bp Band	DMFERGQCGRGYSSRSGSRTRSTKATSTLPEGRSLRRRRGPLPFQGWRSAIPVSLAGLQVMVSLKTHCSATLVY
300 bp Band	DELEDMLASTNMWKSKRLLLRCHRRTPKRS

We concluded that the SNAREs and secretory proteins in *O. savignyi* do not share sufficient sequence homology (to known isoforms) to such an extent that degenerative primers can be used. Therefore, other methods that exploit the structural properties of SNARE proteins, such as protein-protein interactions (see Chapter 4), functional complementation in knockout

yeast and affinity chromatography (see Chapter 5), must be exploited in order to isolate the conserved exocytotic machinery in *O. savignyi*.

3.7. CONCLUSION

By means of polyclonal antibodies directed at rat brain SNAREs, we were able to identify homologues of syntaxin, VAMP and SNAP25 in *O. savignyi* salivary glands. Therefore one can conclude that structural similarity exists between rat, ixodid- and argasid tick isoforms. The localization of the SNARE homologues in the salivary glands of unfed *O. savignyi* is summarized in Figure 3.36.
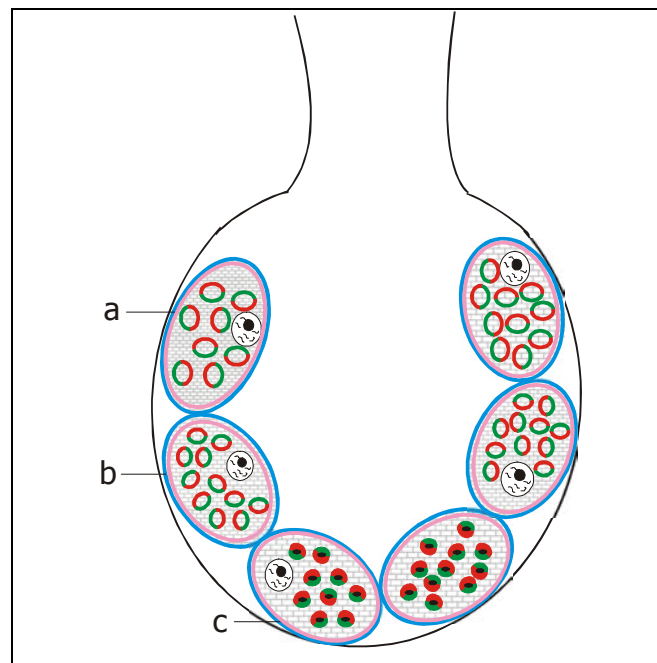
Figure 3.36. Localization of SNAREs and cytoskeletal proteins in the acini of *O. savignyi*. *Syntaxin (Blue), SNAP25 (red), VAMP (green), actin (pink) and tubulin (grey background) are indicated. We hypothesize that the small vesicles enriched in both VAMP and SNAP25 are located to the 'c' cells (filled-circles), and the granule membranes of 'a' and 'b' cells (open circles).*

3'-RACE with degenerative primers were used in an attempt to isolate the various SNARE and secretory protein transcripts from *O. savignyi*. RNA was successfully isolated from the salivary glands of some 100 unfed ticks and converted to cDNA using a poly(T)-anchor primer. As positive control, cDNA created from total rat brain RNA was used. In the latter case, synaptotagmin could be amplified and correctly identified. We also exploited a synaptotagmin I probe, which identified possible positive clones incorrectly in *O. savignyi*.

Possible reasons for not detecting SNAREs or secretory proteins could include: (a) mRNA synthesis is only initiated upon feeding, and (b) the low abundance of the mRNA transcripts.

Therefore, *O. savignyi* ticks were fed to completion on rabbits before isolating total RNA from some 30 glands. Double stranded, cDNA was synthesized from as little as 500 ng total RNA by using the Super SMART system (Clontech). The latter protocol involves equalization of the transcripts by means of suppression PCR. As a positive control, a primer against a high abundance transcript (encoding serine proteases) was used. By means of 3'-RACE, we were able to successfully amplify and clone a trypsin-like serine protease. Studies using the degenerative primers directed against the various SNAREs and secretory proteins were unsuccessful.

Our data indicates that the structural properties of *O. savignyi* secretory proteins does resemble that of rat brain, but since the degenerative primers were unsuccessful in amplifying SNAREs, one can conclude that the nucleotide sequences differ significantly between tick SNAREs and the consensus sequences used for primer design. Alignments of all known syntaxins to date indicated no significant conserved regions useful for primer design amongst the entire family. Therefore, methods exploiting the functional and structural characteristics of the secretory proteins such as protein-protein interactions (Chapter 4), functional complementation in knockout cells (Chapter 5) and affinity (Chapter 5) will be exploited in order to isolate these proteins.

3.8. REFERENCES

Apodaca, G. (2001). Endocytic traffic in polarized epithelial cells: Role of the actin and microtuble cytoskeleton. *Traffic* **2**: 149-159.

Atlas, D. (2001). Functional coupling of voltage-sensitive calcium channels with exocytotic proteins: ramification for the secretion mechanism. *Journal of Neurochemistry* **77**: 972-985.

Banerjee, A., Kowalchyk, J.A., DasGupta, B.R., Martin, T.F.J. (1996b). SNAP-25 is required for a late postdocking step in calcium-dependent exocytosis. *The Journal of Biological Chemistry* **271**(34): 20227-20230.

Betz, A., Okamoto, M., Benseler, F., Brose, N. (1997). Direct interaction of the rat unc-13 homologue Munc13-1 with the N-terminus of syntaxin. *The Journal of Biological Chemistry* **272**(4): 2520-2526.

Burgoyne, R.D., Morgan, A. (2003). Secretory granule exocytosis. *Physiology Reviews* **83**: 581-632.

Castle, J.D., Guo, Z., Liu, L. (2001). Function of the t-SNARE SNAP-23 and secretory carrier membrane proteins (SCAMPs) in exocytosis in mast cells. *Molecular Immunology* **38**: 1337-1340.

Chapman, E.R., Hanson, P.I., An, S., Jahn, R. (1995). Calcium regulates the interaction between synaptotagmin and syntaxin I. *The Journal of Biological Chemistry* **270**(40): 23667-23671.

Clontech Laboratories, I. (2001a). *Super SMART PCR cDNA synthesis kit user manual PT3656-1 (PR 22685)*.

Cobb, B.D., Clarkson, J.M. (1994). A simple procedure for optimizing the polymerase chain reaction (PCR) using modified Taguchi methods. *Nucleic acids research* **22**(18): 3801-3805.

Edelman, L., Hanson, P.I., Chapman, E.R., Jahn, R. (1995). Synaptobrevin binding to synaptophysin: a potential mechanism for controlling the exocytotic fusion machine. *The EMBO Journal* **14**(2): 224-231.

Gerona, R.R.L., Larsen, E.C., Kowalchyk, J.A., Martin, T.F.J. (2000). The C terminus of SNAP25 is essential for calcium-dependent binding of synaptotagmin to SNARE complexes. *The Journal of Biological Chemistry* **275**(9): 6328-6336.

Gerst, J.E. (1999). SNAREs and SNARE regulators in membrane fusion and exocytosis. *Cellular and Molecular Life Sciences* **55**: 707-734.

Graham, M.E., Washbourne, P., Wilson, M.C., Burgoyne, R.D. (2001). SNAP-25 with mutations in the zero layer supports normal membrane fusion kinetics. *Journal of Cell Science* **114**: 4397-4405.

Grimberg, E., Peng, Z., Hammel, I., Sagi-Eisenberg, R. (2003). Synaptotagmin III is a critical factor for the formation of the perinuclear endocytic recycling compartment and determination of secretory granule size. *Journal of Cell Science* **116**(Pt1): 145-154.

Grote, E., Hao, J.C., Bennett, M.K., Kelly, R.B. (1995). A targeting signal in VAMP regulating transport to synaptic vesicles. *Cell* **81**: 581-589.

Grote, E., Novick, P.J. (1999). Promiscuity in Rab-SNARE interactions. *Molecular Biology of the Cell* **10**: 4149-4161.

Haucke, V., De Camilli, P. (1999). AP-2 recruitment to synaptotagmin stimulated by tyrosine based endocytic motifs. *Science* **285**: 1268-1271.

Hodel, A. (1998). SNAP-25. *The International Journal of Biochemistry and Cell Biology* **30**: 1069-1073.

Hudson, A.W., Birnbaum, M.J. (1995). Identification of non-neuronal isoform of synaptotagmin. *Proceedings of the National Academy of Science of the United States of America* **92**: 5895-5899.

Jahn, R. (1999). Membrane fusion and exocytosis. *Annual Reviews in Biochemistry* **68**: 863-911.

Joubert, A.M., Louw, A.I., Joubert, F., Neitz, A.W.H. (1998). Cloning, nucleotide sequence and expression of the gene encoding factor Xa inhibitor from the salivary glands of the tick, *Ornithodoros savignyi*. *Experimental and Applied Acarology* **22**: 603-619.

Karim, S., Essenberg, R.C., Dillwith, J.W., Tucker, J.S., Bowman, A.S., Sauer, J.R. (2002). Identification of SNARE and cell trafficking regulatory proteins in the salivary glands of the lone star tick, *Amblyomma americanum* (L.). *Insect Biochemistry and Molecular Biology* **32**: 1711-1721.

Katz, L., Brennwald (2000). Testing the 3Q:1R Rule: Mutational analysis of the ionic zero layer in the yeast exocytic SNARE complex reveals no requirement for arginine. *Molecular Biology of the Cell* **11**: 3849-3858.

Kauppi, M., Wohlfahrt, G., Olkkonen, V.M. (2002). Analysis of the Munc18b-Syntaxin binding interface. *The Journal of Biological Chemistry* **277**(46): 43973-43979.

Kleizen, B., Braakman, I., de Jonge, H.R. (2000). Regulated trafficking of the CFTR chloride channel. *European Journal of Cell Biology* **79**: 544-556.

Lukyanov, K., Diatchenko, L., Chenchik, A., Nanisetti, A., Siebert, P., Usman, N., Matz, M., Lukyanov, S. (1997). Construction of cDNA libraries from small amounts of total RNA using the suppression PCR effect. *Biochemical and Biophysical Research Communications* **230**: 285-288.

Mans, B.J. (2002a). Functional perspectives on the evolution of argasid tick salivary gland protein superfamilies. *Biochemistry*. Pretoria, University of Pretoria.

Marqueze, B., Berton, F., Seagar, M. (2000). Synatotagmins in membrane traffic: Which vesicles do the tagmins tag? *Biochimie* **82**: 409-420.

Marz, K.E., Lauer, J.M., Hanson, P.I. (2003). Defining the SNARE complex binding of alpha-SNAP. *The Journal of Biological Chemistry* **278**(29): 27000-27008.

Misura, K.M., Scheller, R.H., Weis, W.I. (2000). Three dimensional structure of the neuronal Sec1-syntaxin 1a complex. *Nature* **404**(6776): 355-362.

Neco, P., Giner, D., Frances, M., Viniegra, S., Gutierrez, L.M. (2003). Differential participation of actin- and tubulin-based vesicle transport systems during secretion in bovine chromaffin cells. *European Journal of Neuroscience* **18**: 733-742.

Niemeyer, B.A., Schwarz, T.L. (2000). SNAP-24, a *Drosophila* SNAP-25 homologue on granule membranes, is a putative mediator of secretion and granule-granule fusion in salivary glands. *Journal of Cell Science* **113**: 4055-4064.

Novick, P., Schekman, R. (1979). Secretion and cell-surface growth are blocked in a temperature-sensitive mutant of *Saccharomyces cerevisiae*. *Proceedings of the National Academy of Science of the United States of America* **76**: 1858-1862.

Perin, M.S. (1996). Mirror image motifs mediate the interaction of the COOH terminus of multiple synaptotagmins with the Neurexins and Calmodulin. *Biochemistry* **35**: 13808-13816.

Pfeffer, S.R. (2001). Rab GTPases: specifying and deciphering organelle identity and function. *Trends in Cell Biology* **11**(12): 487-491.

Rothman, J.E. (1994). Mechanisms of intracellular protein transport. *Nature* **372**: 55-62.

Rychlik, W., Rhoades, R.E. (1989). A computer program for choosing optimal oligonucleotides for filter hybridization, sequencing and *in vitro* amplification of DNA. *Nucleic acids research* **17**: 8543-8551.

Rychlik, W., Spencer, W.J., Rhoades, R.E. (1990). Optimisation of the annealing temperature for DNA amplification *in vitro*. *Nucleic acids research* **18**: 6409-6412.

Sollner, T., Whiteheart, S.W., Brunner, M., Erdjument-Bromage, H., Geromanos, S., Tempst, P., Rothman, J.E. (1993). SNAP receptors implicated in vesicle targeting and fusion. *Nature* **362**: 318-324.

Stenbeck, G. (1998). Soluble NSF-attachment proteins. *The International Journal of Biochemistry and Cell Biology* **30**: 573-577.

Stenmark, H., Olkkonen, V.M. (2001). The Rab GTPase family. *Genome Biology* **2**(5): 3007.1-3007.7.

Sudhof, T.C. (2002). Synaptotagmins: Why so many? *The Journal of Biological Chemistry* **277**(10): 7629-7632.

Tagaya, M., Genma, T., Yamamoto, A., Kozaki, S., Mizushima, S. (1996). SNAP-25 is present on chromaffin granules and acts as a SNAP receptor. *FEBS Letters* **394**: 83-86.

Takai, Y., Sasaki, T., Matozaki, T. (2001). Small GTP-binding proteins. *Physiology Reviews* **81**(1): 153-185.

Teng, F.Y.H., Wang, Y., Tang, B.L. (2001). The syntaxins. *Genome Biology* **2**(11): reviews 3012.1-2012.7.

Thompson, J.D., Higgins, D.G., Gibson, T.J. (1994). CLUSTAL W: improving the sensitivity of progressive multiple sequence alignment through sequence weighting, position-specific gap penalties and weight matrix choice. *Nucleic acids research* **22**: 4673-4680.

Torii, S., Zhao, S., Yi, S., Takeuchi, T., Izumi, T. (2002). Granuphilin modulates the exocytosis of secretory granules through interaction with syntaxin 1a. *Molecular and Cellular Biology* **22**(15): 5518-5526.

Voets, T., Moser, T., Lund, P.E., Chow, R.H., Geppert, M., Sudhof, T.C., Neher, E. (2001). Intracellular calcium dependence of large dense-core vesicle exocytosis in the absence of synaptotagmin I. *PNAS* **98**(20): 11680-11685.

Watson, E.L. (1999). GTP-binding proteins and regulated exocytosis. *Critical Reviews in Oral Biological Medicine* **10**(3): 284-306.

CHAPTER 4

INVESTIGATION INTO PROTEIN-PROTEIN INTERACTIONS BETWEEN RAT BRAIN SECRETORY PROTEINS AND AN *O. savignyi* cDNA LIBRARY BY MEANS OF THE GAL4 TWO-HYBRID SYSTEM

4.1. INTRODUCTION

Protein-protein interactions are essential to cellular mechanisms at all levels in biologically responsive systems. These interactions occur extracellularly, and include ligand-receptor interactions, cell adhesion, antigen recognition, immune response and virus-host recognition (Young 1998). Intracellular protein-protein interactions occur in the formation of multi-protein complexes, during the assembly of cytoskeletal elements, between receptor-effector as well as effector-effector molecules of signal transduction pathways and even assembly of transcriptional machinery. These interactions can be defined as the interaction between specific amino acid regions or interacting pockets of the two proteins, which can be studied by various methods such as FRET (fluorescence resonance energy transfer), chemical cross-linking, surface plasmon resonance biosensors, affinity chromatography, immuno-precipitation and fluorescence gel retardation, to name just a few. All of the latter techniques have their advantages as well as disadvantages. One great disadvantage is that most of them require the availability of one protein binding-partner (bait) and is performed on protein level. Therefore, after identification of the interacting partners, one needs to determine their amino acid sequences in order to clone them for further studies. Also, these techniques do not always reflect the *in vivo* reactions, which are usually more complex than *in vitro* reactions. One technique, the two-hybrid assay, is performed *in vivo* and results in the immediate gene isolation of the interacting proteins or protein domains (Frederickson 1998). Since no data is available on the SNAREs and secretory proteins of *O. savignyi*, we exploited the two-hybrid system.

4.1.1. The yeast two hybrid system

In July 1989, Stanley Fields and Ok-kyu Song published the first paper describing a novel genetic system to study protein-protein interaction by taking advantage of the properties of the GAL4 protein of the yeast, *Saccharomyces cerevisiae* (Fields and Song 1989). They investigated the yeast proteins SNF1, SNF4 and the GAL4 protein, which is a transcriptional

activator required for the expression of genes encoding enzymes of galactose utilization. It consists of two separable and functionally essential domains: a N-terminal DNA-binding domain, which binds to specific DNA sequences (UAS$_G$) and a C-terminal activation domain containing acidic regions, which is necessary to activate transcription by directing the RNA polymerase II complex to transcribe the gene downstream of the UAS (Figure 4.1). By generating two hybrid proteins GAL4(1-147)-SNF1 and SNF4-GAL4(768-881), transcription of reporter genes regulated by UAS$_G$ occurred (Fields and Song 1989). Their results further indicated that the DNA-binding domain alone did not activate transcription, nor did the GAL4(1-147)-SNF1 or SNF4-GAL4(768-881) fusion proteins.

Today, we know that many eukaryotic trans-acting transcription factors are composed of physically separable, functionally independent domains. These include a DNA-binding domain (DNA-BD) that binds to a specific enhancer-like sequence, which in yeast is referred to as an upstream activation sequence (UAS). In the case of the native yeast GAL4 protein, the two domains are part of the same protein, but in principle any activation domain (AD) can be paired with any DNA-BD to activate transcription.

In the MATCHMAKER™ GAL4 two-hybrid system that was used in this study, the DNA-BD (amino acids 1–147) and the AD (amino accids 768–881) are both derived from the yeast GAL4 protein. Two different cloning vectors are used to generate fusions of these domains to genes encoding proteins that potentially interact with each other. The recombinant hybrid proteins are co-expressed in yeast and are targeted to the yeast nucleus. An interaction between a bait protein (fused to the DNA-BD) and a library-encoded protein (fused to the AD) creates a novel transcriptional activator with binding affinity for a GAL4-responsive UAS. This factor then activates reporter genes having upstream GAL4-responsive elements in their promoter, and this makes the protein-protein interaction phenotypically detectable. If the two hybrid proteins do not interact with each other, the reporter genes will not be transcribed (Figure 4.1.).
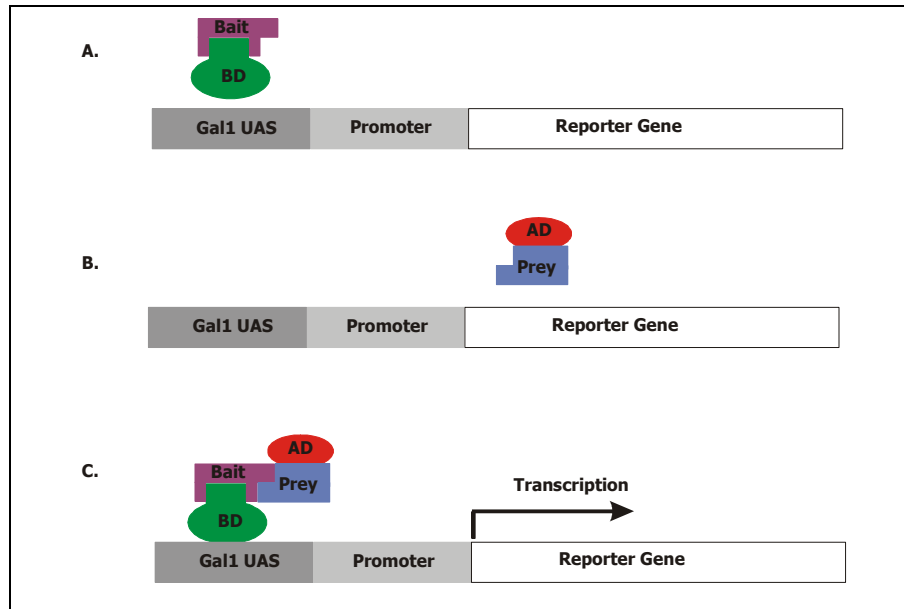
Figure 4.1. Schematic diagram of the GAL4-based two-hybrid system. *(A) The DNA-BD/bait hybrid binds to the Gal1 UAS but cannot activate transcription without the activation domain. (B) In the absence of bait protein, the AD/library fusion protein cannot bind to the Gal1 UAS and thus does not activate transcription. (C) Interaction between the bait and library protein in vivo activates transcription of the reporter gene.*

Constructing a DNA Binding Domain-Bait chimeric protein

Performing a two-hybrid experiment is a complex process involving many different steps, and there are a number of potential problems. When constructing a BD/Bait construct, the technical problems of cloning the gene of interest into a suitable plasmid and the variety of *in vivo* criteria that should be met, are the greatest source of problems (MacDonald 2001). These are discussed in greater detail below.

i. Cloning the gene of interest

In this study the bait proteins were cloned into the pAS2_1 vector (Figure 4.2). This vector includes both bacterial (Col E1) and yeast (2μ) origins of replication and a phenotypic selection marker (*TRP1*) suitable for selection in the yeast strain of choice, AH109. The pAS2_1 vector contains a cycloheximide resistant marker (*CYH2*) that is useful for eliminating false positives that have lost bait plasmid and also ampicillin resistance gene (Amp^r) for selection in bacteria. The multiple cloning site (MCS) in all reading frames was used for directional cloning of the bait (see methods section). Great care was taken to ensure that the bait was cloned in the correct reading frame, i.e. in the reading frame of the GAL4 BD, which forms the N-terminal part of the fusion protein and ensuring that cloning of the gene does not create an in-frame stop codon.
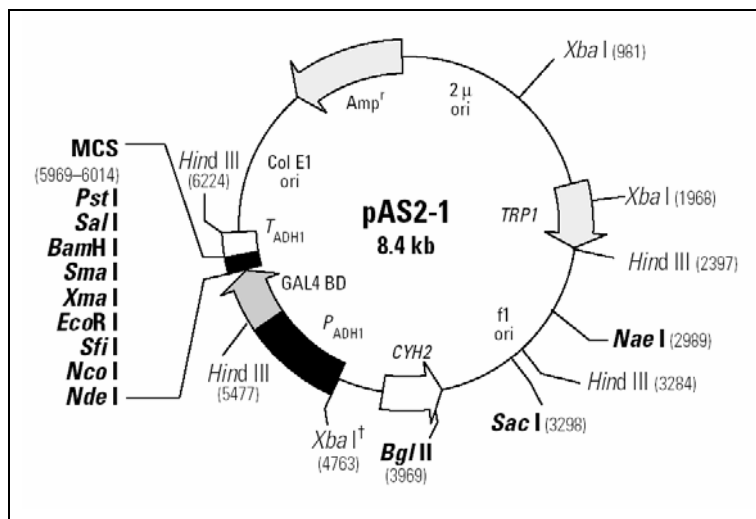
Figure 4.2. pAS2-1 map and MCS (Clontech Laboratories 1997a). *Unique sites are in bold. pAS2-1 is a cloning vector used to generate fusions of a bait protein with the GAL4 DNA-BD (amino acids 1–147). pAS2-1 carries the CYHS2 gene for cycloheximide sensitivity. The hybrid protein is expressed at high levels in yeast host cells from the full-length ADH1 promoter (P_{ADH1}). The Xba I site at bp 4763 (†) is methylation sensitive. pAS2-1 contains the TRP1 gene for selection in Trp– auxotrophic yeast strains.*

Since the interacting complex must be able to localize to the nucleus, care must be taken to choose the correct domain(s) of the protein of interest as bait. In the case of cytosolic proteins such as α-SNAP and Rab3a, full-length constructs were used. For syntaxin, which is an integral membrane protein, both a full-length construct and a truncated construct (lacking the C-terminal transmembrane region) was used to ensure localization to the nucleus.

ii. In vivo criteria

a. Levels of expression: Vector Promoters, Terminators and Copy number

Currently, most two-hybrid vectors utilize the yeast ADH1 promoter to drive expression of the fusion protein and transcription is terminated at the ADH1 transcription termination signal. The ADH1 promoter is available in full-length and truncated (ADH1*) forms, which results in lower expression levels. The pAS2_1 plasmid used in this study contains a full-length ADH1 promoter that results in high levels of constitutively expressed BD/bait fusion protein (Clontech Laboratories 1997a). This enables the detection of weak interactions, but can also increase toxicity and background activation of reporter genes. There is a common belief that higher expression will increase the number of interactions identified. However, in most cases the same interactions are detected with low expression and could even result in better detection of interactions. Therefore, great care should be given to choosing a promoter or even testing a high- and low strength promoter (MacDonald 2001).

The majority of two-hybrid vectors utilize the yeast 2μ origin of replication to maintain plasmids at high copy number (15-30 copies per cell). This elevated copy number has the advantage of increased bait protein expression, but the disadvantage that the copy number is variable and may not be the same for bait and target. This explains the prolonged time needed for cells to amplify plasmids before they are able to activate more stringent reporters such as *ADE2* (MacDonald 2001).

b. Fusion domains, localization to the nucleus and dimerisation

Although different fusion domains (AD and BD) work similarly, there are several potential problems that can sometimes be addressed by switching to an alternative fusion domain. These include poor stability or incorrect folding of the fusion protein or obstruction of a binding site. Unfortunately these are difficult to diagnose, and deciding which domain to use is a matter of trial and error. Some interactions work better with the LexA system, others with GAL4. It has even been found that some interactions are directional, i.e. they do not work if the BD and AD inserts are reversed (MacDonald 2001). The most commonly used fusion domains are derived from the GAL4 and LexA proteins, which both bind DNA as dimers. GAL4 contains a nuclear localization signal (NLS) while LexA fusions enter the nucleus without a NLS. The mechanism by which the LexA fusions enter the nucleus is unknown to date. However, by comparing large and small LexA-baits, it was found that small constructs enter the nucleus more successfully, probably due to the fact that they are below the size exclusion limit of the nuclear pore (MacDonald 2001). Both Gal4 and LexA fusion domains have been shown to exhibit increased efficiency when multiple binding sites are present in the reporter gene promoter, therefore much attention has been given to constructing suitable reporter genes in various yeast cells.

c. Protein Folding

Most two-hybrid vectors produce fusions in which the protein of interest (bait) is fused to the carboxyl terminus of the transcription factor domain (DNA-BD). This could be troublesome if the bait protein requires the N-terminal domain for interaction and therefore this orientation could block the interaction site. The possible solutions are to switch to an amino-terminal fusion approach, such as the LexA system, or use smaller fractions of the bait protein (MacDonald 2001). The latter is however, only viable if the domain structure of the protein is known, as there is a risk of eliminating the interacting site.

Constructing an Activation Domain-Fusion Library

The power of the two-hybrid system is to a very large extent based on it's use to screen AD-fusion libraries for novel genes that interact with the protein of interest. AD-fusion libraries have several critical features (Bartel and Fields 1997):

- AD-fusion libraries are fusion libraries, i.e. each clone encodes a fusion of the AD to whatever polypeptide is encoded in-frame by the cloned insert.
- AD-fusion libraries are expression libraries, i.e. the fusion proteins must be expressed in yeast cells for the assay to work.
- AD-fusion libraries are cDNA libraries, since only protein-coding sequences are of interest.
- AD-fusion libraries must be constructed (or converted) to plasmid vectors to allow transformation, maintenance and selection.

Choice of AD vector

System II utilizes pACT2 as AD vector, which is one of the earliest AD vectors and is an improved version of the pACT1 vector. pACT2 contains an expanded polylinker region, a HA epitope tag and truncated ADH1 promoter, which results in constitutive regulated medium expression levels (Clontech Laboratories 1997a). It also contains yeast and bacterial *ori*, ampicillin resistance and a *LEU2* selection marker (Figure 4.3). The *LEU2* marker can be used for selection in Leu⁻ auxotrophic yeast strains, as well as *E. coli* strains containing the *leu6* mutation (for distinguishing bait and prey plasmids during plasmid rescue).
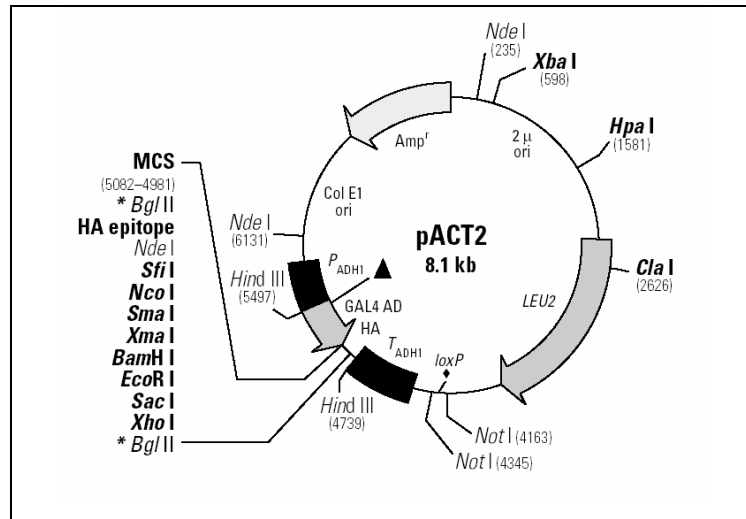
Figure 4.3. pACT2 map and MCS (Clontech Laboratories 1997a). *Unique sites are in bold. The hybrid protein is expressed at medium levels in yeast host cells from an enhanced, truncated ADH1 promoter and is targeted to the yeast nucleus by the SV40 T-antigen nuclear localization sequence (▲). pACT2 contains the LEU2 gene for selection in Leu– auxotrophic yeast strains.*

Source of RNA

Libraries should always be constructed from RNA derived from the appropriate tissue and at a specific differentiation stage. In ticks it has been described that the total protein and RNA increased sixfold in the salivary glands of fed male *A. americanum*. In fed male *D. andersoni* salivary glands, RNA increased approximately 3.5 times. Feeding *D. andersoni* in the presence of females increased total RNA by 25% over those fed in the absence of females (Bior *et al.* 2002). Therefore during this study, ticks were fed prior to RNA isolation. Since fusion libraries are cDNA libraries, it is recommended that library construction start with poly $(A)^+$ RNA. Since obtaining sufficient high quality poly $(A)^+$ RNA from fed tick salivary glands are a laborious process, the SMART technology (Clontech), which enriches and amplifies poly $(A)^+$ from total RNA, was used during this study.

Insert length, priming method and cloning

 Unlike normal cDNA libraries, useful AD fusion libraries do not require full-length cDNA. Based on the assumption that a minimum polypeptide length required for an interaction is in the range of 50 residues, some researchers create libraries with quite short inserts. Shorter inserts also favor more efficient ligation of vector to insert. However, if one wants to detect multiple interactions or interactions that require complex protein folding, longer inserts are required. To date, two priming methods are used for cDNA synthesis. The first method uses random priming. This randomly primed reaction ensures that the library will contain clones

encoding fusions to the amino-terminal and internal domains. This method also generates a wide size range, and subsequent size fractionation is used to control the insert length. The second priming method uses an oligo $(dT)_{25}d(A/G/C)$-primer, which will result in clones enriched in carboxyl-terminal domains (Bartel and Fields 1997; Clontech Laboratories 1997b). Directional cloning, which increases the library complexity two-fold, can be achieved by two methods. The first entails the ligation of adaptor to the ds cDNA followed by subsequent restriction digestion, phosphorylation and ligation into dephosphorylated vector (Clontech Laboratories 1997b). The second method is the one used in this study. In this case, primers containing directional cloning sites are used during SMART cDNA synthesis and directional cloning is achieved after restriction enzyme digestion and ligation (Clontech Laboratories 2001a).

Library complexity

Library complexity is defined as the number of independent clones present in the original, unamplified library. It is most likely the most critical determinant of whether or not screens of an AD-fusion library will be successful. The more independent clones, the higher the complexity of the library, and better the chances of finding even a very rare interacting protein. Generally, a library should contain at least 1×10^6 independent clones (Bartel and Fields 1997). In order to obtain sufficient material for yeast transformation (following amplification of the library), the titer must be $>10^8$ cfu/ml for plasmid libraries (Clontech Laboratories 1998). If sufficient information is available regarding the organism, the sequence representation can be determined (e.g. by using probes against a house-hold gene) to further address library quality. In mammalian libraries, a β-actin probe that cross-reacts with all mammalian β-actin cDNA is mostly used. Human cDNA libraries must show a minimum β-actin frequency of 0.10%, and all other mammalian libraries a minimum frequency of 0.05%. Non-mammalian cDNA libraries can be screened with a ubiquitously expressed species-specific probe (Clontech Laboratories 1998).

Two-Hybrid Yeast: Their Promotors, Phenotypes and Reporter Genes

   i.   *Yeast promoters*

A region containing a loosely conserved sequence (TATA box) precedes all yeast structural genes and determines the transcription start site. Many genes are also associated with *cis*-acting elements, i.e. DNA sequences to which transcription factors and other *trans*-acting regulatory proteins bind and affect transcription levels. The term "promoter" usually refers to

both the TATA box and the associated *cis*-regulatory elements. In this text, "minimal promoter" will refer specifically to the TATA region, exclusive of other *cis*-acting elements. The minimal promoter (or TATA box) in yeast is typically approximately 25 bp upstream of the transcription start site. One type of *cis*-acting transcription element in yeast is upstream activating sequences (UAS), which are recognized by specific transcriptional activators and enhance transcription from adjacent downstream TATA regions. The enhancing function of yeast UASs is generally independent of orientation; however, it is sensitive to distance effects if moved more than a few hundred base pairs from the TATA region. In most cases, the reporter genes (*lacZ, HIS3, ADE2* and *LEU2*) are under control of artificial promoter constructs comprised of a TATA and UAS (or operator) sequence derived from another gene. For GAL4-based systems, either a native GAL UAS or a synthetic UAS$_{G-17-mer}$ consensus sequence provides the binding site for the GAL4 DNA-BD (see Figure 4.4).
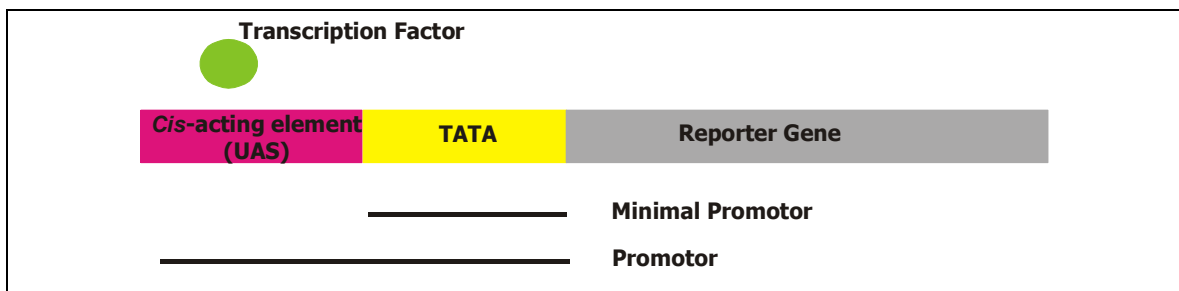
Figure 4.4. Schematic presentation of a yeast promoter.

ii.   *Yeast phenotypes*

Various yeast strains are available for use in two-hybrid assays. All the strains used during this study use the GAL4 promoter system. Their genotype and most important applications are listed in Table 4.1. Strain AH109 was used most since it has an additional reporter gene for adenine. This allows for the selection on not only SD/-His/-Leu/-Trp (TDO, Triple drop out) but also SD/-His/-Leu/-Trp/-Ade (QDO, quadruple drop out).

Table 4.1. MATCHMAKER yeast strain genotypes and applications (Clontech Laboratories 1998; Clontech Laboratories 1999).

Strain	Genotype	Application (s)
AH109	MATa, trp1-901, LEU2-3, 112, ura3-52, HIS3-200, GAL4Δ, gal80Δ, LYS2::GAL1$_{UAS}$-GAL1$_{TATA}$-HIS3,GAL2$_{UAS}$-GAL2$_{TATA}$-ADE2, URA3::MEL1$_{UAS}$-MEL1$_{TATA}$-lacZ	Two-hybrid library screening using HIS3, ADE2 and MEL1
Y187	MATα, ura3-52, HIS3-200, ADE2-101, trp1-901, LEU2-3, 112, GAL4Δ, met⁻, gal80Δ, URA3::GAL1$_{UAS}$ -GAL1$_{TATA}$ -lacZ	Two-hybrid assay of known proteins; Quantitative β-gal assays; Mating partner of CG-1945 and Y190
CG-1945	MATα, ura3-52, HIS3-200, ADE2-101, lys2-801, trp1- 901, LEU2-3, 112, GAL4-542, gal80-538, cyhʳ2, LYS2::GAL1$_{UAS}$ -GAL1$_{TATA}$ -HIS3, URA3::GAL4	Two-hybrid library screening with a highly sensitive HIS3 reporter; cycloheximide counterselection

iii.   Reporter genes in AH109

The yeast strain AH109 (MATCHMAKER system 3), virtually eliminates false positives by using three reporter genes: ADE2, HIS3 and MEL1 (or lacZ), all under the control of distinct GAL4 upstream activating sequences (UASs) and TATA boxes (Figure 4.5). These promoters yield strong and specific responses to GAL4. As a result, two major classes of false positives are eliminated: those that interact directly with the sequences flanking the GAL4 binding site and those that interact with transcription factors bound to specific TATA boxes. The ADE2 reporter alone provides strong nutritional selection, while the option of using HIS3 selection reduces the incidence of false positives and allows one to control the stringency of selection. Furthermore, one has the option of using either MEL1 or lacZ, which encode α-galactosidase and β-galactosidase respectively. Because α-galactosidase is a secreted enzyme, it can be assayed directly on X-α-Gal indicator plates employing blue/white screening.
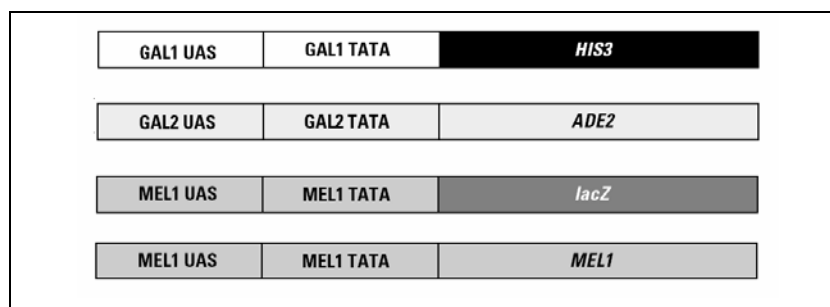
Figure 4.5. Reporter gene constructs in the yeast strains AH109. The HIS3, ADE2, and MEL1/lacZ reporter genes are under the control of three completely heterologous GAL4-responsive UAS and promoter elements, i.e. GAL1, GAL2, and MEL1, respectively.

4.1.2. Using the two-hybrid system for the identification of binding partners of SNAREs and secretory proteins.

In literature, there are many examples of using SNARE- and secretory proteins as bait for the identification of binding partners. These are listed in Table 4.2. The examples listed include cross-species screening, various BD/bait fusion constructs and libraries used.

Table 4.2. The use of various SNAREs and secretory proteins in two-hybrid assays.

Bait	Prey	Proteins identified by two-hybrid assay	Reference
Syntaxin Baits			
Syntaxin 1A & 1B (WT and cytosolic domain)	VAMP 1 & 2 (Cytosolic domains) Munc 18-a WT	Three-hybrid proof that Munc inhibit SNARE assembly	(Perez-Branguli *et al.* 2002)
Rat Syntaxin 1A (181-288)	Fragmented human brain cDNA library (Obtained from Clontech)	α-SNAP (10 clones) β-SNAP (13 clones) SNAP-25 (3 clones) Syntaphilin (2 clones) Syntaxin 1A (5 clones) SNAP-29	(Su *et al.* 2001)
Syntaxin 1A (1-265) Syntaxin 2 (1-266) Syntaxin 3 (1-263) Syntaxin 4 (1-273) Syntaxin 5 (1-284)	Rat SNAP-25 (WT) Human SNAP-23 (WT) Mouse SNAP-23	Specificity of interactions	(Araki *et al.* 1997)
Syntaxin 4 (1-273)	Fragmented human B lymphocyte cDNA library (Obtained from Clontech)	SNAP23	(Ravichandran *et al.* 1996)
Rab Baits			
Rab6a (WT) Rab6a (Val22) Rab6a (Ile126) Rab6a (Leu72) Rab6a (Asn27) Rab5 (WT)	Full length poly (A)$^+$ mouse brain (Stratagene Protocol)	Rab GDI SNIF4 Rabkinesin6	(Janoueix-Lerosey *et al.* 1995) (Stephens and Banting 2000)
Rab3a (WT) Rab3a (Q81L)	Full length poly (A)$^+$ rat brain (Stratagene Protocol)	Rabin 3 (3 clones) PRA1 (Rab6/5 partner C)	(Martincic *et al.* 1997)
SNAP Baits			
dSNAP (*Drosophila* SNAP)	*Drosophila* ovary cDNA library	*Drosophila* syntaxins 1, 5 & 16	(Xu *et al.* 2002)
Bovine α-SNAP (WT)	Fragmented human leukocyte cDNA library (Obtained from Clontech)	Various syntaxin isoforms Novel syntaxin 18 isoform	(Hatsuzawa *et al.* 2000)

Mouse SNAP-25	Fragmented rat brain library	HRS (Hepatocyte growth factor regulated tyrosine kinase substrate) & Syntaxin 1B	(Kwong *et al.* 2000)
SNAP-25B	Rat brain library	EHSH1 (EH/SH3 domain protein) / Intersectin	(Okamoto *et al.* 1999)
Human SNAP-23 (WT)	Fragmented human B lymphocyte cDNA library	Syntaxin 11	(Valdez *et al.* 1999)
γ-SNAP	IIB-Mel-J cell cDNA library	Cytosolic thiolase (22 clones) Gaf-1 (32 clones)	(Chen *et al.* 2001)
Other Proteins used as Baits			
Rat NSF (N-terminal)	Rat lung cDNA library (Obtained from Clontech)	Rab6	(Han *et al.* 2000)
Munc 18-1 Munc 18-2	Various syntaxin constructs	Specificity of Munc-syntaxin interactions	(Hata and Sudhof 1995)
Cytoplasmic synaptotagmin I	Rat brain library (Life Technologies Protocol)	Synaptotagmin I	(Sugita *et al.* 1996)
β-Arrestin 1 (WT)	Fragmented rat brain cDNA library (Obtained from Clontech)	NSF	(McDonald *et al.* 1999)
Kinesin heavy chain (814-963)	Human brain library	SNAP25 & SNAP23	(Diefenbach *et al.* 2002)
Oxysterol-binding protein (WT)	B-cell library	VAP-A (syntaxin-like protein in ER/Golgi)	(Wyles *et al.* 2002)

In our study, syntaxin, Rab3a and α-SNAP constructs were investigated as baits. Therefore emphasis will be placed on studies utilizing these proteins as bait. Studies by Su *et al* and Ravichandran *et al.*, in which syntaxin was used as bait for screening AD-fusion libraries, mostly identified various SNAPs (Ravichandran *et al.* 1996; Su *et al.* 2001). In both cases truncated syntaxin baits were used. In the case of Su *et al.*, the inhibitory N-terminal was removed, but the transmembrane region was kept intact (amino acids 181-288). In contrast, the group of Ravichandran *et al.* removed only the transmembrane region of syntaxin. In both cases, cross-species two-hybrid assays were performed using a fragmented cDNA library. Interestingly, 6 different interacting proteins were identified from brain tissue, while only one partner was identified from B lymphocyte tissue. In the case of Perez-Branguli *et al.* wild type syntaxin was used in a three-hybrid assay (Perez-Branguli *et al.* 2002). During their study they were able to show that wild type syntaxin does bind to its partners Munc and VAMP when they are expressed in high enough levels. Similarly, the study of Araki *et al.*

indicates that syntaxin lacking the transmembrane region is successful in binding SNAP25 (Araki *et al.* 1997). From these studies it is clear that (i) various constructs of syntaxin are useful as bait, (ii) depending on the tissue type, different binding partners were identified and (iii) fragmented libraries were most successful.

In the case of Rab3a, it is evident that wild type and GTPase deficient constructs must be used for the identification of Rab_{GTP} and Rab_{GDP} binding partners, respectively. In both studies listed, full-length poly $(A)^+$ rat brain libraries were used. The use of Rab3a for screening cross-species and various non-neuronal tissues has not been described to date.

Regarding the use of α-SNAP as bait, the study of Hatsuzawa *et al.* is valuable since it describes the cross-species use of α-SNAP as bait. They were able to use bovine α-SNAP as bait for screening a human leukocyte fragmented cDNA library and successfully identified various leukocyte syntaxin isoforms (Hatsuzawa *et al.* 2000).

4.2. HYPOTHESIS

- Cross-species two-hybrid assays are possible between rat brain SNAREs or secretory proteins (bait) and a salivary gland cDNA library of *Ornithodoros savignyi* (prey).

4.3. AIMS

- Construction of both a full-length poly(A)$^+$ and a truncated *Ornithodoros savignyi* salivary gland plasmid AD-fusion library.
- Construction of wild type syntaxin, Rab3a and α-SNAP BD/bait fusion constructs.
- Construction of a transmembrane depleted syntaxin BD/bait fusion construct.
- Construction of a GTPase deficient Rab3a BD/bait fusion construct.
- Two-hybrid assay using rat brain BD/bait constructs and tick salivary gland plasmid AD-fusion libraries.

4.4.   MATERIALS

The MATCHMAKER™ GAL4 two hybrid system 2 was a kind gift from Dr. A. Dhugra, University of Pennsylvania, USA while system 3 was purchased from Clontech Inc. The Super SMART™ cDNA synthesis kit was obtained from Clontech (Southern Cross Biotechnology). KC8 *E. coli* cells were a kind gift from Dr. Hannelie Moolman-Smook, University of Stellenbosh, South Africa. Recombinant NSF, ATPase deficient NSF (D127) and α-SNAP were kinds gifts from Proff. Whiteheart and Rothman of the Memorial Sloan-Kettering Cancer Institute, New York, USA. Recombinant syntaxin, SNAP-25, VAMP, Rab3a and synaptotagmin were a gift from Prof. R.H. Scheller, Stanford University Medical Center, USA. NucleoSpin® Plasmid Quick Pure, NucleoBond® PC2000 and NucleoSpin® Extract kits were from Macherey-Nagel, Germany (Separations). PCR nucleotide mix (10 mM deoxynucleotide solution), *Sfi*I restriction enzyme and Shrimp alkaline phosphatase were from Roche Diagnostics. Peptone, agar and yeast nitrogen base without amino acids were from Difco (Labretoria). Yeast extract and tryptone were purchased from Oxoid Ltd. (England). Deoxyribonucleic acid sodium salt type III from salmon testes, 3-amino-1,2,4-triazole (3-AT), cycloheximide, , RNase Inhibitor, PEG4000, 425-600 micron glass beads, Triton X-100 and all the various amino acids used were from Sigma. Dextrose, Isopropyl β-D-thiogalactopyranoside (IPTG), 5-bromo-4-chloro-3-indolyl-β-D-galactopyranoside (X-gal), L-adenine hemisulphate, lithium acetate, ammonium acetate and ampicillin were from ICN (Separations). DNA polymerase I large (Klenow) fragment, *Taq* Polymerase, *Pfu* DNA polymerase, Proteinase K and various restriction enzymes were from Promega (Wisconsin, USA). TaKaRa Ex Taq (5 U/μl) and T4 DNA Ligase (350 U/μl) were from Takara Bio Inc., Japan (Separations). Primers were synthesized by Inqaba Biotech (Pretoria, South Africa). NaCl, ethylene diamine tetra-acetic acid (EDTA), Tris(hydroxymethyl)aminomethane, methanol, isopropanol and chloroform were obtained from Merck, Germany. Sodium dodecyl sulphate (SDS) was from BDH Laboratory Supplies LTD., England.

4.5.   METHODS

4.5.1.   Full-length GAL4 AD/ library construction

cDNA synthesis and amplification using the Super SMART System™

Tick feeding, salivary gland dissection, RNA isolation, double strand cDNA synthesis and amplification by LD-PCR were performed as described in Chapter 3. In order to allow restriction enzyme digestion and directional cloning, different primers were used. The primers used for plasmid library construction contained a *Sfi* I restriction site, which allows

(i) directional cloning of transcripts into the pACT2 plasmid using a single restriction enzyme step and (ii) a very low abundance restriction enzyme cutting site to limit extensive digestion of the tick transcripts. The sequences of the primers that were used are given in Table 4.3.

Table 4.3. Primers used for synthesis and amplification of cDNA during cDNA library construction.

Primer	Sequence
SMART IV	5' AAGCAGTGGTATCAACGCAGAGTGGCCATGGAGGCCGGG 3' *Sfi*I
CDS III / 3'PCR	5' ATTCTAGAGGCCTCCATGGCCGACATG(T)$_{30}$NN 3' *Sfi* I
5' PCR	5' AAGCAGTGGTATCAACGCAGAGT 3'

INSERT:

```
                                        AGGCCGGG  XXXXXXXXXXX(A)   CATGTCGGCCATGG-OH
                                     HO-ACCTCCGG CCC  XXXXXXXXX NN(T)  GTACAGCCGGT
```

PLASMID (pACT2):

```
                         5' -------GGCCATGG                  AGGCC--------------------
                         3' ------ CCGGT                     ACCTCCGG---------------------
```

DIRECTIONAL CLONING:

```
         -------GGCCATGGAGGCCGGG  XXXXXXXXXXX(A)  CATGTCGGCCATGGAGGCC-------
         ------CCGGT ACCTCCGGCCC  XXXXXXXXXNN(T)  GTACAGCCGGTACCTCCGG--------
```
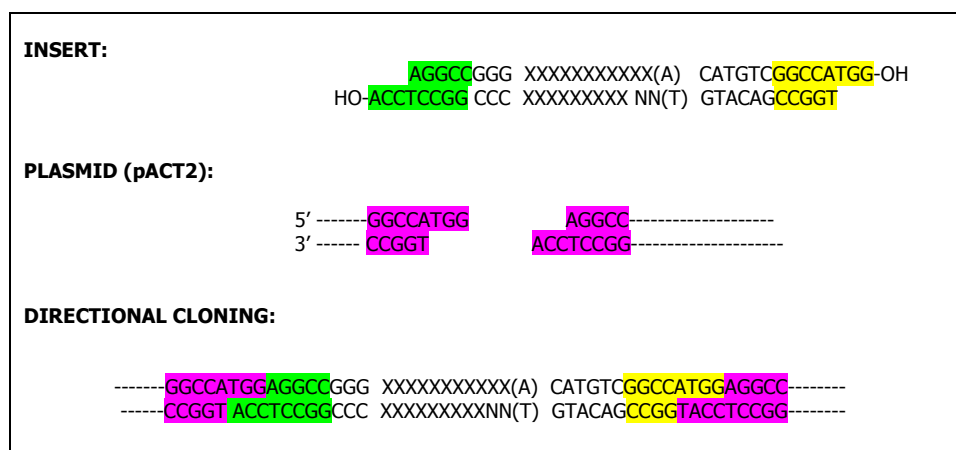
Figure 4.6. Schematic representation of directional cloning using *Sfi*I digestion.

ds cDNA Polishing and size fractionation

Directly after LD-PCR amplification the ds cDNA was polished using the protocol described by Clontech (Protocol # PT3041-1, SMART PCR cDNA synthesis manual). Briefly, the 100μl LD-PCR reaction was divided into two 50 μl samples. To each, 4 μl Proteinase K (10 μg/μl) were added and incubated at 45ºC for 1 hour, before inactivation at 90ºC for 10 minutes. The tubes were immediately chilled (2 min) in ice water to allow for specific re-annealing of strands before the addition of 3μl T4 DNA Polymerase (5 U/μl) and incubation at 16ºC for 30 minutes to allow synthesis of full-length ds cDNA. The reaction was terminated by incubation at 72ºC for 10 minutes. The dsDNA was purified using the NucleoSpin® extract kit (as described previously) and eluted in 50μl buffer NE (5 mM Tris-HCl, pH 8.5). The yield and purity was determined on the Gene Quant Pro system. Typically 1,7-2,5 μg of SMART polished ds cDNA was obtained with a 260nm/280nm ratio greater than 1,8.

Construction of a GAL4 AD/ plasmid library

Polished SMART DNA as well as purified pACT2 plasmid was digested with *Sfi*I at 50ºC for 2 hours, before inactivation of the reaction with the addition of 2 μl Proteinase K (20 μg/ml) and incubation at 45ºC for 1 hour. The latter reaction was terminated at 75ºC for 30 minutes, and the digested products purified using the NucleoSpin extract kit. To avoid ligation of the complementary *Sfi*I generated overhangs of the pACT2 plasmid, the digested plasmid was dephosphorylated with the addition of 10μl Shrimp Alkaline Phosphatase (1 U/μl) and incubated for 30 minutes at 37ºC. The reaction was terminated with the addition of Proteinase K and subsequent heat inactivation (as described previously). To ensure that pACT2 was successfully dephosphorylated prior to ligation of the library, some plasmid was incubated with T4 DNA ligase and analyzed with agarose gel electrophoresis.

In order to optimize library ligation into pACT2, various conditions were tested. These are listed in Table 4.4. Briefly, the various ratios of plasmid and library (insert) were combined with 1μl T4 Ligase (100 U/μl) and incubated overnight at 16ºC, followed by heat inactivation. The ligated products were precipitated in the presence of tRNA and electroporated into BL21 *E. coli* cells (as described in Chapter 3).

Table 4.4. Ligation of the GAL4 AD / plasmid library using the pACT2 vector (8100 bp).

Average Insert size	250 bp			500 bp			1000 bp			1500 bp		
Ligation Ratio	1/1	2/1	5/1	1/1	2/1	5/1	1/1	2/1	5/1	1/1	2/1	5/1
Insert (ng)	4.6	9.3	23	9.3	18.5	46.3	18.5	37	92.6	27.8	55.6	138.9
Vector (ng)	150	150	150	150	150	150	150	150	150	150	150	150
Sample #	1	2	3	2	4	5	4	6	7	8	9	10

After electroporation, the cells were diluted in 1 ml LB-broth and incubated at 30ºC with moderate shaking for 60 minutes. Following incubation, 10μl of cells from each sample were diluted with 40 μl LB-Broth and plated onto a 1.5% agar plate containing ampicillin (50 μg/ml). The plates were inverted and incubated at 37ºC overnight while the remaining transformation mixtures were stored at 4ºC. The next day, the confluent and semi-confluent plates were selected as successful transformation ratios and the remaining transformation mixtures of these ratios were plated among 50 large plates (150 mm diameter) and again incubated overnight. Before pooling the library, the percentage of clones containing inserts

was determined (see the following section). Finally, the cells were scraped from all of these plates, pooled into 500 ml of LB-Broth containing 25% glycerol (on ice) and stored in 1 ml aliquots at –70ºC.

Determining the number of recombinant/independent clones

In order to determine the percentage of recombinant clones in the library, at least 15 isolated colonies were randomly picked from nearly confluent plates, inoculated into 1 ml LB-Broth containing ampicillin and grown overnight. The following day the samples were subjected to miniprep plasmid isolation (as described in Chapter 3), *Eco*RI and *Hind*III digestion and analysis on agarose electrophoresis. A transformation mixture was only added to the pooled library if at least 10 out of 15 clones contained inserts.

Titering plasmid libraries

Prior to freezing the library the titer has to be determined to ensure a representative library. In general the titer should be at least 10-fold higher than the number of independent clones and at least 10^8 cfu/ml for long-term storage. To determine the titer, 1 μl of the pooled library is added to 1 ml LB broth in a 1.5 ml microcentrifuge tube (this is dilution A, $1:10^3$) and mixed by vortexing. 1 μl of Dilution A is added to 1 ml LB broth to create dilution B ($1:10^6$). For plating the cells, 1 μl of dilution A was diluted in 50 μl LB broth, mixed and the entire mixture plated. Two aliquots (50 μl and 100 μl) from dilution B were also plated. Following overnight incubation at 37ºC, the number of colonies was counted and the titer (cfu/ml) calculated according to the following formulas:

- Colony# Dilution A x 10^3 x 10^3 = cfu/ml
- (Colony # Dilution B / plating volume) x 10^3 x 10^3 x 10^3 = cfu/ml

Amplification and large-scale plasmid isolation of library

In order to amplify the cells from the stored library to obtain sufficient plasmid for a library scale transformation of yeast cells, 1 ml of frozen plasmid library was thawed on ice and diluted into 2 litres of LB broth containing ampicillin (250 μl of cells / 500 ml broth). Each 500 ml culture was placed in a 2-litre flask to ensure sufficient oxygenation during amplification at 30ºC with vigorous shaking. Cultures were grown until $A_{600} \sim 0.5 - 0.6$ before collecting the cells with centrifugation (5000 x g, 30 minutes). Large-scale plasmid isolation was subsequently performed using the NucleoBond™ PC2000 system. Briefly, the cells were resuspended in 90 ml of buffer S1 (50 mM Tris-HCl, 10 mM EDTA, 100 μg/ml RNase A, pH

8.0) and lyzed with the addition of 90 ml buffer S2 (1% SDS, 200 mM NaOH) and incubation at room temperature for 3 minutes. The released chromosomal DNA was precipitated with the addition of 90 ml pre-cooled buffer S3 (2.8 M potassium acetate, pH 5.1), mixed by inversion and incubated on ice for 5 minutes. The lysate was clarified by filtering the suspension through a NucleoBond® folded filter in a large funnel and loaded on a pre-equilibrated NucleoBond® AX2000 column (20 ml buffer Equilibration buffer N2, 100 mM Tris-HCl, 15% ethanol, 900 mM KCl, 0.15% TritonX100, adjusted to pH 6.3 with H_3PO_4). The column was subsequently washed twice with 50 ml of buffer N3 (100 mM Tris-HCl, 15% ethanol, 1.15 M KCl, adjusted to pH 6.3 with H_3PO_4) before eluting the plasmid with 25 ml buffer N5 (100 mM Tris-HCl, 15% ethanol, 1 M KCl, adjusted to pH 8.5 with H_3PO_4). During elution, 1 ml fractions were collected, which were immediately precipitated by the addition of 800 μl isopropanol per fraction and centrifuging the samples at 15 000 x g for 30 minutes at 4ºC. The pellets were washed with 70% ethanol, vacuum-dried and dissolved in 50 μl water. Yields were determined spectrophotometrically as described previously.

4.5.2. Truncated GAL4 AD/ library construction

The methodology for creating a fragmented library whereby the coding strand is truncated from the 3' end is given in Figure 4.7. The approach utilizes random hexa-nucleotides and the DNA polymerase I large (Klenow) fragment. Klenow is useful in this case since each of the annealing temperatures of the random hexanucleotides differs, and therefore amplification must be done at low temperatures to allow optimal annealing. In this case extension was performed at 37ºC, which is the optimal temperature of the Klenow enzyme.

SMART ds cDNA

```
5'    AAGCAGTGGTATCAACGCAGAGTGGCCATGGAGGCCGGG- INSERT - NN(A) CATGTCGGCCATGGAGGCCTCTATAAT  3'
3'    TTCGTCACCATAGTTGCGTCTCACCGGTACCTCCGGCCC  - INSERT - NN(T) GTACAGCCGGTACCTCCGGAGATCTTA  5'
                                    SfiI                                    SfiI
```

ANNEAL XhoI-(N)$_6$ PRIMER and EXTEND WITH KLENOW

```
5'    AAGCAGTGGTATCAACGCAGAGTGGCCATGGAGGCCGGG - INSERT- (A)CATGTCGGCCATGGAGGCCTCTATAAT    3'
                              3'<<<<<<<(N)₆GGCGAGCTCGCC 5'
                                             XhoI
```

OR

```
                        XhoI
              5'CCGCTCGAGCGG(N)₆>>>>>>>>>>>3'
3'    TTCGTCACCATAGTTGCGTCTCACCGGTACCTCCGGCCC - INSERT- NN(T)GTACAGCCGGTACCTCCGGAGATCTTA  5'
```

CREATE dsDNA WITH 5' PCR PRIMER AND ExTaq

```
5' AAGCAGTGGTATCAACGCAGAGTGGCCATGGAGGCCGGG - TRUNCATED INSERT- (A) CCGCTCGAGCGG 3'
3' TTCGTCACCATAGTTGCGTCTCACCGGTACCTCCGGCCC  - TRUNCATED INSERT- (N)₆GGCGAGCTCGCC 5'
                            SfiI                                   XhoI
```

Figure 4.7. Schematic representation of fragmenting the full-length *Sfi*I library using random primers.

SMART *Sfi*I dsDNA (1000 ng) was incubated with 650 pmol random hexanucleotide, 2 µl dNTPs (10 mM of each nucleotide) and 2.5 µl Klenow buffer in a 25 µl reaction. The dsDNA was denatured at 94ºC for 1 minute and snap cooled on ice for 5 minutes to allow annealing of the random hexanucleotides. Klenow enzyme (4U) was added and the reactions incubated at 37ºC for 30 minutes before heat inactivation at 70ºC for 15 minutes. Generating dsDNA from only the 5' ends (which are the correct reading frames), was achieved by adding 650 pmol of the 5'PCR primer, 1 µl of dNTP's (10 mM), 2.5 µl ExTaq buffer and ExTaq polymerase (5U) to yield a final volume of 50 µl. The reactions were incubated at 94ºC for 30 seconds, followed by annealing of the 5' PCR primer at 60ºC for 30 seconds and extension at 72ºC for 6 minutes. The fragmented dsDNA was purified using the NucleoSpin™ Extract kit as described previously. In general, there was a 2- 2.5x increase in the amount of dsDNA. In order to directionally clone these fragments, the fragmented DNA and the pACT2 plasmid were digested sequentially with *Sfi*I and *Xho*I. Ligation, transformation, titering of the fragmented library and determination of the percentage of recombinant clones were done as described previously.

4.5.3. Verification of yeast host strains and control vectors

It is important to verify the phenotype of the yeast strains used prior to transformation. This is achieved by plating the yeast cells on standard (SD) or dropout (DO) medium (6,7 g/l

yeast nitrogen base without amino acids, 20 g/l agar, 100 ml of the appropriate 10x dropout solution) and incubating cells at 30ºC for 3-5 days until colonies appear. As a positive control, cells were plated on adenine supplemented YPD media (YPDA, 20 g/l peptone, 10 g/l yeast extract, 20 g/l agar, 20g/l dextrose, 0,03g/l adenine hemisulphate). In the case of testing cycloheximide (CHX) resistance, 10 μg/ml cycloheximide was added to the plates. Additional cultures were propagated from isolated colonies identified on the selection plates. The phenotypes of the various MATCHMAKER yeast strains are listed in Table 4.5.

Table 4.5. MATCHMAKER yeast strain phenotypes. *(+) Indicates growth, while (-) indicates no growth in the various growth media.*

	Selection media							
Strain	**SD/-Ade**	**SD/-Met**	**SD/-Trp**	**SD/-Leu**	**SD/-His**	**SD/-Ura**	**YPDA**	**YPD/CHX**
AH109	-	+	-	-	-	+	+	-
Y187	-	-	-	-	-	+	+	-
CG-1945	-	+	-	-	-	+	+	+

4.5.4.   GAL4 DNA-BD/Bait construction

Native constructs

The full-length recombinant clones containing inserts encoding native rat brain syntaxin, Rab3a and α-SNAP were sequenced to confirm their nucleotide sequences. Primers were designed to PCR amplify and directionally clone these inserts in the correct reading frame into the pAS2_1 plasmid. The sequences of the primers are given in Table 4.6.

To amplify the open reading frame (ORF) of the native inserts, purified plasmid (50 ng), forward and reverse primers (5 pmol) were used. All other conditions were identical to that of 3' RACE described in Chapter 3. The amplified inserts were analyzed on agarose gel electrophoresis and purified using the NucleoSpin® Extract kit. Sequential digestions with the appropriate restriction endonucleases were performed on both the inserts and the pAS2_1 plasmid. The digested inserts and plasmids purified using the NucleoSpin® Extract kit were ligated overnight at 16ºC, precipitated with tRNA and electroporated into DH5α *E. coli* cells.

Table 4.6. Primers used for the amplification of native bait constructs.

Name	Sequence	Tm (ºC)
Syntaxin baits constructs		
Syntaxin forward	GGA ATT C<u>CA TAT G</u>AA GGA CCG AAC CCA G *Nde*I	66.6
Syntaxin reverse	CCA ATG CAT TGG TT<u>C TGC AG</u>C TAT CCA AAG ATG CC *Pst*I	70.6
Rab3a bait constructs		
Rab3a forward	GGA ATT C<u>CA TAT G</u>GC TTC CGC CAC AGA C *Nde*I	64.9
Rab3a reverse	CCG <u>GAA TTC</u> TCA GCA GGC ACA ATC CTG *Eco*RI	65.1
α-SNAP bait construct		
α-SNAP forward	GGA ATT C<u>CA TAT G</u>GA CAA CTC CGG GAA G *Nde*I	67.5
α-SNAP reverse	CCG <u>GAA TTC</u> TTA GCG CAG GTC TTC CTC *Eco*RI	69.0

Truncated syntaxin construct

Syntaxin is an integral membrane protein that is targeted to the plasma membrane. If this occurs a protein-protein interaction could still occur, but the complex would not be able to migrate into the nucleus and activate the two-hybrid marker genes. Therefore, a truncated syntaxin (1-265) construct lacking the transmembrane region was constructed and used as a bait molecule (Figure 4.8).
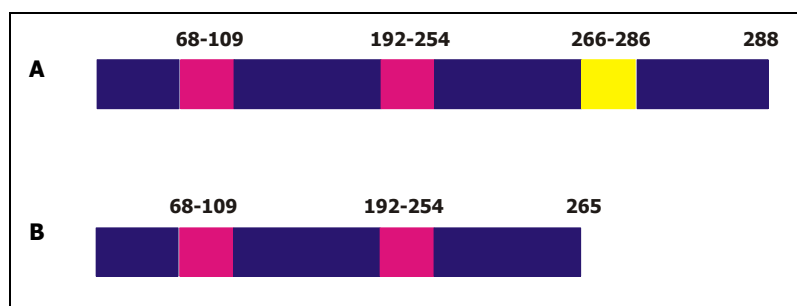
Figure 4.8. Schematic presentation of (A) native syntaxin 1 and (B) truncated syntaxin 1 bait constructs. *The coiled-coiled regions are indicated in pink and the transmembrane region in yellow.*

The reverse primer is given in Table 4.7 and the forward primer of the native construct was used. All procedures are identical to those described for constructing the full-length native constructs.

Table 4.7. Reverse primer used for the amplification of the syntaxin 1-265 construct.

Name	Sequence	Tm (ºC)
Truncated syntaxin	CCA ATG CAT TGG TT<u>C TGC AG</u>T TCT TCC TGC GCG CC *Pst*I	72.2

GTPase deficient Rab3a T36N

When designing a bait molecule, one has to incorporate functional relevance into two-hybrid screens. One such an example is the identification of the Rab6-dependent trafficking machinery. Rab6 is a small GTPase that, like other Rabs, regulate membrane trafficking through the hydrolysis of GTP. This enables the use of mutant Rab6 proteins, constitutively 'locked' in either the GTP or GDP-bound state, to screen two-hybrid libraries for interacting proteins. When using the GDP-bound state the guanine nucleotide dissociation inhibitor protein (Rab GDI) was identified. In contrast, Rabkinesin6 was found to interact with the wild-type or GTP-locked forms, but not the GDP-locked form (Stephens and Banting 2000).

This approach was followed for Rab3a in this study (Figure 4.9). Both native Rab3a as well as a GTP-deficient Rab3a containing a T36N mutation (locked in the GDP form) was used. This mutation was selected based on the mutational analysis of Rab3a as described by Burstein *et al*. In their studies it was shown that, for the T36N mutant, the intrinsic GDP dissociation rate constant ($k_{off\ (GDP)}$) was 61-fold higher than that of wild-type Rab3a, indicating a GDP binding function (Burstein *et al.* 1992).
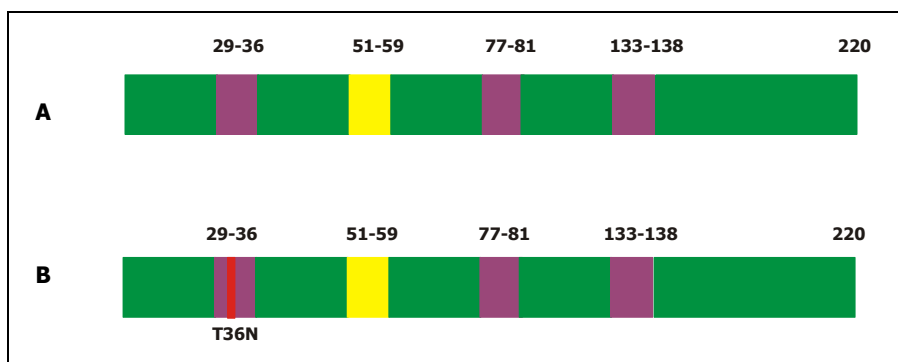
Figure 4.9. Schematic presentation of (A) native Rab3a and (B) mutated Rab3a bait constructs. *The GTP-binding regions are indicated in purple, the effector-binding regions in yellow and the mutated site in red.*

Site directed mutagenesis, based on the principle described in the QuickChange™ Site-directed mutagenesis Kit by Stratagene (La Jolla, California, USA), was used to generate the T36N mutant from the native Rab3a construct. In this protocol, PCR is used to introduce site-specific mutations to any double-stranded supercoiled plasmid containing the insert of

interest. Two complementary primers containing the desired mutation are used to create mutated plasmids with staggered nicks after linear amplification. *Pfu* DNA polymerase (isolated from *Pyrococcus furiosis*) is used to replicate both plasmid strands with high fidelity using its 3'-5' proofreading exonuclease activity. The product is then treated with *Dpn*I (target sequence: 5' Gm^{6}ATC-3') in order to remove the methylated parental template. The mutated plasmid is transformed into *E. coli* cells where the bacterial ligase system repairs the nicks to create double-stranded plasmids.

The mutagenesis reaction (50 μl) contained 50 ng of wild-type Rab3a pAS2_1 plasmid, 125 ng of both the forward and reverse T36N primers (see Table 4.8), 1 x Pfu DNA polymerase reaction buffer, 2.5 mM of each dNTP and 3U *Pfu* DNA polymerase. The cycling parameters were 95ºC for 30 sec, 55 ºC for 1 minute and 68ºC for 8 minutes repeated for 12 cycles in a Perkin Elmer GeneAmp PCR system 9700. After PCR amplification, 20 U of *Dpn*I was added to the 50 μl reaction and incubated for 3 hours at 37ºC. The mutated plasmids were subsequently isolated using the High Pure Plasmid Isolation Kit (Roche), precipitated with tRNA and sodium acetate (pH 5), electroporated into DH5α *E. coli* cells and plated on LB/Amp plates. The nucleotide sequences of positive clones were obtained in order to confirm mutagenesis.

Table 4.8. Primers used for the site-directed mutagenesis of Rab3a. *The mutated nucleotide is underlined.*

Name	Sequence	Tm (ºC)
Rab3a T36N forward	GTG GGC AAA AAC TCG TTC CTC TTC	60
Rab3a T36N reverse	GAA GAG GAA CGA GTT TTT GCC CAC	60

4.5.5.　Small-scale yeast transformation

Small scale yeast transformation was performed according to the method of Dr. Moolman-Smook, Department of Medical Biochemistry, University of Stellenbosch, South Africa (personal communication). Yeast cells were plated on the appropriate plates (YPDA for non-transformed cells or SD for transformed cells) and incubated for a maximum of 2 days at 30ºC. A fresh yeast colony (25-50 μl) was resuspended in 1 ml water (in a 2 ml tube), vortexed, and cells collected by centrifugation (13000 rpm, 30 sec). Yeast cell membranes were made porous (competent) with the addition of 1 ml lithium acetate (LiAc, 100 mM) and incubation at 30ºC for 5 minutes without shaking. For transformation, the following was added to the pelleted LiAc treated cells in the listed order: 240 μl 50% PEG 4000, 36 μl LiAc

(1M), 25 μl heat denatured salmon sperm DNA (2 mg/ml) and 500 ng plasmid in a final volume of 50 μl water. The mixture was vortexed for at least a minute and heat-shocked at 42ºC for 20 minutes in a water bath. The cells were collected with centrifugation, resuspended in 250 μl water and plated on the appropriate agar for selection of the plasmid transformed into the AH109 yeast cells. Plates were incubated upside down at 30ºC for 2-5 days.

4.5.6.   GAL4 DNA-BD/Bait test for autonomous reporter gene activation

The DNA-BD/bait protein constructs were tested for transcriptional activation function before using it to screen a library by plating the transformed host strain (AH109) on SD/-Trp, SD/-His/-Trp (DDO, Double drop out) and SD/-His/-Trp/-Leu (TDO, Triple drop out). If cells survived on DDO or TDO, the construct was not suitable for screening the library. A colony-lift assay (see 4.5.8) for activation of the *lacZ* reporter gene expression was also done to confirm that the bait construct does not activate the *lacZ* gene.

4.5.7.   Sequential library-scale transformation of AH109 yeast cells

For the library-scale transformation of yeast the 30 x TRAFCO protocol described by Agatep R, Kirkpatrick, R.D., Parchaliuk, D.L., Woods, R.A. and Gietz, R.D. was used (http://tto.trends.com). Since sequential transformation was done, AH109 yeast cells containing the DNA-BD/bait construct was inoculated in 50 ml SD/-Trp and grown overnight at 30ºC with shaking. The cell titer was determined, the volume of cell suspension yielding a total of 7.5 x 10^8 cells calculated, the cells collected with centrifugation and diluted in 150 ml pre-warmed YPDA medium. The cells were incubated at 30ºC with shaking for 3-4 hours until the cell titer reached 2 x 10^7 cells/ml before harvesting the cells once more by centrifugation (3000 x g, 5 min). The cells were washed with 75 ml water, collected by centrifugation, resuspended in 3 ml lithium acetate (100 mM) and incubated for 15 minutes at 30ºC without shaking, again collected and the supernatant removed. The following were added to the cells in the listed order: 7,2 ml 50% PEG4000, 1 ml lithium acetate (1 M), 1,5 ml heat denatured salmon-sperm DNA (2 mg/ml), 250 μg DNA-AD/ library pACT2 plasmid in a final volume of 1 ml water. The mixture was vigorously vortexed for 1 minute until the cell pellet was totally resuspended and then incubated at 30ºC for 30 minutes. Subsequently, the cells were heat shocked at 42ºC for 40 minutes and mixed by inversion for 15 seconds every 5 minutes. The cells were collected, gently resuspended in 40 ml water and 1 ml aliquots plated on 40 large SD/-Trp/-Leu plates. Plates were incubated at 30ºC for 3-5 days until co-

transformed colonies appeared. Apart from sequential transformation of AH109 cells with the DNA-BD/bait and DNA-AD/ library constructs, cells were also sequentially transformed with the control vectors. These are listed in Table 4.9.

Table 4.9. Control vectors of the MATCHMAKER™ **GAL4 two-hybrid system 2.**

Control vector	Name	Selection
β-gal positive control	pCL1	*LEU2*
DNA-BD/p53	pVA3	*TRP1*
AD / T-antigen	pTD1	*LEU2*
DNA-BD / lamin C	pLAM5'	*TRP1*
Positive controls for a two-hybrid interaction		
Plasmids	pVA3 + pTD1	*TRP1, LEU2*

4.5.8.   Two-hybrid screening of reporter genes (See appendix 1)

Co-transformed cells were scraped from the plates, collected with centrifugation, resuspended in 10 ml SD/-Trp/-Leu, 3 x 1 ml aliquots were plated on SD/-Trp/-Leu/-His (TDO, Triple drop-out) plates and incubated at 30ºC for 2-8 days, or until colonies appeared. The remaining cells were stored in 1 ml aliquots at −70ºC in SD/-Trp/-Leu containing 25% glycerol. TDO positive colonies were transferred to duplicate TDO master plates with sterile wood sticks and incubated at 30ºC overnight. One master plate was stored at 4ºC as back up while colonies from the second master plate were plated onto SD/-Trp/-Leu/-His/-Ade (QDO, Quadruple drop-out) for further selection. QDO positive colonies were transferred to two master plates. Again, one master plate was stored at 4ºC while the other was used for the colony-lift β-galactosidase filter assay (see 4.5.8) to test activation of the *lacZ* gene.

4.5.9.   Colony-lift β-galactosidase filter assay (Clontech Laboratories 2001b)

QDO positive colonies were grown on a master plate for 2-4 days at 30ºC until 1-3 mm in diameter. Using forceps, a sterile dry filter paper was placed over the surface of the plate of colonies and gently rubbed to help colonies cling to the filter. Holes were poked through the filter into the agar in three asymmetric locations to orient the filter. When the filter was evenly wetted it was carefully lifted from the agar plate with forceps and transferred (colonies facing up) to a pool of liquid nitrogen. Using the forceps, the filter was completely submerged for 10 seconds, removed from the nitrogen and allowed to thaw at room

temperature. This freeze-thaw treatment to permeate the cells, was repeated three times. Finally, the filter was placed on a filter presoaked in 100 ml buffer Z (16,1 g/l $Na_2HPO_4.7H_2O$; 5,50 g/l $NaH_2PO_4.H_2O$; 0,75 g/l KCl; 0,46 g/l $MgSO_4.7H_2O$; pH 7.0) containing 167 μl of X-gal solution (20 mg/ml) and incubated at room-temperature. The filter was checked periodically for the appearance of blue colonies. The time it takes colonies producing β-galactosidase to turn blue varies, typically from 30 minutes up to 3 hours. Prolonged incubation (>8 hr) may give false positives. Yeast transformed with the β-galactosidase positive control plasmid (pCL1) turns blue within 20-30 minutes, while cells co-transformed with plasmid for a two-hybrid interaction (pVA3 and pTD1) give a blue signal within 60 minutes. The colonies, which activated the *lacZ* gene, were identified on the master QDO plate and selected for further screening using nested PCR.

4.5.10.   Nested-PCR screening of positive clones

Nested-PCR screening was performed according to the method of Dr. Moolman-Smook, Department of Medical Biochemistry, University of Stellenbosch, South Africa (personal communication). PCR directly from the yeast cells were performed by inoculating ~1 μl of cells into the PCR mixture (15 pmol pACT2 forward and reverse primers, 1x *Taq* DNA polymerase buffer A, 1.5 mM $MgCl_2$, 200 μM dNTP's and water to a final volume of 20 μl). *Taq* DNA in Buffer A (Promega) was used since buffer A (50 mM Tris-HCl, 100 mM NaCl, 0,1 mM EDTA, 1 mM DTT, 50% glycerol and 1% Triton X100) aids in disrupting the yeast cells. The cells were disrupted at 94ºC for 7 minutes in Perkin Elmer GeneAmp PCR system 9700 and then cooled to 80ºC after which 5 μl of enzyme mix (1.25 U *Taq* DNA polymerase diluted in 1x buffer A) was added. PCR was performed for 30 cycles of denaturation (94ºC, 30 sec), primer annealing (60ºC, 30 sec) and extension (72ºC, 2 min). For the nested PCR, 1 μl of the above PCR product was used as template in a second PCR with the nested primers (Table 4.10) and identical composition otherwise. Nested PCR was performed for 30 cycles of denaturation (94ºC, 30 sec), primer annealing (55ºC, 30 sec) and extension (72ºC, 2 min) before analyzing the products on ethidium bromide agarose gel electrophoresis.

Table 4.10. Nested PCR primers.

Name	Sequence	Tm (ºC)
pACT2 Forward	CTA TTC GAT GAT GAA GAT ACC CCA CCA AAC CC	63.7
pACT2 Reverse	GTG AAC TTG CGG GGT TTT TCA GTA TCT ACG AT	63.9
pACT2 Forward Nested	TGT ATG GCT TAC CCA TAC GAT GTT CC	60.2
pACT2 Reverse Nested	GGG TTT TTC AGT ATC TAC GAT TCA TAG	55.2

4.5.11.   Plasmid isolation from yeast

Plasmid isolation was performed according to the method of Dr. Moolman-Smook, Department of Medical Biochemistry, University of Stellenbosch, South Africa (personal communication). Yeast cells were grown in 1 ml TDO at 30ºC overnight with shaking before adding 4 ml YPDA medium and growing cells for a further 4 hours. Cells were collected by centrifugation (3000 x g, 5 minutes), the supernatant removed and cells resuspended in 200 μl Smash-and-Grab buffer (1% SDS, 2% Triton X-100, 100 mM NaCl, 10 mM Tris-HCl, 1 mM EDTA, pH 8). Glassbeads (~ 100 μl, 425-600 micron) and 200 μl phenol: chloroform: isoamylalcohol (25:24:1) were added and the mixture vortexed vigorously for 3 minutes to break open the yeast cells. The mixture was centrifuged (13 000 rpm, 5 minutes) and the aqueous layer removed. In order to precipitate the plasmid from the solution, 0.5 volumes of ammonium acetate (7.5 M, pH 5) and 2 volumes of 100% ethanol was added and the mixture centrifuged at 4ºC (13000 rpm for 25 minutes). The pellet was washed with 70% ethanol, vacuum dried and dissolved in 20 μl water.

4.5.12.   AD/library plasmid rescue via transformation in KC8 *E. coli*

KC8 *E. coli* cells have a defect in *leuB*, which can be complemented by *LEU2*. Thus, KC8 cells can be used to rescue AD/library plasmids (which carry *LEU2*) from yeast co-transformants that also contain a DNA-BD/bait plasmid. Plasmids isolated from QDO and *LacZ* positive colonies were electroporated into electro-competent KC8 *E. coli* cells. In order to select cells containing AD/library plasmids, cells were plated on M9 minimal medium containing ampicillin and lacking leucine.

4.5.13.   Sequencing of AD/library inserts

KC8 cells containing AD/library plasmid were grown overnight in 1 ml LB/amp medium at 30ºC with shaking. Plasmid was isolated from the cells using the High Pure plasmid isolation kit (Roche) as described previously. Automated nucleotide sequencing of the insert was

performed using the GAL4 AD sequencing primer (5' TACCACTACAATGGATG 3') with the Big Dye Sequencing kit on an ABI Prism 377 DNA sequencer (Perkin Elmer Applied Biosystems, USA) as described in Chapter 3. Sequences obtained were analyzed using the BioEdit Program. DNA and deduced protein sequences were analyzed using various databases and programs. These are described in the results section.

4.6.   RESULTS AND DISCUSSION

4.6.1.   Full-length cDNA GAL4 AD / Plasmid library construction

Figure 4.10 shows a typical gel profile of ds cDNA synthesized using the SMART cDNA synthesis and amplification system. First strand synthesis was done using 120 ng total RNA in a final volume of 11 μl. After amplification of 2 μl of first strand product, a smear from 0.3 -2 kb is visible after the optimal number of cycles (24 cycles) as determined in Chapter 3.
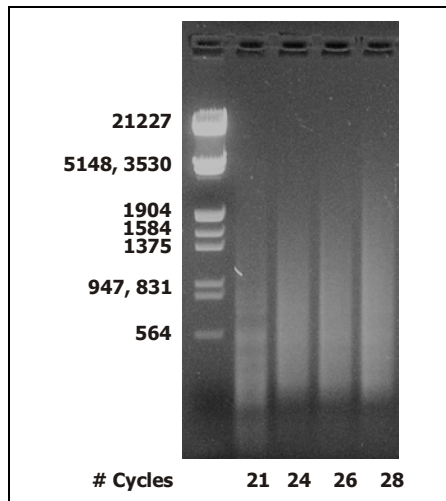
Figure 4.10. Analysis of ds cDNA amplification by LD-PCR using Super SMART™ technology.

Following amplification, the ds cDNA was polished, purified and size fractionated using the NucleoSpin® Extract system. The latter utilizes conventional binding of DNA to a silica membrane in the presence of chaotropic salts. DNA fragments between 200-2000 bp are subsequently eluted from the column with 50 μl alkaline buffer. Using spectrophotometry, we were able to recover more than 95% of the loaded sample with an A260/280 exceeding 1.9.

The purified dsDNA was digested with *Sfi*I (in the presence of acetylated BSA) for 2 hours at 50ºC and again purified using the NucleoSpin® Extract system. Figure 4.11 shows the gel profile of a polished purified sample and a sample following *Sfi*I digestion and the second purification step. In both cases, an intense smear ranging between 200 and 950 base pairs is visible centering around 550 bp. Therefore it can be concluded that *SfiI* is also a rare cutter in *O. savignyi*, and does not completely digest the tick salivary gland dsDNA to small fragments. Therefore, we continued with the *Sfi*I digested dsDNA for constructing the GAL4 AD / plasmid library.
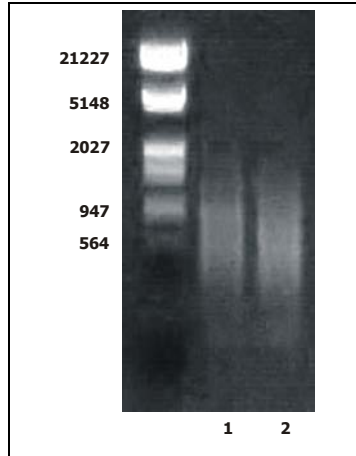
Figure 4.11. Agarose gel electrophoresis of (1) polished ds cDNA and (2) purified *Sfi*I digested ds SMART DNA.

Following *Sfi*I digestion of the pACT2 plasmid, the 5' phosphate groups were removed using Shrimp Alkaline Phosphatase (SAP). Since incomplete dephosphorylation would result in the ligation of intact pACT2 plasmids during ligation, we incubated dephosphorylated pACT2 with T4 DNA Ligase and performed agarose gel electrophoresis to test for complete dephosphorylation. The results in Figure 4.12 indicate that both *Sfi*I digestion and SAP dephosphorylation were successful.
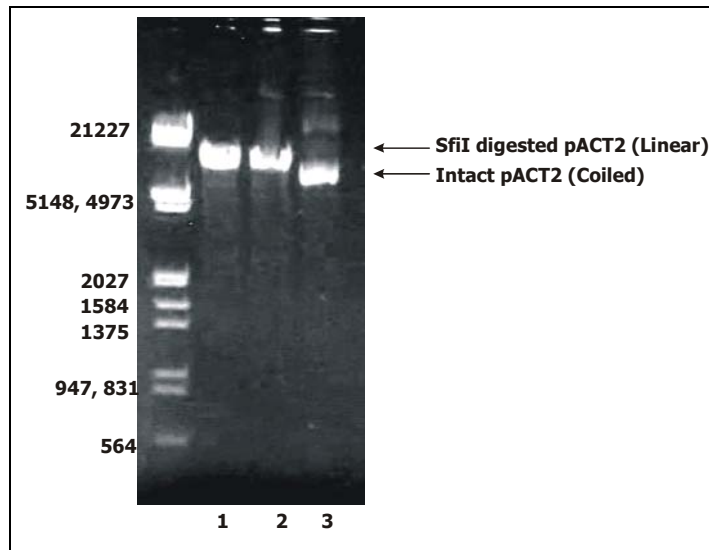
Figure 4.12. Agarose gel electrophoresis of (1) *Sfi*I digested pACT2, (2) *Sfi*I digested pACT2 treated with T4 Ligase and (3) untreated intact pACT2.

Ligation of the *Sfi*I digested dsDNA and dephosphorylated *Sfi*I digested pACT2 plasmid was optimized as described in Table 4.4. Indicated in Figure 4.13 are the results obtained from

166

the various vector: insert ratios obtained for an average insert of 500 bp and 150 ng vector which yielded the highest transformation efficiency. Both the 2:1 and 5:1 ratios exceeded 3 x 10^7 cfu/μg.
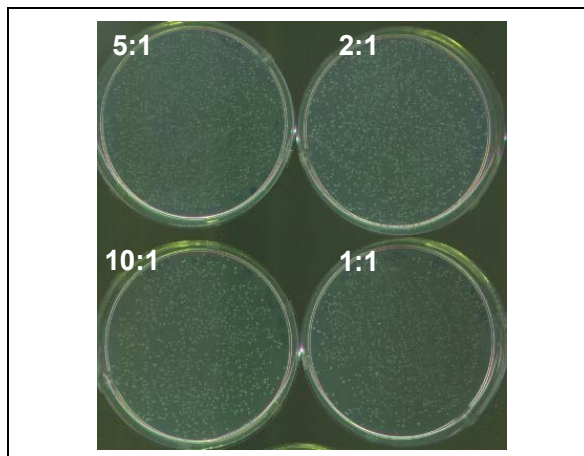
Figure 4.13. Transformation of various insert: vector ratios into electro competent BL21 *E. coli* cells.

The number of independent colonies was determined by restriction enzyme digestion of the fusion plasmids isolated from various clones. From Figure 4.14 it is obvious that numerous clones have similar molecular masses. To investigate whether these clones are identical, DNA sequencing was performed. The sequencing data indicated that clones with similar molecular masses do however contain different DNA sequences, but a high number of *Sfi*I-*Sfi*I linked inserts were detected among the clones that were sequenced (results not shown). Therefore, the library was not used for two-hybrid screens, and a fragmented library containing a *Sfi*I and *Xho*I site for directional cloning was created.
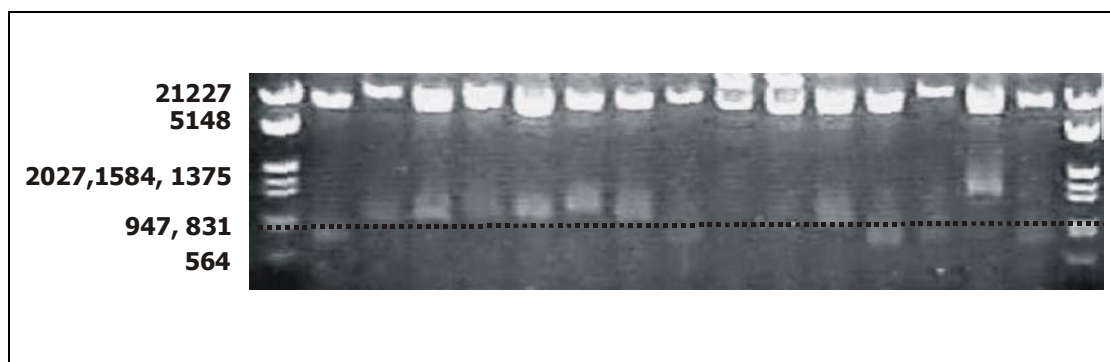
Figure 4.14. Agarose gel electrophoresis of *Sfi*I digested plasmids isolated from GAL4 AD/library transformed BL21 *E. coli* cells. *The first and last lanes correspond to molecular mass markers while lanes 2-16 each corresponds to a single colony.*

4.6.2. Truncated GAL4 AD / Plasmid library construction

Apart from the truncated cDNA library being directionally cloned via two different restriction sites (*Sfi*I and *Xho*I), it also allows for truncation of the coding strands from the 3' end, creating truncated C-terminal ends of the encoded proteins. This is useful since the SNARE proteins syntaxin and VAMP are anchored to the membrane via their C-terminal tails and could therefore now be identified in a two-hybrid assay that require translocation of the fusion protein complex to the nucleus.

As described in the methods section, the random hexa-nucleotides containing a *Xho*I site were annealed to the SMART dsDNA (1200 ng) and extended with Klenow enzyme at low temperatures. After converting the truncated strands to dsDNA the DNA was purified using NucleoSpin® columns. Using spectrophotometry we were able to calculate a two-fold increase in concentration during the truncation process. A typical gel electrophoresis profile of the fragmented *Xho*I digested library is shown in Figure 4.15. Once again a smear from 200- 950 bp was observed that center around ~550-600 bp, indicating *Xho*I to be a rare cutter.
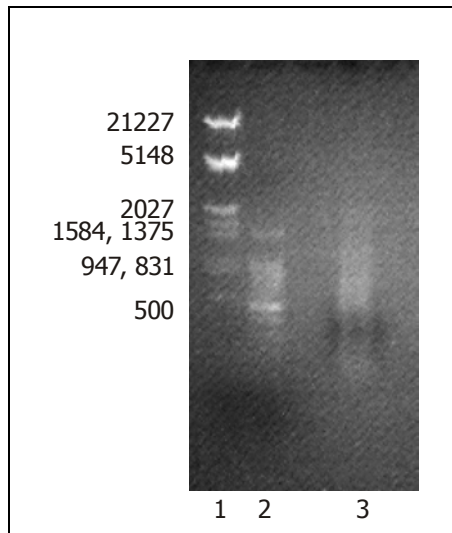
Figure 4.15. Agarose gel electrophoresis of the *Xho*I digested fragmented dsDNA. *Lanes 1 and 2 corresponds to different molecular mass markers, lane 3 corresponds to the XhoI digested, truncated dsDNA.*

The *Sfi*I and *Xho*I digested library was ligated into the pACT2 plasmid and electroporated into BL21 *E. coli* cells (as described previously). Similar to the full-length library, ligations with an average insert size of 500 ng and a 2:1 ratio (insert: plasmid) yielded the highest transformation efficiency, i.e. 9,6 x 10^6 cfu/μg. The number of independent clones was

determined by PCR amplification of the inserts directly from the BL21 *E. coli* cells (Figure 4.16). DNA sequencing of various clones with similar molecular masses were performed to distinguish between them. It was clear that bands with similar molecular masses do contain different DNA sequences (Figure 4.17). Therefore, the percentage of independent clones exceeded 60% and the library was used during a two-hybrid screen (see section 4.5.1. for calculating the number of independent clones). Interestingly, only one clone (419 bp) contained a *Sfi*I-*Sfi*I fused insert. All of the other clones contained a *Xho*I site in the 3' UTR of the transcript indicating incomplete *Sfi*I digestion in the 3' region.
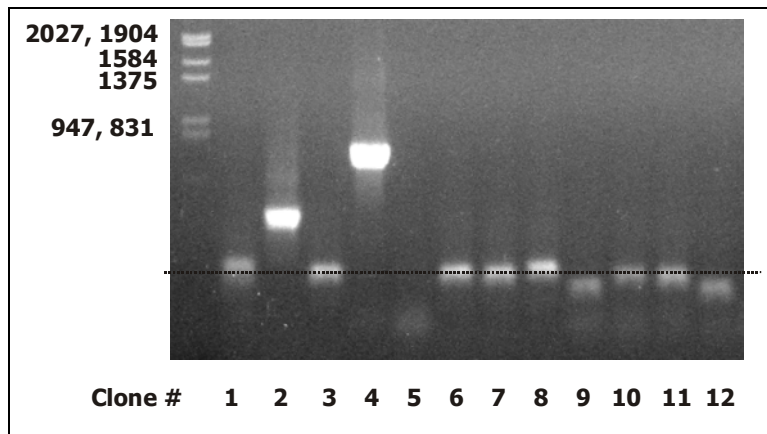
Figure 4.16. PCR screening of cloned inserts from transformed BL21 *E. coli* cells. *PCR amplification of inserts was done directly from the BL21 E. coli cells using the forward and reverse nested primers. Each lane corresponds to a unique clone.*

Figure 4.17. DNA sequence of four similar molecular mass clones from the fragmented *Sfi*I/*Xho*I GAL4AD fusion library. *The following is indicated: pACT2 plasmid regions (yellow), SfiI restriction sites (purple), XhoI restriction site (green) and reading frame (/).*

In order to amplify the library, the remaining cells (~ 2ml) from the 2:1 and 5:1 ratios were plated on 40 large plates (50 μl per plate), grown overnight and the cells collected in 50 ml LB/glycerol. The titer of the library was determined as 3,5 x 10^7 cfu/ml. The cells were aliquoted into 1 ml fractions and stored at –70ºC. To obtain sufficient plasmid for a library scale transformation, 500 μl cells were diluted into 500 ml LB/Amp and grown until A_{600} ~ 0.5 - 0.6 before cells were collected by centrifugation, and a large-scale plasmid isolation (using the NucleoBond™ PC2000 system) performed. On average 800 -1000 μg of plasmid was isolated from 2 liters of culture.

4.6.3.   Bait construction

Full-length and truncated syntaxin

The full-length recombinant clone containing inserts encoding native rat brain syntaxin 1 (D45208) was a gift from Prof. Scheller. Primers were designed to PCR amplify and directionally clone (using the *Nde*I and *Pst*I sites) the entire coding sequence of syntaxin 1 in the correct reading frame. A second primer was used to create a truncated version of the insert. The latter coding sequence was also ligated directionally into the pAS2_1 plasmid using the *Nde*I and *Pst*I sites. Figure 4.18 shows the PCR amplified products obtained from the rat brain syntaxin plasmid. The bands were excised and purified using the NucleoSpin system. DNA sequencing of the obtained clones indicated that both the native and truncated bait constructs were correctly constructed in the pAS2_1 plasmid (Figure 4.19).
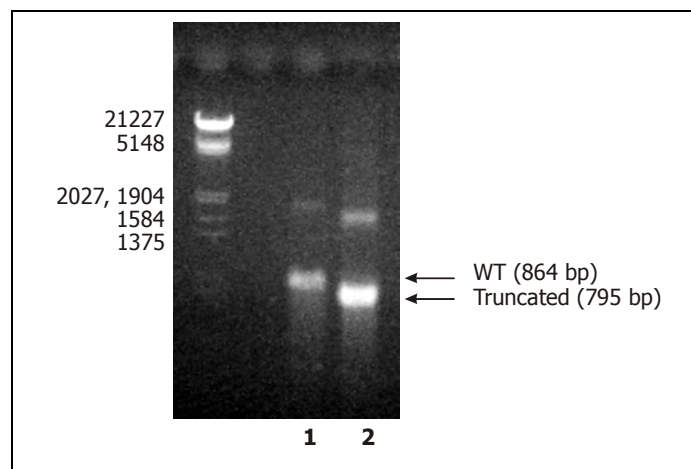
Figure 4.18. PCR amplification of syntaxin bait constructs. *Native (lane 1) and truncated (lane 2) inserts from the rat brain syntaxin1A original construct are shown.*

```
SynBait    MKDRTQELRTAKDSDDDDDVTVTVDRDRFMDEFFEQVEEIRGFIDKIAENVEEVKRKHSA 60
TruncSyn   MKDRTQELRTAKDSDDDDDVTVTVDRDRFMDEFFEQVEEIRGFIDKIAENVEEVKRKHSA 60
D45208     MKDRTQELRTAKDSDDDDDVTVTVDRDRFMDEFFEQVEEIRGFIDKIAENVEEVKRKHSA 60
           ************************************************************

SynBait    ILASPNPDEKTKEELEELMSDIKKTANKVRSKLKSIEQSIEQEEGLNRSSADLRIRKTQH 120
TruncSyn   ILASPNPDEKTKEELEELMSDIKKTANKVRSKLKSIEQSIEQEEGLNRSSADLRIRKTQH 120
D45208     ILASPNPDEKTKEELEELMSDIKKTANKVRSKLKSIEQSIEQEEGLNRSSADLRIRKTQH 120
           ************************************************************

SynBait    STLSRKFVEVMSEYNATQSDYRERCKGRIQRQLEITGRTTTSEELEDMLESGNPAIFASG 180
TruncSyn   STLSRKFVEVMSEYNATQSDYRERCKGRIQRQLEITGRTTTSEELEDMLESGNPAIFASG 180
D45208     STLSRKFVEVMSEYNATQSDYRERCKGRIQRQLEITGRTTTSEELEDMLESGNPAIFASG 180
           ************************************************************

SynBait    IIMDSSISKQALSEIETRHSEIIKLETSIRELHDMFMDMAMLVESQGEMIDRIEYNVEHA 240
TruncSyn   IIMDSSISKQALSEIETRHSEIIKLETSIRELHDMFMDMAMLVESQGEMIDRIEYNVEHA 240
D45208     IIMDSSISKQALSEIETRHSEIIKLETSIRELHDMFMDMAMLVESQGEMIDRIEYNVEHA 240
           ************************************************************

SynBait    VDYVERAVSDTKKAVKYQSKARRKKIMIIICCVILGIIIASTIGGIFG 288
TruncSyn   VDYVERAVSDTKKAVKYQSKARRKK
D45208     VDYVERAVSDTKKAVKYQSKARRKKIMIIICCVILGIIIASTIGGIFG 288
           *************************************************
```

Figure 4.19. Amino acid sequence alignment of the syntaxin baits. *The full-length rat brain syntaxin (SynBait), truncated syntaxin (TruncSyn) and native rat brain syntaxin (D45208) constructs are shown.*

In order to confirm expression of the syntaxin bait proteins, total protein content of native and bait expression yeast cells were isolated and equal amounts of protein were coated onto an ELISA plate. Screening with an antibody against the DNA-BD was not performed, as this approach does not confirm expression of the correct reading frame and hence bait protein. In this approach, a polyclonal antibody directed at rat brain syntaxin 2 was used. We were able to confirm expression of the bait molecules (Figure 4.20). Significant signals were obtained for native AH109 cells, indicating cross-reactivity of the antibody with homologous yeast proteins. The signals are however 1,8 x and 3,6 x higher than the control (native AH109 cells) for AH109 cells expressing native syntaxin and truncated syntaxin, respectively.

A.

B.
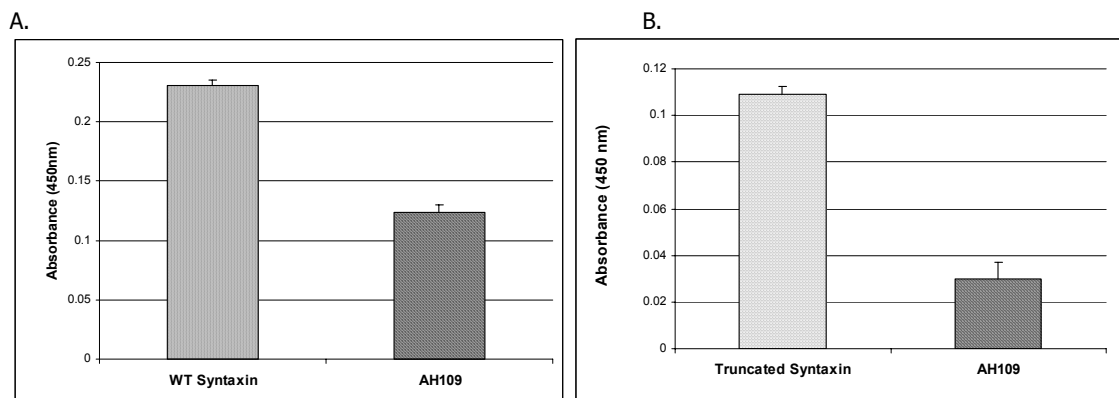
Figure 4.20. ELISA of syntaxin transformed AH109 cells with polyconal anti-syntaxin 2 IgG. *Equal amounts of total yeast protein extract from AH109 cells expressing (A) native syntaxin and (B) truncated syntaxin were investigated.*

Native and GTPase deficient Rab3a baits

Similar to constructing the syntaxin baits, the native Rab3a bait was created from the mouse Rab3a construct that was a kind gift from Prof. Scheller. As described previously, Rab3a is a GTPase with different protein binding partners when in the GTP- and GDP-bound state. Therefore, a GTPase deficient isoform containing the T36N mutation was also constructed. Figure 4.21 indicates the band amplified from the obtained Rab3a construct. Figure 4.23 gives the DNA nucleotide sequence of the native and T36N mutated clones created in pAS2_1.
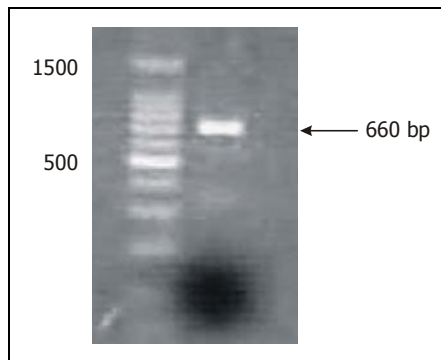
Figure 4.21. PCR amplification of the coding region of native mouse brain Rab3a.

To confirm expression of Rab3a T36N, ELISA of total yeast protein was performed using a polyclonal antibody against mouse brain Rab3a. The result indicates a 1,57 x fold higher signal for AH109 cells expressing the bait construct compared to native AH109 cells. Similar to the results obtained for syntaxin, AH109 cells also cross-reacted with the antibody (Figure 4.22).
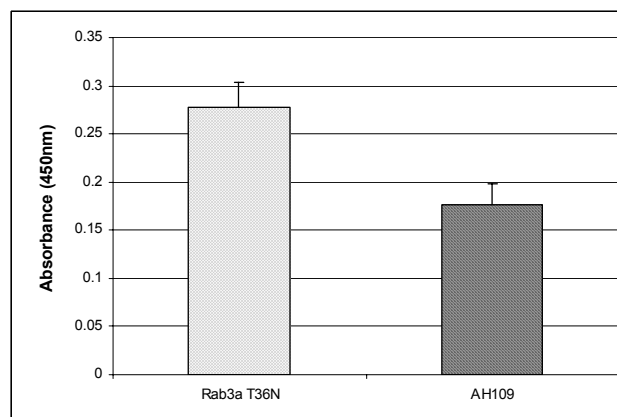
Figure 4.22. ELISA of Rab3a T36N transformed AH109 cells with polyconal anti-Rab3a IgG. *Equal amounts of total yeast protein extract from native AH109 cells and Rab3a T36N transformed cells were investigated.*

```
BaitWT      ATGGCTTCCGCCACAGACTCTCGCTATGGGCAGAAGGAGTCCTCAGACCAGAACTTCGAC 60
T36N        ATGGCTTCCGCCACAGACTCTCGCTATGGGCAGAAGGAGTCCTCAGACCAGAACTTCGAC 60
NM_009001   ATGGCTTCCGCCACAGACTCTCGCTATGGGCAGAAGGAGTCCTCAGACCAGAACTTCGAC 60
            ************************************************************

BaitWT      TATATGTTCAAGATCCTGATCATTGGGAACAGCAGCGTGGGCAAAACCTCGTTCCTCTTC 120
T36N        TATATGTTCAAGATCCTGATCATTGGGAACAGCAGCGTGGGCAAAAACTCGTTCCTCTTC 120
NM_009001   TATATGTTCAAGATCCTGATCATTGGGAACAGCAGCGTGGGCAAAACCTCGTTCCTCTTC 120
            *********************************************** ************

BaitWT      CGCTACGCAGATGACTCCTTCACTCCAGCCTTTGTCAGCACCGTTGGCATAGACTTCAAG 180
T36N        CGCTACGCAGATGACTCCTTCACTCCAGCCTTTGTCAGCACCGTTGGCATAGACTTCAAG 180
NM_009001   CGCTACGCAGATGACTCCTTCACTCCAGCCTTTGTCAGCACCGTTGGCATAGACTTCAAG 180
            ************************************************************

BaitWT      GTCAAAACCATCTACCGCAACGACAAGAGGATCAAGCTGCAGATCTGGGACACAGCAGGG 240
T36N        GTCAAAACCATCTACCGCAACGACAAGAGGATCAAGCTGCAGATCTGGGACACAGCAGGG 240
NM_009001   GTCAAAACCATCTACCGCAACGACAAGAGGATCAAGCTGCAGATCTGGGACACAGCAGGG 240
            ************************************************************

BaitWT      CAAGAGCGGTACCGCACCATCACCACAGCCTATTACCGAGGCGCCATGGGCTTCATCCTA 300
T36N        CAAGAGCGGTACCGCACCATCACCACAGCCTATTACCGAGGCGCCATGGGCTTCATCCTA 300
NM_009001   CAAGAGCGGTACCGCACCATCACCACAGCCTATTACCGAGGCGCCATGGGCTTCATCCTA 300
            ************************************************************

BaitWT      ATGTATGACATCACCAATGAGGAGTCATTTAATGCAGTGCAGGACTGGTCCACTCAGATC 360
T36N        ATGTATGACATCACCAATGAGGAGTCATTTAATGCAGTGCAGGACTGGTCCACTCAGATC 360
NM_009001   ATGTATGACATCACCAATGAGGAGTCATTTAATGCAGTGCAGGACTGGTCCACTCAGATC 360
            ************************************************************

BaitWT      AAAACTTACTCGTGGGACAATGCCCAGGTGCTGCTGGTGGGAAACAAGTGTGACATGGAA 420
T36N        AAAACTTACTCGTGGGACAATGCCCAGGTGCTGCTGGTGGGAAACAAGTGTGACATGGAA 420
NM_009001   AAAACTTACTCGTGGGACAATGCCCAGGTGCTGCTGGTGGGAAACAAGTGTGACATGGAA 420
            ************************************************************

BaitWT      GATGAGCGAGTGGTGTCCTCAGAGCGTGGCCGGCAGCTGGCTGACCACCTGGGCTTTGAG 480
T36N        GATGAGCGAGTGGTGTCCTCAGAGCGTGGCCGGCAGCTGGCTGACCACCTGGGCTTTGAG 480
NM_009001   GATGAGCGAGTGGTGTCCTCAGAGCGTGGCCGGCAGCTGGCTGACCACCTGGGCTTTGAG 480
            ************************************************************

BaitWT      TTCTTTGAGGCCAGCGCCAAGGACAACATTAATGTCAAGCAGACGTTTGAACGTCTGGTG 540
T36N        TTCTTTGAGGCCAGCGCCAAGGACAACATTAATGTCAAGCAGACGTTTGAACGTCTGGTG 540
NM_009001   TTCTTTGAGGCCAGCGCCAAGGACAACATTAATGTCAAGCAGACGTTTGAACGTCTGGTG 540
            ************************************************************

BaitWT      GACGTGATCTGTGAGAAGATGTCAGAGTCCCTGGATACTGCAGACCCTGCGGTCACCGGT 600
T36N        GACGTGATCTGTGAGAAGATGTCAGAGTCCCTGGATACTGCAGACCCTGCGGTCACCGGT 600
NM_009001   GACGTGATCTGTGAGAAGATGTCAGAGTCCCTGGATACTGCAGACCCTGCGGTCACCGGT 600
            ************************************************************

BaitWT      GCCAAGCAGGGCCCGCAGCTCACCGACCAGCAGGCGCCACCTCATCAGGATTGTGCCTGC 660
T36N        GCCAAGCAGGGCCCGCAGCTCACCGACCAGCAGGCGCCACCTCATCAGGATTGTGCCTGC 660
NM_009001   GCCAAGCAGGGCCCGCAGCTCACCGACCAGCAGGCGCCACCTCATCAGGATTGTGCCTGC 660
            ************************************************************

BaitWT      TGA 663
T36N        TGA 663
NM_009001   TGA 663
            ***
```

Figure 4.23. DNA nucleotide sequence alignment of the various Rab3a bait constructs. *The native mouse Rab3a bait (BaitWT), GTPase deficient Rab3a (T36N) and original native mouse brain Rab3a construct (NM_009001) are shown. The mutation resulting in a T36N mutation is indicated in yellow.*

Native α-SNAP bait

α-SNAP is a protein with an exceptionally crucial role in forming the 25S fusion complex. Upon recognizing the SNARE complex it induces a conformational change that renders it

competent for binding and stimulating the ATPase activity of the D1 domain of NSF (Burgoyne and Morgan 2003). From literature it is clear that cytosolic α-SNAP engage in protein-protein interactions with syntaxin, SNAP25, VAMP and NSF that makes it attractive for use in a two-hybrid screen (Table 4.2). The coding region from mouse brain α-SNAP was amplified from the construct obtained from Proff. Whiteheart and Rothman, and directionally cloned in frame into the pAS2_1 plasmid. Figure 4.24 indicates the band obtained after PCR amplification, while the coded sequences obtained from these clones (in frame with the DNA-BD) are indicated in Figure 4.25.
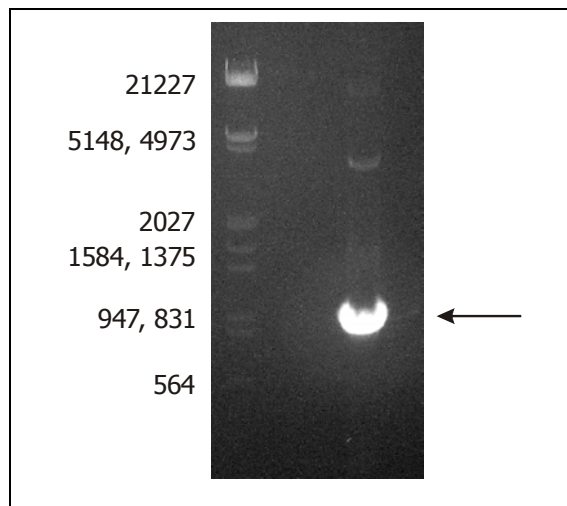
Figure 4.24. PCR amplification of the coding region of native mouse brain α-SNAP.

```
    Clone2          ----------------ERKVKNSQSFFSGLFGGSSKIEEACEIYARAANMFKMAKNWSA 43
    P54921          MDTSGKQAEAMALLAEAERKVKNSQSFFSGLFGGSSKIEEACEIYARAANMFKMAKNWSA 60
    Clone3          ----------------ERKVKNSQSFFSGLFGGSSKIEEACEIYARAANMFKMAKNWSA 43
    Clone5          ----------------ERKVKNSQSFFSGLFGGSSKIEEACEIYARAANMFKMAKNWSA 43
                                    *******************************************

    Clone2          AGSAFCQAAQLHLQLQSKHDAATCFVDAGNAFKKADPQEAINCLMRAIEIYTDMGRFTIA 103
    P54921          AGNAFCQAAQLHLQLQSKHDAATCFVDAGNAFKKADPQEAINCLMRAIEIYTDMGRFTIA 120
    Clone3          AGSAFCQAAQLHLQLQSKHDAATCFVDAGNAFKKADPQEAINCLMRAIEIYTDMGRFTIA 103
    Clone5          AGSAFCQAAQLHLQLQSKHDAATCFVDAGNAFKKADPQEAINCLMRAIEIYTDMGRFTIA 103
                    **.*********************************************************

    Clone2          AKHHISIAEIYETELVDVEKAIAHYEQSADYYKGEESNSSANKCLLKVAGYAAQLEQYQK 163
    P54921          AKHHISIAEIYETELVDVEKAIAHYEQSADYYKGEESNSSANKCLLKVAGYAAQLEQYQK 180
    Clone3          AKHHISIAEIYETELVDVEKAIAHYEQSADYYKGEESNSSANKCLLKVAGYAAQLEQYXK 163
    Clone5          AKHHISIAEIYETELVDVEKAIAHYEQSADYYKGEESNSSANKCLLKVAGYAAQLEQYQK 163
                    ************************************************************

    Clone2          AIDIYEQVGTSAMDSPLLKYSAKDYFFKAALCHFCIDMLNAKLAVQKYEELFPAFSDSRE 223
    P54921          AIDIYEQVGTSAMDSPLLKYSAKDYFFKAALCHFCIDMLNAKLAVQKYEELFPAFSDSRE 240
    Clone3          AIDIYEQVGTSAMDSPLLKYSAKDYFFKAALCHFCIDMLNAKLAVQKYEELFPAFSDSRE 200
    Clone5          AIDIYEQVGTSAMDSPLLKYSAKDYFFKAALCHFCIDMLNAKLAVQKYEELFPAFSDSRE 222
                    ************************************************************

    Clone2          CKLMKKLLEAHEEQNVDSYTES 245
    P54921          CKLMKKLLEAHEEQNVDSYTES 262
    Clone3          CKLMKKLLEAHEEQNVDSYTES 222
    Clone5          CKLMKKLLEAHEEQNVDSYTES 244
                    *********************
```

Figure 4.25. DNA nucleotide sequence alignments of α-SNAP bait constructs. *α-SNAP baits constructed in pAS2_1 (Clones 2, 3 and 5) as well as native mouse brain α-SNAP (P5421) are indicated.*

4.6.4. Transformation of bait/ GAL4 BD constructs into AH109

Using the small-scale yeast transformation protocol, the bait constructs were transformed into AH109 yeast cells. Since the pAS2_1 plasmid contains the *TRP1* reporter gene, the cells were plated on SD/-Trp. In order to confirm that the bait constructs themselves do not activate the two-hybrid reporter genes (*HIS3* and *ADE2*), the cells were also plated on SD/-Leu/-Trp/-His (TDO) and SD/-Leu/-Trp/-His/-Ade (QDO). Indicated in Figure 4.26 are six clones containing the truncated syntaxin bait plated on various selection media. It is evident that this bait does not activate the two-hybrid reporter genes. All baits were screened in this way (results not shown) and none activated the yeast reporter genes.
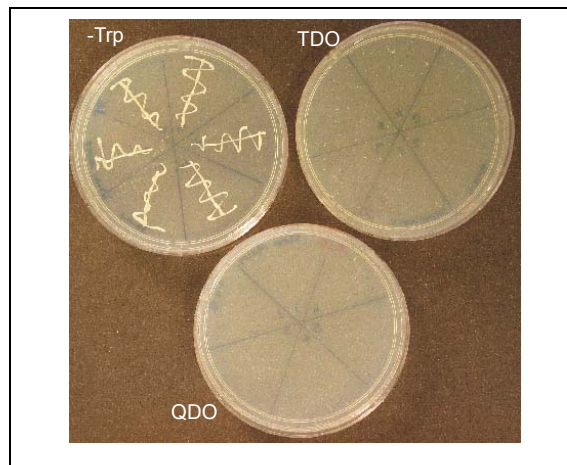
Figure 4.26. AH109 yeast cells containing the pAs2_1 truncated syntaxin bait construct. *Cells are plated on SD/-Trp (-Trp), SD/-Leu/-Trp/-His (TDO) and SD/-Leu/-Trp/-His/-Ade (QDO)*

4.6.5.   Library transformation and two-hybrid screening

Using the 30x scale described by the two-hybrid TRAFCO protocol (http://tto.trends.com) for library scale transformations, AH109 cells containing the various bait plasmids (truncated syntaxin, Rab3a, Rab3a T36N and α-SNAP, respectively) were transformed with 150 μg of library plasmid. Co-transformed cells were directly plated on TDO plates and grown until colonies were visible (2-3 days). The cells were then scraped from the plates and re-plated at various dilutions on QDO plates (see Figure 4.27.i). From here single colonies were picked and plated in duplicate on master QDO plates (Figure 4.27.ii). Only the results of truncated syntaxin are shown, while the results for α-SNAP were identical. Both the truncated syntaxin and α-SNAP co-transformed cells were used for further two-hybrid screening.
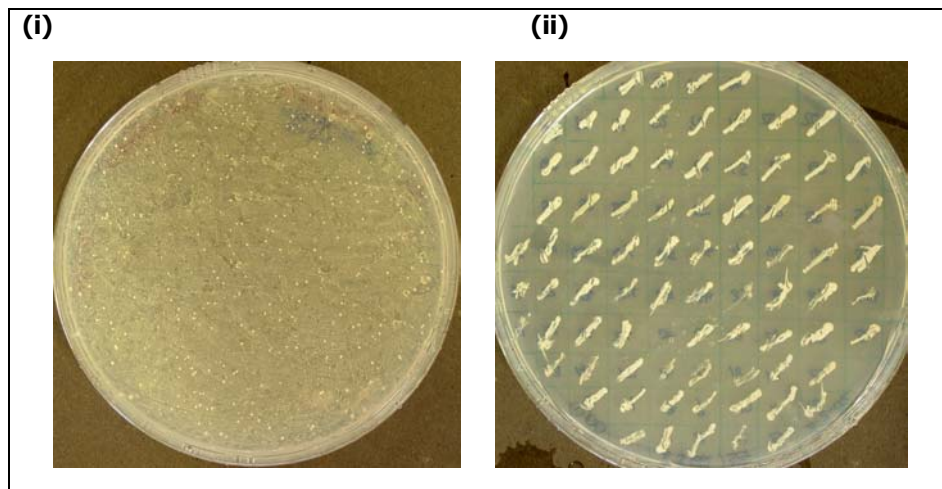
Figure 4.27. AH109 yeast cells co-transformed with truncated syntaxin bait and *Sfi*I/*Xho*I truncated library. *Co-transformed cells were plated on SD/-Leu/-Trp/-His/-Ade (QDO) and grown until single colonies were visible (i). The colonies were then streaked on a master QDO plate (ii) for subsequent storage and analysis.*

When plating cells co-transformed with the Rab3a bait constructs and library, it was noted that the cells turned dark pink on both TDO- and QD-plates. It is known that Ade$^+$ cells remain white to pale pink while Ade$^-$ colonies gradually turn reddish-brown and stop growing. Therefore, stronger *ADE2* expression will be white while in contrast, weaker expression will become progressively more pink and red. In the case of AH109 cells containing the native Rab3a as well as the mutant Rab3a T36N bait constructs, the cells were extremely pink in colour indicating weak expression (Figure 4.28). Therefore, the Rab3a baits were not used during two-hybrid assays. Future studies could exploit use of the Rab3a Q81L mutation as described by Martincic *et al.* (Martincic *et al.* 1997).
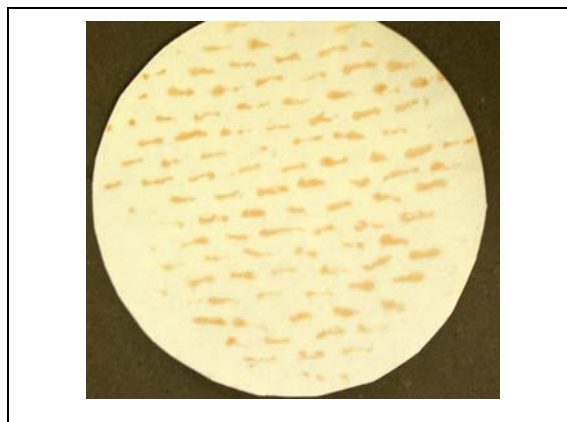
Figure 4.28. AH109 yeast cells containing the pAs2_1 native Rab3a bait construct. *Co-transformed cells plated on SD/-Trp were transferred to filter paper to emphasize the pink color.*

The number of clones screened can be calculated as (cfu/μg) x amount of library plasmid used. In the case of cells co-transformed with truncated syntaxin bait and library, the co-transformation efficiency was calculated at 5,3 x10^4 cfu/μg and the number of clones screened 7,95 x 10^6. In the case of α-SNAP / library co-transformations the co-transformation efficiency was calculated at 3,4 x 10^4 cfu/μg and the number of clones screened 5,1 x 10^6.

4.6.6. Colony-lift β-galactosidase assay

Initial screening of the QDO positive clones was performed using the *lacZ* reporter gene, i.e. positive for β-galactosidase activity. The colony lift assay for β-galactosidase was used to screen large numbers of QDO positive clones in order to identify clones with elevated levels of β-galactosidase activity. Figure 4.29 indicates a typical result obtained using the colony-lift assay. Clones containing control plasmids turned blue within 30-60 minutes. Clones with elevated β-galactosidase activity was identified within 60 minutes and used for further screening with nested PCR.
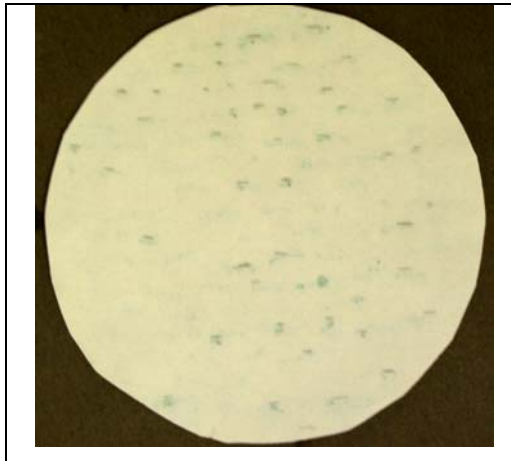
Figure 4.29. A typical β-galactosidase colony lift assay of AH109 yeast cells containing the pAS2_1 truncated syntaxin bait construct. *Co-transformed cells are plated on QDO, transferred to filter paper; lyzed by freeze/thaw cycles and incubated with buffer containing X-gal. Blue colonies are positive for β-galactosidase activity.*

4.6.7. Nested-PCR screening of β-galactosidase positive clones

PCR screening directly from intact yeast cells requires nested PCR due to the high amount of chromosomal DNA present. Indicated in Figure 4.30 are the two sets of primers (indicated in blue and red, respectively) used to amplify the cloned inserts from the pACT2-AD/ library constructs.
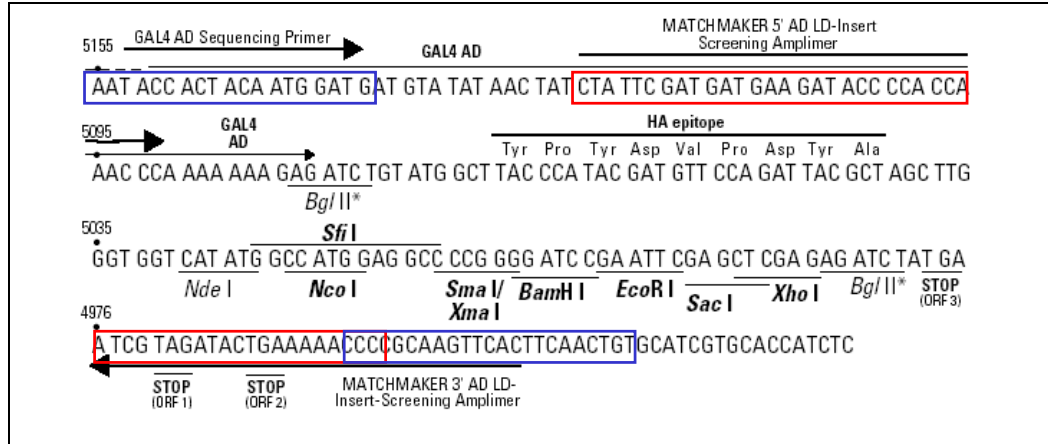
Figure 4.30. Partial sequence of the pACT2 plasmid. *The first (blue) and second (red) set of primers used during nested PCR are indicated. The multiple cloning region, containing the SfiI and XhoI sites used for directional cloning of the library inserts, are also shown.*

Cells (~1 μl) were suspended in PCR mixture containing the first set of nested primers (indicated in blue) and lyzed by incubating the reaction mixture at 94ºC for 7 minutes in a Perkin Elmer GeneAmp PCR system 9700. After cooling the mixture to 80ºC, enzyme mix was added and PCR performed as described previously. Product obtained from this first PCR was used as template for the second (nested) PCR using the second set of primers (indicated in red, Figure 4.30). The final product was analyzed using agarose gel electrophoresis. As indicated in Figure 4.31, it is clear that one cannot distinguish between the various clones after only nested PCR. Therefore, restriction enzyme mapping was done using *Bam*HI and *Hin*dIII. After restriction enzyme mapping, 7 unique clones could be identified from QDO positive clones using truncated syntaxin as bait (Figure 4.32).
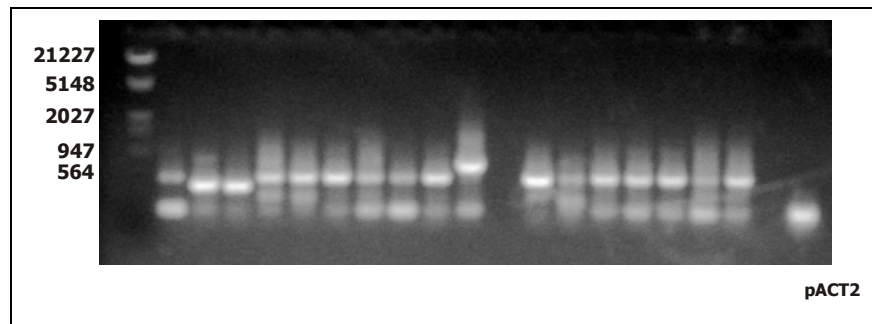
Figure 4.31. Typical agarose electrophoresis pattern obtained after nested PCR of QDO-positive clones containing truncated syntaxin as bait. *Each lane corresponds to a different QDO β-galactosidase positive clone. The last lane indicates the multiple cloning site amplified form native pACT2 plasmid during nested PCR.*
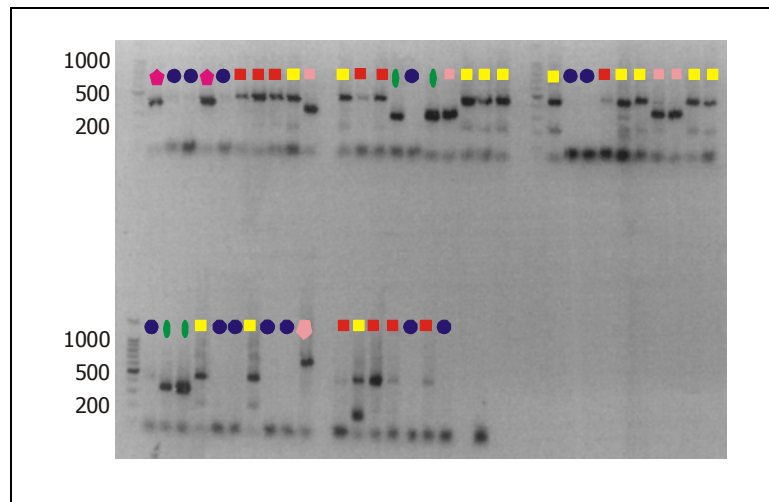
Figure 4.32. Agarose electrophoresis pattern obtained after *Bam*Hi and *Hin*dII digestion of nested PCR products obtained from QDO-positive clones containing truncated syntaxin as bait. *Each lane corresponds to a different QDO β-galactosidase positive clone. Colored symbols are used to indicate unique clones.*

Nested PCR and restriction enzyme digestion (*Bam*HI and *Hin*dIII) of the products obtained from positive clones using α-SNAP as bait resulted in the identification of only a single clone. Indicated in Figure 4.33 are the agarose electrophoresis results from 30 clones that were screened. All of the clones contained a single amplified band of ~500bp.
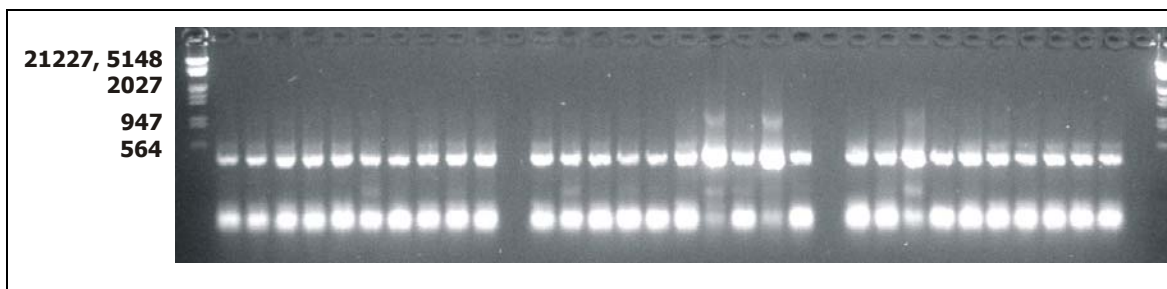
Figure 4.33. Agarose electrophoresis pattern obtained after *Bam*HI and *Hin*dII digestion of nested PCR products obtained from QDO-positive clones containing α-SNAP as bait.

4.6.8. Sequencing and analysis of positive AD/library inserts

The various novel clones identified by both the β-galactosidase assay and nested PCR were identified on the master QDO plates. These clones, however, still contained both the pAS2_1 BD/Bait as well as the pACT2 AD/library plasmids. In order to isolate only the pACT2 AD/library plasmids for DNA sequencing of the interacting inserts, both plasmids were isolated from the clones and transformed into KC8 *E. coli* cells. These KC8 cells have a defect

in *leuB*, which can be complemented by *LEU2* from yeast and will hence only select the pACT2 AD/library plasmids.

The KC8 clones (plated on M9 minimal medium, with ampicillin, lacking leucine) were again screened for pACT2 AD/library plasmids and correct insert as detected during restriction enzyme analysis of QDO positive clones. Following High Pure plasmid isolation from the KC8 cells, the interacting inserts were subjected to DNA sequencing using the GAL4 AD sequencing primer.

Analysis of inserts interacting with truncated rat brain syntaxin1

The proteins encoded for the interacting inserts were deduced from the nucleotide sequences as encoded for by the open reading frame of the DNA activation domain. Two consensus domains that are shared between the five clones were identified. These are colored yellow (domain I) and green (domain II), respectively (Table 4.11).

Table 4.11. Prey molecules identified using truncated syntaxin and truncated library

Clone #	In frame translation
2 & 6	SYPWWKRCGQEQGRLSCQVFIKMCVAT
9	SYPWWKRCGQEQGRLSCQVFIKMCVTEKKKKKKKKKKTCRPWRRGXRRLWRW
10	PIPALPLWAARLRARIALALLRGNYRASAERRKGAPPPNGCTGQTFRSLAEPRQISPAWF
14	GGSEAKTPSAAGPGRAGPPIPALPLWAARLRARIALALLRGNYRASAERRKGAPPQWLHGTNLPVIGRASTDLACLVF
40	TLTGTTRGVAGEAARNAGTSPGTVPGTAIPGGPDRRGTGAGESTVRRARVCVVRSHRITLSRTVAVRTEGDQCPAGPSCSYLDGNLGEI NLRVCKKKKKKKKKKKHVGHGGRGTSSWWXQPPXYWQGLNSSKRCLSRSQGRSDCRQXDGSYPWWKRCGQEQG

Domain I (indicated in yellow, Table 4.11) was shared between clones 2, 6, 9 and partially in the C-terminal of clone 40. We were unable to ascribe an identity to domain I due to the limited length of the encoded peptides. Domain II (indicated in green, Table 4.11) was present in clone 10 and 14.

Since no significant identity could be attributed to clones 10 and 14 using normal BLAST-P, we used PSI-BLAST with the BLOSUM72 matrix (Position Specific Iterated) analysis since it is much more sensitive to detect weak but biologically relevant sequence similarities (Altschul *et al.* 1997). PSI-Blast analysis of only the consensus region (domain II) indicated various possible targets. Amongst these was the protein syntaphilin (gi_57104478), which shared a

44% identity with domain II (Figure 4.34). Syntaphilin has only been isolated from brain tissue to date, where it functions as a molecular clamp that controls free syntaxin-1 and dynamin-1 availability and thereby regulates synaptic vesicle exocytosis and endocytosis. The binding of syntaphilin to syntaxin is regulated via the phosphorylation of syntaphilin by a cAMP-dependent kinase. It is predicted that PKA phosphorylation acts as an "off" switch for syntaphilin, thus blocking its inhibitory function via the cAMP-dependent signal transduction pathway (Das *et al.* 2003; Boczan *et al.* 2004). The expect (E) value, which is a parameter that describes the number of hits one can expect to obtain just by chance when searching a database of particular size, indicated this similarity as not significant. We obtained an E-value of 33, while a lower E-value (closer to zero) indicates a more significant match. It must however be noted that searches with short sequences can be virtually identical and have relatively high E-value because calculation of the E-value also takes into account the length of the query sequence. This is because shorter sequences have a high probability of occurring in the database purely by chance.

```
Domain 2         1  PIPALPLWAARLRARIALALLRGNYRASAERRKGAP  36
                    PIP L      R R+ +A++L  G+ RASA  R G P
Syntaphilin    346    PIPPL----TRTRSLMAMSL-PGSRRASAGSRSGGP
376
```

Figure 4.34. Homology between domain I and syntaphilin using PSI-BLAST.

When the entire coding sequence of clone 10 was subjected to PSI-BLAST analysis, the data indicated similarity to casein kinase I, epsilon isoform from mouse (Q9JMK2) and human (P49674). In both cases 44% identity was observed with an e-value of 0.7, which indicates a greater degree of confidence. The alignments and identical residues are indicated in Figure 4.35. Literature indicates that syntaxin does interact with casein kinase I and gets phosphorylated by both casein kinase I and II (Dubois *et al.* 2002). In order to conclusively identify clone 10 one will have to obtain the entire open reading frame of the protein. Since a partial sequence is known, one can exploit the use of 3' and 5' RACE, or using the cloned insert as a probe for screening the full-length library. No identity could be ascribed for clones 14 and 40 using PSI-BLAST.

```
Clone 10    23  GNYRASAERRKGAPPPNGCTGQTFRSLAEPRQISPA    58
                G  R SA R     PP G T    RS AEP   +PA
Q9JMK2     318  GQLRGSATRALPPGPPTGATANRLRSAAEPVASTPA  353
P49674     318  GQLRGSATRALPPGPPTGATANRLRSAAEPVASTPA  353
```

Figure 4.35. Homology between clone 10 and Casein kinase I epsilon isoform using PSI-BLAST.

Certain analysis programs (the so called threading programs) incorporate both PSI-BLAST, as well as structure prediction from a library of structures in order to identify possible identity. Using the threading programs 3D-PSSM Web Server V 2.6.0 (http://www.igb.uci.edu/tools/scratch/), both clones 10 and 14 were found to share 36% and 24% identity, respectively, to the voltage-gated potassium channel inactivation domain 2 (residues 1 - 75). Once again, the interaction between syntaxin and the voltage-gated potassium channel, in particular the inactivation domain, has been described in literature (Leung *et al.* 2003; Michaelevski *et al.* 2003). Again, no motifs or identity could be determined for clone 40.

Since syntaxin interacts with its binding partners via coiled-coiled regions (α-helical rich regions), we investigated the secondary structure of the identified peptides using the SCRATCH server of 3D-PSSM. This server uses 7 different servers (Sspro2, Sspro8, CONpro, ACCpro, CMAPpro, CCMAPpro and CMAP23Dpro) to assign the most likely secondary structure to an amino acid sequence (http://www.igb.uci.edu/ tools/scratch/). From the data it is clear that all of the identified clones are rich in alpha helical structure (Figure 4.36). Domain I, clone 10 and clone 14 contain a single helix while clone 4 contain 2 helical domains as well as a helical C-terminal. Based on the helical content, one could postulate that these helical domains are most likely to be the ones involved in coil-coil interactions with the syntaxin bait.

```
Domain I:

SYPWWKRCGQEQGRLSCQVFIKMCVAT
...HHHHHTHHTT.EEHEEEEEEEE..
eeee-ee-eeeeeeee-e---e--eee


Clone 10:

PIPALPLWAARLRARIALALLRGNYRASAERRKGAPPPNGCTGQTFRSLAEPRQISPAWF
...HHHHHHHHHHHHHHHHHHHT..H.HHHHTT....TS.TT.EHH.........HT..
eeee-e---ee-e-e------eee-e-eeeeeeeeeeee-eeee-ee-eeeee-eeeee


Clone 14:

GGSEAKTPSAAGPGRAGPPIPALPLWAARLRARIALALLRGNYRASAERRKGAPPQWLHG
...........STT..S....HHHHHHHHHHHHHHHHHHT..H.HHHHTT...G..TT
eeeeeeeeeeeeeeeeeee-ee-e---ee-e--------e-e-e-eeeeeee-eee--e-

Clone 40:

TLTGTTRGVAGEAARNAGTSPGTVPGTAIPGGPDRRGTGAGESTVRRARVCVVRSHRITL
......HHHHHHHHHHTT..TT.....E.......T....S..EEEEEEEEEEEEEEEEE
eeeeeeee--ee--eeeeeeeee-eee--eeeeeeeeeeeeee-ee-e----eeee-e-

SRTVAVRTEGDQCPAGPSCSYLDGNLGEINLRVCKKKKKKKKKKHVGHGGRGTSSWWXQP
EEEEEEEE.T.........GEE.S.THEEEEHHHHHHHHHHHHEEE.........GT...
ee----eeeeee-eeeee-ee-eee-ee-e-e--eeeeeeeeeeeeeeeeeeee-eee-

PXYWQGLNSSKRCLSRSQGRSDCRQXDGSYPWWKRCGQEQG
.HHHHT.....EEE...T........TS..HHHHHHT....
ee--eeeeeeee-eeeeeeeee-eeeeeeee--ee-eeeee
```

Figure 4.36. Structure prediction of syntaxin interacting peptides. *Line 1: The 1-letter code of the protein primary sequence. Line 2: 8-class secondary structure prediction (H: alpha helix, E: extended strand, T: turn, S: bend, G: 310-helix). Line 3: Prediction of relative solvent accessibility (-: The residue is buried, e: The residue is exposed).*

Analysis of inserts interacting with rat brain α-SNAP

All the interacting clones identified during two-hybrid assays using α-SNAP as bait contained an identical ~500 bp insert which encoded a 126 amino acid protein (Table 4.12, row 2). BLAST-P and PSI-BLAST analysis of the encoded protein detected no hits. The Predict protein database, which incorporates functional motifs, composition-bias, protein domains and threading (http://cubic.bioc.comumbia.edu/predictprotein), indicated that the protein shares highest homology with the microtubule-associated protein 1B (also called neuraxin) from rat (P15205), various heat shock proteins and myosin (Table 4.12). In all of these cases the E-value was again not significant.

Table 4.12. Predict protein analysis of α-SNAP interacting protein.

α-SNAP interacting protein sequence:			
GLTTMHTNIKDIKSDLKTTENNISILSARAESIEANVASLGKVHEAVRDLTETSKNLSANVDFLKRKTDDFENRMRRSNLVFY GIPDDPAETWAQSELHVIKLCEQNLGKVVKPEEIERAHRSRDL			

Predict protein analysis results:

	Identity (%)	Accession number	Name
mapb_rat	26	P15205	LIGHT CHAIN LC1
dnak_brume	26	Q8YE76	HSP70
dnak_bruov	26	Q05981	DNAK PROTEIN (HEAT SHOCK)
tpm2_yeast	24	P40414	TROPOMYOSIN 2.
g160_human	23	Q08378	GOLGIN-160
dyna_neucr	22	Q01397	(DP-150)(DAP-150)
myh8_human	21	P13535	MYOSIN HEAVY CHAIN (SKELETAL MUSCLE)
tpm1_yeast	21	P17536	TROPOMYOSIN 1
smc3_yeast	21	P47037	CHROMOSOME SEGREGATION
ra50_sulso	21	Q97WH0	DNA DOUBLE-STRAND BREAK REPAIR PROTEIN
tpm1_chick	22	P04267	ALPHA-TROPOMYOSIN
mys2_dicdi	21	P08799	MYOSIN II HEAVY CHAIN
yhge_bacsu	21	P32399	HYPOTHETICAL 84.1 KDA PROTEIN

When subjecting the protein sequence to the 3D-PSSM threading web server V 2.6.0 it was found to share sequence and structural homology to syntaxin 1A N-terminal, syntaxin 6 and the neuronal synaptic fusion complex. Crystal structure data of syntaxin 1 indicates that the protein contains 4 α-helices linked via three loop regions (Figure 4.37). In order to further investigate possible similarity to the syntaxins, the secondary structure prediction of the α-SNAP binding protein was determined by using the analysis program 3D-PSSM. From the secondary structure prediction it is evident that the isolated protein contains three helical domains, similar to those found for syntaxin (Figure 4.38).

Figure 4.37. Crystal structure of syntaxin 1N. A vertical (i) and rotated (ii) view is shown with the *N-terminal (N), C-terminal (C), helices 1-4 (H1-4) and loops 1-3 (L1-3) labelled.*

Figure 4.38. Secondary structure prediction of the α-SNAP interacting protein. *Data was obtained from 3D-PSSM Web Server V 2.6.0, (http://www.igb.uci.edu/tools/scratch/). aSNAP_SS indicates the predicted secondary Structure for the α-SNAP interacting protein, aSNAP_Seq indicates the α-SNAP interacting protein sequence, Syn1A_Seq indicates the sequence of human syntaxin 1A, Syn1A__SS represents the known secondary structure of the library sequence of syntaxin 1A (Assigned by [STRIDE](link)). Helical regions 1,2 and 3 are indicated (blue), as well as coils (C) and extended strands (E).*

Alignment of various syntaxins and the α-SNAP interacting protein was performed using Pfam (http://www.sanger.ac.uk/Software/Pfam/), which is a comprehensive collection of protein domains and families, with a range of well-established uses including genome annotation. Each family in Pfam is represented by two multiple sequence alignments and two profile-Hidden Markov models (profile-HMMs) (Bateman *et al.* 2004). The results indicated that the sequences do share homology (Figure 4.39). Between the α-SNAP interacting protein (fragment) and the full length syntaxin 1A there is 14% identity and 40% similarity.
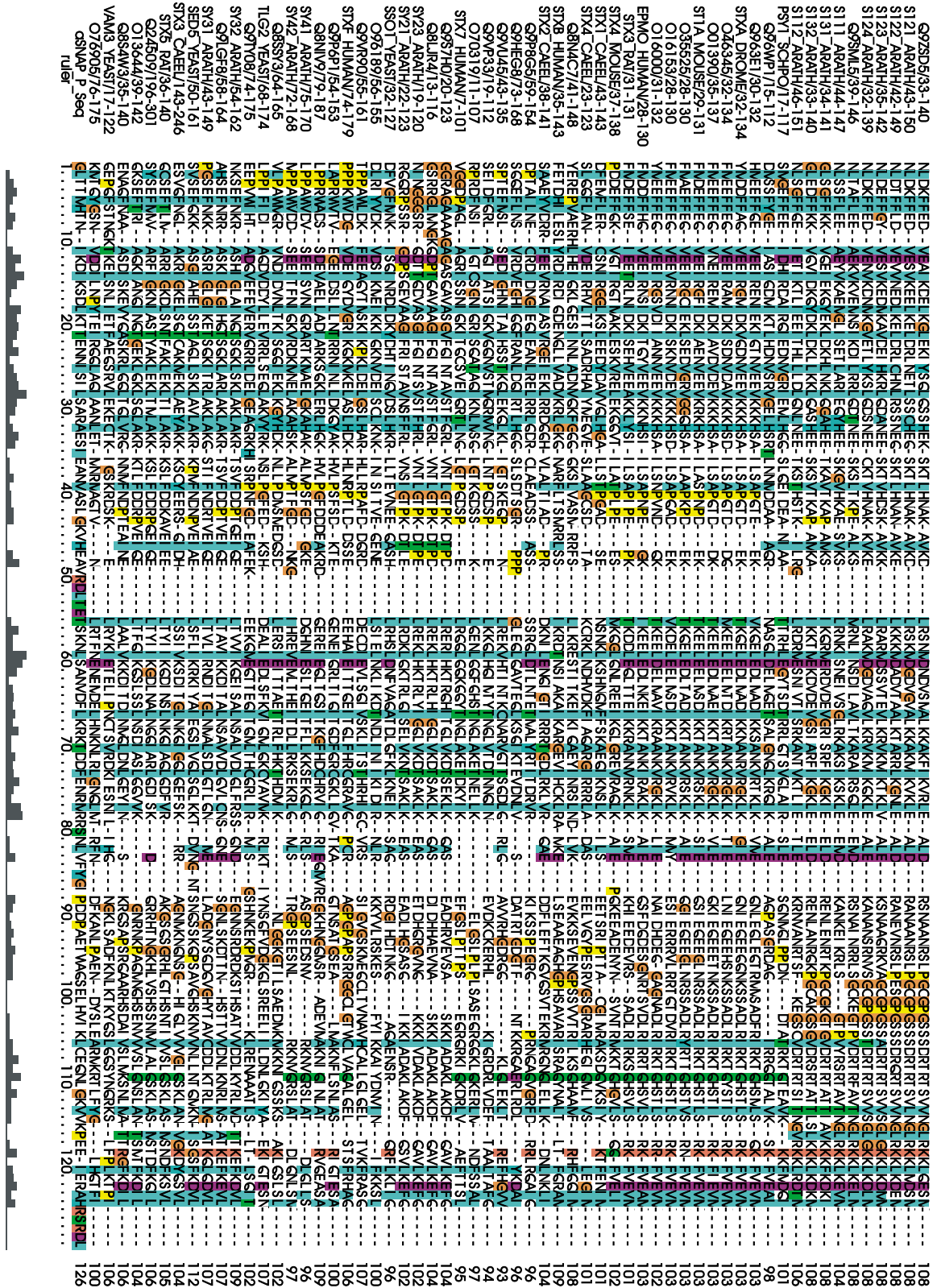
Figure 4.39. Multiple sequence alignment of syntaxins and α-SNAP interacting protein.
Non-polar residues (blue), negative residues (purple), uncharged residues (green), positive residues (orange), and proline (yellow) are indicated. The identified α-SNAP interacting sequence aSNAP_P-Seq as well as a similarity scale (below sequences) is shown.

We continued with the alignments obtained from Pfam and compared the structure of the α-SNAP protein identified to the known crystal structure of syntaxin 1A using Modeller (Sali and Blundell 1993; Fiser and Sali 2000; Marti-Renom *et al.* 2000). Mr Tjaart de Beer from the Comparative Biology and Bioinformatics Unit, University of Pretoria performed all of the modeling studies. From the superimposed structures it is clear that the α-SNAP interacting protein shares structural homology to the N-terminal and three helices of syntaxin (Figure 4.40). In helix 2 we were unable to model the structure of the α-SNAP interacting protein due to lack of crystal structure data of syntaxin 1A (Indicated by an arrow, Figure 4.40.ii).
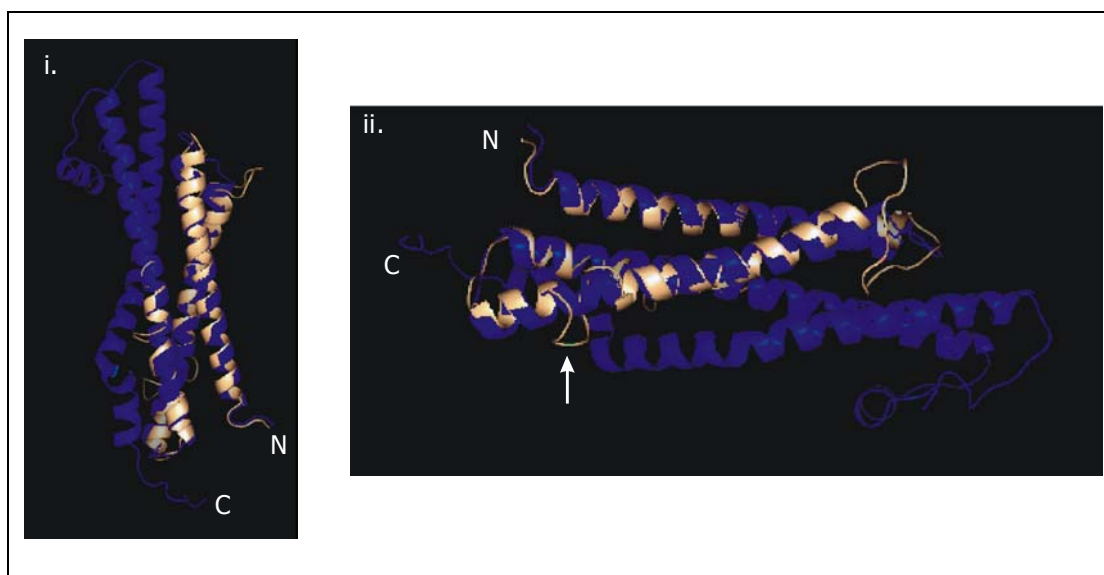
Figure 4.40. Modeled structure of the α-SNAP interacting protein. *Superimposed model of the backbone structure of α-SNAP interacting protein (brown) on that of syntaxin 1A crystal structure (blue). The vertical view (i), horizontal view (ii), N-termini (N), C-terminal (C) and the single region for which no crystal structure data is available (arrow) is indicated. Structures were generated using Modeller and viewed using PyMol.*

Based on the Pfam alignments, secondary structure prediction, threading and modeling results we suggest this protein to be a syntaxin. This finding is similar to that obtained from literature, where the use of α-SNAP as bait resulted in the identification of various syntaxin isoforms (see references in Table 4.2). In order to conclusively label the α-SNAP interacting protein a novel *O. savignyi* syntaxin, one will have to isolate and analyze the entire open reading frame of the protein.

4.7.   CONCLUSION

The aim of this study was to investigate the possibility of exploiting protein-protein interactions across species and tissues in order to identify secretory proteins from *O. savignyi* able to interact with rat brain secretory proteins. This was attempted by using the two-hybrid system. We were able to use the two-hybrid system in detecting and isolating novel domains and proteins involved in binding known secretory proteins. Although our data is not conclusive, we hypothesize a model for the formation of a fusion complex between LDCVs and the plasma membrane in *O. savignyi* salivary glands (Figure 4.41). We hypothesize that fusion complex formation is inhibited by means of a protein similar to syntaphilin/munc/nsec bound to the N-terminal of syntaxin. The other two SNARE proteins, VAMP and SNAP25 are bound to the granule membrane (see Chapter 3) and do not interact with syntaxin prior to stimulation. Upon stimulation, the inhibitory protein is released from syntaxin and fusion complex formation is initiated. This recruits α-SNAP, which binds via syntaxin (as proposed by the two-hybrid results) to the fusion complex. Based on literature, binding of α-SNAP will result in recruiting the ATPase NSF. The possible interaction between syntaxin and the voltage-gated K^+ channel cannot be excluded based on the threading results obtained for clone 10 and 14 when truncated syntaxin was used as a bait molecule.
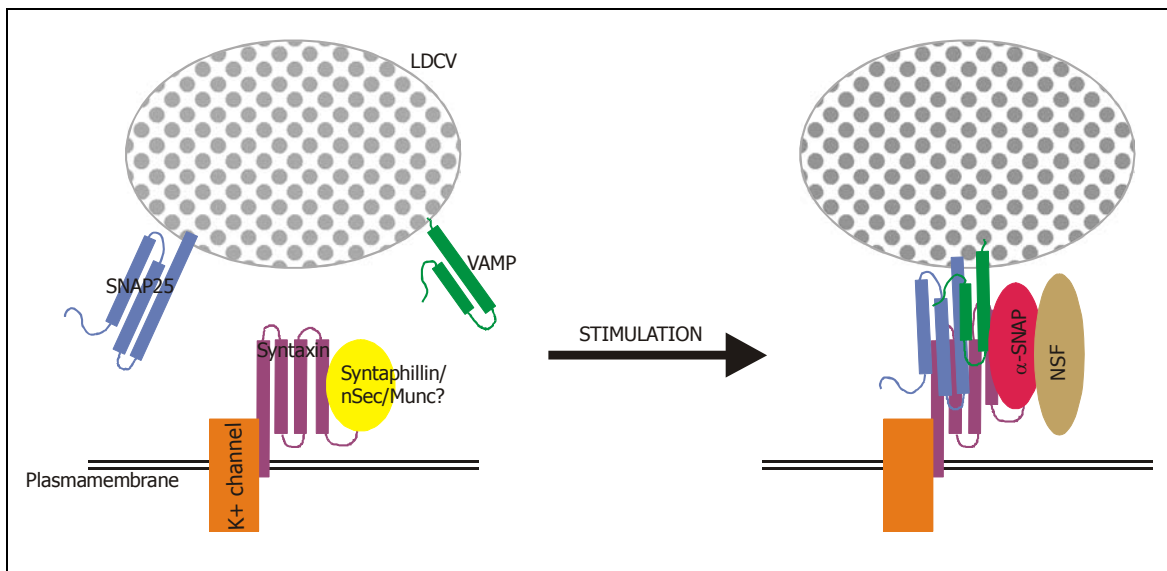
Figure 4.41. Schematic presentation of a possible model for fusion complex formation in the salivary glands of *O. savignyi*.

4.8.   REFERENCES

Altschul, S.F., Madden, T.L., Schaffer, A.A., Zhang, J., Zhang, Z., Miller, W., Lipman, D.J. (1997). Gapped BLAST and PSI-BLAST: a new generation of protein database search programs. *Nucleic acids research* **25**(17): 3389-3402.

Araki, S., Tamori, Y., Kawanishi, M., Shinoda, H., Masugi, J., Mori, H., Niki, T., Okazawa, H., Kubota, T., Kasuga, M. (1997). Inhibition of the binding of SNAP-23 to Syntaxin-4 by Munc-18c. *Biochemical and Biophysical Research Communications* **234**: 257-262.

Bartel, P.L., Fields, S. (1997). *The yeast two-hybrid system*. New York, Oxford, Oxford University Press.

Bateman, A., Coin, L., Durbin, R., Finn, R.D., Hollich, V., Griffiths-Jones, S., Khanna, A., Marshall, M., Moxon, S., Sonnhammer, E.L.L., Studholme, D.J., Yeats, C., Eddy, S.R. (2004). The Pfam protein families database. *Nucleic acids research* **32**: D138-D141.

Bior, A.D., Essenberg, R.C., Sauer, J.R. (2002). Comparison of differentially expressed genes in the salivary glands of male ticks, *Amblyomma americanum* and *Dermacentor andersoni*. *Insect Biochemistry and Molecular Biology* **32**: 645-655.

Boczan, J., Miriam Leenders, A.G., Sheng, Z.-H. (2004). Phosphorylation of Syntaphilin by cAMP-dependent Protein Kinase Modulates Its Interaction with Syntaxin-1 and Annuls Its Inhibitory Effect on Vesicle Exocytosis. *The Journal of Biological Chemistry* **279**(18): 18911-18919.

Burgoyne, R.D., Morgan, A. (2003). Secretory granule exocytosis. *Physiology Reviews* **83**: 581-632.

Burstein, E.S., Brondyk, W.H., Macara, I.G. (1992). Amino acid residues in the Ras-like GTPase Rab3a that specify sensitivity to factors that regulate the GTP/GDP cycling of Rab3a. *The Journal of Biological Chemistry* **267**(32): 22715-22718.

Chen, D., Xu, W., He, P., Medrano, E.E., Whiteheart, S.W. (2001). Gaf-1, a gamma-SNAP binding protein associated with the mitochondria. *The Journal of Biological Chemistry* **276**(16): 13127-13135.

Clontech Laboratories, I. (1997a). *Matchmaker Gal4 Two-hybrid vectors handbook (PT3062-1)*.

Clontech Laboratories, I. (1997b). *Two-hybrid cDNA library construction kit user manual (PT1113-1)*.

Clontech Laboratories, I. (1998). *Matchmaker Gal4 Two-hybrid user manual (PT3061-1)*.

Clontech Laboratories, I. (1999). *Matchmaker Gal4 two-hybrid system 3 & Libraries user manual (PT3247-1)*.

Clontech Laboratories, I. (2001a). *Super SMART PCR cDNA synthesis kit user manual PT3656-1 (PR 22685)*.

Clontech Laboratories, I. (2001b). *Yeast Protocols Handbook (PT3024-1)*.

Das, S., Gerwin, C., Sheng, Z.-H. (2003). Syntaphilin Binds to Dynamin-1 and Inhibits Dynamin-dependent Endocytosis. *The Journal of Biological Chemistry* **278**(43): 41221-41226.

Diefenbach, R.J., Diefenbach, E., Douglas, M.W., Cunningham, A.L. (2002). The heavy chain of conventional kinesin interacts with the SNARE proteins SNAP25 and SNAP23. *Biochemistry* **41**: 14906-14915.

Dubois, T., Kerai, P., Learmonth, M., Cronshaw, A., Aitken, A. (2002). Identification of syntaxin-1A sites of phosphorylation by casein kinase I and casein kinase II. *European Journal of Biochemistry* **269**: 909-914.

Fields, S., Song, O.-K. (1989). A novel genetic system to detect protein-protein interactions. *Nature* **340**: 245-246.

Fiser, A., Sali, A. (2000). Modeling of loops in protein structures. *Protein Science* **9**: 1753-1773.

Frederickson, R.M. (1998). Macromolecular matchmaking: advances in two-hybrid and related technologies. *Current Opinion in Biotechnology* **9**: 90-96.

Han, S.Y., Park, D.Y., Park, S.D., Hong, S.H. (2000). Identification of Rab6 as an N-ethylmaleimide sensitive fusion protein binding protein. *Biochemical Journal* **352**: 165-173.

Hata, Y., Sudhof, T.C. (1995). A novel ubiquitous form of Munc-18 interacts with multiple syntaxins. Use of the yeast two-hybrid system to study interactions between proteins involved in membrane traffic. *The Journal of Biological Chemistry* **270**(22): 13022-13028.

Hatsuzawa, K., Hirose, H., Tani, K., Yamamoto, A., Scheller, R.H., Tagaya, M. (2000). Syntaxin 18, a SNAP receptor that functions in the endoplasmic reticulum, intermediate compartment and cis-Golgi vesicle trafficking. *The Journal of Biological Chemistry* **275**(18): 13713-13720.

Janoueix-Lerosey, I., Jollivet, F., Camonis, J., Matche, P.N., Goud, B. (1995). Two-hybrid screen with the small GTP-binding protein Rab6. *The Journal of Biological Chemistry* **270**(24): 14801-14808.

Kwong, J., Roudabush, F.L., Moore, P.H., Montague, M., Oldham, W., Li, Y., Chin, L.-S., Li, L. (2000). Hrs interacts with SNAP-25 and regulates calcium-dependent exocytosis. *Journal of Cell Science* **113**: 2273-2284.

Leung, Y.M., Kang, Y., Gao, X., Xia, F., Xie, H., Sheu, L., Tsuk, S., Lotan, I., Tsushima, R.G., Gaisano, H.Y. (2003). Syntaxin 1A binds to the cytoplasmic C terminus of Kv2.1 to regulate channel gating and trafficking. *The Journal of Biological Chemistry* **278**(19): 17532-17538.

MacDonald, P.N. (2001). *Two-hybrid systems: Methods and Protocols*. Totowas, New Jersey, Humana Press.

Marti-Renom, M.A., Stuart, A., Fiser, A., Melo, F., Sali, A. (2000). Comparative protein structure modeling of genes and genomes. *Annual Review of Biophysics and Biomolecular Structure* **29**: 291-325.

Martincic, I., Peralta, M.E., Ngsee, J.K. (1997). Isolation and characterization of a dual prenylated Rab and VAMP2 receptor. *The Journal of Biological Chemistry* **272**(43): 26991-26998.

McDonald, P.H., Cote, N.L., Lin, F.-T., R.T., P., Pitcher, J.A., Lefkowitz, R.J. (1999). Identification of NSF as a beta-arrestin1 binding protein. *The Journal of Biological Chemistry* **274**(16): 19677-10680.

Michaelevski, I., Chikvashvilli, D., Tsuk, S., Singer-Lahat, D., Kang, Y., Linial, M., Gaisano, H.Y., Fili, O., Lotan, I. (2003). Direct interaction of target SNAREs with the Kv2.1 channel. Modal regulation of channel activation and inactivation gating. *The Journal of Biological Chemistry* **278**(36): 34320-34330.

Okamoto, M., Schoch, S., Sudhof, T.C. (1999). EHSH1/Intersectin, a protein that contains EH and SH3 domains and binds to dynamin and SNAP-25. *The Journal of Biological Chemistry* **274**(25): 18446-18454.

Perez-Branguli, F., Muhaisen, A., Blasi, J. (2002). Munc18a binding to syntaxin 1A and 1B isoforms defines its localization at the plasma membrane and blocks SNARE assembly in a three-hybrid system assay. *Molecular and Cellular Neuroscience* **20**: 169-180.

Ravichandran, V., Chawla, A., Roche, P.A. (1996). Identification of a novel syntaxin- and synaptobrevin/VAMP-binding protein, SNAP-23, expressed in non-neuronal tissues. *The Journal of Biological Chemistry* **271**(23): 13300-13303.

Sali, A., Blundell, T.L. (1993). Comparative protein modelling by satisfaction of spatial restraints. *Journal of Molecular Biology* **234**: 779-815.

Stephens, D.J., Banting, G. (2000). The use of yeast two-hybrid screens in studies of protein-protein interactions involved in trafficking. *Traffic* **1**: 763-768.

Su, Q., Mochida, S., Tian, J.-H., Mehta, R., Sheng, Z.-H. (2001). SNAP 29: A general SNARE protein that inhibits SNARE disassembly and is implicated in synaptic transmission. *PNAS* **20**(24): 14038-14043.

Sugita, S., Hata, Y., Sudhof, T.C. (1996). Distinct calcium-dependent properties of the first and second C2-domains of synaptotagmin I. *The Journal of Biological Chemistry* **271**(3): 1262-1265.

Valdez, A.C., Cabaniols, J.P., Brown, M.J., Roche, P.A. (1999). Syntaxin 11 is associated with SNAP-23 on late endosomes and the trans-Golgi network. *Journal of Cell Science* **112**: 845-854.

Wyles, J.P., McMaster, C.R., Ridgway, N.D. (2002). Vesicle-associated membrane protein-associated Protein-A (VAP-A) interacts with the oxysterol-binding protein to modify export from the endoplasmic reticulum. *The Journal of Biological Chemistry* **277**(33): 29908-29918.

Xu, H., Boulianne, G.L., Trimble, W.S. (2002). *Drosophila* syntaxin 16 is a Q-SNARE implicated in golgi dynamics. *Journal of Cell Science* **115**(23): 4447-4455.

Young, K.H. (1998). Yeast two-hybrid: So many interactions, in so little time. *Biology of reproduction* **58**: 302-311.

CHAPTER 5

INVESTIGATING SNARE-INTERACTIONS BY FUNCTIONAL COMPLEMENTATION IN *Saccharomyces cerevisiae* AND PULL-DOWN ASSAYS WITH α-SNAP

5.1. INTRODUCTION

In 1977 it was shown that a gene from a higher eukaryote could be expressed in a microorganism, *Escherichia coli*, to produce a biologically active protein, somatostatin (Kingsman *et al.* 1985). It appears, however, that *E. coli* may not be the most suitable host for the expression of all eukaryotic proteins. A disadvantage of the *E. coli* system is the necessity to renature the heterologous polypeptides, since in most cases this organism was found to be unable to produce the proteins in a properly folded, soluble form (i.e. not in inclusion bodies). Moreover, many eukaryotic proteins depend on post-translational modifications such as glycosylation, which prokaryotic hosts are unable to synthesize (Gellissen *et al.* 1992). In many instances yeast became the preferred hosts for heterologous protein and gene expression. The best-characterized species, *Saccharomyces cerevisiae*, was the first to be used for the successful production of eukaryotic proteins such as human α-interferon, hepatitis B surface antigens and enzymes like calf pro-chymosin and *Aspergillus* glucoamylase (Gellissen *et al.* 1992). Furthermore, the availability of the entire genome sequence of *S. cerevisiae*, as well as the *S. cerevisiae* genome deletion project, enables researchers to perform functional complementation in yeast.

5.1.1. *S. cerevisiae*: A model organism for studying protein transport

A basic feature of all eukaryotic cells is compartmental organization, which requires mechanisms for the correct sorting and distribution of molecules to the appropriate target organelle. Due to an impressive conservation of the molecular transport machinery across phyla (Rothman 1996), a great deal of knowledge on the functional interactions has been acquired by the study of *S. cerevisiae*. This yeast is a unicellular eukaryote, organized into the same major membrane-bounded compartments as all other eukaryotic cells and shares the same metabolic processes (Kucharczyk and Rytka 2001).

In *S. cerevisiae* delivery of cargo to the recipient organelle is accomplished by membrane recognition processes known as tethering, docking and fusion, similar to those described in mammalian cells. Tethering factors are peripherally membrane-associated protein complexes, containing up to 10 different subunits. The docking stage involves two specific sets of membrane-anchored SNARE proteins. Firstly the family of v-SNAREs (or synaptobrevin-related receptors) on the vesicle membranes and secondly, the t-SNAREs (or plasma membrane syntaxin related receptors) on the target membrane. The formation of a stable four-helical bundle between the v- and t-SNAREs is believed to generate enough energy to initiate mixing of the lipid bilayers of the fusing membranes (Sutton *et al.* 1998). In yeast, the proteins Sec18p and Sec17p, which are required at all transport steps, regulate complex formation. ATP hydrolysis by Sec18p disassembles the complex, similar to NSF in higher eukaryotic cells. In yeast, similar to mammalian cells, SNARE binding has been proven to be promiscuous and that multi-protein complexes determine the specificity of membrane fusion (Kucharczyk and Rytka 2001). The various interactions between v- and t-SNAREs in yeast are summarized in Figure 5.1. Apart from the functional similarities between yeast SNAREs and those of higher eukaryotes, the remarkable structural similarities have also been well described (Rossi *et al.* 1997; Katz and Brennwald 2000; Antonin *et al.* 2002; Fasshauer 2003).

Apart from the homologous SNAREs in yeast, the small monomeric Rab GTPases (200-230 amino acids) found in higher eukaryotic cells also occur in yeast i.e. the Ypt GTPases. These small Ypt GTPases belong to the Ras-related protein superfamily and play key regulatory roles at the different stages of trafficking. In *S. cerevisiae* this superfamily contains 29 members of which eleven are Ypt GTPases. Other families belonging to this superfamily include Ras that has a regulatory role in the cell cycle, Ran which regulates nuclear import, Arf/Sar which functions during vesicle budding and Rho, which regulates cytoskeletal organization and cell wall biogenesis (Kucharczyk and Rytka 2001).
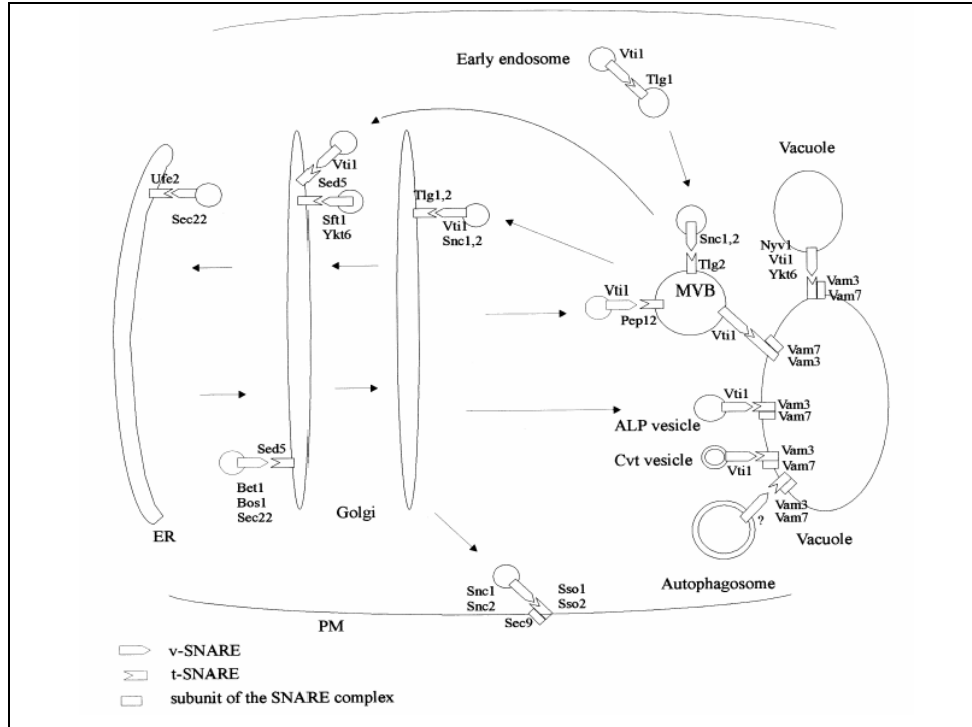
Figure 5.1. Interactions of v- and t-SNAREs in yeast (Kucharczyk and Rytka 2001). *Compartment abbreviations: (ER) endoplasmic reticulum, (PM) plasma membrane and (MVB) multivesicular body. The various yeast v- and t-SNAREs are indicated.*

Similar to higher eukaryotic GTPases, the transport GTPases in yeast also cycle between active GTP-bound and inactive GDP-bound conformations. Furthermore, the cycle is regulated in an identical manner as in mammalian cells by means of GDP-dissociation inhibitors (GDI), GDI displacement factors (GDF) and GTPase-activating proteins (GAP), as described in Chapter 2 (Kucharczyk and Rytka 2001). A high degree of conserved sequence motifs occur between Ras proteins from different species (Table 5.1), enabling functional complementation studies.

Table 5.1. Conserved sequence motifs in Ras proteins from different species (Kucharczyk and Rytka 2001). *G1 binds α and β phosphates of GTP/GDP; G2 is the effector domain essential for GTP hydrolysis; G3 binds γ phosphate of GTP; G4 binds the guanine ring; G5 stabilizes the guanine-G4 interaction.*

	G1	**G2**	**G3**	**G4**	**G5**
Ypt7 (Yeast)	GDSGVGKT	YKATI	WDTAGQE	GNKID	FL-TSAK
p21 / ras (Rat)	GAGGVGKS	YDPTI	LDTAGQE	GNKCD	FIETSAK
RhoH (Human)	GDGGCGKT	YTPTV	WDTAGQD	GCKTD	YHRGQEM
Ran (Mouse)	GDGGTGKT	YVATL	WDTAGQE	GNKVD	YYDISAR

196

Apart from the conserved proteins involved in trafficking, yeast also exhibits signal regulation of the various trafficking steps, i.e. clathrin, Vps34p phosphatidylinositol 3-kinase and the Vps15 protein kinase which has been indicated to regulate the formation of Golgi vesicles, which carry cargo to the multi vesicular body (Conibear and Stevens 1995). It is proposed that Vps15p and Vps34p function together as components of a membrane-associated signal transduction complex that regulates intracellular protein trafficking through protein and lipid phosphorylation (Kucharczyk and Rytka 2001).

The lipid constituents of the plasma membrane, i.e. phosphatidylinositols (PI), sphingolipids and sterols are not only present in *S. cerevisiae*, but have also been proven to be important transport regulators, similar to higher eukaryotic cells (Kucharczyk and Rytka 2001). This confirms that in all eukaryotes, not only proteins, but also lipids play a vital role in trafficking. PIs, which are substrates for various PI kinases and PI phosphatases have been studied extensively. In *S. cerevisiae*, it has been shown that PI-4,5-P_2 plays a role in internalization of clathrin-mediated endocytosis and that PI-3-P functions at a post-internalization step of endocytosis as well as endosomal/vacuolar trafficking. Spingolipids and ergosterol form sterol-sphingolipid-rich domains (rafts) in the plasma membrane. These rafts are believed to define the membrane spatial specificity by recruiting the endocytic machinery to a distinct membrane site and also delivery of some proteins to the plasma membrane (Kucharczyk and Rytka 2001).

Other multi cellular processes linked to transport and trafficking, including actin cytoskeletal dynamics and ubiquitylation, have also been studied extensively in yeast and were shown to resemble processes in higher eukaryotes (Shaw *et al.* 2001).

5.1.2. Functional complementation

Functional complementation involves the controlled expression of a heterologous (e.g. non-yeast) proteins in mutated or knockout cells (e.g. yeast cells) in order to rescue a particular phenotype.

Yeast vectors used for heterologous protein expression

Five common types of plasmids are used for yeast transformation. Vectors of the YIp type (yeast integration plasmid) integrates by homologous recombination of complementation genes contained on the plasmid at the respective mutant loci of suitable auxotrophic

acceptor strains. Integrative transformants are extremely stable and therefore often used as production strains containing or producing a heterologous protein. Vectors of the YRp type (yeast replication plasmid) remain in an extra-chromosomal state after transformation due to the presence of a sequence for autonomous replication (*ARS*). They are present in 3-20 copies, but are very unstable due to abnormal segregation during mitosis or meiosis. The plasmid stability was improved with the addition of a yeast centromeric sequence, leading to the YCp (yeast centromeric plasmid) vectors. Addition of telomeric structures in YAC (yeast artificial chromosomes) lead to linear vectors that can harbour DNA fragments up to 200 kb in size. The most commonly used vectors in yeast engineering are derived from the 2 μm plasmid, termed YEp (yeast episomal plasmid) vectors. They can transform yeast at a frequency of 5 000 – 20 000 recombinants per μg of DNA and transformants contain an average of 40 copies per cell and also exhibit high stability (Gellissen *et al.* 1992). For expression, a heterologous gene is fused to a promoter obtained from a highly expressed *S. cerevisiae* gene (see Chapter 4) as well as a yeast derived termination sequence.

In this study we investigated the use of the pRS 413 plasmid, which is an autonomously replicating single copy centromeric (YCp) plasmid (http://www.atcc.org/Products/prs.cfm). It is also an *S. cerevisiae / E. coli* shuttle vector which allows ampicillin and blue/white selection in *E. coli* (lacZ). It contains the ADH-promoter and termination fragments, as well as a HIS3 selection marker in *S. cerevisiae* (Figure 5.2).
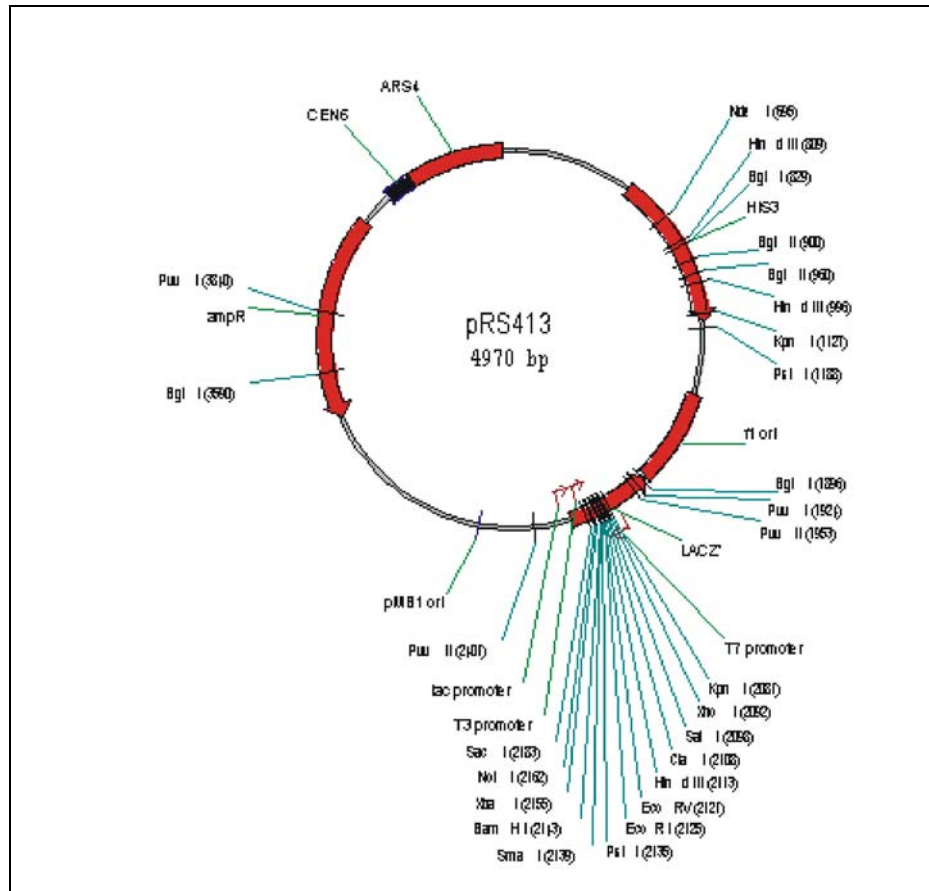
Figure 5.2. Plasmid map of the *S. cerevisiae* / *E. coli* shuttle vector pRS 413 (Clontech Laboratories 1997a).

Subcellular localization of heterologous proteins

It has been shown that the presence or absence of a 'classical' signal sequence on a heterologous protein does not necessarily determine the subcellular localization in *S. cerevisiae* (Kingsman *et al.* 1985). For example, the proteins preprochymosin, prochymosin and chymosin have all been expressed in *S. cerevisiae,* and all forms located to the cell membrane and none in the cytoplasm. Similar results were obtained during the expression of hepatitis B surface antigen, which lacks a signal sequence. Expression of these constructs in a yeast strain with the *pep4-3* mutation (which is deficient in vacuolar proteases) increased the yields, indicating that proteolytic degradation of foreign proteins occurs (Kingsman *et al.* 1985).

Glycosylation

Evidence for the glycosylation of heterologous proteins in *S. cerevisiae* comes from studies on α_1-antitrypsin and mouse immunoglobulins. Expression of the latter yielded high

199

molecular weight forms which were not present in tunicamysin-treated cultures or after endoglycosidase H or chemical de-glycosylation (Kingsman *et al.* 1985). It must be noted that the percentage of glycosylation is low and heterogeneous. Also, *S. cerevisiae* glycoproteins are of the high-mannose type, whereas higher eukaryotic glycoproteins contain a variety of glycosyl residues with complex branching. It is therefore unlikely that glycosylation of heterologous proteins in *S. cerevisiae* will contribute to any biological activity, which requires complex and specific carbohydrate modifications (Kingsman *et al.* 1985).

5.1.3. Functional complementation of SNAREs and trafficking proteins in yeast

In spite of all the obstacles, functional complementation of both *SSO-1* and *SSO-2* (yeast syntaxin) as well as a *pep12* (homologue of yeast and mammalian syntaxins) mutants were successful. In the case of the temperature-sensitive mutations in the yeast syntaxin 1, homologous Sso1p and Sso2p, a screen for high copy number suppressors of the phenotype yielded three genes from a genomic yeast library that are involved in the terminal step of secretion: *SNC1*, *SNC2* (synaptobrevin homologues) and *SEC9* (a SNAP25 homologue) (Jantti *et al.* 2002).

The yeast protein pep12 is a syntaxin homologue, which may function in the trafficking of vesicles from the trans-Golgi network to the vacuole. By means of functional complementation of the yeast pep12 mutant with an *Arabidopsis thaliana* cDNA library, a pep12 homologue was identified. The *Arabidopsis* cDNA encodes a 31 kDa protein which is homologous to yeast pep12 and other members of the syntaxin family (Bassham *et al.* 1995). The existence of plant homologues of syntaxins indicates firstly, that the basic vesicle docking and fusion machinery may be conserved in plants as it is in yeast and mammals and secondly, that cross-species expression and functional complementation of syntaxin homologues are feasible in yeast.

In another functional complementation study using *S. cerevisiae* and an *Arabidopsis thaliana* cDNA library, a homologue that complements the *sec14* mutant was identified. AtSEC14 was able to restore the growth of sec14 temperature sensitive mutants, partly restored protein secretion and enhanced the phosphatidylinositol-transfer activity that is impaired in *sec14* mutants. Interestingly, the best sequence similarity between yeast sec14 and AtSec14 is

found at the amino acid level (36.5% similar) and not the genomic level (Jouannic *et al.* 1998). Our results obtained by the two-hybrid assay (Chapter 4) are similar to the latter.

Transport between secretory pathways also requires SNAREs. By means of functional complementation in *YKT6* knockout yeast (which encodes a novel SNARE involved in ER to Golgi transport), three SNAREs, p14, p28 and p26 were identified from human cDNA libraries. These proteins were found to be homologous to their yeast counterparts, Sft1p, Gos1p and Ykt6p. Important to note is that the SNARE, Ykt6p, which requires membrane localization for protein function, still localized to the membrane in yeast without the isoprenylation signal. Furthermore, this study demonstrated that Ykt6p and its homologues are highly conserved between yeast and human and it is the first example of a human SNARE protein functionally replacing a yeast SNARE. This observation implies that the specific details of the vesicle targeting code, like the genetic code, are conserved in evolution (McNew *et al.* 1997).

In a study by Pullikuth *et al.* the *in vivo* role of the insect NSF (MsNSF), isolated from the insect *Manduca sexta* (the so-called tabacco hormworm) was investigated by heterologous expression in *SEC18* mutated yeast. *M. sexta* MsNSF is believed to regulate hormone release from the endocrine/paracrine cells of the corpora allata. MsNSF was shown to be functional in yeast membrane fusion *in vivo* and rectified defects in the mutated yeast at nearly all discernable steps where Sec18p has been implicated in the biosynthetic route (Pullikuth and Gill 2002).

5.1.4. α-SNAP: Functional properties

It has long been known that *in vitro* α-SNAP binds directly to syntaxin and SNAP25, but not to VAMP (McMahon and Sudhof 1995). Upon formation of a α-SNAP-syntaxin complex, VAMP can be bound. In the presence of all three SNAREs as well as NSF, pull-down assays using immobilized α-SNAP results in the purification of all three SNAREs and NSF. This indicates that syntaxin, VAMP and SNAP25 are SNAP receptors (Hanson *et al.* 1995; McMahon and Sudhof 1995).

Despite limited overall sequence similarity among SNAREs on different membranes, all SNARE complexes examined to date bind α-SNAP and can be disassembled by NSF (Marz *et al.* 2003). All SNARE complexes contain four SNARE helices, are rod-shaped and held

together by interactions among conserved, mostly hydrophobic residues, within the core of the complex. Crystal structures of both the neuronal and endosomal SNARE complexes indicated that these complexes have largely acidic surface potentials, but contain few conserved residues on the outer solvent-exposed surfaces (Antonin *et al.* 2002; Marz *et al.* 2003).

To date, little is known about how α-SNAP recognizes the variety of SNARE complexes. By means of deletion studies in bovine α-SNAP and structural modeling of the data on the Sec17p (yeast α-SNAP homologue) crystal structure, Marz *et al.* were able to show that shape complementarity, sequence conservation and overall surface charge distribution are important factors for protein interactions (Marz *et al.* 2003).

The model proposed for α-SNAP binding to SNARE complexes shows that α-SNAP binds SNAREs in an anti-parralel orientation, positioning the N-terminal near the membrane and the C-terminal away from the membrane where it interacts with NSF. By mutating basic residues, SNARE binding was reduced up to 20% indicating that charged α-SNAP residues (which are distributed over the concave surface) are involved in the binding of SNARE complexes (Figure 5.3).
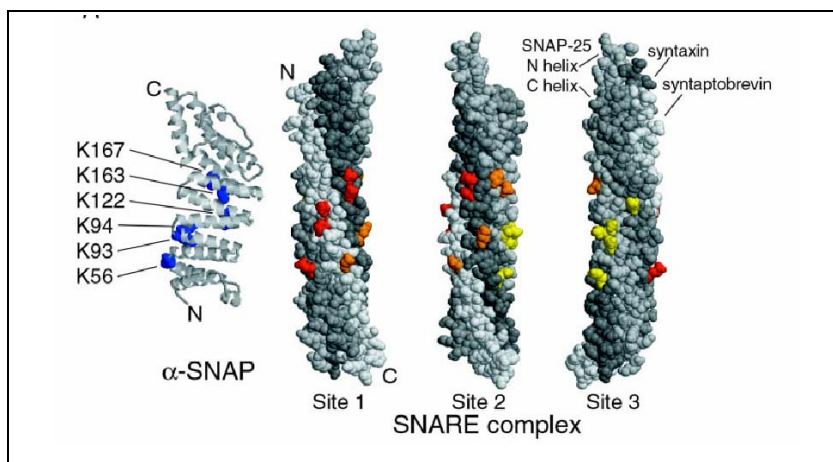
Figure 5.3. Putative α-SNAP binding sites on the SNARE complex (Marz *et al.* 2003). *Left, ribbon diagram of α-SNAP homology model, showing basic residues (blue) whose mutation reduces SNARE complex binding. Right, conserved acidic residues on the SNARE complex define three potential binding sites for α-SNAP. These sites are designated Site 1 (red, syntaxin Asp-214, Asp-218; synaptobrevin Asp-51, Glu-55; SNAP-25 C-terminal helix Glu-183), Site 2 (orange, SNAP-25 N-terminal helix Glu-38, Asp-41; syntaxin Glu-228; synaptobrevin Asp-65), and Site 3 (yellow, SNAP-25 C-terminal helix Asp-166; SNAP-25 N-terminal helix Asp-51, Glu-52, Glu-55; syntaxin Glu-238).*

Previous studies indicated that each 20S complex consists of one SNARE complex, three α-SNAPs and one NSF hexamer (Marz *et al.* 2003). The model created by Marz *et al.* indicated that the basic residues of α-SNAP form a diagonal band across the face of the α-SNAP sheet domain and that this band pairs with a diagonal band of acidic residues on the SNARE complex (Marz *et al.* 2003). Pairing of the charged diagonal bands allowed the authors to align three α-SNAP twisted sheet domains with a single SNARE complex (Figure 5.4). In this arrangement, shape complementarity is maximized and is substantially greater than when SNAPs are placed directly parallel to individual SNARE helixes. This may explain why α-SNAP binding to individual SNAREs is weaker than to the SNARE complex and why α-SNAP dissociates after complex disassembly.
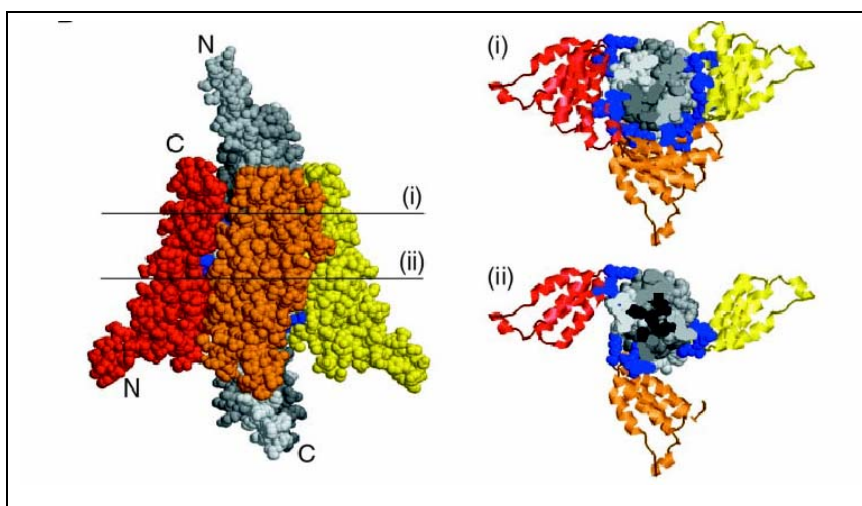
Figure 5.4. Proposed SNAP-SNARE binding model (Marz *et al.* 2003). *Indicated are the three α-SNAP twisted sheet domains bound to the SNARE complex. Each α-SNAP is color-coded according to the SNARE complex site to which it binds. Lines through the model show where slices were made to generate axial views (i) and (ii). Views are from the N-terminal and cytoplasmic ends of the SNARE complex. Basic residues whose mutations reduce SNARE complex binding, are colored blue. The SNARE complex ionic layer is colored black.*

Taking into account all of the above listed properties of α-SNAP, we decided on exploiting recombinant rat brain α-SNAP in order to isolate all of its binding partners from the salivary glands of *O. savignyi* by means of affinity chromatography (pull-down assays).

5.2. HYPOTHESIS

- We hypothesize that the SNARE proteins and α-SNAP of *O. savignyi* share both structural and functional similarity to the SNAREs of other eukaryotic cells, such as yeast and rat brain.

5.3. AIMS

- Functional complementation of the syntaxin 1 homology SSO-1 and SSO-2 mutated yeast strains using an *O. savignyi* salivary gland cDNA library.
- Expression of rat brain α-SNAP.
- Isolation of α-SNAP binding proteins from *O. savignyi* salivary glands using affinity chromatography (pull-down assays) with immobilized recombinant rat brain α-SNAP.

5.4. MATERIALS

The SSO1 and SSO2 mutated yeast strains H603 and H902 were obtained from Dr. Jussi Jantti of the VTT Technical Research Centre of Finland, VTT Biotechnology, Finland and Prof. Hans Ronne from the Department of Plant Biology, Swedish University of Agricultural Sciences, Sweden. Yeast expression plasmids were a kind gift from Prof. Carol Sibley, Department of Genetics, University of Washington, Seattle, USA. The Super SMART™ cDNA synthesis kit was obtained from Clontech (Southern Cross Biotechnology). KC8 *E. coli* cells were a kind gift from Dr. Hannelie Moolman-Smook, University of Stellenbosh, South Africa. Recombinant α-SNAP was a kind gift from Proff. Whiteheart and Rothman at the Memorial Sloan-Kettering Cancer Institute, New York, USA. NucleoSpin® Plasmid Quick Pure, NucleoBond® PC2000, NucleoSpin® Extract kits and Protino® Ni 150 columns were from Macherey-Nagel, Germany (Separations). PCR nucleotide mix (10 mM deoxynucleotide solution), *Sfi* I restriction enzyme and Shrimp alkaline phosphatase were from Roche Diagnostics. Peptone, agar and yeast nitrogen base without amino acids were from Difco (Labretoria). Yeast extract and tryptone were purchased from Oxoid Ltd. (England). Deoxyribonucleic acid sodium salt type III from salmon testes, 3-amino-1,2,4-triazole (3-AT), cycloheximide, , RNase Inhibitor, PEG4000, 425-600 micron glass beads, Triton X-100 and all the various amino acids used were from Sigma. Dextrose, Isopropyl β-D-thiogalactopyranoside (IPTG), 5-bromo-4-chloro-3-indolyl-β-D-galactopyranoside (X-gal), L-adenine hemisulphate, lithium acetate, ammonium acetate and ampicillin were from ICN (Separations). DNA polymerase I large (Klenow) fragment, *Taq* Polymerase, *Pfu* DNA polymerase, Proteinase K and various restriction enzymes were from Promega (Wisconsin, USA). BugBuster™ was from Novagen, USA. TaKaRa Ex Taq (5 U/μl) and T4 DNA Ligase (350 U/μl) were from Takara Bio Inc., Japan (Separations). All primers were synthesized by Inqaba Biotech (Pretoria, South Africa). Anti-IgG (whole molecule) conjugated to peroxidase was from Cappel (Separations). The GelCode® SilverSNAP™ stain kit was from Pierce, USA (Separations).

5.5. METHODS

5.5.1. *O. savignyi* salivary gland cDNA library construction

cDNA libraries were constructed using the Super SMART™ system, as described previously (Chapter 3 and 4). In order to directionally clone the inserts into the pRS413 vector, various restriction enzyme recognition sequences were incorporated into the CDS and SMART primers, respectively. The properties of the primers are listed in Table 5.2.

5.5.2. Growth and maintenance of *SSO*-mutated yeast cells

The SSO1 and SSO2 mutated yeast exhibit a temperature-sensitive phenotype. Therefore, cells from both H603 and H902 strains were grown at 24ºC in a shaking incubator in adenine supplemented YPD media (YPDA, 20 g/l peptone, 10 g/l yeast extract, 20 g/l agar, 20g/l dextrose, 0,03g/l adenine hemisulphate). In order to obtain sufficient cells for library transformation, cells were grown for 4 - 6 days.

5.5.3. Transformation, selection and screening

Large-scale yeast transformation was performed as described in Chapter 4. Following transformation, cells were plated on SD/-His and incubated at 30ºC in order to identify positive transformants with a suppressed phenotype. Clones were screened using nested PCR (see Chapter 4) and unique clones were selected and grown at 30ºC in SD/-His at 30ºC, in a shaking incubator. Plasmid isolation from the positive yeast clones was done as decribed in Chapter 4 and transformed into *E. coli* cells in order to obtain sufficient plasmid for DNA sequencing.

5.5.4. Data analysis

Sequences obtained were analyzed using the BioEdit Program. DNA and deduced protein sequences were analyzed using BLAST-P, PSI-BLAST (www.ncbi.nlm.nih.gov/BLAST) and the threading program 3D-PSSM Web Server V 2.6.0 (www.igb.uci.edu/tools/scratch/). All alignments were performed with Clustal W (www.ebi.ac.uk/clustalw/).

5.5.5. Expression of rat brain α-SNAP

Rat brain α-SNAP (cloned into the pQE-9 vector) was transformed into BL21 *E. coli* cells. Colonies selected from ampicillin-agar plates were grown for 12 hours at 30ºC in 5 ml LB-Broth containing 1:1 000 ampicillin. Four milliliters of culture were diluted into 50 ml LB-Broth and incubated at 30ºC in a shaking incubator until $A_{660} \sim 0.6$. Isopropryl-β-D-thiogalactopyranoside was added to a final concentration of 2.5 mM and cultures incubated for another 3 hours. The cells were collected by centrifugation (10 000 x g, 10 min) and aspirated, before determining the wet weight of the pellet. Cells were completely resuspended in 5 ml BugBuster™ per gram of wet cell paste containing 10 μg/ml DNAse, 1 μg/ml leupeptin, 20 μg/ml aprotonin and 0.5 mM PMSF (phenylmethylsulfonyl fluoride). Cells were incubated on a rotating mixer at 8ºC overnight. Insoluble debris was removed by

centrifugation (13 000 x g, 20 min, 4ºC) and the supernatant transferred to a fresh tube. The supernatant was loaded directly onto a Ni-column or stored at –70ºC until needed.

5.5.6. Salivary gland homogenate preparation

Salivary glands (~20 glands) were dissected from female, unfed *O. savignyi* ticks. Glands were suspended in homogenization buffer (20 mM HEPES pH 7.4, 100 mM KCl, 5 mM ATP, 1 mM mercapto-ethanol, 0,5% Triton X100) containing 1 μg/ml Leupeptin, 20 μg/ml aprotonin and 0.5 mM PMSF and incubated overnight at 8ºC on a rotating platform. Insoluble debris was removed by centrifugation (13 000 x g, 20 minutes, 4ºC) and the supernatant was used immediately for affinity chromatography or stored at –70ºC.

5.5.7. Affinity chromatography (Pull-down assays)

Polyhistidine-tagged recombinant α-SNAP was isolated using the Protino$^{\circledR}$ Ni 150 pre-packed columns from Macherey-Nagel. Columns were equilibrated in 320 μl LEW buffer (50 mM NaH$_2$PO$_4$, 300 mM NaCl, pH 8.0) and the cell lysate, prepared with BugBuster™, was loaded and allowed to elute with gravity. Columns were washed once with 320 μl of LEW before loading the clarified salivary gland homogenates. Non-specific bound proteins were removed by washing the column two times with 320 μl LEW. Specifically bound protein was eluted with 800 μl elution buffer (50 mM NaH$_2$PO$_4$, 300 mM NaCl, 250 mM imidazole, pH 8.0).

5.5.8. ELISA

Samples obtained after affinity chromatography were distributed into a 96 well microtiter plate (50 μl /well), dried under a 150 W lamp in a stream of air generated by an electric fan, and subsequently blocked with 300 μl of TBS (pH 7.4) containing 0.5% casein for 60 minutes. Blocking medium was replaced with 50 μl of primary antibody containing medium (diluted 1:1 000 in blocking buffer) and incubated at 37ºC for 60 minutes. Plates were washed three times in blocking buffer and incubated with an appropriate anti-IgG (whole molecule) peroxidase conjugate at a 1:10 000 dilution. After a second washing step, 100 μl developing buffer (10 ml citrate, 10 mg OPD and 8 mg H$_2$O$_2$, pH 4.5) was added and the reaction monitored at 450 nm.

5.5.9. SDS-PAGE

Samples obtained after affinity chromatography were dialyzed against 20 mM Tris-HCl (pH 8) overnight at 8ºC with stirring and freeze dried prior to SDS-PAGE. SDS-PAGE was performed

using a 5% stacking gel (0.625 M Tris-HCl, 0.5% SDS, pH 6.8) and 12% separating gel (1.88 M Tris-HCl, 0.5% SDS, pH 8.8). The acrylamide gels and the electrophoresis buffer were prepared from an acrylamide stock (30% acrylamide, 0.8% N',N'-methylene bisacrylamide) and electrophoresis buffer stock (0.02M Tris-HCl, 0.06% SDS, 0.1 M glycine, pH 8.3). The gel solutions were polymerized with the addition of 30 μl of 10% ammonium persulphate and 5 μl TEMED. Samples were resuspended in reducing sample buffer (0.06 M Tris-HCl, 2% SDS, 0.1% glycerol, 0.05% β-mercaptoethanol, 0.025% bromophenol blue) and boiled at 95ºC for 5 minutes. Pre-stained molecular mass markers (Pierce, USA) were dissolved in 10 μl water. Electrophoresis was carried out in a Biometra electrophoresis system (Biometra GmbH, Germany) with an initial voltage of 60 V for 45 minutes and thereafter a voltage of 100 V until the bromophenol blue marker reached the bottom of the gel. Gels were stained using the GelCode® SilverSNAP™ stain from Pierce.

5.6. RESULTS AND DISCUSSION

5.6.1. cDNA library construction

Although a cDNA library constructed in the two-hybrid plasmid (pACT2) was available for performing functional complementation studies in the SSO-mutant yeast, we decided to create a new cDNA library that does not contain the DNA-AD domain. In order to clone the inserts directionally, SMART and CDS primers containing *Bam*HI and *Eco*RI sites were designed and used for cDNA and ds DNA construction using the SMART system as described previously. The properties of the primers are listed in Table 5.2.

Table 5.2. Properties of the primers used for SMART cDNA synthesis of the *Bam*H I/*Eco*R I library.

Name	Sequence	Tm (ºC)
*Bam*H I SMART	AAG CAG TGG TAT CAA CGC AGA GTC <u>GGA TCC</u> GGG G *Bam*H I	74.3
*Eco*R I CDS	AAG CAG TGG TAT CAA CGC AGA GT<u>G AAT TC</u>(T)$_{18}$ VN *Eco*R I	67.3

During amplification of the cDNA, a smear ranging from 200 to 2000 bp were obtained (Figure 5.5.i). This is identical to the results described previously (Chapters 3 and 4). After digestion with *Bam*HI and *Eco*RI, the library was digested to such an extent that it was regarded as inadequate for cloning (Figure 5.5.ii). This indicates that there are multiple digestion/recognition sites for *Bam*HI and *Eco*RI in the ds cDNA of *O. savignyi* salivary glands.

Based on the list of frequency of restriction enzyme cutters from BioLabs, (http://www.neb.com/neb/tech/tech_resource/restriction/properties), we designed a new SMART primer which contains a low frequency *Sac* I restriction site. As a CDS primer, we used the CDSIII primer which is decribed in Chapters 3 and 4. This primer contains not only an *Sfi* I site, but also *Xba* I and *Nco* I sites. The properties of the primers are listed in Table 5.3.
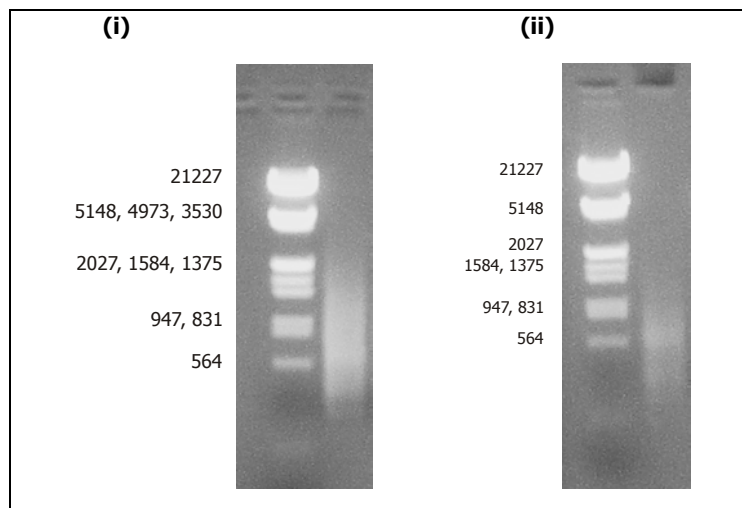
Figure 5.5. Agarose gel electrophoresis of (i) the ds SMART cDNA synthesized using the *Bam*H I SMART- and *Eco*R I CDS primers and (ii) the SMART ds DNA after *Bam*H I and *Eco*R I digestion.

Table 5.3. Properties of the primers used for SMART cDNA synthesis of the *Sac* I/*Xba* I library.

Name	Sequence	Tm (ºC)
Sac I SMART	AAG CAG TGG TAT CAA CGC AGA GTC <u>GAG CTC</u> GGG G *Sac* I	74.3
CDS III / 3'PCR	5' A<u>TT CTA GA</u>**G GCC TCC ATG GCC** GAC ATG (T)$_{30}$NN 3' *Xba* I **Sfi I** *Nco* I	67.3

After cDNA synthesis and LD-PCR amplification we obtained a smear ranging between 200 and 2000 bp (Figure 5.6). Following digestion of the library with *Sac* I and *Xba* I (which is present on the pRS 413 plasmid), the library was completely digested into very small fragments (i.e. *Sac* I and *Xba* I are frequent cutters) and again not regarded as useful for cloning. In order to clone the salivary gland cDNA library, one would need to incorporate a suitable rare cutter restriction enzyme site for *O. savignyi* (such as *Sfi* I) into the pRS413 plasmid, since it does not contain a suitable restriction site. Prior to altering the plasmid, we decided to exploit the possibility of using the full-length *Sfi* I two-hybrid fusion library for the functional complementation studies. Based on the findings in literature that fusion constructs, such as GFP tagged proteins, do not interfere with SNARE binding, localization or function, we decided on using the two-hybrid full-length *Sfi* I cDNA library cloned into the pACT2 vector.
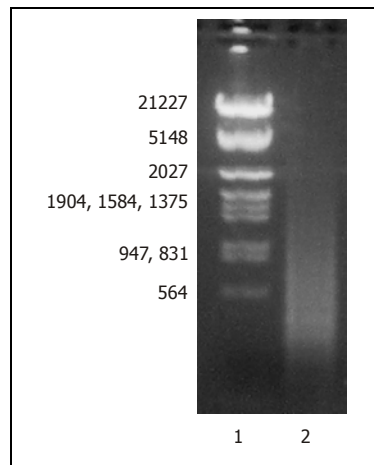
Figure 5.6. Agarose gel electrophoresis of the ds SMART cDNA synthesized using the *Sac* I SMART- and CDS III primer. *Lane 1 corresponds to the molecular mass standards, and lane 2 to the cDNA library obtained after 24 cycles using the Sac I SMART- and CDS III primers.*

5.6.2. Growth and maintenance of syntaxin knockout yeast

During the study of Jäntti *et al.*, various *SSO1* and *SSO2* mutants were generated (Jantti *et al.* 2002). They were able to show that Sso1p is essential for sporulation, while Sso2p is important for protein secretion. Only two strains were used during this functional complementation study, i.e. H603 and H902 that both contain deletions of the *SSO1* gene and contain a mutated *SSO2* gene. The properties of the two strains are listed in Table 5.4. The strains differ in their origin, i.e. H603 is derived from the W303 strain while H902 is derived from the NY179 strain, which contribute the various markers (Table 5.4). Therefore, by performing complementation in both strains, the W303 and NY179 background effects can be investigated. Cells were grown in a shaking incubator in YPDA medium at 24ºC.

Table 5.4. Properties of the SSO-mutated temperature sensitive yeast strains

Name	Genotype	Markers
H603	a, *sso*1-Δ1::*HIS3 sso*2-1	*ade2-1, can 1-100, his3-11, 15leu2-3, 112 trp1-1 ura3-1*
H902	a, *sso*1-Δ1::*LEU2 sso*2-1	*leu2-3, 112, ura3-52*

5.6.3. Transformation, selection and screening

Mutated H603 cells were transformed with the pACT2 full-length *Sfi* I salivary gland cDNA library from fully engorged, female *O. savignyi* salivary glands using the 30x library scale TRAFCO transformation protocol (Chapter 4). Positive H603 transformants were selected on SD/-Leu/-His plates and grown at 37ºC to select inserts that suppress the temperature

211

sensitive phenotype. Nested PCR directly from positive clones were performed using the pACT2-nested primers (Chapter 4). Restriction enzyme mapping (*Bam*HI and *Hind*III) of some 40 clones identified four unique inserts (Figure 5.7). These were isolated and transformed into KC8 *E. coli* cells in order to obtain sufficient plasmid for DNA sequencing. Restriction enzyme mapping of the inserts from KC8 cells confirmed the presence of four unique clones (Figure 5.8), which were isolated and sequenced.
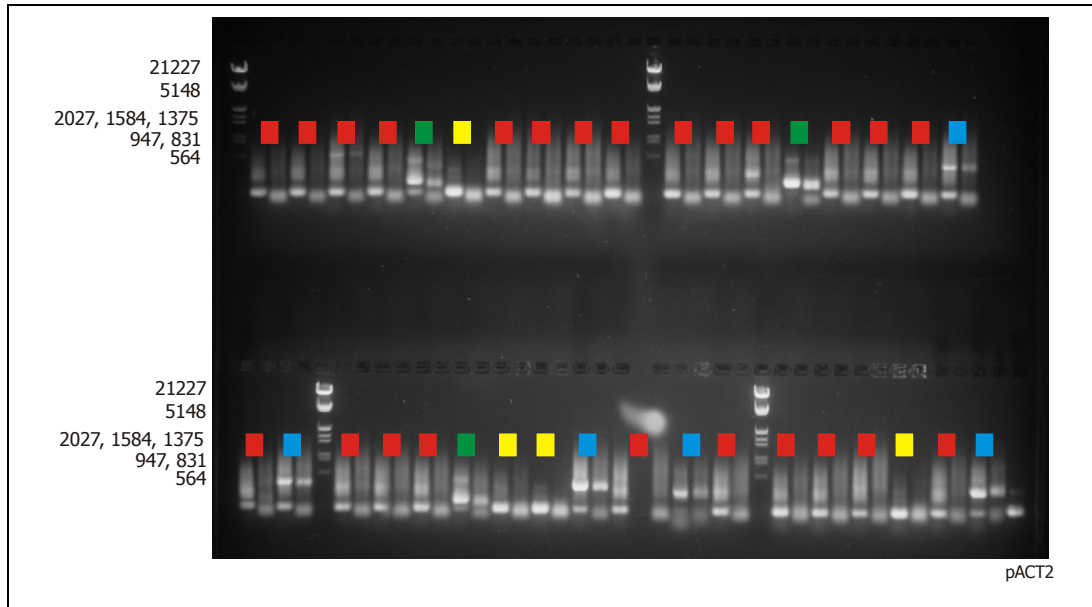
Figure 5.7. Agarose electrophoresis of the nested PCR products from suppressed H603 cells. *For each clone the undigested as well as the BamH I/Hind III digested inserts are shown. Unique inserts (coloured blocks) are indicated.*
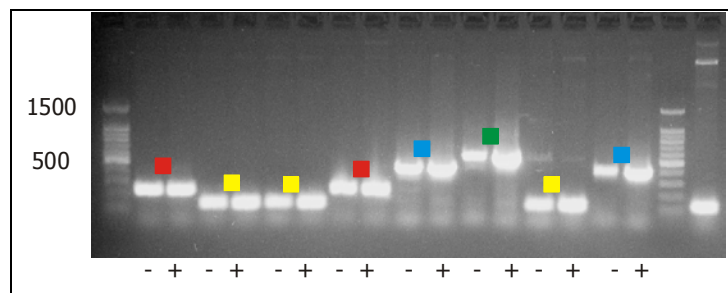
Figure 5.8. Agarose electrophoresis of the nested PCR products from KC8 cells*.

Undigested (-) BamH I and Hind III digested (+) and unique inserts (coloured blocks) are shown.

5.6.4. Data analysis

The deduced amino acid sequences of the four unique inserts were determined and are listed in Table 5.5. These correspond to 30, 81, 135 and 91 amino acid peptides for clone 5, 20, 23 and 27, respectively. The peptides were further analyzed by multiple sequence alignment of the syntaxin family (obtained from Pfam) using Clustal X. By aligning the peptide sequences with the syntaxin family sequences (Figure 5.9) and calculating the similarity and identity between various sequences, we were able to show that clones 20, 23 and 27 share homology with syntaxins sso2 from yeast, syntaxin 7 from human and syntaxin from fungi, respectively (Table 5.6).

Sequence comparisons between various mammalian full-length syntaxins indicated that they share 27-44% similarity (Advani *et al.* 1998). When non-mammalian syntaxins are included, the similarity is reduced to 30-35%. Since the calculated values (given in Table 5.6) are representative of the identified protein fragment (domain) vs. the full-length syntaxins, the calculated values are decreased, but still significant (see Figure 5.10 and 5.11).

Table 5.5. Deduced amino acid sequence of inserts that suppressed the SSO1 temperature sensitive phenotype of H603 cells.

Name	Amino acid sequence
Clone 5	AGHVTRSLTVKLNKWQQRKKKXKKKKKKHV
Clone 20	WSHGPVKVAADAVRGQYSELLEAGSLPHQPKQRVLGLSRVYIRCTCAPCTASTKEKKPGVDVLRCKYLRNGALNKCGSCQA
Clone 23	WGLHPNMVLKCPEITDKDKIYKTLPQPSCIYYCGQEEESGRYKYGFLRDNSTCKLAPTLNGYCYKGHCYKYPGGQQVTTTTEA GVTEKSTGRPSQTRRPSPTRRPSPTRRPSPTKKTKATKKPSDQKKKKKKKKN
Clone 27	GQQADCRNSRAFEKTERRRGAKKAGGRSQNQGRRRSGAFEARETEARARTQREEETERKGKEKLHLQRKLRSQRRKKKKKKK

Table 5.6. Calculated similarities and identities between identified protein domains and various full-length syntaxin isoforms. *The encoded protein sequence of the knockout clones that suppressed the temperature sensitive phenotype, was compared to that of various known syntaxins (column 1) of various organism. The similarity and identity between the isolated fragment (domain) and the full-length syntaxin was calculated using the BioEdit program.*

	Clone 20		Clone 23		Clone 27	
	% Identity	% Similarity	% Identity	% Similarity	% Identity	% Similarity
SSO2_Yeast/36-131	14	30	12	27	10	26
SSO1_Yeast/32-127	7	20	13	26	7	33
Q9P8G5/59-154 (Fungi)	14	24	16	27	17	35
Q9VU45/43-135 (Drosophila)	13	27	13	25	17	32
O70319/11-107 (Rat)	13	24	14	26	15	33
1Dn1_B/Syntaxin 1 (Human)	8	13	12	19	9	18
STX7_Human/7-101	16	27	16	29	19	34
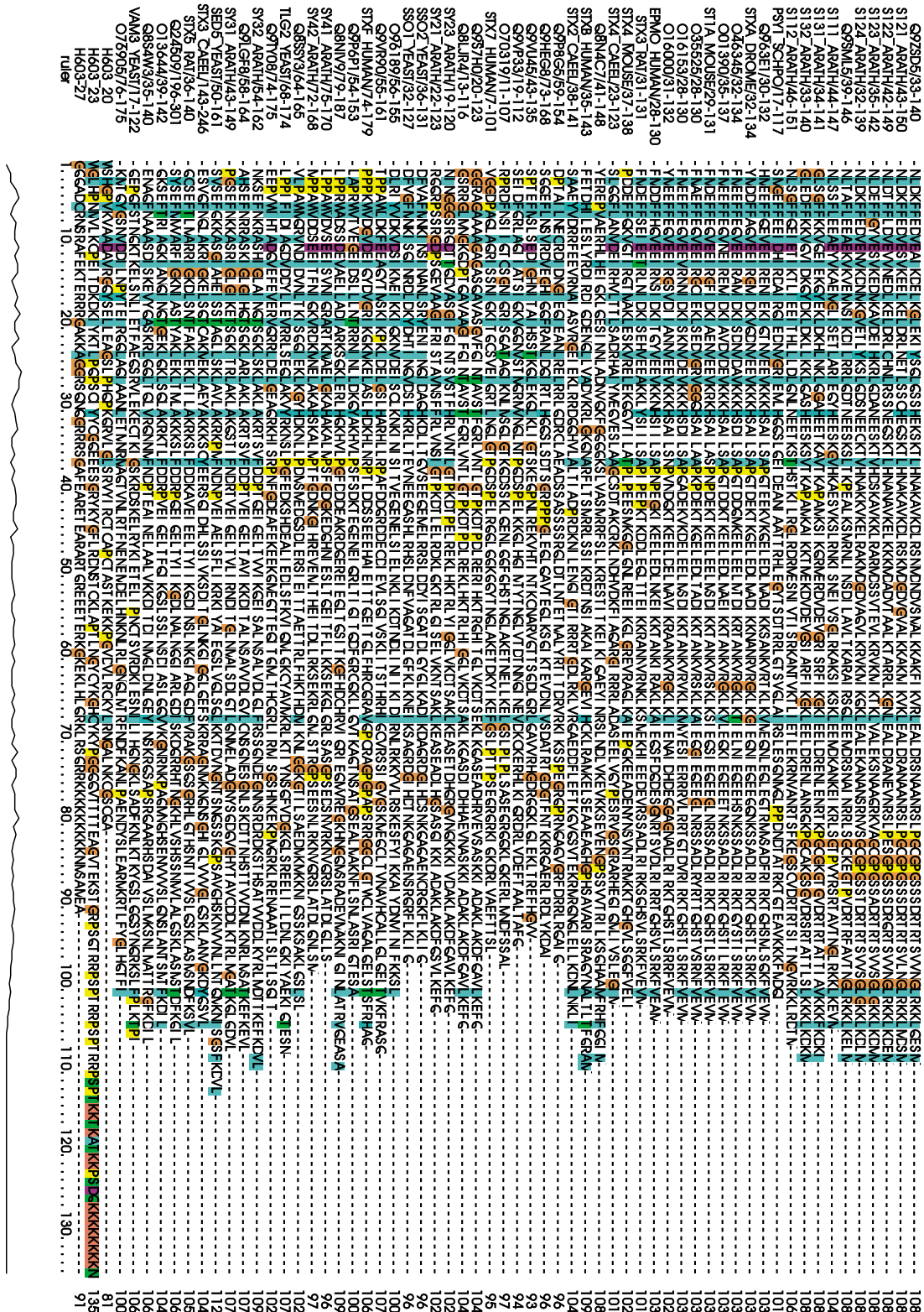
Figure 5.9. Multiple sequence alignment of syntaxins and knockout suppressor peptides. *Non polar-(blue), negative charged- (purple), uncharged – (green), positive charged – (orange) and proline (yellow) residues are indicated. The three isolated peptides (H603 clones 20, 23 and 27) as well as a similarity scale are shown.*

215

Alignment of the peptide encoded by clone 20 with the human syntaxin 1 (1Dn1_B, used for modelling in Chapter 4) indicated the aligned regions of the sequences to share 23% identity and 38% similarity with the C-terminal domain (residues 237-273) of syntaxin 1 (Figure 5.10). Similarly, the peptide encoded by clone 27 shares 19% identity and 37% similarity to the aligned N-terminal domain (residues 27-83) of human syntaxin 1 (Figure 5.11). Clone 23 did not align to human syntaxin 1.

```
1Dn1_B    237   -RIEYNVEHAVDYVERAVSDTKKA--VKYQSKARRKKIM 273
H603_20     6   W-SHGPVEVAADAVRGQYSELLEAGSLPHQPKQIVLGLS 44
```
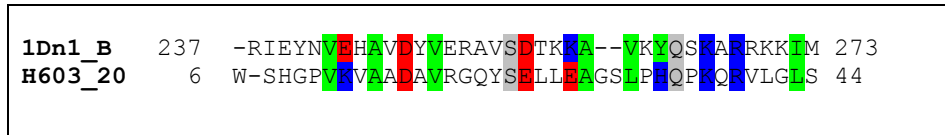
Figure 5.10. Multiple sequence alignments of clone 20 (H603_20) and human syntaxin 1 (1Dn1_B).
Non-polar (green), negative charged (red), positive charged (blue) and polar uncharged (grey) residues are indicated.

```
1Dn1_B    27   DRFMDEFFEQVEEIRGFIDKIAENVEEVKRKHSAILASPNPDEKTKEELEELMSDI 83
H603_27    1   DCRNSRAFEKTERRRG-AKKAGGRSQNQGRRRSGAFEARETEALANTQREEETERK 59

1Dn1_B    84   KKTANKVRSKLKSIEQSIEQEEGLNRSSADLR 115
H603_27   60   GREKLHLQRKLRSQREKKKKKKKKKNMSAMEA 91
```
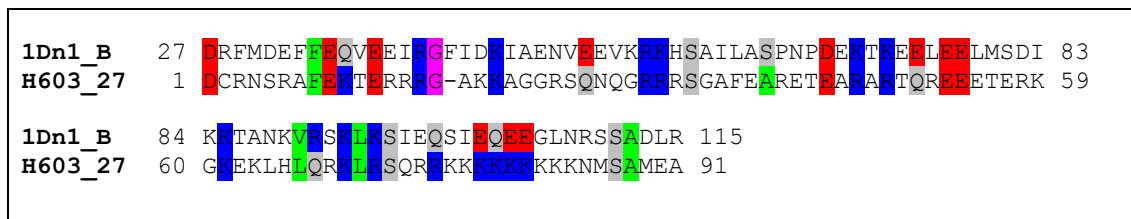
Figure 5.11 Multiple sequence alignments of clone 27 (H603_27) and human syntaxin 1 (1Dn1_B).
Non-polar (green), negative charged (red), positive charged (blue) and polar uncharged (grey) residues are indicated.

Secondary structure prediction of the peptides indicated that clones 20 and 27, which align best with the syntaxins, are rich in alpha helical structure (Figure 5.12). Both clones 20 and 27 contain two α-helical domains while clone 23 only contains a short 9 residue C-terminal α-helix.

Threading analysis of clone 20 did not identify any significant similarities, but clone 23 was found to share 24% structural identity to the SH3 domain of human intersectin 2 (which acts as a scaffold during Clathrin mediated endocytosis). Clone 27 shares 29% structural identity to the complexin/SNARE complex, also known as the synaphin/SNARE complex (Figure 5.13). The latter complex contains the normal four-helix SNARE complex with complexin bound in an anti-parallel α-helical conformation in the groove between VAMP and syntaxin helices. Complexin is believed to stabilize the interface between the latter two helices, which bears the repulsive forces between the opposed membranes (Chen *et al.* 2002).

```
Clone 20:

WSHGPVKVAADAVRGQYSELLEAGSLPHQPKQRVLGLSRVYIRCTCAPCTASTKEKKPGV
...S.HHHHHHHHHHHHHHHHHTT......T.EEEEEEEEEEEEEE.............TT.
eeeeeee---ee-eee-ee--eeeeeeeeeeee-ee--e---e-e-ee-eeeeeeeeeee

DVLRCKYLRNGALNKCGSCQA
.EEEHHHHHHHHHHHTTS....
e--e-ee-eeeeeee-ee-ee

Clone 23:

WGLHPNMVLKCPEITDKDKIYKTLPQPSCIYYCGQEEESGRYKYGFLRDNSTCKLAPTLN
....TTEEEE......TTHEEEE.....EEEEE..EEETSEEEEEEEE.T...EE....T
eeeeee---e-ee-eeeee-eee-eeee-----eeeeeeee-e----eeeee-ee-ee-e

GYCYKGHCYKYPGGQQVTTTTEAGVTEKSTGRPSQTRRPSPTRRPSPTRRPSPTKKTKAT
EEEEETEEEE.TT..EEEEEEETTEEE...S.........................E..
-e--e-e--e-eeeee-eeeeeee-eeeeeeeeeeeeeeeeeeeeeeeeeeeeeeeeeee

KKPSDQKKKKKKKKNV
....HHHHHHHHHT..
eeeeeeeeeeeeeeee


Clone 27:

GQQADCRNSRAFEKTERRRGAKKAGGRSQNQGRRRSGAFEARETEARARTQREEETERKG
......T..HHHHHHHHHHT.HHTT.....TT....HHHHHHHHHHHHHH..HHHHHHHT
eeeee-eeeeeeeeeeeee-eeeeeeeeeeeeeeeeeeeeeeeeeeeeeeeeeeeeeeee

KEKLHLQRKLRSQRRKKKKKKKKKNMSAMEA
HHHHHHHHHHHHHHHHHHHHHHHHHHHHHH..
eeeee-eeeeeeeeeeeeeeeeee-eeeee
```

Figure 5.12. Secondary structure prediction of the knockout suppressor peptides. *Line 1: The 1-letter code of the protein primary sequence. Line 2: 8-class secondary structure prediction (H: alpha helix, E: extended strand, T: turn, S: bend, G: 310-helix). Line 3: Prediction of relative solvent accessibility. Symbols corresponds to (-) the residue is buried, and (e) the residue is exposed.*

(i) **(ii)**
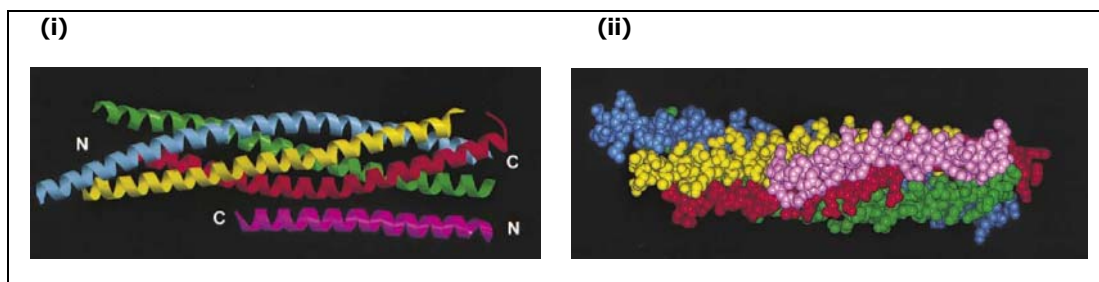
Figure 5.13. Structure of the Complexin / SNARE Complex (Chen *et al.* 2002). (i) Ribbon diagram with the following coloring code: yellow, syntaxin; red, synaptobrevin; blue, SNAP-25 N-terminal SNARE motif; green, SNAP-25 C-terminal SNARE motif; pink, complexin. (ii) Space filling model of the complexin/ SNARE complex.

Finally, we modeled the peptide encoded by clone 27 on the known crystal structure of syntaxin 1A using Modeller. From the model it is clear that the peptide share structural homology to the N-terminal domain of syntaxin 1A (Figure 5.14).
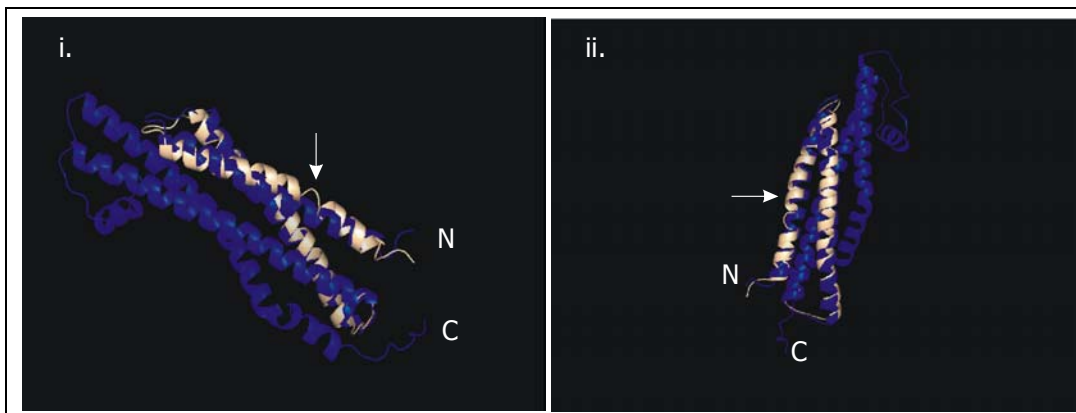
Figure 5.14. Modeled structure of the knockout fragment encoded by clone 27. *Superimposed model of the backbone structure of the knockout peptide from clone 27 (brown) on that of syntaxin 1A crystal structure (blue). The horizontal view (i), horizontal view (ii), N-terminal (N), C-termianl (C) and the single region for which no crystal data is available (arrow) is indicated. Structures were generated using Modeller and viewed using PyMol.*

In order to finally classify clone 20 and 27 as syntaxins, we need to obtain the full-length sequence of the encoded transcript and also investigate their effect on protein secretion from the H603 cells, as described by Jantti *et al*. (Jantti *et al.* 2002). To confirm that the suppressor effects are not due to the W303 cell background, these plasmids must be tested in H902 cells as well. The data obtained during this study is inconclusive in suggesting a possible identity for clone 23. Determining the entire open reading frame of the transcript is essential for identification. Regarding clone 5, no significant analysis could be performed due to the short length of the deduced peptide.

5.6.5. Pull-down assays

Isolation of the SNAREs from *O. savignyi* salivary glands were done by affinity chromatography, using immobilized recombinant rat brain α-SNAP and allowing salivary gland homogenates to bind. Eluates were investigated for the presence of SNAREs using ELISA and SDS-PAGE. ELISA with syntaxin, SNAP25, VAMP and Rab3a (negative control) polyclonal antibodies indicated signals 2.6 and 22.7 fold that of the negative control (Figure 5.15), confirming the presence of all three SNARE proteins in the eluate.
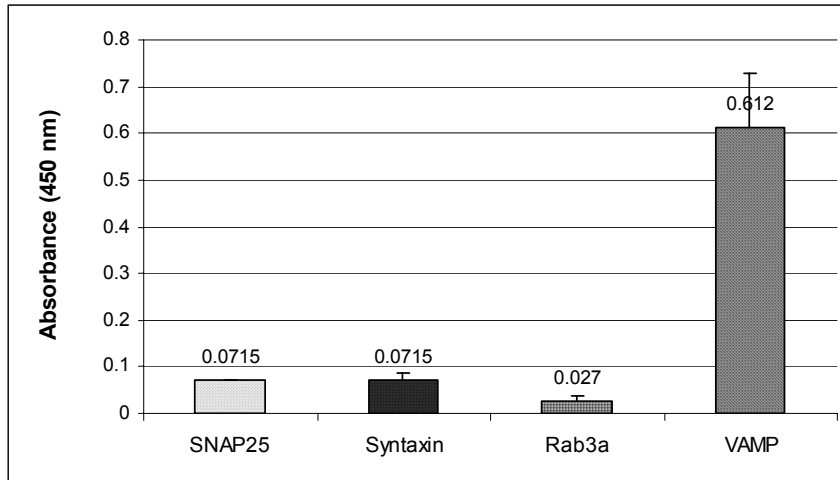
Figure 5.15. ELISA of pull-down eluates using polyclonal antibodies against the various SNAREs and Rab3a.

SDS-PAGE of the eluate confirmed the ELISA results. In the absence of salivary gland homogenates only recombinant α-SNAP is detected, but the three tick SNAREs (as determined by Western blotting, results not shown) are detected in samples obtained after performing the pull-down assay (Figure 5.16). The elevated level of VAMP is visible, explaining the high signal obtained during ELISA. In all cases, the migration rate of α-SNAP increased (lane 2), possibly due to proteolytic cleavage of α-SNAP by a protease present in the salivary gland homogenate. This must however be confirmed during future studies.
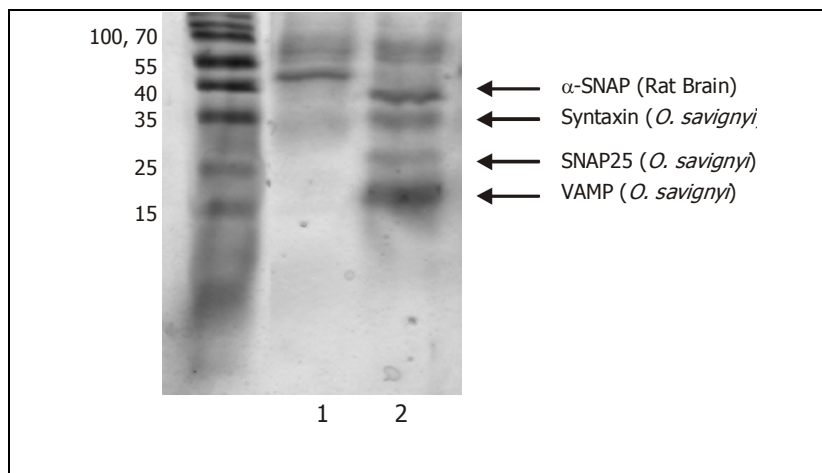
Figure 5.16. SDS-PAGE of pull-down eluates. *Lane 1 corresponds to recombinant α-SNAP isolated using the nickel column, while lane (2) corresponds to the eluate obtained after pull-down assays with O. savignyi salivary gland homogenates.*

Interestingly, very high amounts of VAMP were isolated compared with that of syntaxin and SNAP25. This can be explained from literature where it has been shown that the α-SNAP-syntaxin as well as the α-SNAP-syntaxin-SNAP25 complexes forms high affinity biding sites for VAMP (Hanson *et al.* 1995; McMahon and Sudhof 1995). Future studies will entail the protein sequencing of these SNAREs, amplification of their encoding transcripts and comparing their sequences to those of known SNAREs and those identified during functional complementation and two-hybrid studies.

5.7. CONCLUSION

During this study, functional complementation was used to successfully identify fragments of a putative syntaxin homologue from an *O. savignyi* salivary gland cDNA library. This *in vivo* system requires a functional protein domain in order to rescue the phenotype (temperature sensitive, secretion impaired), indicating that the identified domain is biologically capable of doing so. The syntaxin homologue identified differs from the syntaxin homologue that was identified using the two-hybrid system with α-SNAP as bait (Figure 5.17). The two domains share a similar charge distribution, but only 25% similarity and 13% identity to each other.

```
Knockout    1   --------------------------------GQQAD---CRNS-RAFE-TE-RRGA-  21
αSNAP       1   GLTTMHTNIKDIKSDLKTTENNISILSARAESIEANVASLGKVHEAVEDLTETSKNLSAN  60

Knockout   21   ----KKAGGRSQKQGKRSGAFEAR-FTEARARTQRKEETEKKGKEKIH--L-QRKI-KS  72
αSNAP      61   VDFLKKKTDDFENFMKESRLVFYGIPDDPAETWAQSRLHVIKLCRQNLGKVVKPEKIEKA  120

Knockout   73   QK-RKK  77
αSNAP     121   HKSKDL  126
```
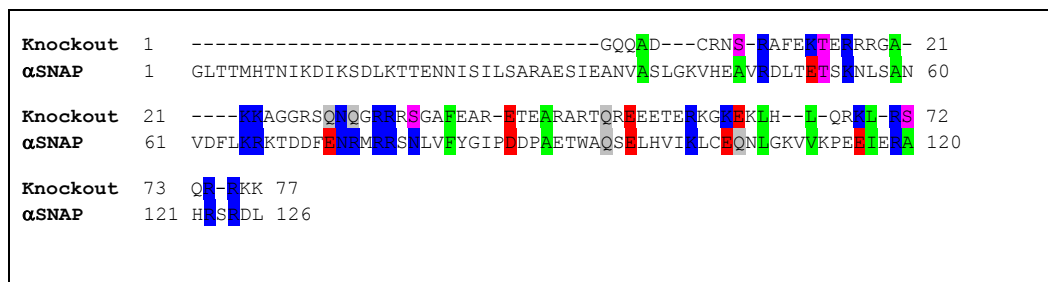
Figure 5.17. Multiple sequence alignment of the putative syntaxins isolated from *O. savignyi* salivary glands. *The sequence identified during functional complementation (Knockout) and two-hybrid screening using α-SNAP as bait (αSNAP) is shown. Non-polar (green), negative charged (red), positive charged (blue) and polar uncharged (gray) residues are indicated*.

Binding of syntaxin to α-SNAP is promiscuous and does not specifically relate to interactions occurring at the plasma membrane, while functional complementation requires biological activity in rescuing secretion at the plasma membrane of the yeast. It could therefore be that the two domains are representative of two different syntaxin isoforms. This must be further investigated by determining the entire coding regions of the domains and amino acid sequence comparison.

A novel feature of the knockout yeast used during this study is the possibility of investigating the effect of the various domains on protein secretion. These studies will be conducted during future investigations, in order to confirm their biological relevance.

By using affinity chromatography with α-SNAP we were able to identify the protein homologue of syntaxin, VAMP and SNAP25 from crude homogenates of *O. savignyi* salivary glands. These proteins share structural similarity to SNAREs found in rat brain, since they

cross-reacted with anti-rat brain SNARE antibodies. Amino acid sequencing of these will be indispensable for further cloning and investigations on the SNAREs of *O. savignyi*.

5.8. REFERENCES

Advani, R.J., Bae, H.R., Bock, J.B., Chao, D.S., Doung, Y.C., Prekeris, R., Yoo, J.S., Scheller, R.H. (1998). Seven novel mammalian SNARE proteins localize to distinct membrane compartments. *The Journal of Biological Chemistry* **273**(17): 10317-10324.

Antonin, W., Fasshauer, D., Becker, S., Jahn, R., Schneider, T.R. (2002). Crystal structure of the endosomal SNARE complex reveals common structural principles of all SNAREs. *Nature Structural Biology* **9**(2): 107-111.

Bassham, D., Gal, S., Conceicao, A., Raikhel, N.V. (1995). An *Arabidopsis* syntaxin homologue isolated by functional complementation of a yeast *pep12* mutant. *Proceedings of the National Academy of Science of the United States of America* **92**: 7262-7266.

Chen, X., Tomchick, D.R., Kovrigin, E., Arac, D., Machius, M., Sudhof, T.C., Rizo, J. (2002). Three-dimensional structure of the complexin/SNARE complex. *Neuron* **33**: 397-409.

Clontech Laboratories, I. (1997a). *Matchmaker Gal4 Two-hybrid vectors handbook (PT3062-1)*.

Conibear, E., Stevens, T.H. (1995). Vacuolar biogenesis in yeast: Sorting out the sorting proteins. *Cell* **83**: 513-516.

Fasshauer, D. (2003). Structural insights into the SNARE mechanism. *Biochimica et Biophysica Acta* **1641**: 87-97.

Gellissen, G., Melber, K., Janowicz, Z.A., Dahlems, U.M., Weydemann, U., Piontek, M., Strasse, A.W.M., Hollenberg, C.P. (1992). Heterologous protein production in yeast. *Antonie van Leeuwenhoek* **62**: 79-93.

Hanson, P.I., Otto, H., Barton, N., Jahn, R. (1995). The N-ethylmaleimide sensitive fusion protein and alpha-SNAP induce a conformational change in syntaxin. *The Journal of Biological Chemistry* **270**(28): 16955-16961.

Jantti, J., Aalto, M.K., Oyen, M., Sundqvist, L., Keranen, S., Ronne, H. (2002). Characterization of temperature-sensitive mutations in the yeast syntaxin 1 homologues Sso1p and Sso2p, and evidence of a distinct function for Sso1p in sporulation. *Journal of Cell Science* **115**: 409-420.

Jouannic, N., Lepetit, M., Vergnolle, C., Cantrel, C., Gardies, A.M., Kader, J.C., Arondel, V. (1998). Isolation of a cDNA from *Arabidopsis thaliana* that complements the sec14 mutant of yeast. *European Journal of Biochemistry* **258**: 402-410.

Katz, L., Brennwald (2000). Testing the 3Q:1R Rule: Mutational analysis of the ionic zero layer in the yeast exocytic SNARE complex reveals no requirement for arginine. *Molecular Biology of the Cell* **11**: 3849-3858.

Kingsman, S.M., Kingsman, A.J., Dobson, M.J., Mellor, J., Roberts, N.A. (1985). Heterologous gene expression in *Saccharomyces cerevisiae*. *Biotechnology and Genetic Engineering Reviews* **3**: 377-416.

Kucharczyk, R., Rytka, J. (2001). *Saccharomyces cerevisiae* - a model organism for the studies on vacuolar transport. *Acta Biochimica Polonica* **48**(4): 1025-1042.

Marz, K.E., Lauer, J.M., Hanson, P.I. (2003). Defining the SNARE complex binding of alpha-SNAP. *The Journal of Biological Chemistry* **278**(29): 27000-27008.

McMahon, H.T., Sudhof, T.C. (1995). Synaptic core complex of synaptobrevin, syntaxin and SNAP25 forms high affinity alpha-SNAP binding site. *The Journal of Biological Chemistry* **270**(5): 2213-2217.

McNew, J.A., Sogaard, M., Lampen, N.M., Machida, S., Ye, R.R., Lacomis, L., Tempst, P., Rothman, J.E., Sollner, T. (1997). Ykt6p, a prenylated SNARE essential for endoplasmic reticulum - Golgi transport. *The Journal of Biological Chemistry* **272**(28): 17776-17783.

Pullikuth, A.K., Gill, S.S. (2002). *In vivo* membrane trafficking role for an insect N-ethylmaleimide sensitive factor which is developmentally regulated in endocrine cells. *The Journal of Experimental Biology* **205**: 911-926.

Rossi, G., Saliminen, A., Rice, L.M., Brunger, A.T., Brennwald, P. (1997). Analysis of a yeast SNARE complex reveals remarkable similiarity to the neuronal SNARE complex and a novel function for the C terminus of the SNAP-25 homolog, Sec9. *The Journal of Biological Chemistry* **272**(26): 16610-16617.

Rothman, J.E. (1996). The protein machinery of vesicle budding and fusion. *Protein Science* **5**: 185-194.

Shaw, J.D., Cummings, K.B., Huyer, G., Michaelis, S., Wendland, B. (2001). Yeast as a model system for studying endocytosis. *Experimental Cell Research* **271**: 1-9.

Sutton, R.B., Fasshauer, D., Jahn, R., Brunger, A.T. (1998). Crystal structure of a SNARE complex involved in synaptic exocytosis at 2.4 A. *Nature* **395**: 347-353.

CHAPTER 6

CONCLUDING DISCUSSION

The mechanisms underlying regulated exocytosis of large dense core vesicles/granules (LDCVs) from the salivary glands of *O. savignyi*, and also from other argasid ticks, have not been addressed before. Knowledge regarding the secretion of compounds essential for tick feeding is vital since both the signaling mechanisms, as well as the components involved in transport, docking and fusion of the granules are all possible targets for designing an anti-tick feeding strategy.

During this study, the release of the enzyme apyrase, which has been localized to LDCVs of the 'a' cells, was investigated. In all cases, the amount of enzyme secreted from the glands was extremely low. This is consistent with the findings of Mans, who indicated that after feeding or stimulation with dopamine, acini revealed no detectable secretion of granules (Mans 2002a). Further studies also indicated that during feeding of ticks (until fully engorged), only ~17% of the total apyrase activity and 37% of the total salivary gland proteins were secreted, compared to unfed ticks. This indicates that fusion in *O. savignyi* most likely occurs via the kiss-and-run hypothesis and that the granule membrane does not get fully incorporated into the plasma membrane.

Extracellular stimuli indicated that the adrenerigic receptor is involved in controlling exocytosis, and not cholinergic receptors, supporting the observations of Mans in *O. savignyi* (Mans 2002a) and McSwain *et al*. for *A. americanum* (McSwain *et al.* 1992a). The effect of other external stimuli, such as GABA and brain extracts which affected ixodid tick exocytosis, must still be investigated (Lindsay and Kaufman 1986; McSwain 1989). The similarity of the response between argasid and ixodid ticks with dopamine is remarkable. In both cases, cAMP levels are increased and PKA is activated, while elevated cAMP levels are inadequate for stimulating exocytosis. In argasid ticks, elevated cAMP levels were found to inhibit exocytosis. We therefore hypothesize that cAMP acts as an "off switch", regulating exocytosis from salivary glands of *O. savignyi*. The possible downstream effects of PKA regulated protein (described in Chapter 2) must be investigated in order to completely understand the role of cAMP during tick feeding.

225

Prostaglandins, especially PGE$_2$, have been shown to be critical for activating exocytosis in ixodid ticks. In *O. savignyi*, stimulation of glands with PGE$_2$ did however not result in activation of exocytosis. We did however indicate the role of an active phospholipase. In order to address this phenomenon, the generation of free arachidonic acid and the conversion thereof must be investigated during future studies. In *A. americanum*, the presence of an EP1-receptor, linked to a G$_q$-protein (which increase IP$_3$ and DAG) explains the positive effect on exocytosis. One possibility of the non-excitory effect of PGE$_2$ in *O. savignyi*, could be the possibility of an EP2, EP3 or EP4 receptor (Table 2.7). These do not result in activation of PLC, but rather modulate cAMP levels. The latter has been proposed for the salivary glands of the blowfly, *Calliphora erythrocephala,* where PGs act by attenuating the 5-hydroxytryptamine effects by down regulating adenylyl cyclase, or by up-regulating cAMP degradation via interaction with phoshodiesterase (Stanley-Samuelson and Pedibhotla 1996). In insects, prostaglandins (PGs) are known for regulating ion and water transport similarly to that of other animals e.g. frog skin glands, toad urinary bladder, bivalve gill tissue, tick salivary glands, insect Malpighian tubules and insect rectal tissue (Stanley-Samuelson and Pedibhotla 1996). Therefore, the effect of PGs on fluid secretion and not protein secretion in *O. savignyi* must be investigated. Finally, the possibility of increased levels of other prostaglandins, such as PGF$_{2a}$ and PGD$_2$ which are elevated in ixodid ticks upon feeding, must also be addressed (Bowman 1995d).

In most stimulatory cells, intracellular calcium is usually stored in ER, and released upon stimulation e.g. via activation of the IP$_3$ receptor. In *O. savignyi* we were able to show that an active PLC as well as an increase in intracellular calcium is essential for secretion of apyrase. Previous studies indicated that in granule containing cells of *O. savignyi* the ER and Golgi is not readily visible. This raises an interesting question as to the storage of intracellular calcium. In some cells, such as gonadotrophs, the poorly visible ER was found to locate close to secretory granules and are attached to the plasma membrane (Burgoyne and Morgan 2003).

During this study, we were the first to indicate the essential role of the cytoskeleton during exocytosis from tick salivary glands. We propose that the actin barrier is an important regulator of exocytosis and that upstream signaling pathways, such as PKA and PKC, regulate its assembly and disassembly. Interestingly, microtubules are also required for

exocytosis, and therefore one can hypothesize that the LDCVs still need to be transported to the site of fusion.

We identified homologues of the SNAREs syntaxin, VAMP and SNAP25 as well as the GTPase Rab3a, in the salivary glands of *O. savignyi*. Similar to secretory cells, studies performed in *A. americanum* indicated these proteins to be essential for exocytosis. RNA-interference directed against synaptobrevin (VAMP) and nSec1 were found to decrease expression of the transcript, levels of the protein and also inhibited PGE_2 stimulated anticoagulant secretion (Karim *et al.* 2004a; Karim *et al.* 2004b).

RNA isolation from salivary glands of unfed *O. savignyi* was found to contain only the 18*S* rRNA subunit. In contrast, RNA isolated from the entire fed *O. savignyi* tick (excluding the salivary glands) as well as from the fed argasid tick larvae of *Argas (P.) walkerae*, contained the 28*S*, 18*S* and 5*S* rRNA subunits. Universally, rRNA genes are organized in tandem repeats, separated by short transcribed spacers to form a single transcript unit of ~7500 bp, the 45*S* primary transcript (Voet and Voet 1995). These genes are transcribed by RNA polymerase I and post-transcriptionally processed and assembled with ribosomal proteins. Although not evident from the RNA gels in this study, a high molecular mass band has been observed during denaturing agarose electrophoresis of RNA from unfed *O. savignyi* salivary glands (Mans 2002). Therefore, one possible explanation is that rRNA is not post-transcriptionally processed in unfed *O. savignyi*. Secondly, similarly to the stringent response of prokaryotes (where the rate of rRNA synthesis is proportional to the rate of protein synthesis), signaling mechanisms could be involved in controlling rRNA synthesis and hence protein synthesis in *O. savignyi*. During non-feeding stages, which could be as long as 5-6 years, energy saving is essential and once feeding starts, signaling mechanisms could "switch on" the pathways regulating rRNA synthesis, processing and hence protein synthesis.

Although probes of SNAREs have been used with great success in the identification of SNARE homologues in other organisms or tissues (Table 3.6), they were unsuccessful during this study, as well as for identifying SNAREs in *A. americanum* (personal communication with Dr. S. Karim, Oklahoma State University, Stillwater, USA). Similarly, degenerate primers for SNAREs were also unsuccessful, most likely due to the difference in nucleotide sequence between known SNAREs and those of *O. savignyi*. This is supported by the data obtained during this study, where syntaxin was identified and found to share little sequence homology

with known syntaxins in the regions where primers were designed. In *A. americanum*, gene specific primers were used successfully in order to clone the SNARE synaptobrevin/VAMP (Karim *et al.* 2004a) as well as the regulatory protein nSec1 (Karim *et al.* 2004b). In both cases, the identified sequences shared identity to those of human and mouse only on amino acid sequence level. VAMP from *A. americanum* shared 65% identity to human VAMP, while nSec shared 74% identity to nSec1 from *Mus musculus*.

During two-hybrid studies, the syntaxin bait identified two novel domains that interact with syntaxin. Since these domains were repeatedly identified, we regard them as significant. Future studies are however needed to confirm their identity. By using αSNAP as bait as well as during functional complementation, putative syntaxin homologues were identified in *O. savignyi*. In both cases, the N-terminal domains of the syntaxin homologues were identified. This is noteworthy since it has been described that the N-terminal domains are involved in controlling membrane fusion in eukaryotes (Dietrich *et al.* 2003).

Pull-down assays with α-SNAP isolated all SNAREs indicating that the protein-protein interactions between SNAREs in *O. savignyi* resemble those of eukaryotes. Amino acid sequencing of these identified SNAREs will be valuable in designing *O. savignyi* sequence specific primers for cloning of these proteins.

In conclusion, this is the first study describing the mechanism underlying exocytosis from an argasid tick. Although their feeding pattern differs greatly from those of ixodid ticks (Chapter 1), the mechanism regulating exocytosis is remarkably similar. Similar to all eukaryotes, from yeast to man, argasid ticks seem to use the same conserved core machinery in a preserved mechanism in order to control exocytosis from LDCVs.

REFERENCES

Bowman, A.S., Sauer, J.R., Zhu, K., Dillwith, J.W. (1995d). Biosynthesis of salivary prostaglandins in the lone star tick, *Amblyomma americanum*. *Insect Biochemistry and Molecular Biology* **25**(6): 735-741.

Burgoyne, R.D., Morgan, A. (2003). Secretory granule exocytosis. *Physiology Reviews* **83**: 581-632.

Dietrich, L.E.P., Boeddinghaus, C., LaGRassa, T.J., Ungermann, C. (2003). Control of eukaryotic membrane fusion by N-terminal domains of SNARE proteins. *Biochimica et Biophysica Acta* **1641**: 111-119.

Karim, S., Ramakrishnan, V.G., Tucker, J.S., Essenberg, R.C., Sauer, J.R. (2004a). *Amblyomma americanum* salivary glands: double stranded RNA-mediated gene silencing of synaptobrevin homologue and inhibition of PGE_2 stimulated protein secretion. *Insect Biochemistry and Molecular Biology* **34**: 407-413.

Karim, S., Ramakrishnan, V.G., Tucker, J.S., Essenberg, R.C., Sauer, J.R. (2004b). *Amblyomma americanum* salivary gland homolog of nSec1 is essential for saliva protein secretion. *Biochemical and Biophysical Research Communications* **324**: 1256-1263.

Lindsay, P.J., Kaufman, R. (1986). Potentiation of salivary fluid secretion in ixodid ticks: A new receptor system for gamma-aminobutyric acid. *Canadian Journal of Physiology and Pharmacology* **64**: 1119-1126.

Mans, B.J. (2002). Functional perspectives on the evolution of argasid tick salivary gland protein superfamilies. *Biochemistry*. Pretoria, University of Pretoria**:** 282.

McSwain, J.L., Essenberg, R.C., Sauer, J.R. (1992a). Oral secretion elicited by effectors of signal transduction pathways in the salivary glands of *Amblyomma americanum* (Acari: Ixodiddae). *Journal of Medical Entomology* **29**(1): 41-48.

McSwain, J.L., Tucker, J.S., Essenberg, R.C., Sauer, J.R. (1989). Brain factor induced formation of inositol phosphates in tick salivary glands. *Insect Biochemistry* **19**: 343-349.

Stanley-Samuelson, D.W., Pedibhotla, V.K. (1996). What can we learn form the prostaglandins and related eicosanoids in insects? *Insect Biochemistry and Molecular Biology* **26**(3): 223-234.

Voet, D., Voet, J.G. (1995). *Biochemistry*. New York, Chichester, Brisbane, Toronto, Singapore, John Wiley & Sons, Inc.

SUMMARY

Title of Thesis:	The mechanisms regulating exocytosis of the salivary glands of the soft tick, *Ornithodoros savignyi*
Student:	Christine Maritz -Olivier
Supervisor:	Prof. A.W.H. Neitz
Co-supervisor:	Prof. A.I. Louw
Department:	Biochemistry
Degree:	*Philisophiae doctor*

Numerous bioactive compounds are secreted from large dense core granules in tick salivary glands during feeding. Investigations into the signalling pathways regulating secretion indicated that they are similar for Argasidae (fast feeding ticks) and Ixodidae (slow-feeding ticks). In both cases, dopamine is the external signal that activates adenylyl cyclase, subsequently cyclic AMP levels are increased and Protein Kinase A (PKA) is activated, resulting in the phosphorylation of proteins. Secretion was also found to be highly calcium dependant. Firstly, it requires extracellular calcium (via a L-type voltage-gated calcium channel located on the plasma membrane) and secondly, intracellular calcium which is released presumably in response to IP_3. In contrast to numerous exocrine cells, membrane depolarisation and elevation of the cAMP levels are not sufficient for inducing exocytosis from *O. savignyi* salivary glands. Pathways such as the activation of Phospholipase C, inositol-phosphate kinases, Na^+K^+-ATPases, as well as the disassembly of the actin barrier, have been shown to be essential. Finally, our research also indicated a need for the ATPase NSF, an intact microtubule network and an active cytosolic Phospholipase A_2 for exocytosis. A model has been suggested, but a great deal of research is needed to elucidate all the mechanisms of regulated exocytosis.

All secretory eukaryotic cells to date require SNARE proteins for fusion of granules with the plasma membrane, leading to the release of granular content. By means of Western blotting we identified the tick homologues of the SNAREs syntaxin, SNAP25 and VAMP, as well as the small GTPase Rab3a, all enriched within the membrane fraction. We also identified the SDS-resistant 20*S* complex, which forms during the docking of granules and is composed of the three SNARE proteins. Confocal microscopy of the SNARE proteins indicates SNAP25 and

VAMP localize to the granule membranes, while syntaxin localises strictly to the plasma membrane.

In order to isolate the tick SNARE homologues we exploited protein-protein interactions by means of the yeast two-hybrid system. Screening of an *O. savignyi* cDNA salivary gland library using rat brain α-SNAP as bait, we identified a transcript encoding a tick syntaxin homologue. It encoded a 126 residue protein which shares 14% identity and 40% similarity with human syntaxin 1. Furthermore, we were able to successfully model the identified protein onto the known crystal structure of human syntaxin 1 and indicate that it shares structural homology with helices 1, 2, 3 and the connecting two loop regions. Following screening of the library with a truncated syntaxin bait construct, two novel domains were identified in all the interacting clones. To date their identity remains unknown.

Functional complementation in the syntaxin knockout yeast strain H603 with an *O. savignyi* cDNA library resulted in the identification of four novel transcripts, which suppressed the temperature sensitive phenotype. Two of these share homology with the N- and C-terminals of syntaxins respectively and were successfully modelled onto the human syntaxin 1 crystal structure. Finally, by exploiting the extensive SNARE binding properties of recombinant rat brain α-SNAP, we were able to isolate the *O. savignyi* SNAREs, i.e. syntaxin, SNAP25 and VAMP, using pull-down assays. These purified proteins will soon be subjected to amino acid sequencing, and their sequences used to confirm the identified transcripts as true syntaxins. By enhancing our understanding of the molecular basis underlying tick feeding, as well as the proteins involved in the processes, we hope to identify possible targets for the rational design of a viable tick vaccine.

APPENDIX

Construct Gal4-BD/Bait
Section 4.5.4.

Construct Gal4 AD/Library
Section 4.5.1. & 4.5.2.

Test for Autonomous Activation
Section 4.5.6.

Titer and Amplify Library
Section 4.5.1.

Transform AH109 Yeast Cells
Sequential Transformation Section 4.5.7.

Select Transformants
Low Stringency: SD/-Leu/-Trp **Medium Stringency:** SD/-Leu/-Trp/-His **High Stringency:** SD/-Leu/-Trp/-His/-Ade/X-gal Sections 4.5.8. & 4.5.9.

Nested PCR Screening
Section 4.5.10.

Plasmid Isolation & Transformation into KC8 *E. coli*
Sections 4.5.11. & 4.5.12.

DNA sequencing of AD/Library positive clones
Section 4.5.13.

Scheme 1: Overview of performing a yeast two-hybrid screen.